Numéro ordre C.N.R.S.
A.O 10712

THÈSE

présentée à

L'UNIVERSITE SCIENTIFIQUE ET MEDICALE ET L'INSTITUT NATIONAL POLYTECHNIQUE DE GRENOBLE

pour obtenir le grade

DOCTEUR ES-SCIENCES PHYSIQUES

par

Jean-Paul JAY-GERIN

SUJET

ETUDE DES PROPRIETES THERMOELECTRIQUES ET THERMOMAGNETIQUES DU GRAPHITE A BASSES TEMPERATURES

ETUDE DE LA "TRANSITION STATISTIQUE" PAR UN CHAMP MAGNETIQUE INTENSE DANS LES SEMICONDUCTEURS EN REGIME EXTREME QUANTIQUE

Soutenue le 12 mai 1975 devant la commission d'Examen

MM.	A. LACAZE	Président
	S. ASKENAZY	Examinateurs
	M. CYROT	
	R. MAYNARD	
	P.R. WALLACE	

UNIVERSITE SCIENTIFIQUE
ET MEDICALE DE GRENOBLE

M. Michel SOUTIF
M. Gabriel CAU

INSTITUT NATIONAL POLY-
TECHNIQUE DE GRENOBLE

Présidents M. Louis NEEL
Vice-Présidents MM. Lucien BONNETAIN
Jean BENOIT

MEMBRES DU CORPS ENSEIGNANT DE L'U.S.M.G.

PROFESSEURS TITULAIRES

MM.	ANGLES D'AURIAC Paul	Mécanique des fluides
	ARNAUD Georges	Clinique des maladies infectieuses
	ARNAUD Paul	Chimie
	AUBERT Guy	Physique
	AYANT Yves	Physique approfondie
Mme	BARBIER Marie-Jeanne	Electrochimie
MM.	BARBIER Jean-Claude	Physique expérimentale
	BARBIER Reynold	Géologie appliquée
	BARJON Robert	Physique nucléaire
	BARNOUD Fernand	Biosynthèse de la cellulose
	BARRA Jean-René	Statistiques
	BARRIE Joseph	Clinique chirurgicale
	BEAUDOING André	Pédiatrie
	BERNARD Alain	Mathématiques Pures
Mme	BERTRANDIAS Françoise	Mathématiques Pures
MM.	BEZES Henri	Chirurgie générale
	BLAMBERT Maurice	Mathématiques Pures
	BOLLIET Louis	Informatique (IUT B)
	BONNET Georges	Electrotechnique
	BONNET Jean-Louis	Clinique ophtalmologique
	BONNET-EYMARD Joseph	Pathologie médicale
	BOUCHERLE André	Chimie et Toxicologie
	BOUCHEZ Robert	Physique nucléaire
	BOUSSARD Jean-Claude	Mathématiques Appliquées
	BRAVARD Yves	Géographie
	CABANEL Guy	Clinique rhumatologique et hydrologie
	CALAS François	Anatomie
	CARRAZ Gilbert	Biologie animale et pharmacodynamie
	CAU Gabriel	Médecine légale et Toxicologie
	CAUQUIS Georges	Chimie organique
	CHABAUTY Claude	Mathématiques Pures
	CHARACHON Robert	Oto-Rhino-Laryngologie
	CHATEAU Robert	Thérapeutique
	CHIBON Pierre	Biologie animale
	COEUR André	Pharmacie chimique et chimie analytique
	CONTAMIN Robert	Clinique gynécologique
	COUDERC Pierre	Anatomie Pathologique
	CRAYA Antoine	Mécanique
Mme	DEBELMAS Anne-Marie	Matière médicale
MM.	DEBELMAS Jacques	Géologie générale
	DEGRANGE Charles	Zoologie
	DEPORTES Charles	Chimie minérale
	DESRE Pierre	Métallurgie
	DESSAUX Georges	Physiologie animale
	DODU Jacques	Mécanique appliquée
	DOLIQUE Jean-Michel	Physique des plasmas
	DREYFUS Bernard	Thermodynamique
	DUCROS Pierre	Cristallographie
	DUGOIS Pierre	Clinique de Dermatologie et Syphiligraphie
	FAU René	Clinique neuro-psychiatrique

MM.	GAGNAIRE Didier	Chimie physique
	GALLISSOT François	Mathématiques Pures
	GALVANI Octave	Mathématiques Pures
	GASTINEL Noël	Analyse numérique
	GAVEND Michel	Pharmacologie
	GEINDRE Michel	Electroradiologie
	GERBER Robert	Mathématiques Pures
	GERMAIN Jean-Pierre	Mécanique
	GIRAUD Pierre	Géologie
	KAHANE André	Physique générale
	KLEIN Joseph	Mathématiques Pures
	KOSZUL Jean-Louis	Mathématiques Pures
	KRAVTCHENKO Julien	Mécanique
	KUNTZMANN Jean	Mathématiques Appliquées
	LACAZE Albert	Thermodynamique
	LACHARME Jean	Biologie végétale
	LAJZEROWICZ Joseph	Physique
	LATREILLE René	Chirurgie générale
	LATURAZE Jean	Biochimie pharmaceutique
	LAURENT Pierre	Mathématiques Appliquées
	LEDRU Jean	Clinique médicale B
	LLIBOUTRY Louis	Géophysique
	LONGEQUEUE Jean-Pierre	Physique nucléaire
	LOUP Jean	Géographie
Mle	LUTZ Elisabeth	Mathématiques Pures
	MALGRANGE Bernard	Mathématiques Pures
	MALINAS Yves	Clinique obstétricale
	MARTIN-NOEL Pierre	Séméiologie médicale
	MAZARE Yves	Clinique médicale A
	MICHEL Robert	Minéralogie et Pétrographie
	MOURIQUAND Claude	Histologie
	MOUSSA André	Chimie nucléaire
	NEEL Louis	Physique du Solide
	OZENDA Paul	Botanique
	PAYAN Jean-Jacques	Mathématiques Pures
	PEBAY-PEYROULA Jean-Claude	Physique
	RASSAT André	Chimie systématique
	RENARD Michel	Thermodynamique
	REULOS René	Physique industrielle
	RINALDI Renaud	Physique
	ROGET Jean	Clinique de pédiatrie et de puériculture
	DE ROUGEMONT Jacques	Neuro-chirurgie
	SEIGNEURIN Raymond	Microbiologie et Hygiène
	SENGEL Philippe	Zoologie
	SOUTIF Michel	Physique générale
	TANCHE Maurice	Physiologie
	TRAYNARD Philippe	Chimie générale
	VAILLANT François	Zoologie
	VALENTIN Jacques	Physique Nucléaire
	VAUQUOIS Bernard	Calcul électronique
Mme	VERAIN Alice	Pharmacie galénique
M.	VERAIN André	Physique
MM.	VEYRET Paul	Géographie
	VIGNAIS Pierre	Biochimie médicale
	YOCCOZ Jean	Physique nucléaire théorique

PROFESSEURS ASSOCIES

MM.	ASCARELLI Gianni	Physique
	CHEEKE John	Thermodynamique
	GILLESPIE John	I.S.N.
	ROCKAFELLAR Ralph	Mathématiques appliquées
	WOHLFARTH Erich	Physique du solide

PROFESSEURS SANS CHAIRE

Mle	AGNIUS-DELORD Claudine	Physique pharmaceutique
	ALARY Josette	Chimie analytique
MM.	BELORIZKY Elie	Physique
	BENZAKEN Claude	Mathématiques appliquées
	BERTRANDIAS Jean-Paul	Mathématiques appliquées
	BIAREZ Jean-Pierre	Mécanique
Mme	BONNIER Jane	Chimie générale
MM.	BRUGEL Lucien	Energétique
	CARLIER Georges	Biologie végétale
	CONTE René	Physique
	DEPASSEL Roger	Mécanique des Fluides
	GAUTHIER Yves	Sciences biologiques
	GAUTRON René	Chimie
	GIDON Paul	Géologie et Minéralogie
	GLENAT René	Chimie organique
	HACQUES Gérard	Calcul numérique
	HOLLARD Daniel	Hématologie
	HUGONOT Robert	Hygiène et Méd.Préventive
	IDELMAN Simon	Physiologie animale
	JANIN Bernard	Géographie
	JOLY Jean-René	Mathématiques pures
	JULLIEN Pierre	Mathématiques appliquées
Mme	KAHANE Josette	Physique
MM.	KUHN Gérard	Physique
	LUU-DUC-Cuong	Chimie Organique
	MAYNARD Roger	Physique du solide
	MULLER Jean-Michel	Thérapeutique
	PERRIAUX Jean-Jacques	Géologie et minéralogie
	PFISTER Jean-Claude	Physique du solide
Mle	PIERY Yvette	Physiologie animale
MM.	REBECQ Jacques	Biologie (CUS)
	REVOL Michel	Urologie
	REYMOND Jean-Charles	Chirurgie générale
	ROBERT André	Chimie papetière
	SARRAZIN Roger	Anatomie et chirurgie
	SARROT-REYNAULD Jean	Géologie
	SIBILLE Robert	Construction Mécanique
	SIROT Louis	Chirurgie générale
Mme	SOUTIF Jeanne	Physique générale
MM.	VIALON Pierre	Géologie
	VAN CUTSEM Bernard	Mathématiques appliquées

MAITRES DE CONFERENCES ET MAITRES DE CONFERENCES AGREGES

MM.	AMBLARD Pierre	Dermatologie
	AMBROISE-THOMAS Pierre	Parasitologie
	ARMAND Yves	Chimie
	BEGUIN Claude	Chimie organique
Mme	BERIEL Héléne	Pharmacodynamique
M.	BILLET Jean	Géographie
	BOUCHARLAT Jacques	Psychiatrie adultes
Mme	BOUCHE Liane	Mathématiques (CUS)
MM.	BOUCHET Yves	Anatomie
	BRODEAU François	Mathématiques (IUT B)
	BUISSON Roger	Physique
	BUTEL Jean	Orthopédie
	CHAMBAZ Edmond	Biochimie médicale
	CHAMPETIER Jean	Anatomie et organogénèse
	CHERADAME Hervé	Chimie papetière
	CHIAVERINA Jean	Biologie appliquée (EFP)

MM.	COHEN-ADDAD Jean-Pierre	Spectrométrie physique
	COLOMB Maurice	Biochimie médicale
	COULOMB Max	Radiologie
	CROUZET Guy	Radiologie
	CYROT Michel	Physique du solide
	DELOBEL Claude	M.I.A.G.
	DUSSAUD René	Mathématiques (CUS)
Mme	ETERRADOSSI Jacqueline	Physiologie
MM.	FAURE Jacques	Médecine légale
	FONTAINE Jean-Marc	Mathématiques Pures
	GENSAC Pierre	Botanique
	GIDON Maurice	Géologie
	GRIFFITHS Michaël	Mathématiques Appliquées
	GROS Yves	Physique (stag.)
	GROULADE Joseph	Biochimie médicale
	GUITTON Jacques	Chimie
	IVANES Marcel	Electricité
	JALBERT Pierre	Histologie
	KRAKOWIAK Sacha	Mathématiques appliquées
Mme	LAJZEROWICZ Jeanninе	Physique
MM.	LEROY Philippe	Mathématiques
	LOISEAUX Jean-Marie	Physique Nucléaire
	MACHE Régis	Physiologie végétale
	MAGNIN Robert	Hygiène et Médecine préventive
	MARECHAL Jean	Mécanique
	MARTIN-BOUYER Michel	Chimie (CUS)
	MICHOULIER Jean	Physique (I.U.T. "A")
Mme	MINIER Colette	Physique
MM.	MICOUD Max	Maladies infectieuses
	NEGRE Robert	Mécanique
	PARAMELLE Bernard	Pneumologie
	PECCOUD François	Analyse (IUT B)
	PEFFEN René	Métallurgie
	PELMONT Jean	Physiologie animale
	PERRET Jean	Neurologie
	PHELIP Xavier	Rhumatologie
	RACHAIL Michel	Médecine interne
	RACINET Claude	Gynécologie et obstétrique
	RAYNAUD Hervé	M.I.A.G.
	RENAUD Maurice	Chimie
Mme	RENAUDET Jacqueline	Bactériologie
M.	RICHARD Lucien	Botanique
Mme	RINAUDO Marguerite	Chimie macromoléculaire
MM.	ROMIER Guy	Mathématiques (IUT B)
	SHOM Jean Claude	Chimie Générale
	STIEGLITZ Paul	Anesthésiologie
	STOEBNER Pierre	Anatomie pathologique
	VROUSOS Constantin	Radiologie

MAITRES DE CONFERENCES ASSOCIES

MM.	CRABBEE Pierre	C.E.R.M.O.
	CABOT	Mathématiques appliquées
	CURRIE Jan	Mathématiques appliquées

CHARGES DE FONCTIONS DE MAITRES DE CONFERENCES

MM.	BARGE Michel	Neuro-chirurgie
	CONTAMIN Charles	Chirurgie thoracique et cardio-vasculaire
	CORDONNIER Daniel	Néphrologie
	DENIS Bernard	Cardiologie
	KOLODIE Lucien	Hématologie
	RAMBAUD Pierre	Pédiatrie
	ROCHAT Jacques	Hygiène et hydrologie

MEMBRES DU CORPS ENSEIGNANT DE L'I.N.P.G.

PROFESSEURS TITULAIRES

MM.	BENOIT Jean	Radioélectricité
	BESSON Jean	Electrochimie
	BONNETAIN Lucien	Chimie Minérale
	BONNIER Etienne	Electrochimie, Electrométallurgie
	BRISSONNEAU Pierre	Physique du solide
	BUYLE-BODIN Maurice	Electronique
	COUMES André	Radioélectricité
	FELICI Noël	Electrostatique
	PAUTHENET René	Physique du solide
	PERRET René	Servomécanismes
	SANTON Lucien	Mécanique
	SILBER Robert	Mécanique des Fluides

PROFESSEUR ASSOCIE

M.	BOUDOURIS Georges	Radioélectricité

PROFESSEURS SANS CHAIRE

MM.	BLIMAN Samuel	Electronique
	BLOCH Daniel	Physique du solide et Cristallographie
	COHEN Joseph	Electrotechnique
	DURAND Francis	Métallurgie
	MOREAU René	Mécanique
	POLOUJADOFF Michel	Electrotechnique
	VEILLON Gérard	Informatique fondamentale et appliquée
	ZADWORNY François	Electronique

MAITRES DE CONFERENCES

MM.	BOUVARD Maurice	Génie mécanique
	CHARTIER Germain	Electronique
	FOULARD Claude	Automatique
	GUYOT Pierre	Chimie minérale
	JOUBERT Jean Claude	Physique du solide
	LACOUME Jean Louis	Géophysique
	LANCIA Roland	Physique atomique
	LESPINARD Georges	Mécanique
	MORET Roger	Electrotechnique nucléaire
	ROBERT François	Analyse numérique
	SABONNADIERE Jean Claude	Informatique fondamentale et appliquée
Mme	SAUCIER Gabrièle	Informatique fondamentale et appliquée

MAITRE DE CONFERENCES ASSOCIE

M.	LANDAU Ioan Doré	Automatique

CHARGE DE FONCTIONS DE MAITRES DE CONFERENCES

M.	ANCEAU François	Mathématiques appliquées

Fait à St Martin d'Hères JANVIER 1974

REMERCIEMENTS

Monsieur le Professeur A. LACAZE, Directeur du Centre de Recherches sur les Très Basses Températures, me fait l'honneur de présider le jury de cette thèse. Je tiens à lui exprimer toute ma reconnaissance.

Je suis très heureux que Monsieur S. ASKENAZY, Maître de Conférence à l'Institut National des Sciences Appliquées de Toulouse, participe à cette Commission d'examen, et je l'en remercie vivement.

Que Monsieur M. CYROT, Maître de Conférence à l'Université Scientifique et Médicale de Grenoble, qui a bien voulu faire partie de ce jury, accepte ici mes remerciements sincères.

Je suis extrêmement reconnaissant envers Monsieur le Professeur R. MAYNARD, qui a toujours manifesté beaucoup d'intérêt pour ce travail. Je tiens à le remercier pour les nombreux conseils et encouragements qu'il m'a prodigués, pour sa présence amicale et pour d'utiles discussions concernant l'organisation et la présentation de ce mémoire.

La plus grande partie de cette étude a été réalisée sous la direction de Monsieur le Professeur P.R. WALLACE de l'Université McGill, Montréal (Canada). Lors des séjours que j'ai effectués à Montréal (octobre 1970- avril 1972), à Toulouse (janvier 1973) et à Oxford (juin-juillet 1973), il m'a communiqué son enthousiasme scientifique et touché par son amitié. C'est un grand plaisir de pouvoir aujourd'hui lui exprimer ma profonde gratitude.

Je remercie tout particulièrement Messieurs A. BRIGGS, Chargé de Recherches au C.N.R.S., J.D.N. CHEEKE, Professeur à l'Université de Sherbrooke (Canada), et A. DE COMBARIEU, Ingénieur au Centre d'Etudes Nucléaires de Grenoble, pour leur constante amitié et pour de très nombreuses discussions.

Je voudrais remercier aussi Monsieur L. BOCHIROL, Directeur du Service des Basses Températures du Centre d'Etudes Nucléaires de Grenoble, qui m'a accepté comme "Collaborateur Extérieur" dans son laboratoire.

Je remercie enfin Madame DEVILLERS pour la frappe rapide et efficace du manuscrit, et Madame TREVISSON pour le tirage final de la thèse.

Grenoble,
janvier 1975.

TABLE DES MATIERES

PARTIE I

ETUDE DES PROPRIETES THERMOELECTRIQUES ET THERMOMAGNETIQUES DU GRAPHITE A BASSES TEMPERATURES

RESUME

L'idée centrale de la première partie de ce travail est d'étudier l'interaction électron-phonon dans le graphite dans les conditions de Kohn, c'est-à-dire lorsque le vecteur d'onde des phonons est exactement égal au diamètre transverse de la surface de Fermi. Nous montrons qu'en raison de l'anisotropie considérable de la surface de Fermi, renforcée encore par l'anisotropie des surfaces de dispersion des phonons de nature quasi-bidimensionnelle, il existe un couplage très intense entre les phonons de Kohn et les électrons. En admettant que les seuls phonons effectivement entraînés sont ceux situés dans le régime de Kohn, nous trouvons que la composante de "phonon-drag" du pouvoir thermoélectrique (prédominante dans le domaine de basses températures considéré) reflète ce fort couplage. Un tel modèle permet d'expliquer, de manière satisfaisante, l'anomalie de pouvoir thermoélectrique observée dans le graphite vers 40 K. Cette idée s'est aussi révélée fructueuse pour expliquer le changement de signe du pouvoir thermoélectrique du graphite irradié aux électrons, par suppression de la contribution de "phonon-drag". Nous avons enfin étendu cette idée à l'analyse des coefficients de transport (pouvoir thermoélectrique et coefficient Nernst-Ettingshausen) en présence d'un champ magnétique, suffisamment faible pour pouvoir négliger les effets de quantification des niveaux d'énergie électroniques. Les résultats obtenus sont en accord satisfaisant avec les récentes mesures expérimentales de Takezawa, Mangez, Hewes, Dresselhaus et Tsuzuku (1973).

CHAPITRE I

Le graphite est certainement le semimétal qui a été le plus étudié depuis le début du siècle, tant du point de vue théorique qu'expérimental. Cet intérêt particulier est fondé sur le fait que le graphite constitue un corps unique dans le domaine de la Physique du Solide. Sa structure cristallographique est très anisotrope : le réseau est hexagonal, formé d'un empilement ordonné de plans graphitiques parallèles se succédant dans l'ordre alterné A B A B ... (Fig. 1).

Chaque plan graphitique est un assemblage hexagonal d'atomes distants de 1.46 Å. La distance $c_o/2$ entre deux de ces plans consécutifs est de 3.35 Å. La maille élémentaire représentée sur la Fig. 1 contient quatre atomes A, B, A', B'. Notons que ces atomes sont de deux sortes, ceux qui ont un voisin immédiat au-dessus et au-dessous d'eux dans les plans graphitiques suivants, tels que les atomes A et B de la Fig. 1, et ceux qui n'en ont pas, tels A' et B'. Le volume de la maille élémentaire est $\sqrt{3}\ a_o^2\ c_o/2$. A cette large anisotropie de structure est liée une grande anisotropie des forces interatomiques : les liaisons entre atomes d'un même plan graphitique, de nature covalente, sont environ deux ordres de grandeur plus intenses que les liaisons entre plans, de type van der Waals. Une telle structure physique se reflète évidemment sur le spectre d'énergie, et les relations de dispersion dans le graphite sont profondément différentes de celles que l'on a dans les cristaux ordinaires isotropes. Cette situation conduit tout naturellement à des problèmes très particuliers et intéressants dans l'étude théorique des propriétés électriques, thermiques et mécaniques du graphite. Cette étude a cependant longtemps été gênée sur le plan expérimental par la très grande difficulté de trouver des monocristaux de graphite naturel d'assez grandes dimensions et surtout libres de défauts et d'impuretés. Ce n'est qu'à partir de 1961-63 que l'on a su préparer, par traitement thermique sous pression, des échantillons de graphite "pyrolytique" qui, sans être monocristallins, sont constitués par l'assemblage de cristallites de grande taille (de 1 à 10 μ), ayant leurs axes c sensiblement parallèles à la direction de compression (dans les meilleurs échantillons actuels, la dispersion des axes c est moins que 1°). L'obtention de ces échantillons de haut degré d'organisation a évidemment permis un élargissement considérable du champ d'investigation sur le matériau idéal, contribuant ainsi de manière décisive à la détermination de ses propriétés intrinsèques.

STRUCTURE DE BANDES DU GRAPHITE

Une quantité considérable de travaux, tant expérimentaux que théoriques, ont contribué à obtenir une information détaillée sur la structure électronique et la surface de Fermi du graphite. Plusieurs mises au point particulièrement complètes et détaillées sont apparues dans la littérature durant ces dix dernières années (Hearing

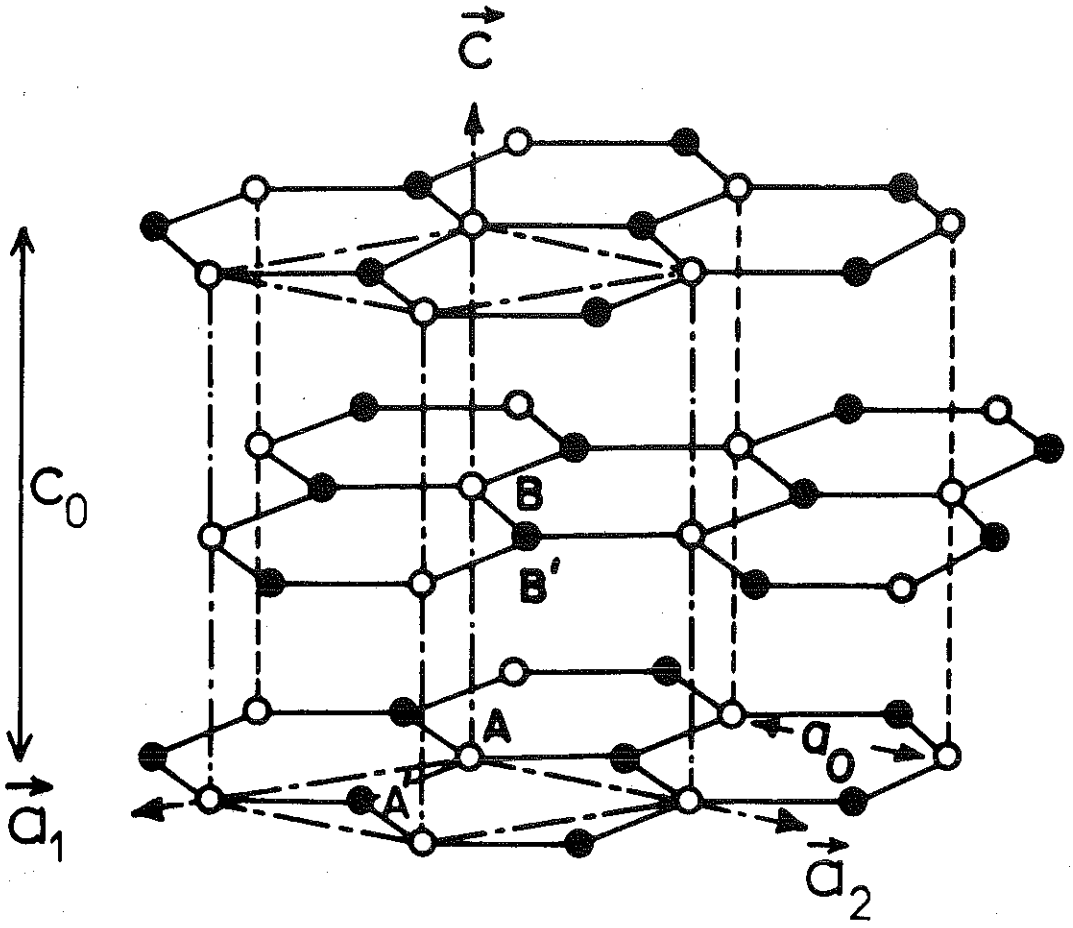

Fig.1

The crystal structure of graphite, showing the stacking sequence A B A B ... . Atoms of type α with neighbors directly above and below in adjacent planes are shown with open circles; those of type β, with full circles. The unit cell with four atoms A, B, A', B' is shown. The cell height c_0 is 6.708 Å and the basal dimension a_0 = 2.46 Å. The in-plane bond length AA' is 1.46 Å. (From I.L. Spain, "The Electronics Properties of Graphite", in "Chemistry and Physics of Carbon", edited by P.L. Walker, Jr. and P.A. Thrower (Marcel Dekker, Inc. New York, 1973), vol. 8, p. 1).

et Mrozowski 1960, Mc Clure 1964, Le Groupe Français d'Etude des Carbones 1965, Reynolds 1968, Cracknell 1971, Mc Clure 1971 et Spain 1973). Dans ce qui suit, nous nous limiterons à rappeler un certain nombre de résultats considérés actuellement comme acquis qui nous seront utiles dans le reste de notre étude.

Le graphite doit ses propriétés intéressantes aux électrons (π), et c'est la répartition de ceux-ci qui est principalement en cause. L'existence de quatre atomes de carbone dans la maille élémentaire, chaque atome possédant un électron (π), a pour conséquence un nombre de bandes (π) égal à quatre. Comme une bande peut accommoder deux électrons par maille, de spins opposés, au zéro absolu nous devons remplir complètement deux bandes (bandes de valence) pour contenir l'ensemble des électrons (π), les deux autres bandes définissant alors les bandes de conduction. Il est aujourd'hui bien établi, à la fois théoriquement et expérimentalement, que les bandes de valence et de conduction dans le graphite se recouvrent légèrement en énergie, sur une largeur d'environ 30 à 40 meV, au voisinage immédiat des six arêtes verticales HKH du prisme hexagonal représentant la zone de Brillouin (Fig. 2).

Le recouvrement de ces deux bandes a pour conséquence, compte tenu de la position du niveau de Fermi au dessous du sommet de la bande de valence aux points H et au dessus du bas de la bande de conduction au point K, l'existence à 0K à la fois de trous et d'électrons libres. Dans un schéma de zone répétée, les surfaces de Fermi de ces porteurs sont représentées par de petites poches en forme de cigares, de très faibles sections perpendiculairement à l'axe k_z, allongées le long des arêtes verticales HKH de la zone de Brillouin. L'étude détaillée de ces surfaces indique en fait une structure fine compliquée qui est associée à une forte déformation dans le plan (k_x, k_y), de symétrie trigonale autour de l'axe k_z. La surface de Fermi du graphite est illustrée Figs. 3, 4 et 5, d'après les travaux de Mc Clure (1957), de Soule, Mc Clure et Smith (1964), de Dresselhaus et Mavroides (1964) et en dernier lieu de Schroeder, Dresselhaus et Javan (1968) : la poche centrale autour du point K (k_z=0) contient les électrons, tandis que les deux poches autour des points H contiennent les trous ; ces surfaces sont extrêmement anisotropes : pour les électrons (trous), la longueur suivant la direction k_z est égale à 17 (12.1) fois la largeur perpendiculairement à cette même direction.

Parmi les divers travaux théoriques qui ont été proposés pour décrire la structure de bandes du graphite, le modèle qui rend compte, de la manière la plus satisfaisante, des propriétés du graphite, est celui de Slonczewski et Weiss (1958) (que nous désignerons dans ce qui suit par les initiales S.-W.). Il reprend le modèle bidimensionnel de Wallace (1947) consistant à traiter les plans graphitiques comme s'ils étaient indépendants, mais en tenant compte du caractère tridimensionnel du réseau, c'est-à-dire en introduisant la faible interaction qui existe entre plans graphitiques différents. Fondé à la fois sur l'utilisation de la théorie des groupes

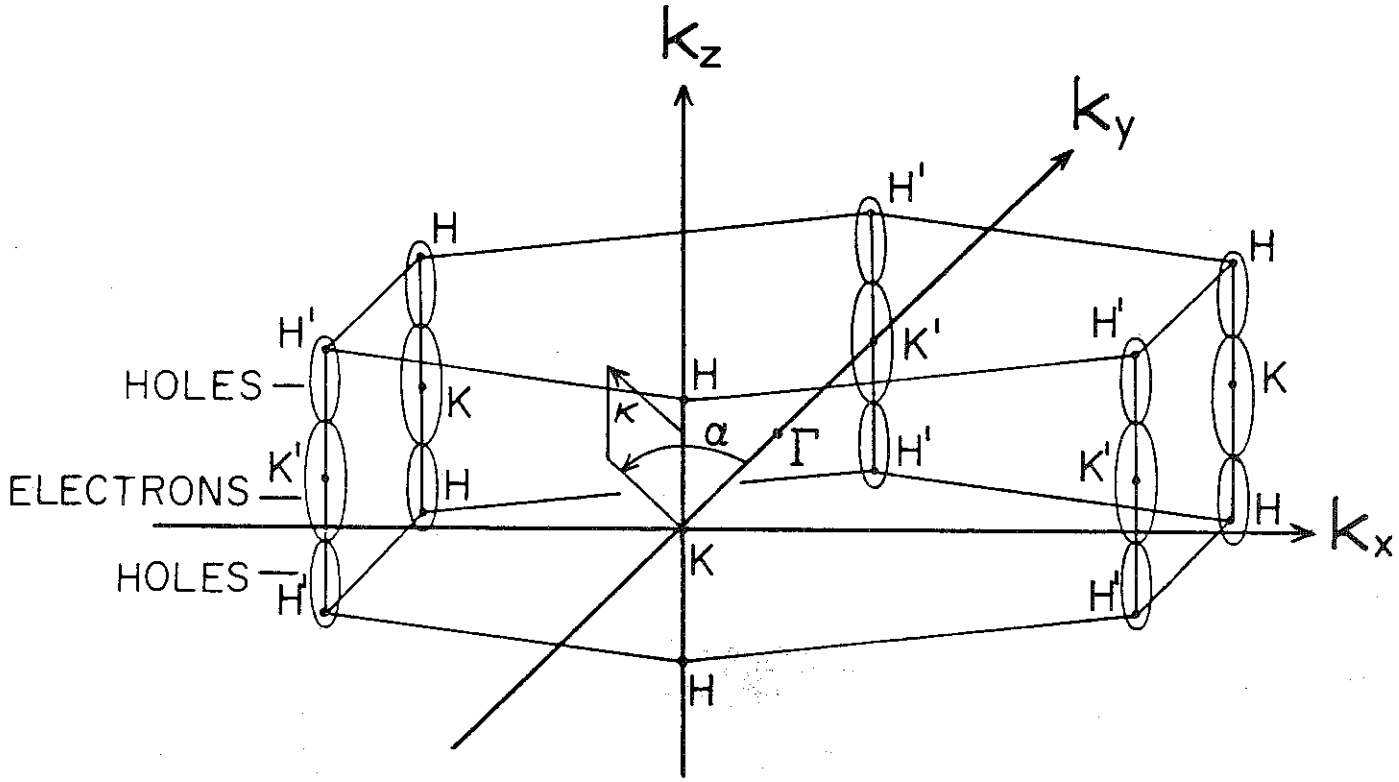

Fig. 2 Brillouin zone of graphite. The lattice parameters are a_o = 2.456 Å and c_o = 6.712 Å for single-crystal graphite, where c_o is twice the distance between layer planes. Electron and hole pockets formed by the π bands are centered on the vertical zone edges HKH.
The angle α is made by the basal wavevector component $\kappa = (k_x^2 + k_y^2)^{1/2}$ with the line joining the point K with the center of the zone, Γ.
Distance ΓK is $4\pi/3\, a_o$, and the zone height $2\pi/c_o$.
(From J. Williamson, S. Foner, and M.S. Dresselhaus, Phys. Rev. 140, A1429 (1965)).

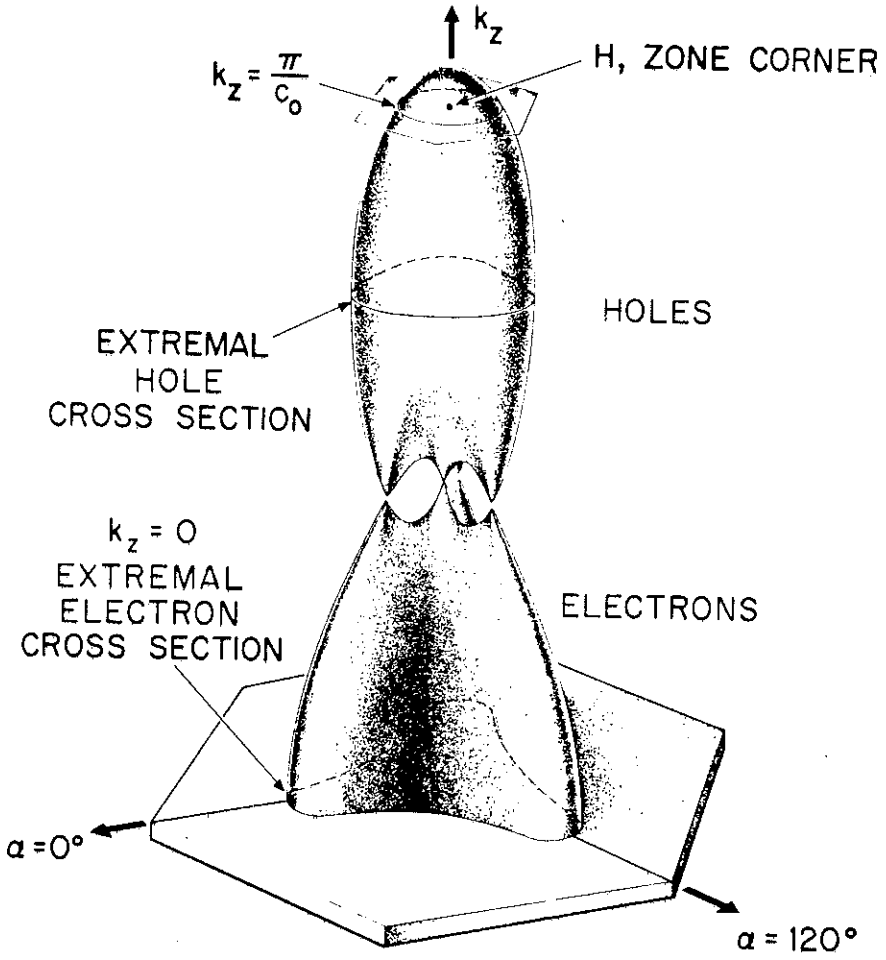

GRAPHITE FERMI SURFACE

Fig. 3

Electron and hole surfaces for $k_z > 0$ at the vertical zone edge HKH are shown in an extended zone scheme. The trigonal warping of the surfaces, which is most pronounced at $k_z = 0$, is caused by an interaction characterized by the band parameter γ_3. To emphasize this trigonal anisotropy, the scale perpendicular to the k_z axis has been expanded by a factor of 5.
(From M.S. Dresselhaus and J.G. Mavroides, IBM J. Res. Develop. 8, 262 (1964)).

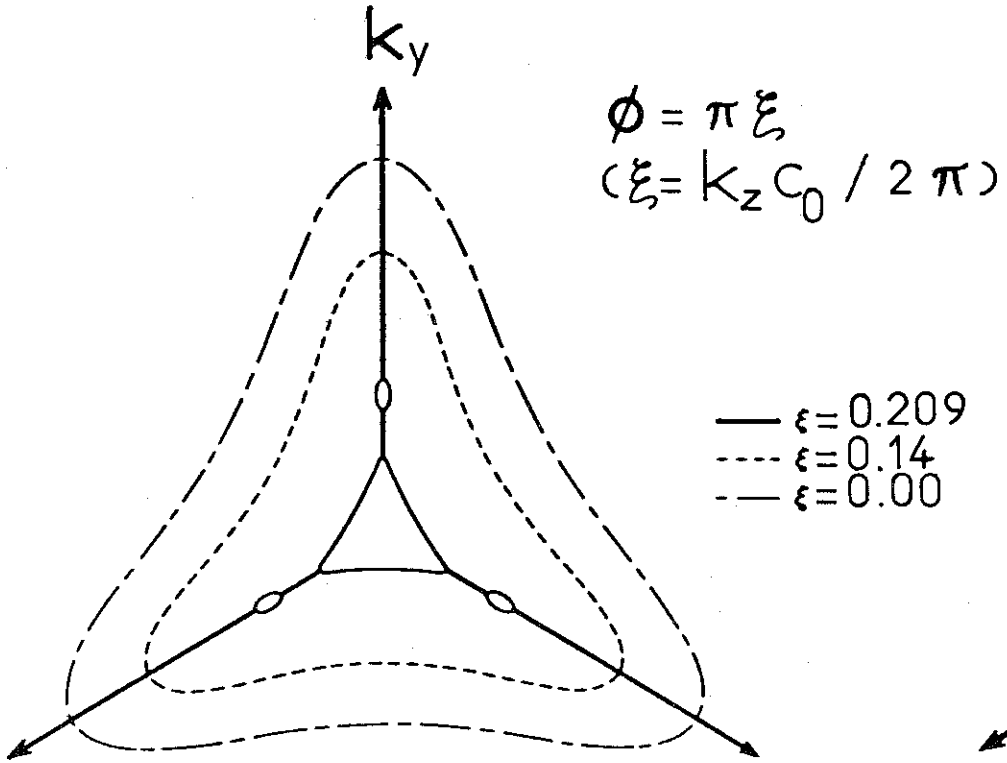

Fig.4

Scale drawings of selected electron cross sections of the Fermi surface showing the variation from the extremal at $\xi = 0$ to the cross sections near the electron "feet". The maximum radius at the extremal cross section is only 1.2 % of the distance from the Brillouin zone center to the zone edge.

6 (From M.S. Dresselhaus and J.G. Mavroides, IBM J. Res. Develop. 8, 262 (1964)).

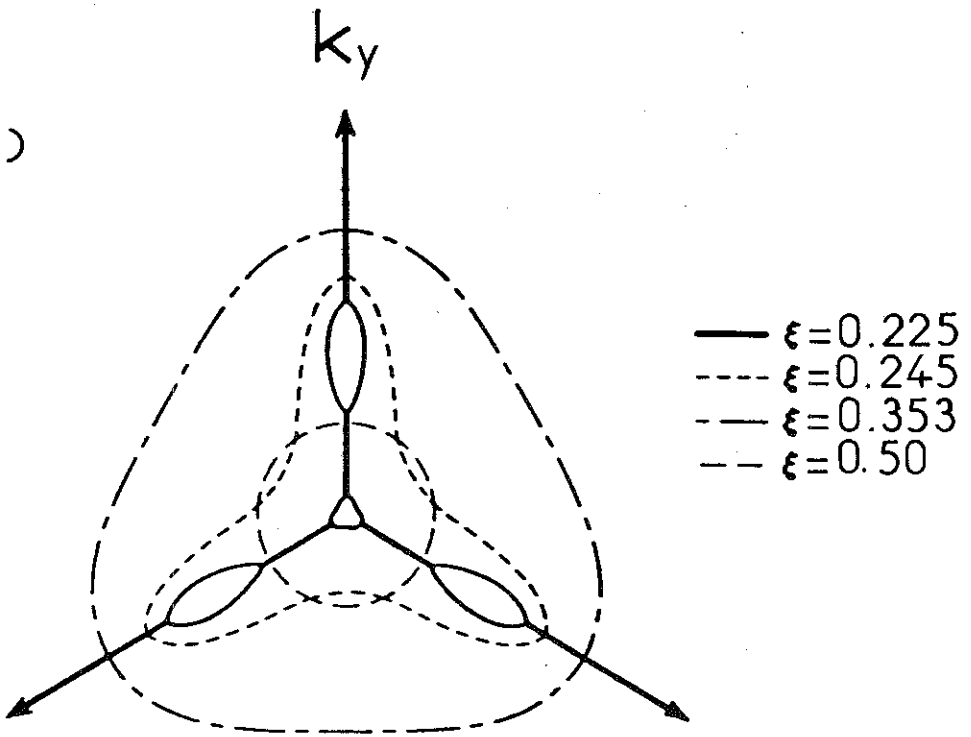

Fig.5

Scale drawings of selected hole cross sections of the Fermi surface: the extremal cross section at $\xi = 0.353$, the warped cross section at $\xi = 0.245$, one of the hole "feet" cross sections at $\xi = 0.225$ and the circular cross section at the Brillouin zone boundary, $\xi = 0.50$. The maximum radius at the extremal cross section is only 0.8 % of the distance from the Brillouin zone center to the zone edge.

et sur un traitement de théorie de perturbation, le modèle de S.-W. donne les relations de dispersion exprimant l'énergie électronique en fonction du vecteur d'onde $\vec{k}$, pour les quatre bandes (π) le long des arêtes verticales HKH de la zone de Brillouin et au voisinage immédiat de celles-ci. Les résultats du calcul de S.-W. peuvent être décrits par l'Hamiltonien (4x4) $\mathcal{H}$ (Mc Clure 1957, 1971).

$$\mathcal{H} = \begin{bmatrix} \varepsilon_1^0 & 0 & H_{13} & H_{13}^* \\ 0 & \varepsilon_2^0 & H_{23} & -H_{23}^* \\ H_{13}^* & H_{23}^* & \varepsilon_3^0 & H_{33} \\ H_{13} & -H_{23} & H_{33}^* & \varepsilon_3^0 \end{bmatrix}, \qquad \text{(I-1)}$$

où

$$\varepsilon_1^0 = \Delta + 2\gamma_1 \cos\phi + 2\gamma_5 \cos^2\phi, \qquad \text{(I-2)}$$

$$\varepsilon_2^0 = \Delta - 2\gamma_1 \cos\phi + 2\gamma_5 \cos^2\phi, \qquad \text{(I-3)}$$

$$\varepsilon_3^0 = 2\gamma_2 \cos^2\phi, \qquad \text{(I-4)}$$

$$H_{13} = \frac{\sqrt{3}}{2\sqrt{2}} (2\gamma_4 \cos\phi - \gamma_0) a_0 \kappa e^{i\alpha}, \qquad \text{(I-5)}$$

$$H_{23} = \frac{\sqrt{3}}{2\sqrt{2}} (2\gamma_4 \cos\phi + \gamma_0) a_0 \kappa e^{i\alpha}, \qquad \text{(I-6)}$$

$$H_{33} = \sqrt{3} (\gamma_3 \cos\phi) a_0 \kappa e^{i\alpha}, \qquad \text{(I-7)}$$

$$\text{et} \quad \phi = \frac{k_z c_0}{2}. \qquad \text{(I-8)}$$

Dans ces expressions, $\vec{\kappa}$ ($\kappa^2 = k_x^2 + k_y^2$) est le vecteur d'onde mesuré à partir de l'arête HKH de la zone de Brillouin dans un plan horizontal, α est l'angle polaire entre le vecteur $\vec{\kappa}$ et l'axe Γk_y (Fig. 2) et Δ, γ_0, γ_1, γ_2, γ_3, γ_4 et γ_5 sont des paramètres ajustables correspondant aux interactions entre sites atomiques différents du réseau graphitique (Table 1). La figure 6 illustre la signification de ces divers paramètres d'interaction.

L'allure des courbes de dispersion dépend, de manière très sensible, des valeurs des différents paramètres d'interaction. Ces valeurs ont été déterminées à

TABLE 1

Les divers paramètres d'interaction décrivant les bandes d'énergie du graphite

γ_0 paramètre d'interaction entre un atome de type α et un atome de type β voisins dans le même plan graphitique

γ_1 paramètre d'interaction entre deux atomes de type α voisins appartenant à deux plans voisins

γ_2 paramètre d'interaction entre deux atomes de type β voisins appartenant à deux plans seconds voisins

γ_3 paramètre d'interaction entre deux atomes de type β voisins appartenant à deux plans voisins. Ce paramètre produit la déformation trigonale des bandes.

γ_4 paramètre d'interaction entre un atome de type α et un atome de type β voisins appartenant à deux plans voisins

γ_5 paramètre d'interaction entre deux atomes de type α voisins appartenant à deux plans seconds voisins

Δ traduit la différence de nature cristallographique entre les atomes du type α et du type β

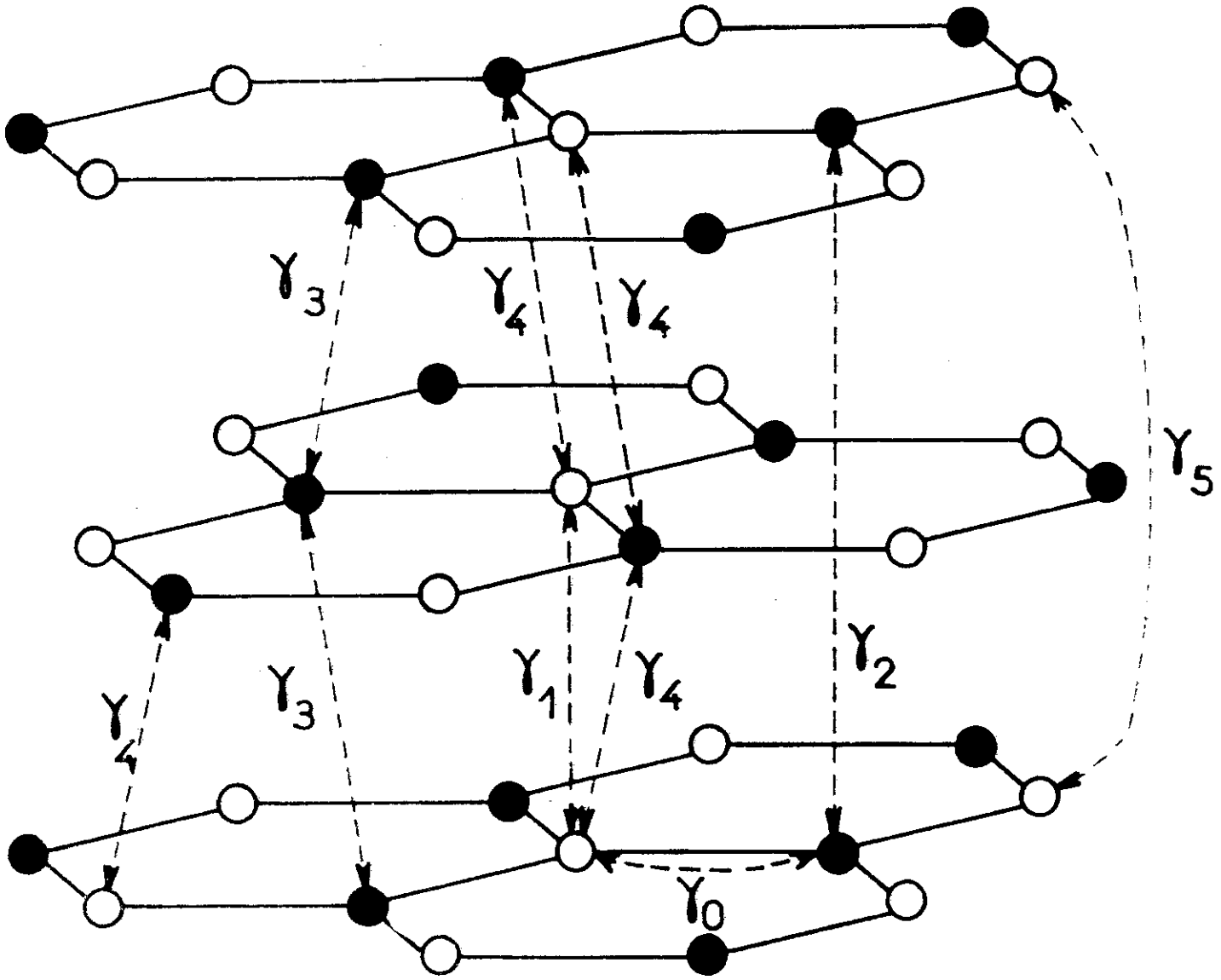

Fig. 6 Overlap parameters describing the energy bands of graphite (Table 1).
Atoms of type α with neighbors directly above and below in adjacent planes are shown with open circles; those of type β, with full circles.

partir d'un grand nombre d'expériences, comprenant principalement l'effet de Haas-van Alphen, l'effet Shubnikov-de Haas et les mesures de magnéto-réflexion et de résonance cyclotron (Mc Clure 1957, Nozières 1958, Mc Clure 1960, Mc Clure et Yafet 1962, Dresselhaus et Mavroides 1964, Williamson, Foner et Dresselhaus 1965, Schroeder, Dresselhaus et Javan 1968, Mc CLure 1971, Toy, Hewes et Dresselhaus 1973 et Sharma, Johnson et Mc Clure 1974). La Table 2 reproduit la gamme des valeurs obtenues et actuellement acceptées.

Les variations de l'énergie le long des arêtes verticales HKH de la zone de Brillouin ($\kappa = 0$) sont données par les formules pour ε_1^0, ε_2^0 et ε_3^0, Eqs. (I-2), (I-3) et (I-4) (Fig. 7) : ε_1^0 et ε_2^0 correspondent à des niveaux d'énergie simples non dégénérés (sauf au point H), ε_3^0 à un niveau dégénéré d'ordre deux.

Pour une valeur fixée de k_z, les bandes de conduction et de valence se touchent exactement à ε_3^0, mais pour différentes valeurs de k_z, ces bandes se recouvrent légèrement, avec un recouvrement maximum de $2|\gamma_2|$. Ainsi, le niveau de Fermi doit se trouver entre 0 et $2\gamma_2$. Cette disposition a pour conséquence l'existence, même à 0K, d'un petit nombre d'électrons libres occupant la bande de conduction, et d'un nombre égal de trous dans la bande de valence : c'est la raison pour laquelle le graphite est appelé un semimétal compensé. Au voisinage des arêtes HKH de la zone de Brillouin, les valeurs de l'énergie s'écartent des valeurs ε_1^0, ε_2^0 et ε_3^0, et la dégénérescence du niveau ε_3^0 est levée. Dans le cas où le paramètre $\gamma_3 = 0$, les valeurs propres de l'énergie, calculées à partir de l'Hamiltonien $\mathcal{H}$ Eq.(I-1) , sont données rigoureusement par :

$$\varepsilon_{1\pm}(\kappa,\phi) = \frac{\varepsilon_1^0 + \varepsilon_3^0}{2} \pm \left[\left(\frac{\varepsilon_1^0 - \varepsilon_3^0}{2}\right)^2 + \frac{3}{4} a_o^2 (\gamma_0 - 2\gamma_4 \cos\phi)^2 . \kappa^2\right]^{1/2} \qquad (I\text{-}9)$$

ou

$$\varepsilon_{2\pm}(\kappa,\phi) = \frac{\varepsilon_2^0 + \varepsilon_3^0}{2} \pm \left[\left(\frac{\varepsilon_2^0 - \varepsilon_3^0}{2}\right)^2 + \frac{3}{4} a_o^2 (\gamma_0 + 2\gamma_4 \cos\phi)^2 . \kappa^2\right]^{1/2} . \qquad (I\text{-}10)$$

A cette approximation, il n'apparaît pas d'anisotropie dans le plan (k_x,k_y), puisque l'énergie ne dépend pas de α : les surfaces d'égale énergie sont alors des surfaces de révolution autour de k_z. Les relations de dispersion (I-9) et (I-10) permettent de tracer les courbes donnant localement les variations de l'énergie autour de l'arête HKH pour une valeur donnée de k_z. La figure 7 indique l'allure de ces courbes pour une valeur de k_z correspondant au point (a). On voit bien sur cette figure comment la dégénérescence du niveau ε_3^0 est levée : deux des niveaux, $\varepsilon_{1-}(\kappa)$ et $\varepsilon_{2+}(\kappa)$, sont tangents en ε_3^0 pour $\kappa = 0$. L'introduction du paramètre γ_3 a pour effet essentiel de faire apparaître une modulation des surfaces d'égale énergie avec l'angle polaire α, de symétrie trigonale autour de l'arête HKH (voir Figs. 3,4 et 5). Cette modulation

TABLE 2

Paramètre	Gamme des valeurs actuellement admises (eV)
γ_0	2.8 à 3.2
γ_1	0.27 à 0.40
γ_2	-0.018 à -0.021
γ_3	0.22 à 0.29
γ_4	0.1 à 0.3
γ_5	-0.003 à -0.02
Δ	-0.008 à 0.1

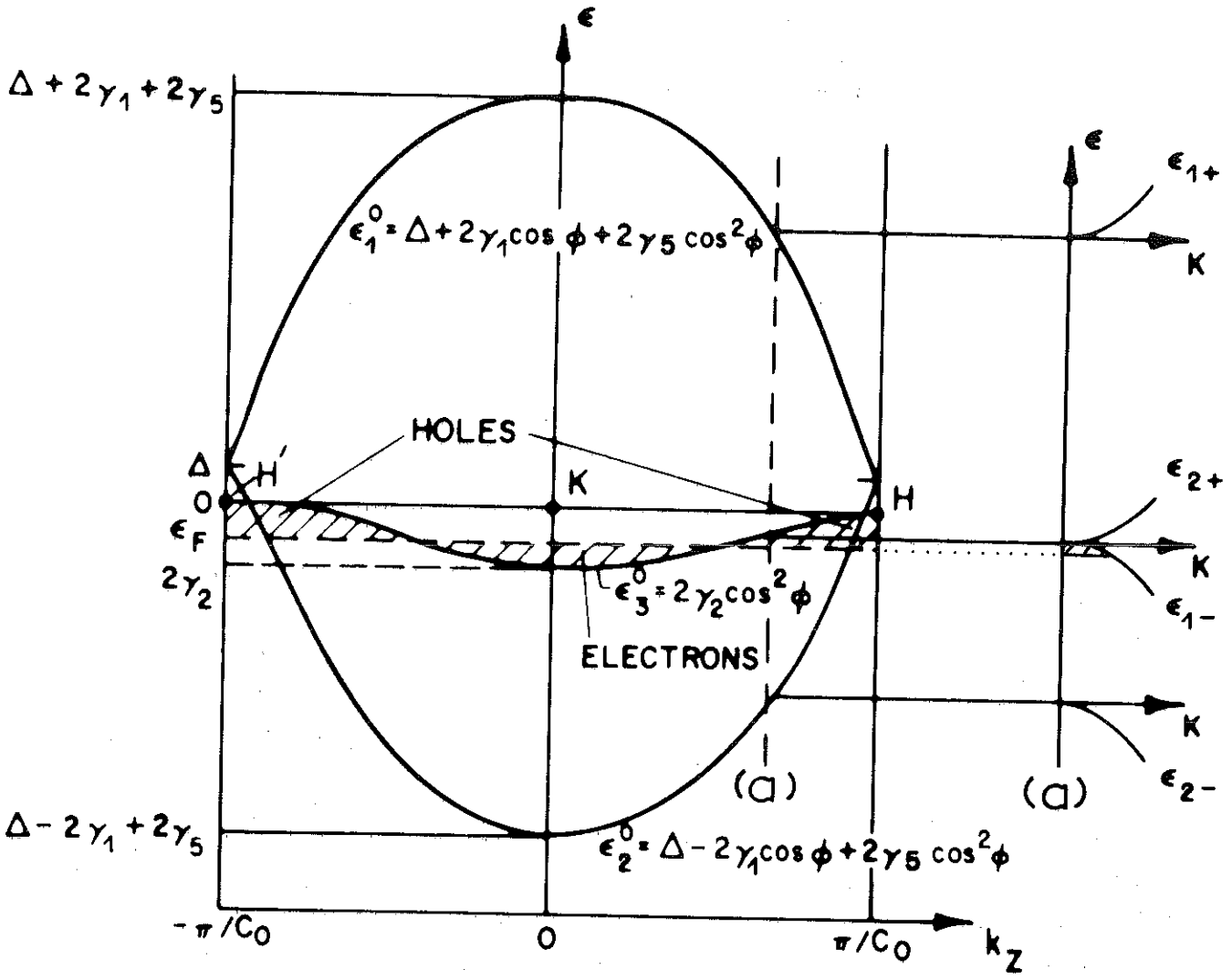

Fig. 7

Energy/wave-number curves for graphite.

Variation in the parameters $\varepsilon_1^0, \varepsilon_2^0$, and ε_3^0 along the zone edge HKH ($\phi = k_z c_0/2$). A negative value of γ_2 and a positive value of Δ are chosen. At 0 K, electrons from the top of the valence band fill up states at the bottom of the conduction band to the Fermi level ε_F as shown.

The variation of energy with the basal component of wave-vector κ is indicated, with states labeled as in the text.

(From I.L. Spain, "The Electronics Properties of Graphite", in "Chemistry and Physics of Carbon", edited by P.L. Walker, Jr. and P.A. Thrower (Marcel Dekker, Inc. New York, 1973), vol. 8, p. 1).

trigonale ("trigonal warping") est tout particulièrement importante près du point K dans la zone de Brillouin ($\xi = 0$), mais devient de moins en moins marquée au fur et à mesure que l'on se rapproche du point H ($\xi = 1/2$). Une telle différence résulte de la forme même de l'Hamiltonien S.-W., $\mathcal{H}$ [Eqs.(I-1)-(I-8)], dans lequel γ_3 apparaît toujours en association avec le facteur $\cos(\pi\xi)$. Les plus récentes estimations du paramètre γ_3 (Sharma, Johnson et Mc Clure 1974 et Dresselhaus 1974) semblent définitivement s'accorder sur une valeur très voisine de 0.29 eV.

LE SPECTRE DE VIBRATIONS DE RESEAU DU GRAPHITE

Le modèle de "semi-continuum" du graphite, initialement proposé par Komatsu et Nagamiya (1951, 1954) et Komatsu (1955) pour expliquer la loi de variation en T^2 de la chaleur spécifique de réseau à basses températures, rend compte, avec un succès remarquable, de la plupart des propriétés thermiques du graphite. Nous pouvons renvoyer, par exemple, à l'excellent article de revue de Kelly et Taylor (1973), particulièrement complet et détaillé. Dans ce modèle, le graphite est traité comme un système de membranes élastiques faiblement couplées les unes aux autres. Les vibrations possibles de ce système se séparent en deux catégories approximativement indépendantes : la première correspond à des déplacements d'atomes dans le plan (vibrations "dans le plan"), et les vecteurs de polarisation $\vec{\varepsilon}_\ell(\vec{q})$ et $\vec{\varepsilon}_t(\vec{q})$ d'un mode $\vec{q}$ sont respectivement parallèle (vibration longitudinale, (ℓ)) et perpendiculaire (vibration transverse, (t)) à $\vec{q}_\perp$, projection du vecteur d'onde $\vec{q}$ sur le plan (Fig. 8); la seconde catégorie correspond à des déplacements d'atomes perpendiculaires au plan (vibrations "hors du plan", (c)), et les vecteurs de polarisation de ces modes sont dirigés parallèlement à l'axe c (Fig. 8). Les relations de dispersion s'écrivent, pour les deux branches de polarisation (ℓ) et (t) (Dreyfus et Maynard 1967) :

$$\omega_\ell^2 = \Omega_\ell^2 (\sigma_x^2 + \sigma_y^2) + 4\,\Omega_\zeta^2 \sin^2(\frac{\sigma_z}{2}) \qquad \text{(I-11)}$$

$$\omega_t^2 = \Omega_t^2 (\sigma_x^2 + \sigma_y^2) + 4\,\Omega_\zeta^2 \sin^2(\frac{\sigma_z}{2}) \quad . \qquad \text{(I-12)}$$

Dans ces expressions, $\vec{q} = (q_x, q_y, q_z)$, vecteur d'onde du phonon, est relié à $\vec{\sigma}$ par la relation $\vec{\sigma} = (c_o/2)\vec{q}$, $(c_o/2) = 3.35$ Å est la distance interplan, Ω_ℓ et Ω_t sont proportionnels aux vitesses du son, longitudinale et transverse, $v_\ell = (c_o/2)\Omega_\ell$, $v_t = (c_o/2)\Omega_t$ et $\Omega_\ell \simeq 457$ K, $\Omega_t \simeq 280$ K, et le coefficient $\Omega_\zeta \simeq 12.5$ K (valeur ajustée à la conductibilité thermique à basses températures (Dreyfus et Maynard 1967)) correspond au couplage entre plans graphitiques qui provient de l'interaction de van der Waals. Les surfaces d'égale énergie des phonons (ℓ) et (t) ont une forme très allongée suivant l'axe c, ellipsoïdale pour $\omega < 2\Omega_\zeta$ ($\simeq 25$ K) et quasi-cylindrique pour $\omega > 2\Omega_\zeta$

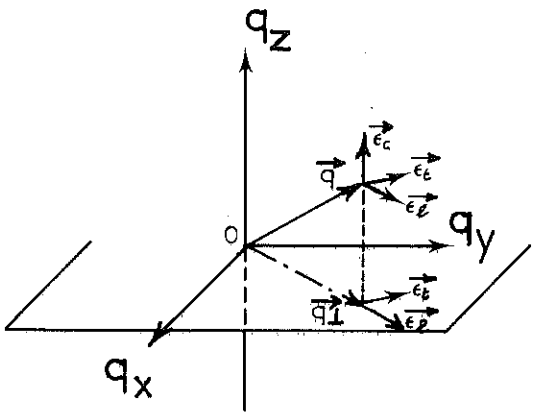

Fig. 8

$\vec{\varepsilon}_\ell$, $\vec{\varepsilon}_t$ et $\vec{\varepsilon}_c$: vecteurs de polarisation correspondant aux trois branches (ℓ), (t) et (c). $\vec{q}_\perp$ projection de $\vec{q}$ sur le plan xOy. $\vec{\varepsilon}_\ell$ // $\vec{q}_\perp$; $\vec{\varepsilon}_t \perp \vec{q}_\perp$ (dans le plan xOy) et $\vec{\varepsilon}_c$ // Oz.
(D'après R. Maynard, Thèse de Doctorat d'Etat, Grenoble, 1967).

(Fig. 9-a). Cette forme traduit clairement le caractère bidimensionnel de ces phonons: les vitesses de propagation, dirigées suivant les normales aux surfaces d'équiénergie, sont presque toutes parallèles aux plans graphitiques. Dans l'analyse du pouvoir thermoélectrique et des divers coefficients thermogalvanomagnétiques que nous présentons dans cette étude, nous avons délibérément assimilé ces surfaces de dispersion à des cylindres pour toutes les valeurs de ω. Une telle approximation, qui conduit à des simplifications considérables, revient à annuler Ω_ζ dans les relations (I-11) et (I-12), c'est-à-dire à négliger l'interaction entre plans graphitiques : les relations de dispersion des phonons (ℓ) et (t) s'écrivent alors, dans ce schéma "cylindrique" :

$$\omega_j = v_j \, q_\perp \quad , \qquad j = \ell, \, t \tag{I-13}$$

où $v_\ell = 2.01 \times 10^6$ cm/s, $v_t = 1.23 \times 10^6$ cm/s et $q_\perp = (q_x^2 + q_y^2)^{1/2}$. La densité d'états, $F_j(\omega)$, par unité d'énergie et de volume, de la branche de polarisation $j(= \ell, t)$ augmente linéairement avec ω, et est donnée par :

$$F_j(\omega) = \frac{1}{2\pi} \, \frac{\omega}{v_j^2 \, (c_o/2)} \, . \tag{I-14}$$

Les phonons (c) ont une relation de dispersion plus compliquée (voir, par exemple, Dreyfus et Maynard 1967) et présentent des surfaces d'égale énergie (Fig. 9-b) quasi-sphériques dans le domaine des basses températures ($2 \text{ K} \lesssim \omega \lesssim 180 \text{ K}$) : les vitesses de propagation sont donc distribuées de manière presque isotrope, montrant ainsi le caractère tridimensionnel de ces phonons dans cette région. L'étude complète et détaillée des vibrations "hors du plan" a été développée par Maynard (1967) en vue de l'analyse de la conductibilité thermique K(T). Cet auteur a montré que les phonons (c) contribuent seuls à $K_{//}$, conductibilité mesurée parallèlement à l'axe c, tandis que leur contribution à $K_\perp$, conductibilité mesurée perpendiculairement à l'axe c, est très faible et négligeable par rapport à celle des phonons (ℓ) et (t). Cette même propriété se retrouve dans l'analyse du phénomène de "phonon-drag" le long des plans graphitiques : la contribution du mode (c) peut être négligée devant la contribution des phonons (ℓ) et (t). Le premier argument qui conduit à l'élimination du mode (c) est lié à l'existence des petites cristallites à l'intérieur des échantillons de graphite "pyrolytique". Celles-ci sont en forme de disques plats dont les plans de base sont parallèles aux plans graphitiques et dont le diamètre d et l'épaisseur e sont tels que $d >> e$. Cette forme des cristallites, vérifiée par des études aux rayons X et au microscope électronique, permet d'expliquer la très grande valeur du rapport $K_\perp/K_{//} \simeq 10^2$ à basses températures (Dreyfus et Maynard 1967). Avec une telle forme de cristallites, les phonons (c), qui ont un caractère tridimensionnel

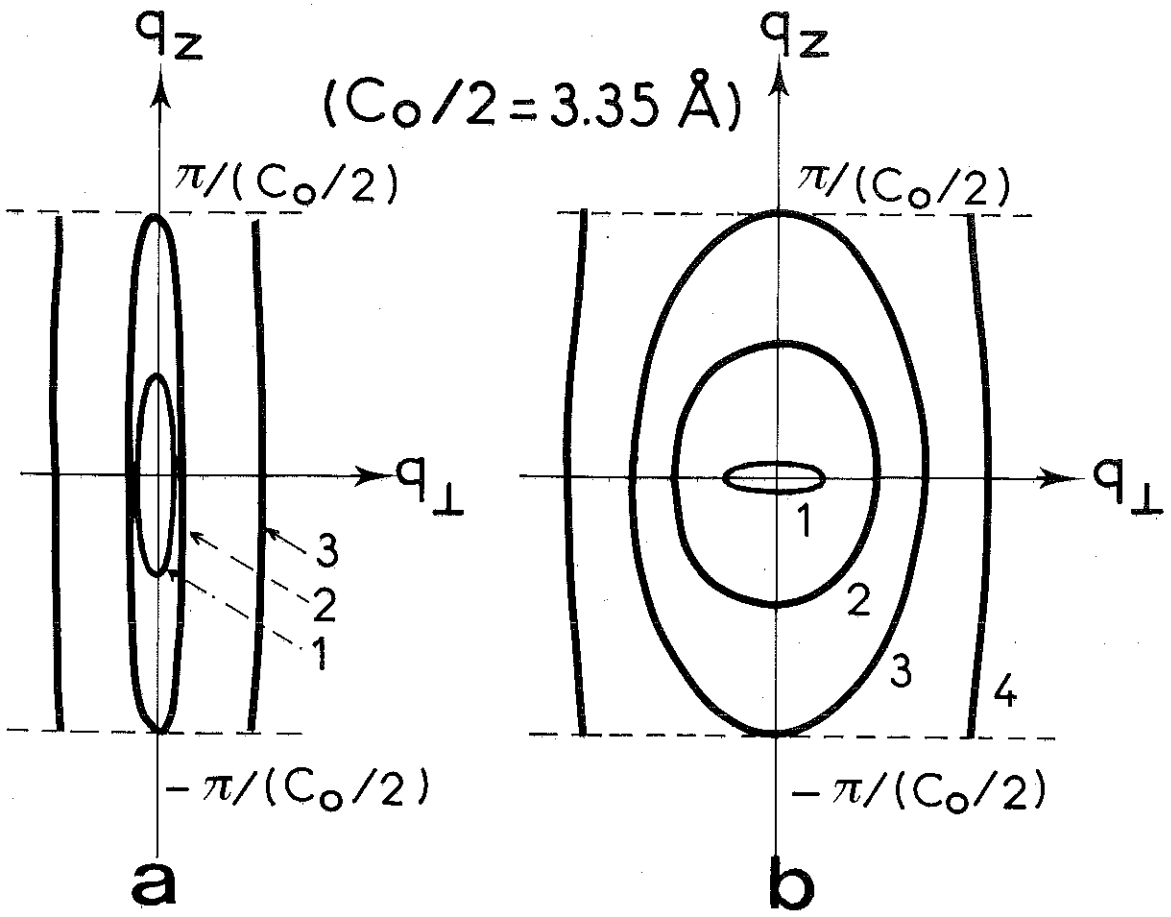

(l) and (t) phonons

$1 \longrightarrow \omega \lesssim 25\ °K$

$2 \longrightarrow \omega \eqsim 25\ °K$

$3 \longrightarrow \omega \gtrsim 25\ °K$

(c) phonons

$1 \text{ —} \quad \omega < 2\ °K$

$2 \text{ —} \quad 2\ °K \lesssim \omega \lesssim 180\ °K$

$3 \text{ —} \quad \omega \eqsim 180\ °K$

$4 \text{ —} \quad \omega \gtrsim 180\ °K$

Fig. 9

Surfaces of constant energy in $\vec{q}$ space for "in-plane" and "out-of-plane" modes.
(From R. Maynard, Ph. D. Thesis (Université de Grenoble, 1967)).

dans le domaine de température considéré, ont un libre parcours moyen de l'ordre de la plus petite dimension e (Casimir 1938) et par suite beaucoup plus petit (dans le rapport $\frac{d}{e}$) que le libre parcours moyen des phonons (ℓ) et (t). Un deuxième argument conduisant à l'élimination du mode (c) est lié à l'interaction électron-phonon : la constante de couplage électron-phonon pour la branche (c) est 6 fois plus faible que celle pour les branches (ℓ) et (t) (Sugihara et Sato 1963).

L' INTERACTION ELECTRON - PHONON DANS LE GRAPHITE

Le calcul de l'interaction électron-phonon dans le graphite a été développé par Sugihara et ses collaborateurs (Sugihara et Sato 1963, Ono et Sugihara 1966, 1968). Leur analyse, basée sur le modèle de l'ion rigide (le potentiel de chaque atome est supposé rigidement fixé à l'atome, et se déplace avec lui), fournit les éléments de matrice $M^{\vec{q}j}_{\vec{k},\vec{k}'}$ pour la diffusion d'un électron d'un état initial $\vec{k}$ vers un état final $\vec{k}'$ par un phonon de vecteur d'onde $\vec{q}$, de polarisation j et d'énergie $\hbar\omega_{\vec{q}}$. Evidemment, les seules collisions permises sont celles pour lesquelles les lois de conservation de l'énergie et du moment sont satisfaites, à savoir :

$$\vec{k} \pm \vec{q} = \vec{k}' + \vec{G}, \qquad \text{(I-15)}$$

$$\varepsilon \pm \hbar\omega_{\vec{q}} = \varepsilon' \quad , \qquad \text{(I-16)}$$

où le signe + correspond à l'absorption et le signe - à l'émission d'un quantum de vibration de réseau. Les collisions pour lesquelles le vecteur du réseau réciproque $\vec{G}$ est nul sont appelées "collisions normales", tandis que celles pour lesquelles $\vec{G} \neq 0$ sont appelées "collisions Umklapp". Pour le cas très général de processus de diffusion électron-phonon "intravallées" et "intervallées", mettant en jeu des phonons des deux types, "dans le plan" et "hors du plan", quatre éléments de matrice $M^{\vec{q}j}_{\vec{k},\vec{k}'}$ doivent être considérés. D'après Sugihara et ses collaborateurs (voir également, Kaganov et Semenenko 1967), ceux-ci peuvent être écrits sous la forme habituelle (Ziman 1961)

$$M^{\vec{q}j}_{\vec{k},\vec{k}'} = \vec{\varepsilon}_j(\vec{q}) \cdot (\vec{k}'-\vec{k})\, \mathcal{C}(|\vec{k}'-\vec{k}|), \qquad \text{(I-17)}$$

où $\vec{\varepsilon}_j(\vec{q})$ est le vecteur de polarisation du mode $\vec{q},j$. Ainsi, si $\vec{q} = \vec{k}'-\vec{k}$, nous obtenons un facteur $\vec{\varepsilon}_j(\vec{q}).\vec{q}$, qui semble nous indiquer, à priori, que les phonons transverses (t) sont inefficaces à diffuser les électrons. En fait, ceci n'est pas exact dans le cas du graphite, où la surface de Fermi touche la limite de la zone de Brillouin : la plupart des processus électron-phonon sont en effet de type Umklapp, où

$$\vec{\varepsilon}_j(\vec{q}).(\vec{k}'-\vec{k}) = \vec{\varepsilon}_j(\vec{q}).(\vec{q}-\vec{G}) \quad . \qquad \text{(I-18)}$$

Evidemment, l'équation (I-18) ne s'annule pas systématiquement pour les modes transverses. En conséquence, dans le graphite, les modes transverses doivent contribuer sensiblement de la même manière que les modes longitudinaux à la diffusion des électrons. La fonction $\mathcal{C}(|\vec{k}'-\vec{k}|)$, qui a les dimensions d'une énergie, est définie par la transformée de Fourier du potentiel dû à un ion individuel et décrit essentiellement la dépendance angulaire de la transition entre les états $\vec{k}$ et $\vec{k}'$ envisagés. Sugihara et ses collaborateurs ont montré que, pour les processus "intravallées", $\mathcal{C}(|\vec{k}'-\vec{k}|)$ est proportionnelle à cosΛ, où Λ est l'angle entre $\vec{k}_\perp$ et $\vec{k}'_\perp$ ($k_\perp^2 = \kappa^2 = k_x^2 + k_y^2$), tandis que pour les processus "intervallées", $\mathcal{C}(|\vec{k}'-\vec{k}|)$ est proportionnelle à sinΛ. La forme particulière de cette fonction joue un rôle important dans notre étude. En effet, près du régime de Kohn, c'est-à-dire pour $\vec{q} \approx 2\vec{k}_F$, où $2k_F$ est un "diamètre" de la surface de Fermi, $\Lambda \approx \pi$ et $\sin\Lambda \approx 0$, alors que $|\cos\Lambda| \approx 1$. Puisque l'objet de ce présent travail repose précisément sur l'analyse de l'interaction électron-phonon dans le graphite au voisinage du régime de Kohn, nous pouvons donc raisonnablement négliger les processus de diffusion "intervallées". D'autre part, la présence du terme cosΛ dans l'expression des éléments de matrice pour les processus "intravallés" contribue de manière appréciable à réduire le couplage électron-phonon pour les phonons éloignés du régime de Kohn, c'est-à-dire pour les phonons tels que $q < 2k_F$. Cette dernière remarque se révèlera très précieuse dans la suite de notre analyse. En définitive, les seuls processus de diffusion électron-phonon, qui sont efficaces pour l'effet de "phonon-drag" dans le graphite le long des plans de base, résultent de l'interaction entre les phonons acoustiques "dans le plan", $\omega_j = v_j\, q_\perp$ [j = (ℓ) et (t)], et les électrons (et les trous) à travers les collisions "intravallées". Pour cette classe de particules interagissantes, l'élément de matrice $M^{\vec{q}j}_{\vec{k},\vec{k}'}$ s'écrit, d'après Sugihara et Sato (1963) :

$$\left|M^{\vec{q}j}_{\vec{k},\vec{k}'=\vec{k}+\vec{q}}\right|^2 = \frac{\hbar\, C^2\, q_\perp\, \cos^2\Lambda}{2\,\Omega\,\rho\,v_j} \quad , \qquad \text{(I-19)}$$

où Ω est le volume de l'échantillon, $\rho = 2.26$ g/cm^3 la densité du graphite et C la constante de couplage électron-phonon pour le mode de vibration "dans le plan" considéré.

CHAPITRE II

ANOMALIE D'ECRAN DE KOHN DANS LE GRAPHITE

Il est bien connu (Kohn 1959, Woll et Kohn 1962, Afanas'ev et Kagan 1963 et Taylor 1963) que, dans un métal, l'interaction des électrons de conduction avec les vibrations de réseau cristallin peut conduire à des anomalies dans la loi de dispersion $\omega(\vec{q})$ des phonons. En particulier, dans le cas d'une surface de Fermi sphérique de diamètre 2 k_F, la dérivée de la fréquence $\omega(\vec{q})$ par rapport à $\vec{q}$ présente une singularité logarithmique pour les phonons qui ont un vecteur d'onde $\vec{q}$ tel que $q = 2\ k_F$. L'origine d'une telle singularité réside dans le comportement non-analytique de la fonction de réponse diélectrique du gaz d'électrons à $q = 2\ k_F$: la facilité des électrons à écranter une perturbation de nombre d'onde $\vec{q}$ chute soudainement lorsque q augmente de 2 k_F, ce qui entraîne une augmentation brusque de la fréquence de vibration de réseau $\omega(\vec{q})$. Pour une étude détaillée de la théorie de l'effet Kohn, nous pouvons renvoyer aux exposés particulièrement complets de Pines (1964), Ziman (1965) et Taylor (1970).

L'anomalie d'écran de Kohn se reflète également par des singularités dans le coefficient d'absorption de phonon $\Gamma(\vec{q})$, dû au couplage électron-phonon. Naturellement, il n'est pas surprenant que l'existence de singularités dans le spectre d'énergie de phonons corresponde à des singularités dans le coefficient d'absorption, puisque ces grandeurs, en raison du principe physique de causalité, sont conjuguées l'une à l'autre par des relations semblables aux relations de Kramers-Kronig (Pines 1964 et Kaganov et Semenenko 1966). Ainsi, lorsque $q = 2\ k_F$, le coefficient d'absorption $\Gamma(\vec{q})$ présente une brusque discontinuité vers zéro.

Kaganov et Semenenko (1966) ont montré que le caractère de la singularité de $\Gamma(\vec{q})$ à $q = 2\ k_F$ (nous l'appellerons simplement "singularité de Kohn") dépend d'une manière extrêmement critique de la géométrie de la surface de Fermi. Dans ce chapitre, nous nous proposons de discuter ce point en détail pour le cas particulier du graphite, où la surface de Fermi est constituée par des "cigares" quasi-cylindriques d'électrons et de trous (voir chapitre I). Nous allons voir que, pour un tel cas, il apparaît une intensification abrupte de la singularité de Kohn.

Le coefficient d'absorption de phonon $\Gamma(\vec{q})$ est donné d'une manière très générale par l'expression :

$$\Gamma(\vec{q}) = \frac{2\pi}{\hbar} \sum_{\vec{k},\vec{k}'} \left| M^{\vec{q}}_{\vec{k},\vec{k}'} \right|^2 \Delta(\vec{k}'-\vec{k}-\vec{q})\ \delta(E_{\vec{k}'}-E_{\vec{k}}-\hbar\omega_{\vec{q}})\ (f^{\circ}_{\vec{k}}-f^{\circ}_{\vec{k}'}) \ , \qquad \text{(II-1)}$$

où $E_{\vec{k}}$ est l'énergie d'un électron dans l'état $\vec{k}$, $f^{\circ}_{\vec{k}} = f^{\circ}(E_{\vec{k}})$ la fonction de distribution de Fermi-Dirac et $|M^{\vec{q}}_{\vec{k}\,\vec{k}'}|^2$ le carré de l'élément de matrice pour la transition d'un électron de l'état $\vec{k}$ vers $\vec{k}'$ avec absorption d'un phonon $\vec{q}$ et d'énergie $\hbar\omega_{\vec{q}}$. $\Delta(\vec{k}'-\vec{k}-\vec{q})$ est la fonction delta de Kronecker et la fonction $\delta(E_{\vec{k}'}-E_{\vec{k}}-\hbar\omega_{\vec{q}})$ traduit la loi de conservation de l'énergie. A T = 0 K et dans la limite élastique des collisions électron-phonon, l'expression (II-1) de $\Gamma(\vec{q})$ se réduit simplement à :

$$\Gamma(\vec{q}) = \frac{2\pi}{\hbar}\hbar\omega_{\vec{q}} \sum_{\vec{k}} |M^{\vec{q}}_{\vec{k},\vec{k}+\vec{q}}|^2 \delta(E_{\vec{k}}-E_F)\,\delta(E_{\vec{k}+\vec{q}} - E_{\vec{k}}) , \qquad \text{(II-2)}$$

où E_F est l'énergie de Fermi.

La sommation sur $\vec{k}$ dans (II-2) s'effectue aisément, et nous obtenons :

$$\Gamma(\vec{q}) = \frac{2\pi}{\hbar}\hbar\omega_{\vec{q}}\,\frac{\Omega}{(2\pi)^3}\int_{E_{\vec{k}}=E_F} \frac{|M^{\vec{q}}_{\vec{k},\vec{k}+\vec{q}}|^2\, dS}{\hbar|\vec{v}_{\vec{k}}|}\,\delta(E_{\vec{k}+\vec{q}} - E_{\vec{k}}) , \qquad \text{(II-3)}$$

où Ω est le volume de l'échantillon, $\vec{v}_{\vec{k}} = \frac{1}{\hbar}\vec{\nabla}_{\vec{k}}E_{\vec{k}}$ la vitesse de groupe d'un électron dans l'état $\vec{k}$ et dS l'élément d'aire sur la surface d'équiénergie $E(\vec{k})$.

Comme l'indique clairement l'équation (II-3), la détermination de $\Gamma(\vec{q})$ nécessite une connaissance précise de la forme géométrique de la surface de Fermi.

Bien que la surface de Fermi du graphite possède une géométrie relativement compliquée dont la description mathématique n'est pas simple (voir chapitre I), il est possible dans une première approximation d'assimiler les différents "cigares" de Fermi à des <u>cylindres</u> de révolution autour des arêtes verticales de la zone de Brillouin. Nous avons alors :

$$E_{\vec{k}} = \frac{\hbar^2\vec{k}_\perp^2}{2m_\perp} , \qquad \text{(II-4)}$$

où $m_\perp$ est la masse effective d'un électron perpendiculaire à l'axe c et $\vec{k}_\perp$ la projection du vecteur d'onde $\vec{k}$ sur le plan équatorial $k_z = 0$. L'intégration (II-3), compte-tenu de (II-4), conduit à une divergence du coefficient d'absorption $\Gamma(\vec{q})$ en $1/\sqrt{4k_{\perp F}^2 - q_\perp^2}$ à la condition de Kohn $q_\perp = 2\,k_{\perp F}$. En d'autres termes, les phonons qui sont situés au voisinage du régime de Kohn (nous les appellerons simplement "phonons de Kohn") sont très violemment couplés avec les électrons ($\Gamma(\vec{q}) \to \infty$). Pour voir l'origine physique de la divergence de $\Gamma(\vec{q})$ à $q_\perp = 2\,k_{\perp F}$, reportons-nous à l'équation (II-2). Celle-ci nous indique que $\Gamma(\vec{q})$ n'est pas nul seulement pour les valeurs du vecteur d'onde de phonon $\vec{q}$ telles que la surface de Fermi $E_{\vec{k}} = E_F$ <u>coupe</u> la surface identique $E_{\vec{k}+\vec{q}} = E_F$ déplacée de $-\vec{q}$ (Fig. 10).

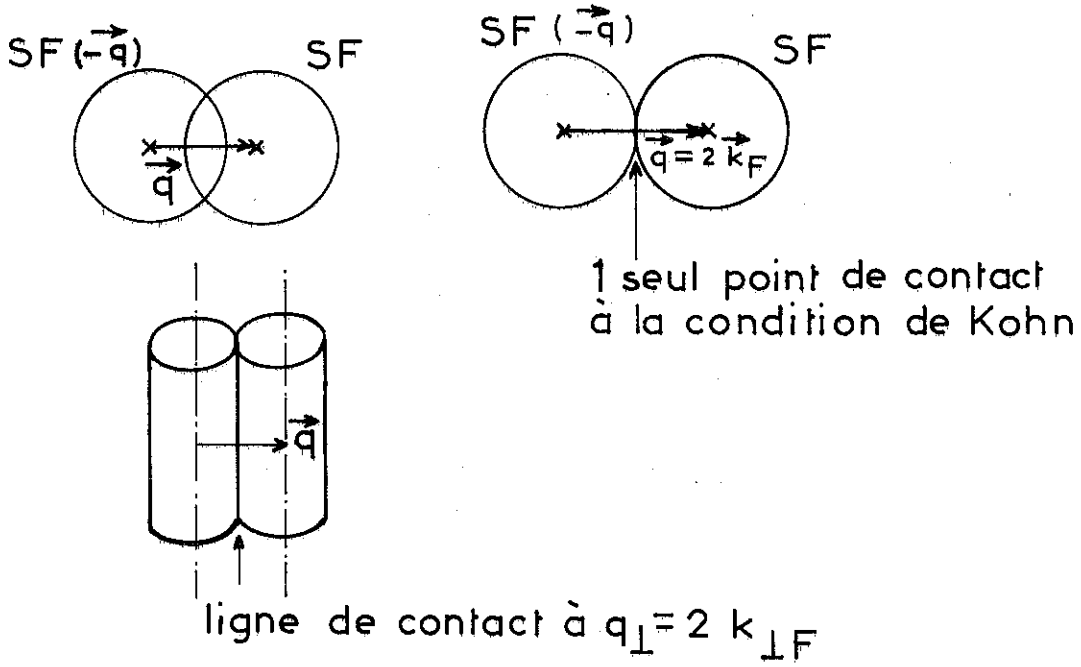
SF (−q)
SF
q
SF (−q)
SF
q = 2 k_F
1 seul point de contact
à la condition de Kohn
q
ligne de contact à q⊥ = 2 k⊥F

Fig. 10

A la limite, lorsque les deux surfaces prennent contact, c'est-à-dire pour $\vec{q} = 2\vec{k}_F$, $\Gamma(\vec{q})$ présente une singularité dont le caractère est étroitement lié à la nature du contact. Dans le cas du modèle cylindrique de la surface de Fermi du graphite, le contact des surfaces $E_{\vec{k}} = E_F$ et $E_{\vec{k}+\vec{q}} = E_F$ à $q_\perp = 2\,k_{\perp F}$ s'établit suivant une ligne : c'est cette multiplicité d'états qui conduit à la divergence de $\Gamma(\vec{q})$. Par contre, dans le cas des électrons libres, c'est-à-dire pour une surface de Fermi sphérique, l'intersection des surfaces à $\vec{q} = 2\vec{k}_F$ se réduit à un point, et la singularité de $\Gamma(\vec{q})$ se caractérise par une simple discontinuité finie. Dans ce dernier cas, les "phonons de Kohn" ne jouent pas de rôle privilégié. Une telle remarque nous amène naturellement à penser que la moindre déformation au modèle cylindrique de la surface de Fermi du graphite doit changer de manière radicale le comportement analytique de $\Gamma(\vec{q})$ au voisinage de la condition de Kohn.

Afin d'étudier la stabilité des résultats avancés quant au rôle prédominant joué par les "phonons de Kohn" dans le graphite, nous avons repris le calcul de $\Gamma(\vec{q})$ pour le cas d'une surface de Fermi ellipsoïdale, de révolution autour des arêtes de la zone de Brillouin et de mêmes dimensions que la surface cylindrique précédemment considérée. Nous avons alors la relation de dispersion :

$$E_{\vec{k}} = E(\vec{k}_\perp, k_z) = \frac{\hbar^2 \vec{k}_\perp^{\,2}}{2m_\perp} + \frac{\hbar^2 k_z^2}{2m_z} \quad , \qquad \text{(II-5)}$$

où $m_\perp$ et m_z sont les masses effectives respectivement perpendiculaire et parallèle à l'axe c. L'intégration (II-3), compte-tenu de (II-5), conduit à une singularité de $\Gamma(\vec{q})$ à $\vec{q} = 2\vec{k}_F$ qui se réduit à une simple discontinuité, exactement comme pour le cas d'une surface de Fermi isotrope. A ce stade, les "phonons de Kohn" n'ont aucun rôle particulier. Cependant, la fonction dont nous avons besoin dans l'étude des propriétés de transport n'est pas $\Gamma(\vec{q})$, mais plutôt $\Gamma(\omega)$, la valeur moyenne de $\Gamma(\vec{q})$ sur une surface d'équiénergie de phonon $\omega_{\vec{q}} = \omega$ = constante. Or, dans le graphite à basses températures, nous avons une situation tout à fait remarquable, en ce sens que les surfaces d'égale énergie des phonons polarisés dans les plans graphitiques sont pratiquement cylindriques pour toutes les valeurs de ω (voir chapitre I). L'anisotropie combinée de la surface de Fermi et du spectre de vibrations de réseau conduit à un maximum aigu de $\Gamma(\omega)$ pour les phonons de Kohn. Pour voir ce résultat simplement, nous pouvons établir dans l'espace des $\vec{q}$, une comparaison directe entre la surface lieu géométrique des points singuliers de $\Gamma(\vec{q})$ à $\vec{q} = 2\vec{k}_F$ (cette surface est appelée la "surface de Kohn") et une surface d'équiénergie de phonon $\omega = v_j q_\perp$ (Fig. 11). Par suite de la coupure dans $\Gamma(\vec{q})$, les seuls phonons d'énergie $\hbar\omega$ qui sont effectivement couplés aux électrons sont situés sur une petite portion du cylindre d'équiénergie $\hbar\omega$ = constante, de hauteur $2\,q_z^{max}$. $\Gamma(\omega)$ est alors défini comme la valeur moyenne de $\Gamma(\vec{q})$ sur le segment $2\,q_z^{max}$:

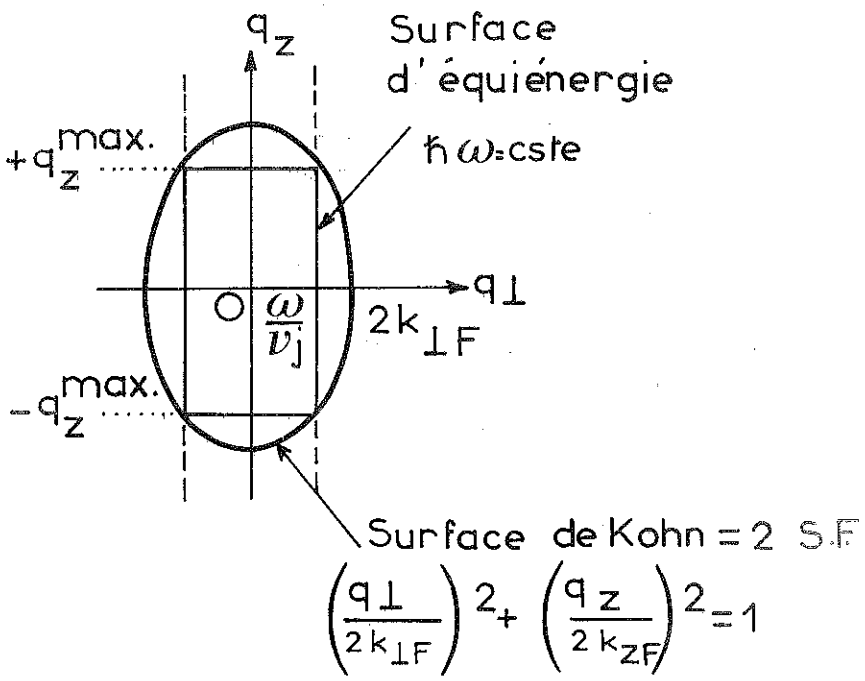
q_z
Surface
d'équiénergie
$\hbar\omega$=cste
$+q_z^{max.}$
$-q_z^{max.}$
$q\perp$
O
$\frac{\omega}{v_j}$
$2k_{\perp F}$
Surface de Kohn = 2 S.F
$\left(\frac{q\perp}{2k_{\perp F}}\right)^2 + \left(\frac{q_z}{2k_{zF}}\right)^2 = 1$

Fig. 11

$$\Gamma(\omega) = \frac{1}{2\pi/(c_o/2)} \int_{-q_z^{max}}^{+q_z^{max}} \Gamma(q_\perp, q_z) dq_z \quad . \qquad \text{(II-6)}$$

Si ω_K est la fréquence maximale des phonons effectifs, la figure (11) montre clairement que pour $\omega \lesssim \omega_K$ un nombre très important de phonons se situe près de la condition de Kohn. Par contre, pour $\omega < \omega_K$, ce nombre diminue très rapidement. Les conditions nécessaires pour obtenir un pic aigu de $\Gamma(\omega)$ au voisinage de la condition de Kohn $\omega = \omega_K$ sont donc satisfaites. Nous avons illustré sur la figure (12) les résultats obtenus pour $\Gamma(\omega)$ dans les deux modèles (cylindrique et ellipsoïdale) de la surface de Fermi du graphite, à T = 0 K et dans la limite élastique des collisions électron-phonon. Bien que les formes analytiques de $\Gamma(\omega)$ soient très différentes, il apparaît une propriété caractéristique commune aux deux cas étudiés : $\Gamma(\omega)$ présente un maximum aigu au voisinage de $\omega = \omega_K$ (pour le cas cylindrique, $\Gamma(\omega) \equiv \Gamma(q_\perp)$ diverge près de cette valeur). Les "phonons de Kohn" $\omega \lesssim \omega_K$ sont donc très violemment couplés aux électrons dans le graphite. C'est cette propriété des "phonons de Kohn" que nous avons utilisée dans les chapitres suivants pour analyser le phénomène de "phonon-drag" dans les effets thermoélectriques et thermomagnétiques du graphite : le pic de $\Gamma(\omega)$ près de la condition de Kohn se reflète dans ces effets par le fait que nous pouvons argumenter que les seuls phonons entraînés par les électrons sont les "phonons de Kohn".

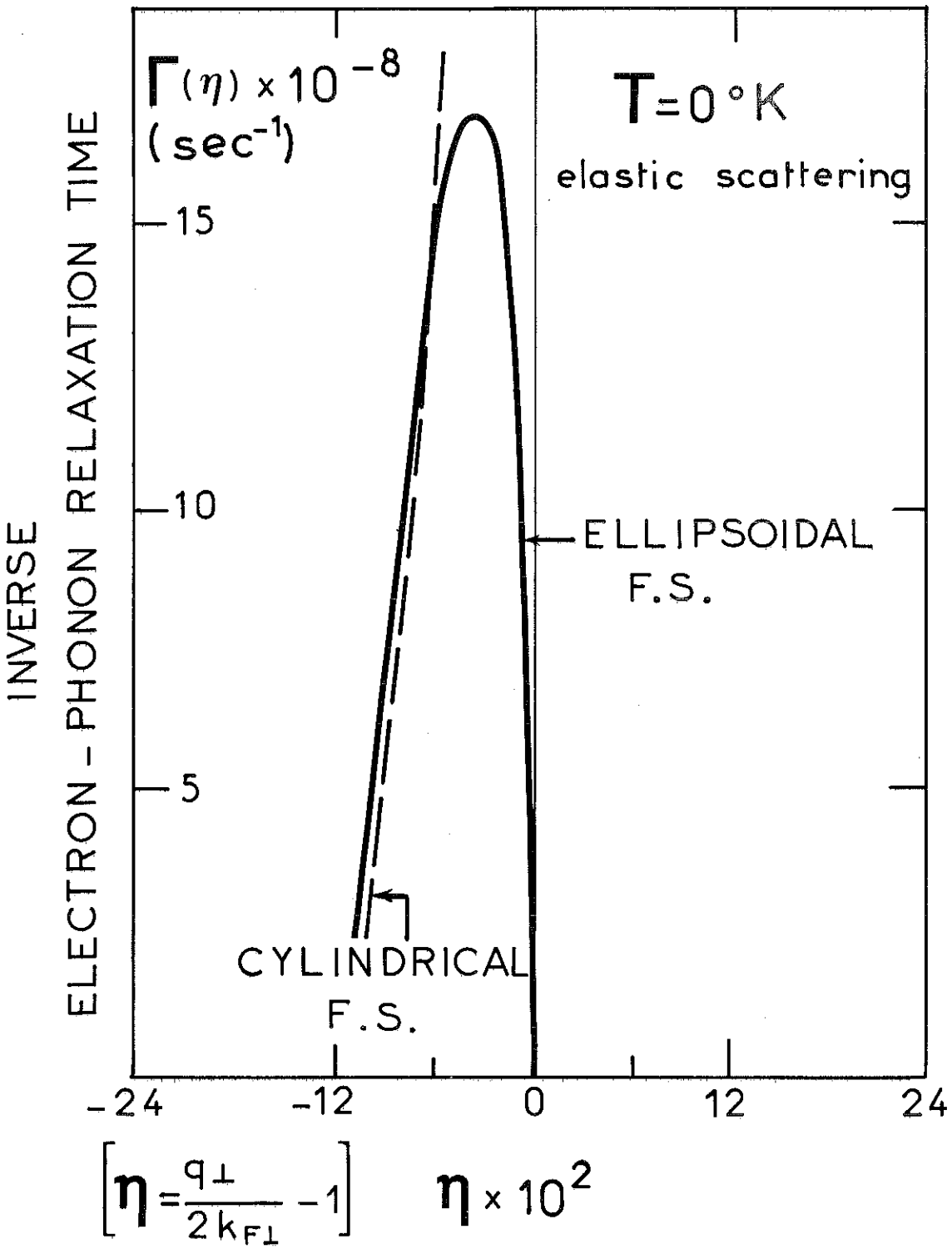
INVERSE
ELECTRON - PHONON RELAXATION TIME
Γ(η) x 10^-8
(sec^-1)
T=0°K
elastic scattering
15
10
5
ELLIPSOIDAL
F.S.
CYLINDRICAL
F.S.
-24
-12
0
12
24
[η = q⊥ / 2k_F⊥ - 1]
η x 10^2

Fig.12

CHAPITRE III

ANALYSE DU POUVOIR THERMOELECTRIQUE DU GRAPHITE A BASSES TEMPERATURES EN L'ABSENCE DE CHAMP MAGNETIQUE

Dans ce chapitre, nous présentons une analyse théorique du pouvoir thermoélectrique, S = S(T), du graphite à basses températures, en l'absence de champ magnétique. Cependant, avant d'aborder le détail de l'exposé, nous trouvons intéressant de rappeler brièvement l'origine de l'effet thermoélectrique. Pour une revue complète, nous renvoyons aux excellents ouvrages de Mac Donald (1962) et de Barnard (1972). Un gradient de température $\vec{\nabla}T$ appliqué à un conducteur en l'absence de tout champ électrique, donne naissance, en général, non seulement à un courant de chaleur, mais également à un courant électrique effectif, appelé "courant thermoélectrique" ("approche Seebeck"). Si ΔV est la "force thermoélectrique absolue" du conducteur, le pouvoir thermoélectrique absolu (on l'appelle aussi coefficient Seebeck), S, est défini par (Fig. 13)

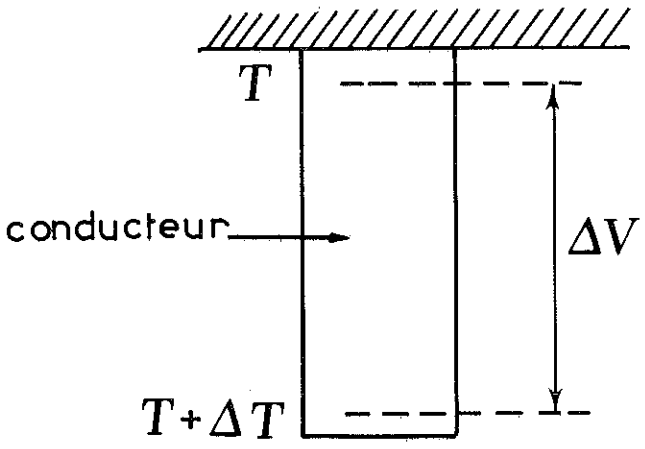

Fig. 13

$$S = \frac{\Delta V}{\Delta T} , \qquad \text{(III-1)}$$

où S est généralement exprimé en microvolt par degré. Analytiquement, il est préférable, dans beaucoup de cas, de traiter les effets thermoélectriques en accédant à la définition (III-1) du pouvoir thermoélectrique de la manière suivante : le conducteur, placé dans des conditions isothermes $\vec{\nabla}T \equiv 0$, est soumis à un champ électrique $\vec{E}$ ("approche Peltier") (Herring 1954 et Herring, Geballe et Kunzler 1958). Si $\vec{U}$ désigne la densité de courant de chaleur et $\vec{J}$ la densité de courant électrique, les équations de transport s'écrivent alors simplement ($\vec{\nabla}T \equiv 0$) (Ziman 1965)

$$\vec{J} = \sigma\vec{E}, \qquad \text{(III-2)}$$

$$\vec{U} = \pi\vec{J}, \qquad \text{(III-3)}$$

où σ est la conductivité électrique et π le coefficient Peltier. S et π ne sont pas indépendants, mais connectés par la relation de Kelvin-Onsager de la Thermodynamique

des processus irréversibles (Onsager 1931),

$$S = \frac{1}{T}\pi \ , \qquad \text{(III-4)}$$

ce qui nous enseigne que les approches "Seebeck" et "Peltier" à la définition du pouvoir thermoélectrique sont équivalentes.
Dans certaines conditions, S peut s'exprimer comme une somme de deux contributions principales

$$S = S_e + S_{ph} \ . \qquad \text{(III-5)}$$

S_e est la composante de diffusion électronique, qui provient de l'effet direct du gradient de température $\vec{\nabla}T$ sur les électrons. S_{ph} est la composante dite de "phonon-drag", qui résulte de l'interaction entre le système d'électrons et la distribution de phonons non en équilibre sous l'influence de $\vec{\nabla}T$. C'est l'entraînement des électrons par le courant de phonons, créé dans le réseau par le gradient de température, qui constitue ce que l'on appelle l'effet de "phonon-drag", ou encore "effet Gurevich" (Gurevich 1945, 1946). Cet effet peut modifier radicalement la variation en température et l'amplitude du pouvoir thermoélectrique. Cependant, il n'est observable expérimentalement que si les phonons sont beaucoup plus fortement diffusés par les électrons que par tous les autres processus de relaxation auxquels ils peuvent participer (impuretés, défauts, limites de l'échantillon, interaction phonon-phonon). Une telle situation ne peut évidemment être réalisée que dans certaines conditions, à savoir : (1) le conducteur doit être placé à basses températures, (2) être de bonne qualité, (3) satisfaire un état de grande pureté, (4) avoir des dimensions raisonnables, et enfin (5) posséder un couplage électron-phonon suffisamment intense.

Les mesures du pouvoir thermoélectrique, S(T), du graphite, effectuées perpendiculairement à l'axe c, c'est-à-dire suivant la direction des plans graphitiques, ont été réalisées jusqu'à ce jour par un certain nombre d'auteurs, tant sur des monocristaux naturels purifiés que sur des échantillons pyrolytiques très bien orientés (Rasor 1955, De Combarieu 1968, Takezawa, Tsuzuku, Ono et Hishiyama 1969, Tamarin, Shalyt et Volga 1969 et Tsuzuku, Takezawa, Hishiyama et Ono 1972). Les diverses courbes obtenues sont montrées Fig.(14). Elles présentent toutes une ressemblance remarquable dans leur forme : S(T) est fortement négatif à basses températures, avec un minimum très accentué apparaissant vers environ 40 K. La valeur de ce minimum varie d'un échantillon à un autre, suivant les auteurs, entre -10 µV/K et - 30 µV/K. C'est ce comportement anormal du pouvoir thermoélectrique du graphite que nous nous proposons d'analyser dans ce chapitre. Nous montrons que l'introduction de l'effet de "phonon-drag" permet d'interpréter de manière tout à fait satisfaisante la variation

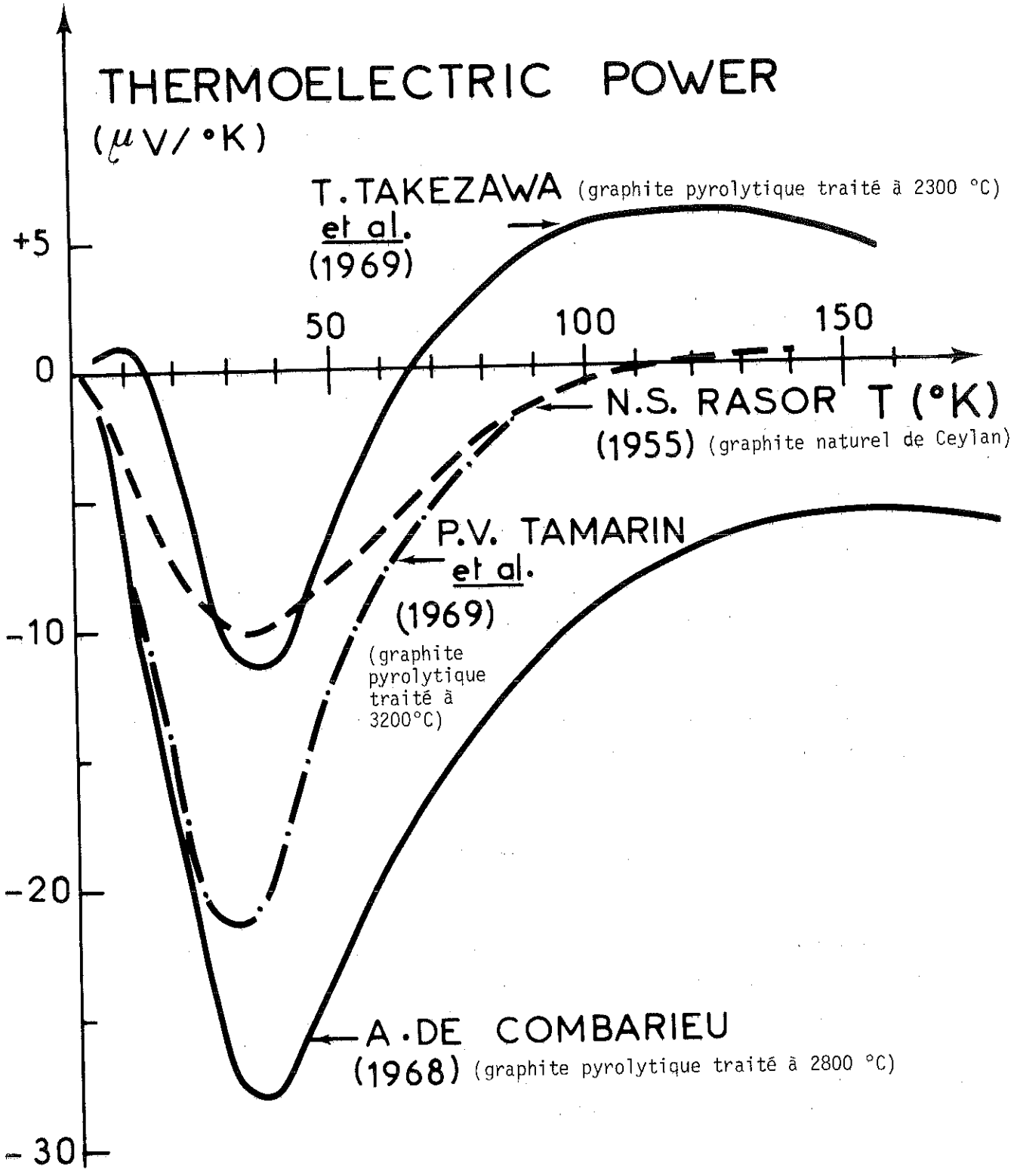
THERMOELECTRIC POWER
(μV/°K)
T. TAKEZAWA (graphite pyrolytique traité à 2300 °C)
et al.
(1969)
+5
0
50
100
150
T (°K)
N.S. RASOR
(1955) (graphite naturel de Ceylan)
P.V. TAMARIN
et al.
(1969)
(graphite pyrolytique traité à 3200°C)
-10
-20
-30
A. DE COMBARIEU
(1968) (graphite pyrolytique traité à 2800 °C)

Fig.14

de S en fonction de la température. Cette interprétation a été confirmée récemment par le fait que le minimum de S(T) vers 40 K se trouve très fortement augmenté en présence d'un champ magnétique (Takezawa, Tsuzuku, Ono et Hishiyama 1971 et Takezawa, Mangez, Hewes, Dresselhaus et Tsuzuku 1973). Nous discuterons ce dernier point plus en détail au chapitre V.

L'étude proposée ici repose essentiellement sur l'analyse du couplage électron-phonon dans le graphite au voisinage de la condition de Kohn. Comme nous l'avons souligné au chapitre II, les phonons dont le vecteur d'onde $\vec{q}$ satisfait la condition $\vec{q} = 2\,\vec{k}_F$, où $\vec{k}_F$ est le vecteur d'onde d'un électron à la surface de Fermi, sont très violemment couplés aux électrons dans des cristaux tels que le graphite où l'anisotropie de la surface de Fermi et du spectre de vibration de réseau est extrêmement grande. Le coefficient d'atténuation acoustique, calculé pour deux modèles possibles de la surface de Fermi du graphite (cylindre et ellipsoïde allongé), présente un maximum aigu pour les phonons dans le régime de Kohn. Le flou thermique des contours de la surface de Fermi qui s'établit, avec l'augmentation de la température, sur un intervalle d'énergie de l'ordre de $k_B T$, conduit à un affaiblissement de l'amplitude de ce pic suivant une loi en T^{-1}. La validité de ces résultats n'est pas affectée de manière appréciable lorsque la déformation trigonale de la surface de Fermi du graphite est prise en considération. En supposant que les seuls phonons effectivement entraînés sont ceux situés dans le régime de Kohn, nous trouvons une contribution maximum à la composante de "phonon-drag" du pouvoir thermoélectrique à une température

$$T_K = \frac{\hbar\omega_K}{k_B} \simeq 43{,}5 \text{ K} , \qquad \text{(III-6)}$$

où $\hbar\omega_K$ est l'énergie des phonons de Kohn. En dépit de nombreuses simplifications adoptées dans les calculs, un accord satisfaisant est obtenu avec les résultats expérimentaux, moyennant l'utilisation d'un seul paramètre ajustable. Le modèle donne, enfin, une description correcte du signe négatif de l'anomalie thermoélectrique, et se trouve ainsi en faveur de la nouvelle affectation des électrons au voisinage du point K le long des arêtes de la zone de Brillouin (Schroeder, Dresselhaus et Javan 1968).

En conclusion, nous devons insister sur les deux résultats fondamentaux que nous révèlent la présente étude, à savoir que :

(1) le pic à $T = T_K$ dans le terme de "phonon-drag" du pouvoir thermoélectrique provient de la structure bidimensionnelle du graphite ;

(2) la décroissance de ce terme pour $T > T_K$ ne provient pas des interactions anharmoniques, comme il est généralement invoqué dans un tel contexte, mais de l'élargissement thermique des contours de la surface de Fermi qui croît avec la température et diminue la force de couplage électron-phonon.

Journal of Low Temperature Physics, Vol. 3, No. 4, 1970

Phonon Drag in Graphite

J. P. Jay-Gerin and R. Maynard

Centre de Recherches sur les Très Basses Températures
Cedex No. 166, 38 Grenoble-Gare, France

(Received June 29, 1970)

This paper is principally concerned with the electron–phonon interaction near the Kohn condition ($\mathbf{q} = 2\mathbf{k}_F$) in crystals such as graphite, where the anisotropy of both the Fermi surface and the vibration spectrum is extremely large. By neglecting the trigonal warping of the Fermi surface of graphite, the inverse phonon lifetime is evaluated and is found to have a sharp maximum for the phonons in the Kohn regime. With increasing temperature, the thermal smearing of the Fermi surface leads to a lowering of the magnitude of this peak which decreases approximately as T^{-1}. The previous conclusions seem to remain valid when the trigonal warping is taken into account. By arguing that the effectively dragged phonons are just the phonons within the Kohn regime we have found that the phonon-drag component of the thermoelectric power reflects this strong coupling. In spite of numerous approximations in the calculations, a one-parameter fit to the experimental results seems to give satisfactory agreement. The model furthermore predicts the right negative sign of the thermoelectric anomaly, provided the new carrier assignment of Schroeder et al. *is used.*

1. INTRODUCTION

A number of measurements[1–4] of the thermoelectric power (TEP) of very-well-oriented, nearly ideal graphite crystals at low temperatures have been reported. The curves exhibit an anomaly near 40°K which at first suggests a phonon-drag contribution to the TEP.

This paper deals with a theory of the electron–phonon interaction in graphite near the Kohn[5] condition $\mathbf{q} = 2\mathbf{k}_F$ and suggests a probable phonon-drag contribution to TEP. In Section 2 we shall show that phonons near the Kohn condition—which we shall call Kohn phonons—are strongly coupled to the electrons when the extreme anisotropy of both the Fermi surface (FS) and the vibration spectrum of graphite is taken into account explicitly. Of particular interest in this connection is the limiting case of a cylindrical FS. The damping rate, $\Gamma(\mathbf{q})$ of the phonon $\mathbf{q}$ (proportional to the imaginary part of the polarization operator) diverges like $(4k_{F\perp}^2 - q_\perp^2)^{-1/2}$ where $q_\perp$ is the component of the phonon wave vector $\mathbf{q}$ on the graphitic planes and $2k_{F\perp}$ is the diameter of the transverse cross section of the

cylindrical FS. This result is not exact because it is obtained in the elastic approximation where the phonon energy transfer between the two electrons is neglected. Despite this simplification, the result clearly shows the physical origin of the strong coupling of the Kohn phonons. $\Gamma(\mathbf{q})$ is proportional to the initial and final density of interacting electronic states which satisfy the conservation laws of energy and momentum. These densities may be represented on the FS by finding the intersection of the FS and another identical surface, shifted by $-\mathbf{q}$ (in the elastic approximation). At the Kohn condition, this line collapses to a point for a corrugated FS, whereas it persists in the cylindrical case. It is this multiplicity of states which leads to the singularity of $\Gamma(\mathbf{q})$ at $q_\perp = 2k_{F\perp}$. When the inelasticity of the scattering is taken into account, $\Gamma(\mathbf{q})$ no longer diverges, but a large peak nevertheless subsists near the Kohn condition.

It is tempting to use this model for graphite although its applicability will depend to a large extent on how well the graphite FS can be approximated by a cylinder. Any deviation from this simple geometry (such as an elongated ellipsoid) radically changes the analytical behavior of $\Gamma(\mathbf{q})$ near $\mathbf{q} = 2\mathbf{k}_F$. (For instance, Afanas'ev and Kagan[6] have shown that $\partial\omega(\mathbf{q})/\partial q_\perp$ has a root singularity at $q_\perp = 2k_{F\perp}$ in the cylindrical case. This singularity becomes logarithmic when some corrugation of the cylindrical FS is introduced.) We start in Section 2 by neglecting the trigonal warping of the FS of graphite and by considering the elongated ellipsoids which are tangent to the belly of the cigar-shaped FS. For this case $\Gamma(\mathbf{q})$ is of the usual form, with a simple discontinuity at $\mathbf{q} = 2\mathbf{k}_F$ as in the isotropic case. At this stage, the Kohn phonons do not play a privileged role. However, what we need for the transport properties is $\Gamma(\omega)$ instead of $\Gamma(\mathbf{q})$ which is some average value of $\Gamma(\mathbf{q})$ over a constant energy phonon surface $\hbar\omega(\mathbf{q}) = \hbar\omega$. For graphite, we find at this point a peculiar behavior in that the phonon surfaces (polarized in the graphitic planes) are practically cylindrical in the temperature range of the TEP anomaly ($\simeq 40°K$). Anisotropy of the vibration spectrum combined with the anisotropic electron gas thus leads to a sharp peak in $\Gamma(\omega)$.

In Section 3, we consider the thermal variations of $\Gamma(\omega)$. While in an ordinary metal $\Gamma(\omega)$ does not depend on T, temperature dependence is possible in a semimetal like graphite, where the Fermi energy is of the order of 250°K. The thermal smearing of the FS involves an averaging procedure within a range of energy k_BT around E_F, and so the peak of $\Gamma(\omega)$ is spread out. We find by means of a simplified calculation that the maximum of Γ decreases as T^{-1}.

In Section 4, we discuss briefly the effect of the trigonal warping and conclude from a geometrical argument that it does not drastically change the previous conclusion.

Starting from the usual expression for the phonon-drag TEP, it is shown in Section 5 that the peak in $\Gamma(\omega)$ near the Kohn condition can be reflected by the phonon drag if we suppose that the single phonons dragged by electrons are Kohn phonons. A very simplified theoretical expression of the TEP has been deduced and provides a good fit to the experimental results. The negative sign of the TEP anomaly is correctly predicted and favors the new carrier assignment of Schroeder *et al.*[7]

2. LIFETIME OF PHONONS NEAR THE KOHN CONDITION

Since 1957, the band structure of graphite has been described by the model of Slonczewski and Weiss,[8] which needs six overlap parameters fitted to the galvanomagnetic measurements. From this, one obtains a very anisotropic FS, where the electrons and holes are situated on the fluted cigars of the FS along the vertical edges of the hexagonal Brillouin zone. Recent studies of Schroeder *et al.*,[7] using magnetoreflection measurements, indicate that the electrons are located at point K of the Brillouin zone instead of holes as previously assumed. The current evidence for this new assignment, supported by the analysis of Spain[9] and Kechin[10] of the galvanomagnetic data, is now very strong and we will adopt it in the following treatment. The bands in graphite are quite complex, involving nonparabolic energy wave-vector relationships and trigonal warping perpendicular to the c axis. This last effect is controlled by the γ_3 overlap parameter which could be quite large.[11] This, however, complicates the treatment of the phonon–electron interaction considerably and we will neglect it at first (this approximation will be discussed in Section 4). Besides, for the evaluation of the phonon lifetime near the Kohn condition that we have in view, we do not need the whole energy spectrum of the entire FS, but only the dispersion relation in the neighborhood of the maximal transverse cross section of the FS. By replacing the real FS by the elongated ellipsoids tangent to the belly of the cigars, we can use the simple dispersion relation

$$\varepsilon(\mathbf{k}_\perp, k_z) = \frac{\hbar^2 \mathbf{k}_\perp^2}{2m_\perp} + \frac{\hbar^2 k_z^2}{2m_z} \tag{1}$$

With this, only two parameters are needed to characterize these portions of the FS: the anisotropy ratio $\alpha^2 = m_z/m_\perp$ and the maximum radius perpendicular to the c axis, $k_{F\perp}$ (more exactly, $k_{F\perp}$ has to be defined as a mean maximum radius, when the trigonal warping is taken into account). The values of these parameters can be deduced from various experiments; for example, in the light of the new assignment interchanging electrons and holes in the Soule *et al.*[12] paper, one can use the following values:

for electrons: $\alpha = 17$, $k_{F\perp} = 1.42 \times 10^6\ \mathrm{cm}^{-1}$, $m_\perp = 0.057\ m_0$

for holes: $\alpha = 12.1$, $k_{F\perp} = 1.21 \times 10^6\ \mathrm{cm}^{-1}$, $m_\perp = 0.039\ m_0$.

There are two distinct classes of acoustical phonons: the "in-plane" vibrations with two-dimensional character and the "out-of-plane" modes. For the former, the dispersion relation $\omega(\mathbf{q})$ is nearly cylindrical: $\omega = v_s q_\perp$ when ω is larger than 25°K; the "out of plane" branch is more complicated (the index $\perp$ refers to the component in the plane perpendicular to the c axis. v_s is the sound velocity).

To describe the interband and intraband transitions by the two types of phonons, four matrix elements must be considered. These matrix elements have been evaluated by Sugihara and Sato[13] in the hard-ion approximation and can be written in the usual way:

$$g^{\mathbf{q},\mu}_{\mathbf{k},\mathbf{k}'} \simeq \boldsymbol{\varepsilon}_\mu(\mathbf{q}) \cdot \mathbf{q} C(|\mathbf{k}' - \mathbf{k}|)$$

where $\varepsilon_\mu(\mathbf{q})$ is the polarization vector of the μ mode and $C(|\mathbf{k}' - \mathbf{k}|)$ is a function of the scattering angle of electrons ($\mathbf{k}' = \mathbf{k} + \mathbf{q}$). These authors have found $C(|\mathbf{k}' - \mathbf{k}|)$ proportional to cos Λ for the intraband transitions and to sin Λ for the interband, where Λ is the angle between $\mathbf{k}_\perp$ and $\mathbf{k}'_\perp$. This particular form is due to the existence of a trigonal symmetry and to the position of the FS on the edges of the Brillouin zone. Near the Kohn regime, $\Lambda \simeq \pi$ and $|\cos \Lambda| \simeq 1$, whereas $\sin \Lambda \simeq 0$, and consequently the interband transitions can be neglected. Elimination of the "out-of-plane" phonons also seems reasonable: the electron–phonon coupling constant of this branch is quite negligible[13] and from thermal conductivity measurements parallel to the basal planes the mean free path is approximately 100 times shorter than for the "in-plane" phonons.[14] "Out-of-plane" phonons are therefore neglected in the present calculation.

For this restricted class of transitions, the matrix element of the electron–phonon interaction is, following Sugihara and Sato,[13]

$$|g^{\mathbf{q}}_{\mathbf{k},\mathbf{k}'}|^2 = \frac{\hbar}{2\Omega\rho v_s} q_\perp C^2 \cos^2 \Lambda \tag{2}$$

The acoustic absorption coefficient is calculated according to the usual relation:

$$\Gamma(\mathbf{q}) = \frac{2\pi}{\hbar} \sum_{\mathbf{k},\mathbf{k}'} |g^{\mathbf{q}}_{\mathbf{k},\mathbf{k}'}|^2 \Delta(\mathbf{k}' - \mathbf{k} - \mathbf{q}) \delta(\varepsilon_{\mathbf{k}'} - \varepsilon_{\mathbf{k}} - \hbar\omega_{\mathbf{q}})(f^0_{\mathbf{k}} - f^0_{\mathbf{k}'}) \tag{3}$$

where $f^0_{\mathbf{k}}$ is the Fermi distribution function and the other symbols have their conventional meaning. Now, let us consider the simplest limit where the inelasticity of the collision is neglected and let $T = 0°\text{K}$. Then, we can approximate $\delta(\varepsilon_{\mathbf{k}'} - \varepsilon_{\mathbf{k}} - \hbar\omega_{\mathbf{q}})$ by $\delta(\varepsilon_{\mathbf{k}+\mathbf{q}} - \varepsilon_{\mathbf{k}})$ and $f^0_{\mathbf{k}} - f^0_{\mathbf{k}'}$ by $\hbar\omega_{\mathbf{q}}\delta(\varepsilon_{\mathbf{k}} - \varepsilon_F)$. By means of a straightforward integration over the whole ellipsoidal FS, one gets

$$\Gamma(q) = \begin{cases} \dfrac{2\pi}{\hbar}\hbar\omega_{\mathbf{q}}|g^{\mathbf{q}}_{\mathbf{k},\mathbf{k}'}|^2 \dfrac{\Omega}{4\pi^2} \dfrac{m_\perp^2}{\hbar^4 q'}\alpha & \text{for } q' \leq 2k_{F\perp} \\ 0 & \text{for } q' \geq 2k_{F\perp} \end{cases} \tag{4}$$

with

$$q'^2 = q_\perp^2 + \frac{1}{\alpha^2} q_z^2$$

Note that $\cos^2 \Lambda$ has been treated rather crudely since it depends on $k_\perp$ and it was left out of the integration which leads to relation (4). The main effect of $\cos^2 \Lambda$ is to reduce $\Gamma(\mathbf{q})$ for the phonons far away from the Kohn condition. This may be seen in an approximative way, from the expression

$$\cos^2 \Lambda = \left[1 - 2\left(\frac{q_\perp}{2k_{F\perp}}\right)^2\right]^2 \tag{5}$$

More important is the discontinuity of $\Gamma(\mathbf{q})$ at $q' = 2k_{F\perp}$, which defines a surface in the phonon space:

$$\left(\frac{q_\perp}{2k_{F\perp}}\right)^2 + \left(\frac{q_z}{2k_{Fz}}\right)^2 = 1 \tag{6}$$

On this surface, all the phonons are just within the Kohn regime and caliper the FS (we will call it after Roth *et al.*[15] the Kohn surface). In our case the Kohn surface is an ellipsoid whose semiaxes are just twice as large as the semiaxes of the simplified FS.

The most interesting function for the transport properties that we have in mind is not $\Gamma(\mathbf{q})$ but rather $\Gamma(\omega)$, the mean value of $\Gamma(\mathbf{q})$ on a constant energy phonon surface $\omega = \text{const}$. We define the average value $\Gamma(\omega)$ as

$$\Gamma(\omega) = \Gamma_{xx}(\omega) = \frac{\displaystyle\int_{\omega=\text{const}} \frac{dS}{|\mathbf{v}_\mathbf{q}|} \mathbf{v}_\mathbf{q}^x \mathbf{v}_\mathbf{q}^x \Gamma(\mathbf{q})}{\displaystyle\int_{\omega=\text{const}} \frac{dS}{|\mathbf{v}_\mathbf{q}|} \mathbf{v}_\mathbf{q}^x \mathbf{v}_\mathbf{q}^x} \tag{7}$$

where the weighting factor $dS(\mathbf{v}_\mathbf{q}^x)^2/|\mathbf{v}_\mathbf{q}|$ represents the effective number of phonons in the x direction, parallel to the electric current ($\mathbf{v}_\mathbf{q}$ is the group velocity of the phonon $\mathbf{q}$). Expression (7) for $\Gamma(\omega)$ is related to the variational solution of the Boltzmann equation for transport problems due to Ziman.[16]

Now, let us see how $\Gamma(\omega)$ is able to reflect the cutoff in $\Gamma(\mathbf{q})$. To do this we make a direct comparison between the Kohn surface and a cylindrical constant energy surface of "in-plane" phonons (the height of this cylinder is equal to $2\pi/c_0$, where $c_0 = 3.35$ Å is the graphitic interplane distance). Due to the cutoff in $\Gamma(\mathbf{q})$, those phonons of energy ω which are effectively coupled to the electrons, are situated on a small cylindrical portion of the equienergy surface $\omega = \text{const}$ inside the Kohn surface. Let $2q_z^{\max}$ be the height of this portion ($q_z^{\max}$ is obtained by the equation $q' = 2k_{F\perp}$ for a fixed value of $q_\perp$) and let ω_K be the maximum frequency of the effective phonons. With decreasing ω from ω_K, $\Gamma(\omega)$ increases very rapidly just like $q_z^{\max}$ while the other terms included in formula (4)—and particularly $\cos^2 \Lambda$—tend to decrease $\Gamma(\omega)$. *The conditions for obtaining a sharp peak of* $\Gamma(\omega)$ *near the maximum frequency* ω_K *are thus fulfilled.* For cylindrical constant energy phonon surfaces, $\Gamma(\omega)$ is simply equal to the mean value of $\Gamma(\mathbf{q})$ on the $2q_z^{\max}$ segment:

$$\Gamma(\omega) = \frac{1}{2\pi/c_0} \int_{-q_z^{\max}}^{+q_z^{\max}} dq_z \Gamma(q_\perp, q_z) \tag{8}$$

where $q_\perp$ has a fixed value equal to ω/v_s. As the q_z dependence of Γ on this segment is very small, we will neglect it and write

$$\Gamma(\omega) \simeq \Gamma(q_\perp, 0) \frac{2q_z^{\max}}{2\pi/c_0} \tag{9}$$

With (4) and (9) one obtains

$$\Gamma(\omega) = \frac{c_0}{4\pi^2} \frac{C^2}{\hbar^3} \frac{m_\perp^2}{\rho} q_\perp \alpha^2 \left[1 - 2\left(\frac{q_\perp}{2k_{F\perp}}\right)^2\right]^2 (4k_{F\perp}^2 - q_\perp^2)^{1/2} \tag{10}$$

Near the Kohn condition, one can expand $\Gamma(\omega)$ as a function of the new variable: $\eta = (\omega/\omega_K) - 1 = (q_\perp/2k_{F\perp}) - 1$. In the lowest order, we find

$$\Gamma(\omega) = \gamma(1 + 9\eta)\,\mathfrak{Re}[(-2\eta)^{1/2}] \tag{11}$$

with

$$\gamma = \frac{c_0}{\pi^2}\frac{C^2}{\hbar^3}\frac{m_\perp^2}{\rho}k_{F\perp}^2\alpha^2 \quad \text{(for one ellipsoid)}.$$

$\mathfrak{Re}(\ldots)$: real part of $(\ldots)$

This function has a maximum value at $\eta_{\max} = -1/27$ and $\Gamma_{\max} = 0.181\gamma$. The values of the different parameters which appear in (11) are obtained from the resistivity analysis of Ono and Sugihara:[17]

$$C = 30.1 \text{ eV}, \rho = 2.26 \text{ g/cm}^3, \text{ and } c_0 = 3.35 \text{ Å} \tag{12}$$

For the electrons one must consider two ellipsoids, while four are required for holes. Since γ is proportional to $\alpha^2 m_\perp^2$ and since the anisotropy is more pronounced for the electrons than for holes (17 instead of 12.1), the amplitude of the peak of Γ is larger for electrons than for holes. One obtains, therefore, $\gamma_e = 94.2 \times 10^8\ s^{-1}$ for electrons instead of $\gamma_h = 34 \times 10^8\ s^{-1}$.

3. INELASTICITY AND THERMAL SMEARING

The $\Gamma(\omega)$ function is cut off at ω_K and is sharply peaked near this value so that one can expect a great sensitivity of the damping rate to any smearing of the FS. By taking first the inelasticity we have to modify the previous calculation in two ways. (1) The phonon energy transfer in the δ function should be restored, thus ensuring the energy conservation rule: $\delta(\varepsilon_{\mathbf{k}+\mathbf{q}} - \varepsilon_{\mathbf{k}} - \hbar\omega_{\mathbf{q}})$ instead of $\delta(\varepsilon_{\mathbf{k}+\mathbf{q}} - \varepsilon_{\mathbf{k}})$. Since v_s/v_F is small ($\simeq \frac{1}{18}$ for the graphite) this modification is of no consequence and will be neglected. (2) The Fermi factor $f^0(\varepsilon_{\mathbf{k}}) - f^0(\varepsilon_{\mathbf{k}} + \hbar\omega_{\mathbf{q}})$ must be treated more correctly. Instead of considering this factor as a δ function, which involves only the FS, we must average $\Gamma(\omega)$ in an interval of energy $\hbar\omega$ near ε_F. (For instance, $f^0(\varepsilon_{\mathbf{k}}) - f^0(\varepsilon_{\mathbf{k}} + \hbar\omega_{\mathbf{q}})$ is just one when $\varepsilon_{\mathbf{k}}$ is between $\varepsilon_F - \hbar\omega_{\mathbf{q}}/2$ and $\varepsilon_F + \hbar\omega_{\mathbf{q}}/2$ and zero elsewhere. Then, the ε dependence of Γ needs to be considered explicitly: $\Gamma(\omega, \varepsilon)$. In fact, it is simply expression (11) with $k_{F\perp}$ replaced by $k_{M\perp} = (2m_\perp\varepsilon/\hbar^2)^{1/2}$ where $k_{M\perp}$ is the radius of the transverse cross section of the ellipsoidal equienergy surface ε. [Then the expression (11) can be rewritten as: $\Gamma(\omega, \varepsilon_F)$.]

If we now consider the thermal smearing, the rapid ε variation of $\Gamma(\omega, \varepsilon)$ near ε_F excludes the use of the classical formula which involves only the second derivative of Γ at ε_F. Actually, the simplest treatment consists of averaging $\Gamma(\varepsilon)$ in a small interval of the order of $k_B T$ near ε_F. So let us define

$$\Gamma(\omega, T) = \frac{1}{k_B T}\int_{\varepsilon_F - k_B T/2}^{\varepsilon_F + k_B T/2} d\varepsilon\Gamma(\omega, \varepsilon) \tag{13}$$

By comparing both these effects, one can distinguish two ranges of temperature for $\Gamma(\omega, T)$. (1) Low temperatures $T < T_K = 43.5°\text{K}$, where the thermal effect is negligible compared with the inelasticity. $\Gamma(\omega, T)$ is then temperature invariant

and can be approximated by $\Gamma^{\text{inel}}(\omega) = \Gamma(\omega, T_K)$. (2) Higher temperatures $T > T_K$, where the thermal smearing of the FS prevails over the inelastic smearing. Here, $\Gamma(\omega, T)$ must be calculated from (13). Let us expand (11) near ε_F and ω_K as a function of $\eta = \omega/\omega_K - 1$ and $x = \varepsilon/\varepsilon_F - 1$:

$$\Gamma(\omega, \varepsilon) = \Gamma(\eta, x) \simeq \gamma\, \mathfrak{Re}\,[(x - 2\eta)^{1/2}(1 - 4x + 9\eta)] \tag{14}$$

[for $x = 0$ or $\varepsilon = \varepsilon_F$ one can find (11) again].

The calculation of the thermal average $\Gamma(\omega, T)$ is straightforward, from (13) we get:

$$\Gamma(\omega, T) = \Gamma(\eta, T) = \gamma \frac{T_F}{T}[y_+(\eta, T) - y_-(\eta, T)]$$

with (15)

$$y_\pm(\eta, T) = \mathfrak{Re}\left[\frac{2}{3}(1 + \eta)\left(\pm\frac{T}{2T_F} - 2\eta\right)^{3/2} - \frac{8}{5}\left(\pm\frac{T}{2T_F} - 2\eta\right)^{5/2}\right]$$

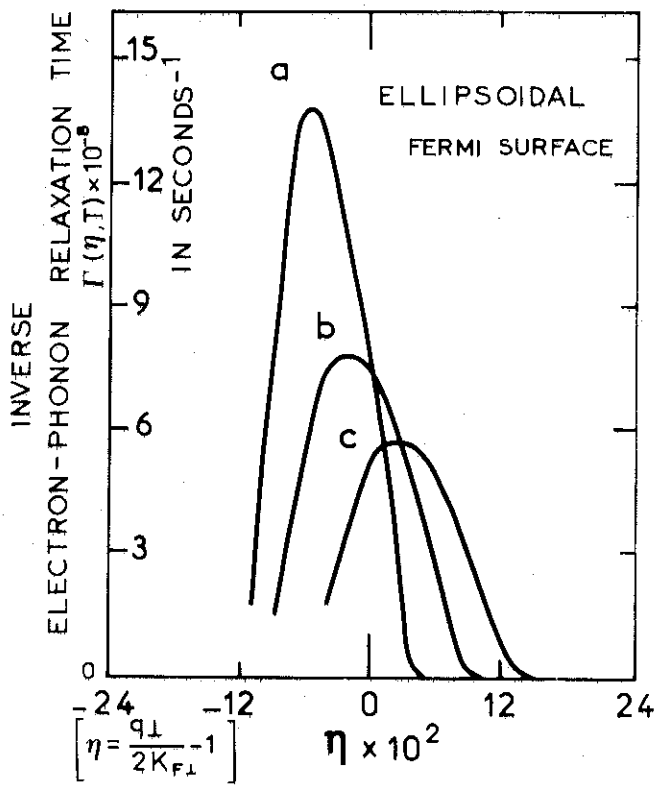

Fig. 1. The ellipsoidal Fermi surface. The inverse phonon lifetime $\Gamma(\omega, T)$ according to formula (15) as a function of $\eta = (\omega/\omega_K) - 1$, the relative departure of the frequency from the Kohn frequency ω_K. Curves a, b, and c correspond respectively to the temperature $T = T_K = 43.5°\text{K}$, $T = 2\,T_K$, and $T = 3\,T_K$. The theoretical curves were stopped at low frequency (large negative value of η) where the η expansion is no longer valid.

This function is represented in Fig. 1 and shows a general lowering of the peak with increasing temperature. One can estimate this decrease by calculating the coordinates of the maximum value Γ_M and η_M. In fact, when $T > 0.218\ T_F$, η_M is between $-T/4T_F$ and $+T/4T_F$ where $y_-(\eta, T)$ is 0. Then, we have $\eta_M = -0.103 + 0.224\ T/T_F$ and $y_+(\eta_M, T) = 2.5 \times 10^{-2}(1 + T/4T_F)^{5/2}$.

Neglecting $T/4T_F$ in the last expression (since $T_F = 230°K$ for graphite) and with the numerical values of (12), one finds for the two electronic ellipsoids

$$\Gamma_{max}(T) = \begin{cases} 12.5 \times 10^8 & T \leq T_K \\ 12.5 \times 10^8 \dfrac{T_K}{T} & T \geq T_K \end{cases} \tag{16}$$

It may now be interesting to compare this result with the one we obtain from a truly cylindrical FS which exactly surrounds the previous ellipsoid. This has been

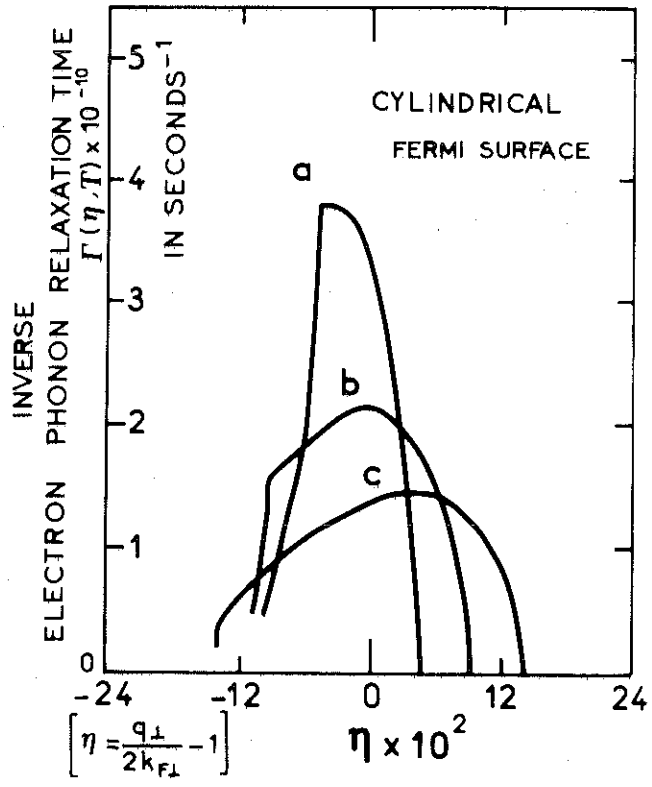

Fig. 2. The cylindrical Fermi surface. The inverse phonon lifetime $\Gamma(\omega, T)$ according to formula (A4) as a function of $\eta = (\omega/\omega_K) - 1$, the relative departure of the frequency from the Kohn frequency ω_K. Curves a, b, and c correspond respectively to the temperature $T = T_K = 43.5°K$, $T = 2\ T_K = 87°K$, and $T = 3\ T_K = 130.5°K$. The theoretical curves were stopped at low frequency (large negative value of η) where the η expansion becomes invalid. Note that the scale of the inverse relaxation time is a hundred times larger than on Fig. 1.

done in the appendix. In this case, the elastic approximation leads to a real square root divergence at $q_\perp = 2k_{F\perp}$.

Furthermore, for reasons of symmetry, $\Gamma(\mathbf{q})$ depends only on $q_\perp$. One can then drop the averaging procedure (7) on the constant energy phonon surface: $\Gamma(\omega) \equiv \Gamma(q_\perp)$. Although the mathematical expression of $\Gamma(\omega, T)$ is different from (15), the general shape is nearly the same with a peak value near $q_\perp = 2k_{F\perp}$ as is shown in Fig. 2. However, it is important to mention that the absolute values of Γ are about 30 times greater than those of Fig. 1 for the same values of the parameters (note that phonons continue to be well defined—even, at the maximum value, the ratio $\Gamma_{max}/\omega_K \simeq 0.01$). A small cylindrical portion of the FS is enough to produce a strong electron–phonon coupling at the Kohn condition. It is thus possible that some semimetals, like bismuth whose FS is very elongated, may be treated in a similar way although phonon gas isotropy will introduce differences.

4. THE EFFECT OF THE TRIGONAL WARPING OF THE FS

All the preceding results have been obtained with the assumption of a circular cross section of the FS. But the observation of a large number of cyclotron resonance harmonics by Williamson *et al.*[11] indicates that the trigonal warping is very large. We have reproduced in Fig. 3 the maximum cross section of the electron FS due to Ono and Sugihara[18] for $\gamma_3 = 0.2$ eV (γ_3 is the overlap parameter which controls the trigonal warping in the Slonczewski–Weiss model). This contour has been obtained by these authors from a fourth-order secular equation which can be solved only numerically. The calculation of the phonon damping rate Γ for such a FS is a difficult task, since it requires laborious numerical computations and we prefer to discuss this effect from a geometrical point of view. To do this, the contour of the cross section of the Kohn anomaly surface for the warped FS has been constructed point by point by connecting the callipering pairs of states such as AB in Fig. 3 on the FS, where the group velocities are antiparallel. (Other sheets of the Kohn anomaly surface corresponding to parallel group velocity pairs of points, such as BC, are not outlined in Fig. 3 because they give shorter Kohn wave vectors.) This contour has a sixfold symmetry (the initial trigonal symmetry multiplied by the inversion symmetry) and consequently is less anisotropically distorted than the original FS. Now, if $\Gamma(\mathbf{q})$ does not differ strongly from the previous relation (4), the evaluation of $\Gamma(\omega)$ needs a supplementary averaging procedure, using those portions of the circular phonon equienergy surface cut out by the rosette of the Kohn surface. This leads to a broadening of the peak of Γ between the maximum radius and the minimum radius of the rosette. In fact, a glance at Fig. 3 shows that the dispersion of the Kohn surface radius q_K does not exceed the value of 20%, which is just of the same magnitude as the width of the peak, when the inelasticity or the thermal smearing is taken into account. Without any rigorous proof we are thus lead to believe that the warping of the FS acts as a geometrical smearing and does not affect dramatically the preceding conclusions obtained with $\gamma_3 = 0$.

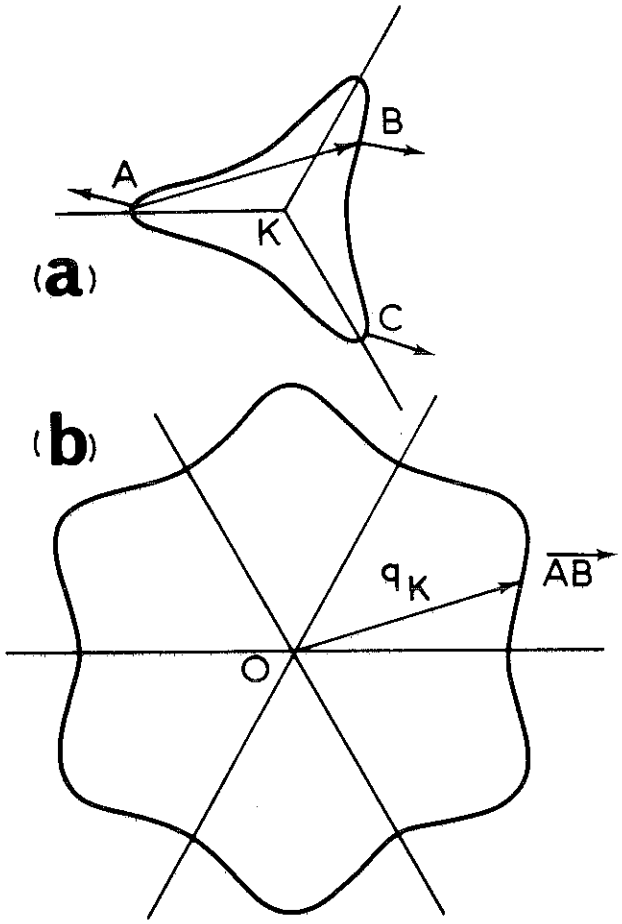

Fig. 3. (a) Maximum cross section of the electron Fermi surface due to Ono and Sugihara[18] for the value $\gamma_3 = 0.2$ eV of the trigonal warping parameter. (b) The cross section of the Kohn anomaly surface corresponding to the FS cross section (a). This contour is generated by the vectors $\mathbf{q}_K$ which join two callipering points such as AB of the FS where the group velocities are antiparallel.

5. PHONON-DRAG TEP CONTRIBUTION

Are the transport properties sensitive to the peak in the phonon lifetime? The sharpness of the peak probably prevents its affecting the thermal conductivity. On the other hand $\Gamma(\omega)$ is directly responsible for the phonon drag by electrons (in the Peltier approach for instance) and plays an essential role in this type of transport property. More precisely, the phonon-drag TEP S_{ph} is defined by the relation

$$S_{ph} = \frac{1}{T}\frac{U_{ph}}{J_{el}} \tag{17}$$

where U_{ph} is the phonon thermal flux which accompanies the electron current J_{el} under isothermal conditions. The elementary solutions of the coupled Boltzmann equations (electrons and phonons) contain the factor

$$\frac{\Gamma(\omega)}{\Gamma(\omega) + 1/\tau_{ph}} \tag{18}$$

where $1/\tau_{ph}$ is the inverse relaxation time for all collisions other than the electron–phonon scattering. This ratio describes the efficiency of the drag, i.e., the relative frequency of electron–phonon collisions to the general set of phonon collisions. [Note that, more exactly, it is the ratio $\Gamma(\mathbf{q})/\Gamma(\mathbf{q}) + 1/\tau_{ph}$ instead of (18) which appears in the *elementary* solutions of the coupled Boltzmann equations. The factor (18) is connected with the variational solutions due to Ziman.[16]] Then, the general expression for S_{ph} can be written as[19]

$$S_{ph}(T) = \frac{k_B}{e}\frac{\overline{\cos^2\theta}}{n_e}\sum_{\mu}\int_0^{\omega_{max}} d\omega F_{\mu}(\omega) C_{ph}\left(\frac{\omega}{T}\right)\frac{\Gamma(\omega, T)}{\Gamma(\omega, T) + 1/\tau_{ph}} \tag{19}$$

where $\overline{\cos^2\theta}$ is the mean value of θ—the angle between the group velocity $\mathbf{v_q}$ and the direction of the electric field—on a phonon equienergy surface ($\overline{\cos^2\theta} = \frac{1}{3}$ for spherical surfaces and $\frac{1}{2}$ for "cylindrical" phonons), n_e is the electron density (per unit volume) ($=2.80 \times 10^{18}$ cm^{-3}), $F_{\mu}(\omega)$ is the spectral density of the branch of polarization μ, and $C_{ph}(\omega/T) = x^2[e^x/(e^x - 1)^2]$ and $x = \hbar\omega/k_B T$, the Einstein specific heat for the mode ω.

Let us recall that Umklapp collisions are taken into account and do not play a particular role here, because the momentum transfer from the electrons to the phonons occurs through the group velocity $\mathbf{v_k}$ and not through $\mathbf{k}$. (The calculation of $\Gamma(\omega)$ using the whole FS in a repeated zone scheme is valid *a posteriori*.) Furthermore, to establish (19) a unique energy dependence of the electron relaxation times has been assumed.[20] This point would need to be handled with some caution for graphite where the anisotropy is considerable. Nevertheless, without any precise information on the problem, we will neglect this complication.

The expression (19) shows that S_{ph} can reflect a peak in $\Gamma(\omega)$ via the efficiency ratio (18), which is stronger for the Kohn phonons than the others, as is shown in Fig. 1. The simplest model then consists in restricting $\Gamma(\omega)$ only to Kohn phonons with an amplitude $\Gamma_{max}(T)$ from (16) and a frequency width $\Delta\omega$:

$$\Gamma(\omega) \simeq \Gamma_{max}(T)\,\Delta\omega\,\delta(\omega - \omega_K) \tag{20}$$

Combining (20) and (19), we get directly

$$S_{ph}(T) \simeq \frac{k_B}{e}\frac{\overline{\cos^2\theta}}{n_e}\sum_{\mu} F_{\mu}(\omega_K) C_{ph}\left(\frac{\hbar\omega_K}{k_B T}\right)\frac{\Gamma_{max}(T)\,\Delta\omega}{\Gamma_{max}(T) + 1/\tau_{ph}} \tag{21}$$

The important feature of the expression (21) is the prediction of a maximum in $|S_{ph}(T)|$ at $T \simeq T_K$. Indeed, at low temperatures $T < T_K$, Γ_{max} is constant and $|S_{ph}(T)|$ varies exponentially like the Einstein function $C_{ph}(\omega_K/T)$. But, when

$T \gtrsim T_K$, the Einstein function is saturated, while $\Gamma_{max}(T)$ begins to decrease. In fact, $\Gamma_{max}(T)$ is smaller than $1/\tau_{ph}$ and the temperature dependence is just that of $\Gamma_{max}(T)$, i.e., T^{-1}. Let us emphasize that this reduction of $|S_{ph}(T)|$ above T_K does not arise from the anharmonicity, which is usually invoked in this context. Actually, the frequency of Kohn phonons is too low for them to be effectively damped by the phonon–phonon interaction. This decrease comes essentially from the thermal smearing of the FS.

To illustrate the experimental situation, we have plotted in Fig. 4, the measurements of de Combarieu[1] which are typical of the TEP anomaly. The reason for this choice is that $1/\tau_{ph}$ is known from the thermal conductivity measurements on the

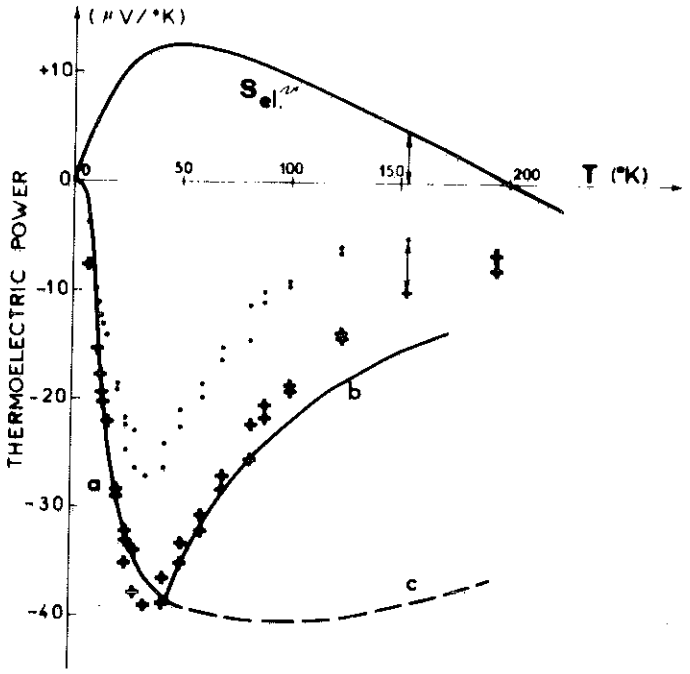

Fig. 4. The comparison of the calculated values of phonon-drag TEP with the measured values. The experimental points marked by a black circle are due to de Combarieu's measurements (Ref. 1). The upper solid line, marked S_{el}, is the electronic component of the TEP from Ref. 21. The cross points are obtained from the measured values by subtracting the diffusion component S_{el}. They represent the estimated phonon drag from experiment. The three lines, marked a, b, and c, are the theoretical curves. The a and b portions are respectively the low- and high-temperature calculated values, using the two-regime formula (21). The dashed curve c is an extrapolation of the low-temperature expression with the usual phonon–phonon interaction, but without any thermal smearing of the FS.

same sample: at T_K the dominant relaxation process is of the Casimir type and $1/\tau_{ph} = 26.5 \times 10^8\ \text{sec}^{-1}$ for the longitudinal "in-plane" phonons.

However, before confronting theory with experiment, we must subtract from the experimental values the electronic TEP contribution (the diffusion TEP). The procedure adopted is standard and was proposed first by Klein[21] and discussed by Spain *et al.*[22] and by Takezawa *et al.*[2] It is based on the so-called simple two-band model of the FS of graphite with an equal number of electrons and holes, and the mobility ratio (electron vs. hole) extracted from the galvanomagnetic measurements. Even if the values obtained for the diffusion TEP shown in Fig. 4 are imprecise, we can argue that the expected curve must be smooth and without dramatic consequences on the extrapolated S_{ph}. Since the sign of the TEP anomaly is negative in Fig. 4, we consider at first only the electron pocket contribution and neglect the holes.

With the values (12) and $v_l = 2.01 \times 10^6\ \text{cm sec}^{-1}$, $v_t = 1.23 \times 10^6\ \text{cm sec}^{-1}$, everything is known in (21) except $\Delta\omega$ or $\Delta\omega/\omega_K = \Delta\eta$ which is the only adjustable parameter. The value of $\Delta\eta$, which induces only a shift of the curve without deformation, has been determined in the ellipsoidal FS approximation: $\Delta\eta = 0.06$. This value seems reasonable and is found within the width of $\Gamma(\omega, T)$ (Fig. 1).

In Fig. 4, the general shape is well described by the two-regime theoretical formula ($T < T_K = 43.5°\text{K}$ and $T > T_K$) obtained from (21) and (16). However, the fit is less satisfactory below the maximum. This comes probably from the transverse "in-plane" phonons which have been rather crudely counted as longitudinal phonons leading in (21) to a spectral density: $F_l(\omega) + F_t(\omega) = \omega(2\pi c_0)^{-1}(v_l^{-2} + v_t^{-2})$. Actually, they could be more independent and have a maximum frequency ω_K^t different from ω_K^l, $\omega_K^t = v_t 2k_{F\perp} = 3.49 \times 10^{12}\ \text{sec}^{-1}$ ($= 26.6°\text{K}$). In this condition, S_{ph} should be analysed as the superposition of both contributions of longitudinal and transverse phonons and could provide an inflexion near 25°K. However, this type of analysis needs so many unknown parameters (at least four: $\Delta\eta_l, \Delta\eta_t, C_l, C_t$) that the interpretation would be less convincing. A more detailed analysis may be needed to explain the recent measurements of the Nernst coefficient, by Tamarin *et al.*,[4] which also show a phonon-drag anomaly.

Based on a low-temperature expansion $T < T_F \simeq 230°\text{K}$, it is not surprising that the theoretical curve departs at higher temperatures ($T > 100°\text{K}$) from the experimental points. Also the phonon–phonon relaxation time, which is known from the thermal conductivity analysis[14] ($1/\tau_{ph\text{-}ph} = 1.26 \times 10^{-11}\omega T^3$) is quite incapable of reducing $|S_{ph}|$ sufficiently above the maximum. To illustrate this point, we have plotted in Fig. 4 a dotted curve which corresponds to the usual theory with the following ingredients: a rigid temperature invariant $\Gamma(\omega)$ plus the Casimir term and the phonon–phonon relaxation time previously indicated.

Let us return briefly to the problem of the negative sign which has led us to neglect the hole contribution in the previous evaluation of S_{ph}. Since in graphite the number of holes is equal to the number of electrons this neglect must be justified. Using the parameters characterizing the hole pocket of the FS, one can estimate the positive contribution of holes to S_{ph} from (21). First, the general shape

of this positive contribution is very different from the electronic contribution and has its maximum at $T_K = 37°K$ instead of $T_K = 43.5°K$ on account of the small difference between the mean maximum radius of the holes' cigars $k_{F\perp} = 1.21 \times 10^6\ cm^{-1}$ instead of $k_{F\perp} = 1.42 \times 10^6\ cm^{-1}$ for the electrons' pockets. The less important anisotropy of the hole pocket of the FS, however, provides a weaker magnitude of the damping rate $\Gamma(\omega)$, as noted in Section 3. In fact, using the same value of the electron–phonon coupling constant C for both the carriers and the same band width for Kohn phonons, one finds a contribution three times smaller for holes than for electrons and, consequently, a negative sign for the phonon-drag TEP. Although the holes' contribution is not completely negligible, it is weaker than the electrons' contribution. So, this analysis of the phonon-drag effect, developed in a semiquantitative way, shows that the observed negative sign of the thermoelectric anomaly is quite in favor of the new assignment of electrons near the K point of the Brillouin zone edge, where the anisotropy ratio is largest.

6. CONCLUSIONS

In this paper, we have tried to show that the Kohn phonons—i.e., phonons with $\mathbf{q} = 2\mathbf{k}_F$—are strongly coupled to the electrons in a semimetal like graphite, where the anisotropy of both the electrons and phonons is extreme. This property has consequences for the phonon-drag TEP contribution S_{ph} that we summarize as follows:

(1) The phonon drag is predominantly due to the Kohn phonons within a small width band $\Delta\omega$, near ω_K, defined as $\omega_K = v_l 2k_{F\perp}$.

(2) The temperature of the maximum value $|S_{ph}|$ is near T_K which is related to the Kohn phonon frequency ω_K ($T_K = \hbar\omega_K/k_B$).

(3) For $T < T_K$, $|S_{ph}|$ decreases exponentially with eventually some inflections arising from other acoustical phonon branches.

(4) For $T > T_K$, the decrease of $|S_{ph}|$ results from the weakening of the electron–phonon interaction on account of the thermal smearing of the FS and not from anharmonicity, as is usually assumed.

(5) The negative sign of the TEP anomaly deduced from this model is in agreement with the new assignment of the electrons at point K in the Brillouin zone of graphite.

Despite the simplifications used in the calculation, the agreement with the experimental results is reasonably satisfactory. It is planned to apply this approach to a study of semimetals like bismuth whose T_K seems to correspond to the temperature of the maximum $|S_{ph}|$.

APPENDIX

We calculate here in the inverse phonon relaxation time $\Gamma(\omega, T)$ from a model of a cylindrical FS whose cross section radius is $k_{F\perp}$ and the height Δk_z. Instead of

(1), the energy dispersion law is now described by

$$\varepsilon(\mathbf{k}_\perp) = \frac{\hbar^2}{2m_\perp}\mathbf{k}_\perp^2 \tag{A1}$$

First the elastic formula must be calculated. With the same electron–phonon interaction matrix (2), the use of the $\cos^2\Lambda$—expression (5)—(which is not an approximation here) and the same notations of Section 3, $\eta = (q_\perp/2k_{F\perp}) - 1$, $x = (\varepsilon/\varepsilon_F) - 1 = (k_\perp/k_{F\perp})^2 - 1$ one obtains from (3) the damping rate $\Gamma(\eta, x)$ for the electronic equienergy surface ε:

$$\Gamma(\eta, x) = \gamma' \,\mathfrak{Re}\,[(x - 2\eta)^{-1/2}(1 - 4x + 9\eta)] \tag{A2}$$

with

$$\gamma' = \frac{C^2 m_\perp^2 \,\Delta k_z}{2\pi^2\hbar^3\rho} = 58.3 \times 10^8 \text{ sec}^{-1} \tag{A3}$$

where the value (12) has been used and $\Delta k_z = 2k_{F\perp}\alpha$, which corresponds to one cylinder of the same dimensions as the previous ellipsoid.

As $\Gamma(\eta, x)$ depends only on $q_\perp = \omega/v_s$, the averaging procedure (7) is superfluous here and we can carry out the thermal smearing method directly to obtain $\Gamma(\omega, T)$. From (13), we find in the same way as (15)

$$\Gamma(\omega, T) = \gamma'\frac{T_F}{T}[y'_+(\eta, T) - y'_-(\eta, T)]$$

with (A4)

$$y'_\pm(\eta, T) = 2\,\mathfrak{Re}\left[(1 + \tilde{\eta})\left(\pm\frac{T}{2T_F} - 2\eta\right)^{1/2} - \frac{4}{3}\left(\pm\frac{T}{2T_F} - 2\eta\right)^{3/2}\right]$$

Comparing formula (A4) with (A2), one notes that the square-root divergence at $q_\perp = 2k_{F\perp}$ has disappeared when one takes the correct inelastic limit at $T = 0°\text{K}$ and sets $T = T_K$ instead of $T = 0°\text{K}$ in (A4). The damping rates given by (A4) have been plotted in Fig. 2 for three temperature values; namely, $T = T_K$ the correct low-temperature limit, $T = 2T_K$ and $T = 3T_K$. The temperature evolution of $\Gamma(\omega, T)$ can be simply characterized by the temperature dependence of the maximum value of these curves: $\Gamma_{\max}(T)$. By a straightforward calculation, one obtains

$$\Gamma_{\max}(T) = \begin{cases} 352 \times 10^8 \text{ sec}^{-1} & T \leq T_K \\ 352 \times 10^8 \times \dfrac{T_K}{T} & T \geq T_K \end{cases} \tag{A5}$$

These values are nearly 30 times greater than for the ellipsoidal FS model. This result shows that $\Gamma(\mathbf{q})$ has to be evaluated carefully when one suspects that even a small portion of the FS can be cylindrical in shape.

ACKNOWLEDGMENTS

The authors would like to express their sincere thanks to A. de Combarieu of the Centre d'Etudes Nucléaires, Grenoble, for communicating his unpublished experimental results. We also wish to thank Professor B. Dreyfus and Dr. J. D. N. Cheeke for fruitful discussions and valuable comments.

REFERENCES

1. A. de Combarieu, Centre d'Etudes Nucléaires, Grenoble, private communication.
2. T. Takezawa, T. Tsuzuku, A. Ono, and Y. Hishiyama, *Phil. Mag.* **19**, 623 (1969).
3. N. S. Rasor, Nuclear Engineering and Manufacturing N.A.A., Downey, California (1955).
4. P. V. Tamarin, S. S. Shalyt, and V. I. Volga, *Fiz. Tverd. Tela* **11**, 1725 (1969) [English transl., *Soviet Phys.-Solid State* **11**, 1399 (1969)].
5. W. Kohn, *Phys. Rev. Letters* **2**, 393 (1959); P. L. Taylor, *Phys. Rev.* **131**, 1995 (1963); E. J. Woll, Jr., and W. Kohn, *Phys. Rev.* **126**, 1693 (1962).
6. A. M. Afanas'ev and Yu. Kagan, *Zh. Eksperim. i Teor. Fiz.* **43**, 1456 (1962) [English transl., *Soviet Phys.—JETP* **16**, 1030 (1963)].
7. P. R. Schroeder, M. S. Dresselhaus, and A. Javan, *Phys. Rev. Letters* **20**, 1292 (1968).
8. J. C. Slonczewski and P. R. Weiss, *Phys. Rev.* **109**, 272 (1958).
9. I. L. Spain, *J. Chem. Phys.* **52**, 2763 (1970).
10. V. V. Kechin, *Fiz. Tverd. Tela* **11**, 1788 (1969) [English transl., *Soviet Phys.—Solid State* **11**, 1448 (1970)].
11. S. J. Williamson, M. Surma, H. C. Praddaude, R. A. Patten, and J. K. Furdyna, *Solid State Commun.* **4**, 37 (1966).
12. D. E. Soule, J. W. McClure, and L. B. Smith, *Phys. Rev.* **134**, A453 (1964).
13. K. Sugihara and H. Sato, *J. Phys. Soc. Japan* **18**, 332 (1963).
14. B. Dreyfus and R. Maynard, *J. Physique* **28**, 955 (1967).
15. L. M. Roth, H. J. Zeiger, and T. A. Kaplan, *Phys. Rev.* **149**, 519 (1966).
16. J. M. Ziman, *Advan. Phys.* **10**, 1 (1961).
17. S. Ono and K. Sugihara, *J. Phys. Soc. Japan* **21**, 861 (1966).
18. S. Ono and K. Sugihara, *J. Phys. Soc. Japan* **24**, 818 (1968).
19. D. K. C. MacDonald, *Thermoelectricity* (John Wiley and Sons, New York, 1962).
20. On the problem of the anisotropy of the electronic relaxation times see, for example, J. S. Dugdale and M. Bailyn, *Phys. Rev.* **157**, 485 (1967).
21. C. A. Klein, *J. Appl. Phys.* **35**, 2947 (1964).
22. I. L. Spain, A. R. Ubbelohde, and D. A. Young, *Phil. Trans.* **A262**, 345 (1967).

CHAPITRE IV

EFFETS D'IRRADIATION AUX ELECTRONS SUR LE POUVOIR THERMOELECTRIQUE DU GRAPHITE A BASSES TEMPERATURES

Dans ce chapitre, nous présentons l'analyse théorique détaillée d'une étude expérimentale réalisée au Service des Basses Températures du Centre d'Etudes Nucléaires de Grenoble (De Combarieu) sur le pouvoir thermoélectrique, à basses températures, d'un échantillon de graphite qui a été soumis à divers traitements d'irradiation et de recuit thermique (Fig. 15) :

(1) Irradiation à 333 K par des électrons de 3 MeV avec une dose intégrée de 5.6×10^{18} électrons par cm^2. La proportion d'atomes déplacés par une telle irradiation peut être estimée sensiblement égale à (Bochirol et Bonjour 1968) :

$$\frac{N_d}{N_o} \simeq 140 \text{ ppm } (1.40 \times 10^{-4}).$$

(2) Recuit thermique pendant 2 heures à 410 K.

(3) Recuit thermique pendant 2 heures à 520 K.

Il est remarquable de noter que, comme la conductibilité thermique $K_\perp$ (De Combarieu 1967, Dreyfus et Maynard 1967), le pouvoir thermoélectrique du graphite à basses températures, mesuré le long des plans graphitiques, est extrêmement sensible à la présence des défauts créés dans le réseau par irradiation. Ainsi, après l'endommagement de l'irradiation, le pouvoir thermoélectrique change de signe et devient positif dans toute la gamme de températures au-dessus de 5 K. D'autre part, l'anomalie de "phonon-drag" vers 40 K (voir chapitre III) disparaît presque totalement (Fig. 15). Parallèlement, on peut noter que la conductibilité thermique $K_\perp$ subit une très forte diminution (facteur 7.5 à 25 K). Les deux traitements de recuit thermique, à 410 K et à 520 K, conduisent à une restauration progressive à la fois de $K_\perp$ et de l'anomalie de "phonon-drag" du pouvoir thermoélectrique (Fig. 15).

L'étude des défauts créés dans le réseau du graphite par irradiation a donné lieu à une quantité considérable de recherches (voir, par exemple, les mises au point de Simmons 1965, Reynolds 1966, Maynard 1967 et Rouby 1974). En ce qui nous concerne, nous rappellerons simplement ici que l'endommagement d'un échantillon de

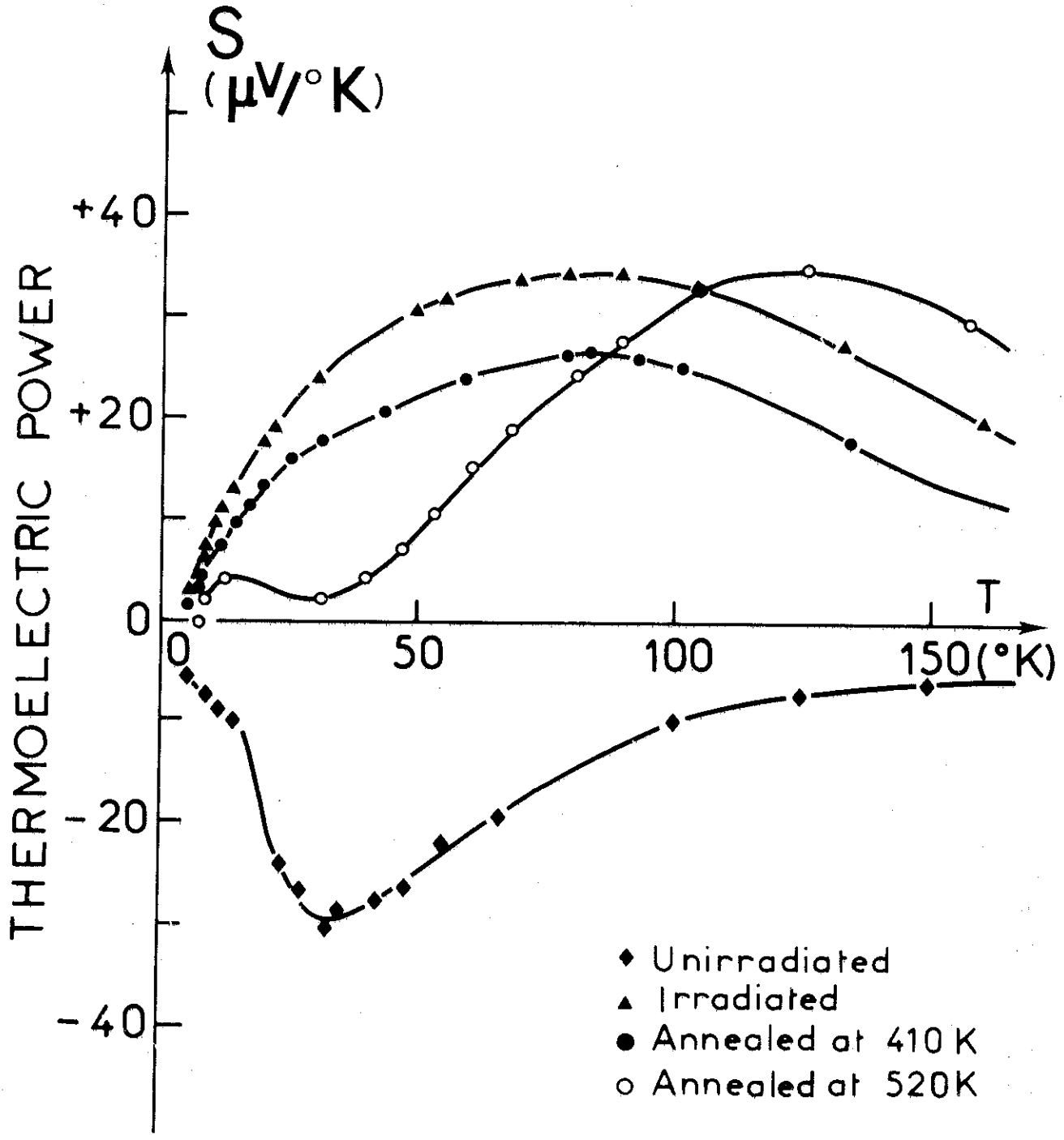
S
(μV/°K)
+40
+20
0
-20
-40
THERMOELECTRIC POWER
0
50
100
150(°K)
T
◆ Unirradiated
▲ Irradiated
● Annealed at 410 K
○ Annealed at 520K

Fig. 15

graphite irradié aux électrons est constitué essentiellement de deux types principaux de défauts :

- les défauts de masse, ou lacunes, situés à l'intérieur des plans graphitiques ;

- les défauts interstitiels, situés entre plans graphitiques voisins.

La présence de ces défauts affecte de manière importante l'une et l'autre des deux composantes du pouvoir thermoélectrique, S_e et S_{ph} (voir chapitre III). Les effets de l'irradiation sur la composante de diffusion électronique S_e sont dus essentiellement à une réduction de la mobilité des électrons et des trous et à un phénomène de piégeage des électrons par les défauts. Moyennant certaines hypothèses simplificatrices concernant les variations du rapport des mobilités et du rapport des concentrations des deux types de porteurs, il est possible d'obtenir la courbe $S_e(T)$ à basses températures par extrapolation de la branche hautes températures (disons, $T > 100$ K) du pouvoir thermoélectrique mesuré. La composante de "phonon-drag" $S_{ph}(T)$ est alors déterminée par simple différence entre la courbe expérimentale et $S_e(T)$.

Il est frappant de constater que les courbes $|S_{ph}(T)|$ ainsi obtenues pour l'échantillon de graphite irradié, puis recuit à 410 K et à 520 K, présentent toutes un maximum très marqué vers 40 K. L'existence d'un tel maximum à $T \simeq T_K$ ($k_B T_K = \hbar\omega_K$, où $\hbar\omega_K$ est l'énergie des phonons de Kohn (voir chapitre III)), confirme très clairement que le minimum trouvé dans les courbes expérimentales du pouvoir thermoélectrique vers 40 K est effectivement associé à une contribution de "phonon-drag", et donne une justification "à postériori" des hypothèses simplificatrices utilisées pour la détermination de $S_e(T)$.

L'analyse détaillée des différentes courbes $S_{ph}(T)$ nous conduit naturellement à examiner la diffusion des phonons de Kohn "dans le plan" (ℓ), (t) par les défauts créés par l'irradiation et en particulier par les interstitiels. En fait, le traitement théorique du problème très général des interactions entre les différentes branches de phonons et les divers types de défauts précités a été donné par Dreyfus et Maynard (1967) et par Maynard (1967) dans le cadre de l'étude de la conductibilité thermique à basses températures du graphite irradié aux neutrons. Ces auteurs ont montré que pour interpréter les résultats expérimentaux, et en particulier pour expliquer la très forte diminution de $K_\perp$ signalée à 25 K, seule la diffusion (ℓ) ou (t) → (c) due aux interstitiels I (voir Fig. 16) doit être prise en considération, les deux autres types d'interstitiels possibles A et W (Fig. 16), étant soit inexistants, soit en nombre insuffisant pour imposer leur loi à $K_\perp$.

Le temps de relaxation associé avec la transition (ℓ), (t) → (c) due aux interstitiels I (supposés en nombre suffisant) est de la forme $\tau_I^{-1} \sim n_I \omega q_z^2$, où n_I est la concentration d'interstitiels sur le site I, ω la fréquence du phonon (ℓ) ou (t)

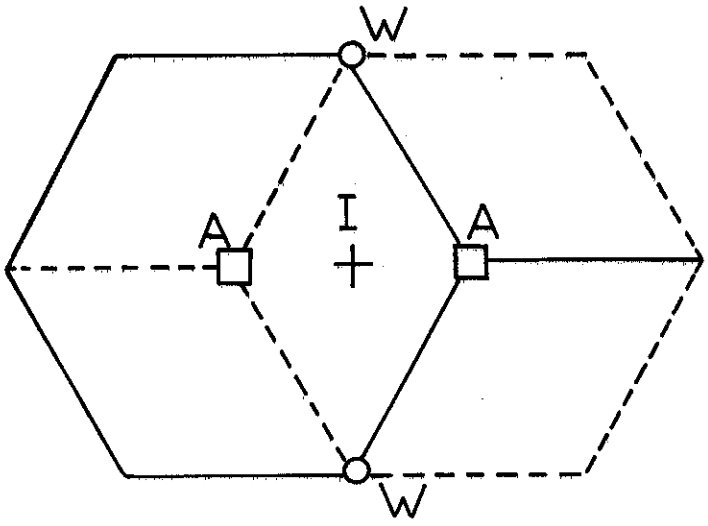

Fig.16

Sites intersticiels A, W et I dans le graphite hexagonal.

A : T. Iwata, F.E. Fujita et H. Suzuki,
J. Phys. Soc. Japan 16, 197 (1961).

W : P.R. Wallace,
Solid State Commun. 4, 521 (1966).

I : B. Dreyfus et R. Maynard,
J. Physique 28, 955 (1967).

incident et q_z la projection du vecteur $\vec{q}$ parallèlement à l'axe c. La présence du terme q_z^2 dans l'expression de τ_I^{-1} est une propriété caractéristique du couplage entre plans graphitiques. Elle montre que tous les phonons d'une même surface d'équiénergie ne sont pas diffusés de la même manière. Ainsi, les états situés au voisinage du plan équatorial ($q_z \tilde{\sim} 0$) des surfaces de dispersion sont peu affectés par les interstitiels, tandis que les autres sont fortement diffusés. Pour évaluer l'effet d'un tel temps de relaxation sur S_{ph} , nous avons supposé que seuls les états de la zone équatoriale de la surface $\omega = \omega_K$, où ω_K est la fréquence des phonons de Kohn (voir chapitre III), contribuent à l'effet de "phonon-drag". Leur nombre s'obtient simplement en combinant ce temps de relaxation avec celui de Casimir ; il est proportionnel à $1/\sqrt{n_I}$, ce qui permet d'écrire S_{ph} après irradiation sous la forme :

$$S_{ph} \tilde{\propto} \left(\frac{1}{\sqrt{n_I}}\right) S^{\circ}_{ph} \quad , \qquad \text{(IV-1)}$$

où S°_{ph} est la composante de "phonon-drag" du pouvoir thermoélectrique avant irradiation (voir chapitre III). Cette loi, qui n'est évidemment valable qu'à partir d'une certaine dose-seuil, montre clairement que S_{ph} se déduit de S°_{ph} par un simple facteur multiplicatif, sans changement de la forme des courbes $S_{ph}(T)$.

Les trois courbes $S_{ph}(T)$, correspondant respectivement au graphite irradié, puis recuit à 410 K et à 520 K, peuvent donc être interprétées par la relation (IV-1) pour trois valeurs différentes de la concentration d'interstitiels n_I. Nous avons comparé les valeurs ainsi obtenues pour n_I avec les valeurs correspondantes déduites des mesures de conductibilité thermique $K_{\perp}$ ($\simeq \frac{1}{\sqrt{n_I}}$) sur le même échantillon, après l'irradiation et les deux recuits thermiques, à T ≃ 25 K, domaine de température où les interstitiels agissent le plus vigoureusement (Maynard 1967). Un accord très satisfaisant est obtenu, ce qui donne une bonne confirmation de notre analyse.

J. Phys. Chem. Solids, 1973, Vol. 34, pp. 189–195. Pergamon Press. Printed in Great Britain

THERMOELECTRIC POWER OF ELECTRON-IRRADIATED GRAPHITE AT LOW TEMPERATURES

A. DE COMBARIEU
Centre d'Etudes Nucléaires de Grenoble, B.P. 85–38041, Grenoble, France

and

J. P. JAY-GERIN*
Eaton Laboratory, McGill University, Montreal, Canada

and

R. MAYNARD
Centre de Recherches sur les Très Basses Températures, Cédex 166, 38-Grenoble-Gare, France

(*Received* 21 *October* 1971; *in revised form* 6 *March* 1972)

Abstract—The thermoelectric power (TEP) of very well oriented, nearly single-crystal graphite irradiated at 333 K by 3 MeV electrons was measured along the basal plane direction above 5 K. Changes in the low-temperature dependence of the TEP after different stages of annealing, at 410 and 520 K, have also been investigated. Analysing carefully the experimental data, the phonon-drag component S_{ph} of the TEP is extracted and compared with the theory of Jay-Gerin and Maynard. As a check of the concentration of the irradiation defects, deduced from this analysis, measurements of the thermal conductivity were made on the same samples. The results are found to be in good agreement.

1. INTRODUCTION

As is now well known, the thermoelectric power (TEP) of very well oriented, nearly single-crystal graphite is found to exhibit a sharp negative dip near 40 K[1–3]. This low-temperature anomaly in TEP is ascribed to phonon-drag. Two of the present authors have recently presented[4] a theoretical analysis of that phenomenon in pure graphite.

In this work, we present an experimental study of TEP of graphite both irradiated with 3 MeV electrons at 333 K, and then annealed at 410 and 520 K. The most striking result is the high sensitivity of the low-temperature TEP to lattice defects introduced by irradiation. The measured TEP values become positive after irradiation damage, and the anomalous dip near 40 K disappears. Annealing treatments lead to a progressive recovery of the anomaly. Following a description of the experiments and results, a theoretical analysis of the different TEP curves is presented and related to the thermal conductivity measurements on the same materials.

2. EXPERIMENTAL DETAILS AND RESULTS

The graphite specimen used in the present experiments was obtained from 'Le Carbone-Lorraine' Society. The sample is a hot-pressed pyrolitic graphite, such as was originally made by Moore *et al.*[5]. It was prepared from pyrolitic graphite deposited at 2100°C and recrystallised for 10–15 min at 2800°C under pressure of 200 kg/cm². Although not a single crystal, the material consists of large size crystallites with c axes aligned along the direction of compression and mean basal plane dimensions estimated about 7·6 μm from thermal conductivity measurements at low temperatures. Moreover, the materials showed a chemical impurity content of 20–30 ppm, and the number of stacking faults remained large. The dimensions of the specimen were approximately $1 \times 5 \times 50$ mm, with the direction of the c axis perpendicular to the largest face.

The experimental arrangement and measur-

*On leave from Centre de Recherches sur les Très Basses Températures de Grenoble, Grenoble, France.

ing apparatus have been reported in a preceding paper[6]. However, Au–Fe/Chromel thermocouples, more sensitive at low temperatures, were used in the present experiments instead of Au–Co/Cu thermocouples. These thermocouples were used both for determining the temperature drop across the specimen and for measuring the thermoelectric voltage between the two gold wires or between the two chromel wires. The absolute TEP of graphite was calculated on using the absolute TEP of chromel[7]. Since the thermal current passing through the specimen was also determined, the measurements of both TEP and thermal conductivity along the basal graphitic planes were obtained.

The experimental TEP results of our graphite samples as a function of temperature are recorded in Fig. 1 for temperatures ranging from 5 to 200 K, and for the material before irradiation and after the following treatments:

(1) Irradiation at 333 K by 3 MeV electrons with an exposure of $5{\cdot}6 \times 10^{18}$ electrons/cm^2. The proportion N_d/N_0 of atoms displaced by such an irradiation has been evaluated by the method of Bochirol and Bonjour[8]; on taking $\sigma_d = 25$ barns as displacement cross-section for 3 MeV electrons, and $\theta \sim 0°$ as the angle between the c axis and the direction of incident electrons, N_d/N_0 is estimated as $1{\cdot}4 \times 10^{-4}$. However, considering the irradiation temperature used here, the displaced atoms do not remain isolated and are probably aggregated forming small interstitial clusters [9, 10].

(2) Two hr annealing at 410 K.

(3) Two hr annealing at 520 K.

These annealing temperatures of 410 and 520 K lie within the Wigner annealing zone, which ranges from 320 to 600 K as described by Bochirol and Bonjour[8]. In this temperature range, the restoration of the irradiation effects is generally interpreted as due to the formation of large interstitial complexes with annihilation of vacancies.

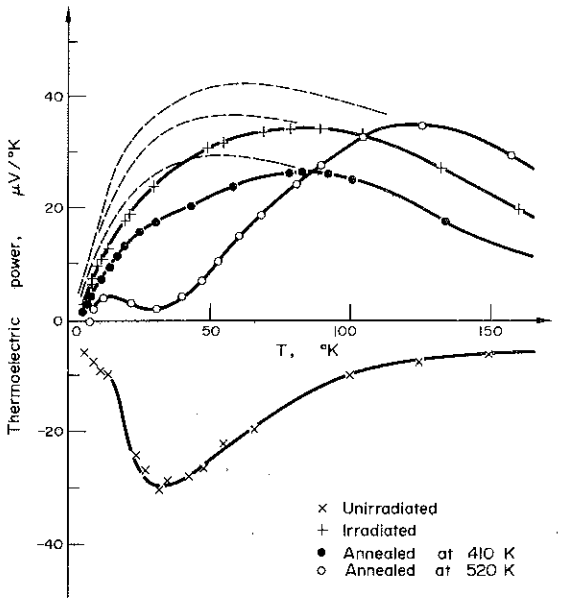

Fig. 1. Temperature dependence of the thermoelectric power of graphite measured along the basal planes before irradiation and after 3 MeV electron irradiation at 333 K. Prior to irradiation, the TEP exhibits a sharp negative dip near 40 K. After irradiation, it becomes positive and the dip has disappeared. Effects of 2 hr annealing at 410 and 520 K on the irradiated sample lead to a progressive recovery of the low-temperature anomaly. The solid lines represent the experimental TEP measurements. The dashed lines indicate the electronic component S_{el} as calculated from equation (1) on using $\mathbf{a} = 1$, $E_0 = 0{\cdot}01$ eV, and the linear extrapolation $\mathbf{b}(T) = \alpha T + \beta$ obtained from the high-temperature TEP values with

$\alpha = 1{\cdot}72 \times 10^{-3}$ K^{-1}, $\beta = 0{\cdot}51$ for the irradiated sample,
$\alpha = 1{\cdot}70 \times 10^{-3}$ K^{-1}, $\beta = 0{\cdot}58$ for the 410 K annealed sample, and
$\alpha = 1{\cdot}67 \times 10^{-3}$ K^{-1}, $\beta = 0{\cdot}47$ for the 520 K annealed sample.

The experimental results of the thermal conductivity of the same graphite samples as a function of temperature are shown in Fig. 2. The effect of the electron bombardment at 333 K gives a decrease in the thermal conductivity by a factor of 10. The 410 K annealing produces a very limited restoration, whereas the 520 K annealing leads to an almost total recovery.

3. ANALYSIS AND DISCUSSION

For temperatures below about 100 K, the TEP of graphite measured along the basal

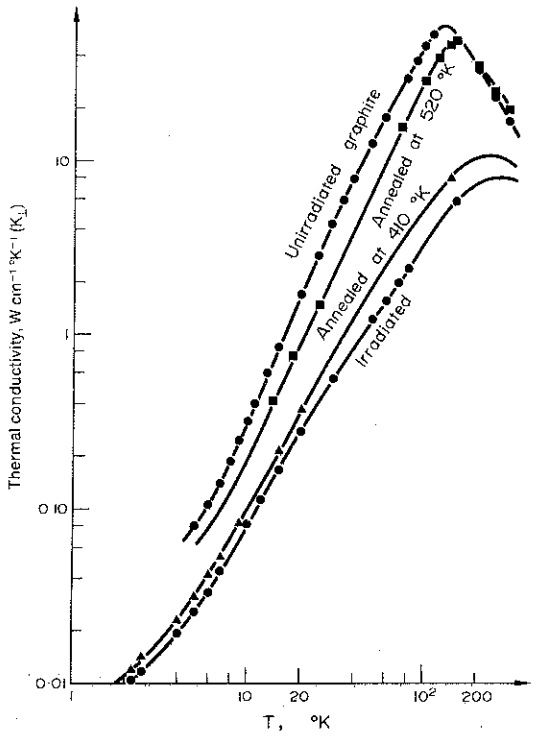

Fig. 2. Temperature dependence of the thermal conductivity $K_\perp$ of graphite along the basal plane direction before irradiation and after 3 MeV electron irradiation at 333 K. Effects of irradiation give a decrease in the thermal conductivity by a factor of 10. The 410 K annealing produces a very limited restoration, whereas the 520 K annealing leads to an almost total recovery. The various symbols are experimental points, and the solid lines are fits of the experimental data.

planes is quite well accounted for by the sum of two contributions: S_{el}, the usual electronic diffusion component and S_{ph}, the phonon-drag component. Using a simple ellipsoidal band model for graphite, two of the present authors have recently carried out a theoretical analysis of the phonon-drag effect in graphite on the basis of the enhanced coupling by anisotropy of the Kohn[11] phonons ($\mathbf{q} = 2\,\mathbf{k}_F$) with electrons[4]. The present work is a continuation of this previous study.

However, the phonon-drag component S_{ph} cannot be obtained directly from experiment. As usual, S_{ph} can be determined by subtracting from the measured TEP values the calculated value of S_{el}. An appropriate evaluation of S_{el} can be obtained on using the so-called simple two band model (STB model), first proposed by Klein[12], and discussed by Spain *et al.*[13] and by Takezawa *et al.*[1]. In this simplified model, the constant energy surfaces for both electrons and holes are approximated by cylinders. Such an approximation is probably very crude compared to the actual band model of graphite. However, because of the relative insensitivity of S_{el} to the various details of the Fermi surface, this simplification is quite justified. Accordingly, the extrapolated $S_{ph}(T)$ component will be sufficiently well defined in the low-temperature range we are concerned with. Then, on the STB basis, S_{el} is expressed as follows

$$S_{el}(T) = \frac{k_B}{e}\left(\frac{\mathbf{a}-\mathbf{b}}{\mathbf{a}+\mathbf{b}}\right)\left\{\frac{2F_1(E_0/2k_BT)}{F_0(E_0/2k_BT)} - \frac{E_0}{2k_BT}\right\} \quad (1)$$

where e is the magnitude of the electronic charge, k_B the Boltzmann constant, F_0 and F_1 tabulated Fermi integrals[14], E_0 the overlap energy of the two bands, $\mathbf{a} = n_h/n_e$ the carrier-density ratio, and $\mathbf{b} = \mu_e/\mu_h$ the carrier-mobility ratio.

In a pure graphite, the number of electrons is equal to the number of holes, and $\mathbf{a} = 1$. On the other hand, the experimental results of Cooper *et al.*[15] on neutron-irradiated material (single crystal coded JPS) show that **a** varies from 1·09 for the sample before irradiation to 1·31 for the sample after irradiation with $5{\cdot}6 \times 10^{16}$ ntv. Such an irradiation dose corresponds to $1{\cdot}4 \times 10^{19}$ displaced atoms per unit volume[16]. This number is very close to the one estimated for our irradiated sample, i.e. $1{\cdot}5 \times 10^{19}$. In the light of these results, we may simply adopt $\mathbf{a} = 1$ for all our samples. The overlap parameter E_0 can be taken as 0·01 eV from low-temperature data[12]. Finally, we shall use a linear extrapolation of $\mathbf{b}(T)$ as a function of temperature*, as originally obtained

*In fact, $\mathbf{b}(T)$ can be measured experimentally. In the absence of such data, this procedure may seem arbitrary. The details of the justification are discussed in the Appendix.

by Soule[17] (crystal EP 14) from low-field Hall effect measurements.

Equation (1) shows that the sign of $S_{el}(T)$ is essentially determined by the difference between **a** and **b** as a function of temperature. As the carrier-mobility ratio is always less than unity over the entire temperature range studied, $S_{el}(T)$ yields a positive contribution to the total TEP.

Now, let us consider the effects of electron irradiation. As seen in Fig. 1, the low-temperature TEP is markedly affected by irradiation, and its value becomes positive and large. For instance, the TEP is about $+30\ \mu$V/K at 50 K.

As is well known, irradiation introduces within the crystal a small number of lattice defects: vacancies in the carbon networks, and interstitial atoms lying between the graphitic planes[9, 10]. The changes produced by these defects in S_{el} are attributed partly to a reduction of the mobility of carriers due to electron scattering by defects, and partly to electron trapping by these defects. In this case, a direct calculation of $S_{el}(T)$ from equation (1) is difficult because of the lack of information about the variation of both the carrier-mobility and the carrier-concentration ratios. Despite of these difficulties, the separation of the measured TEP into its two components, S_{el} and S_{ph}, can be achieved with reasonable accuracy in the following way. Since at high temperatures (about $T > 100$ K) the influence of S_{ph} becomes negligible, the experimental TEP value is approximately equal to S_{el}. The curve obtained by extrapolating the high-temperature branch of the measured TEP to lower temperatures using equation (1) under the conditions $\mathbf{a} = 1$, $E_0 = 0{\cdot}01$ eV, and $\mathbf{b}(T) = \alpha T + \beta$ can then be interpreted as $S_{el}(T)$. The dashed lines, in Fig. 1, show $S_{el}(T)$ as a function of temperature calculated in this way for all materials.

Below about 100 K, these curves depart from the experimental TEP. It is just this difference that we ascribe to $S_{ph}(T)$. The quantities $|S_{ph}(T)|$ obtained in this way are represented in Fig. 3. We note that these different curves in Fig. 3 are very similar in their form to the $|S_{ph}(T)|$ curve obtained for the unirradiated graphite specimen. It is remarkable that all extrapolated $|S_{ph}(T)|$ curves pass through a maximum near 40 K. Such a maximum near $T = T_K (k_B T_K = \hbar\omega_K$, ω_K being the Kohn phonon frequency[4]) is the most striking evidence for a phonon-drag contribution.

The defects produced by electron irradiation strongly scatter phonons both by modifying the binding of atoms in graphitic planes (vacancies) and by forming covalent bonds of interstitial carbon atoms with atoms in the adjacent graphite layers. The problem of pho-

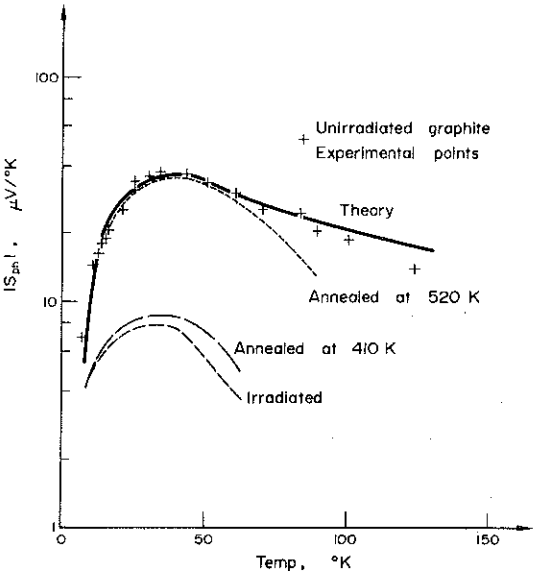

Fig. 3. Phonon-drag TEP of the different materials as a function of temperature. $|S_{ph}(T)|$ is obtained from the measured TEP values by subtracting the calculated electronic component S_{el}. Cross points represent the estimated phonon-drag TEP from experiment for the unirradiated graphite sample, whereas the solid line reproduces the theoretical curve as obtained in Ref. [4]. Dashed curves are the estimated phonon-drag TEP from experiment for the sample which has been subjected to 3 MeV electron irradiation at 333 K, and then annealed at 410 and 520 K. The shape of these last three curves is very similar to that of the theoretical curve. Particularly, the common position of the temperature of the maximum of $|S_{ph}(T)|$ near 40 K confirms the assumption of a phonon-drag contribution to the TEP at low temperatures.

non scattering by these types of defects has previously been discussed theoretically [18, 19] in analysing the low-temperature thermal conductivity. According to this analysis, vacancies are ineffective in the scattering of both longitudinal and transverse 'in-plane' Kohn phonons, which predominantly contribute to the phonon-drag phenomenon along the layer planes [4]. Then, the dominant effect comes from the coupling between graphitic layers. Such a coupling can be carried out by *I*-type interstitials. In fact, the problem is complicated and practically intractable if we take into account that at the irradiation temperature of 333 K many interstitial atoms are annealed or form small clusters of two or more displaced atoms. We shall only consider here the elementary problem of the scattering of the 'in-plane' phonons by isolated *I*-type interstitials. In this assumption, the relaxation time associated with that phonon scattering type, is given by [18, 19]

$$\tau_I^{-1} = n_I E(1-\cos q_z c_0)\omega, \qquad (2)$$

Here, n_I is the isolated *I*-type interstitial concentration, ω the phonon frequency, c_0 the interlayer spacing ($c_0 = 3{\cdot}35$ Å), q_z the hexagonal axis component of the wave vector **q**, and E measures the intensity of coupling between the *I*-type interstitial and its neighbours in adjacent planes.

The occurrence of q_z in equation (2) is quite unusual. Arising from the anisotropy of both phonons and defects, this particular law is characteristic of the interaction between graphitic planes. Equation (2) clearly shows that the phonons situated near the equatorial plane ($q_z = 0$) of the cylindrical phonon constant energy surface ω are not significantly affected by *I*-type interstitials. Therefore, the mean free path of those phonons is only limited by scattering processes on grain boundaries involving a relaxation time of Casimir type τ_C. On the other hand, the other phonon states at $q_z \neq 0$ are strongly damped by the interstitials, and we can neglect their contributions to heat transport provided n_I is sufficiently large. Hence, the critical value q_z^0, which divides phonons into these two regimes, is obtained by making $\tau_I = \tau_C$. Then, we can deduce

$$q_z^0 \simeq \left(\frac{1}{\tau_C E n_I \omega_K c_0^2/2}\right)^{1/2} \qquad (3)$$

which is only valid in the limit $q_z^0 \ll \pi/c_0$.

Accordingly, the only phonons that significantly contribute, with a relaxation time τ_C, to heat transfer in the phonon-drag phenomenon are located on the cylinder of height $2\,q_z^0$ near the equatorial plane of the $\omega = \omega_K$ phonon constant energy surface. Therefore, the number of Kohn phonons dragged by electrons is reduced by the factor $q_z^0/(\pi/c_0)$, and we can write for S_{ph}, the phonon-drag thermopower modified by irradiation

$$S_{ph} \simeq \left(\frac{q_z^0}{\pi/c_0}\right) S_{ph}^0 \quad (q_z^0 \ll \pi/c_0) \qquad (4)$$

where S_{ph}^0 is the phonon-drag thermopower before irradiation [4]. Equation (4) shows that S_{ph} is deduced from S_{ph}^0 by a scaling factor without any change of shape. The unchanged position of the maximum temperature of $|S_{ph}(T)|$ in Fig. 3 must be considered as a confirmation of the present analysis.

The three $|S_{ph}(T)|$ curves (see Fig. 3), which correspond respectively to the different treatments to which our graphite specimen was subjected can be interpreted by equation (4) for three different values of n_I. Using equations (3) and (4) with the estimated phonon-drag thermopower of Fig. 3 at $T = 40$ K, a numerical evaluation of n_I can be carried out. Taking τ_C^{-1} and E to be $26{\cdot}5 \times 10^8\,\mathrm{sec}^{-1}$ and 21, respectively [4, 19], we find $n_I = 1{\cdot}16 \times 10^{-4}$, $0{\cdot}90 \times 10^{-4}$, and $0{\cdot}11 \times 10^{-4}$ for the material after 3 MeV electron irradiation at 333 K, and then annealed at 410 and 520 K, respectively. From these numerical values of n_I, the ratios

$$\frac{n_I^{333\,K\ \text{irradiation}}}{n_I^{410\,K\ \text{annealing}}} \simeq 1{\cdot}3, \text{ and}$$

$$\frac{n_I^{333\,K\ \text{irradiation}}}{n_I^{520\,K\ \text{annealing}}} \simeq 10{\cdot}6 \qquad (5)$$

are calculated. According to Refs. [18] and [19], we know that the basal plane thermal conductivity of graphite $K_\perp$ varies as $T^{3/2}/n_I^{1/2}$ in the limit where n_I is sufficiently large and at $T = 25$ K, temperature at which the interstitials are the most effective. Therefore, from the $K_\perp(T)$ experimental curves of Fig. 2, we can deduce the corresponding ratios

$$\left[\frac{K_{\perp(T=25\,K)}^{410\,K\text{ annealing}}}{K_{\perp(T=25\,K)}^{333\,K\text{ irradiation}}}\right]^2 \simeq \frac{n_I^{333\,K\text{ irradiation}}}{n_I^{410\,K\text{ annealing}}} \simeq 1{\cdot}9$$

$$\left[\frac{K_{\perp(T=25\,K)}^{520\,K\text{ irradiation}}}{K_{\perp(T=25\,K)}^{333\,K\text{ irradiation}}}\right]^2 \simeq \frac{n_I^{333\,K\text{ irradiation}}}{n_I^{520\,K\text{ annealing}}} \simeq 12{\cdot}5. \quad (6)$$

The ratios given in equation (5) are close to the corresponding ratios given in equation (6) and derived from the analysis of the $K_\perp(T)$ curves. A good consistency is thus obtained between the thermal conductivity measurements and our present TEP analysis.

Furthermore, as we can see in Figs. 2 and 3, the annealing stage at 520 K gives a very large recovery of both S_{ph}^0 and $K_\perp$ obtained with the unirradiated graphite specimen. On the other hand, the value $n_I = 1{\cdot}16 \times 10^{-4}$, obtained on using this present model for the irradiated material, is in good agreement with the value $n_I = 1{\cdot}4 \times 10^{-4}$ found by the method of Bochirol and Bonjour[8]. Such results confirm quite well our analysis.

4. CONCLUSION

In this paper, we have pointed out that, like thermal conductivity, the phonon-drag component of the TEP of graphite is highly sensitive to the presence of defects. This explains the disappearance of S_{ph} for small concentrations ($\sim 10^{-4}$) of defects, particularly *I*-type interstitials, created by the small exposures to electron irradiation reported here. Accordingly, the change of sign of the low-temperature TEP is also explained.

Because of this extreme sensitivity of its phonon-drag component at low temperatures, the TEP is capable of giving a clear evidence for the quality of the measured samples, provided that the electronic component is known with a good accuracy.

Acknowledgements—One of us (J.P. J-G) would like to thank his colleagues in the Theoretical Physics Group of Eaton Laboratory for helpful discussions. Particularly, he is very grateful to Prof. P. R. Wallace for his generous hospitality and for his constant interest, encouragement, and many fruitful discussions.

APPENDIX

We consider here the justification of our assumption $\mathbf{b}(T) = \alpha T + \beta$. First of all, the linear extrapolation of $\mathbf{b}(T)$ can be justified, in a self-evident manner, *a posteriori*. In fact, two arguments strongly support this assumption. All the $|S_{ph}(T)|$ curves, deduced with $\mathbf{b}(T) = \alpha T + \beta$, show a sharp maximum near 40 K, exactly at the Kohn condition, whatever the annealing stage of the defects created by irradiation. Such a result so obviously agrees with the results of Ref. [4] that it seems to justify by itself the extrapolation made on $\mathbf{b}(T)$. The second argument comes from the satisfactory agreement for various samples between the concentration of defects deduced from our analysis and that obtained from low-temperature thermal conductivity measurements on the same sample.

The linear variation of $\mathbf{b}$ with T is also supported by the following analysis. If S_{ph} is neglected, $\mathbf{b}(T)$ can be deduced directly from the measured TEP values using equation (1). $\mathbf{b}(T)$, obtained in this manner, is plotted in Fig. 4 for the irradiated sample for which $|S_{ph}|$ is the smallest possible. For high temperatures ($T > 100$ K) where S_{ph} is indeed negligible, $\mathbf{b}(T)$ shows a linear variation. For lower temperature there is a small departure from linearity, which is attributable to S_{ph}. Since S_{ph} is negative, this can be taken into account by using in equation (1) a value of S_{el} higher than the measured TEP. When this is done, the curve $\mathbf{b}(T)$ is depressed towards smaller values of $\mathbf{b}$ and comes nearer the linear extrapolation.

A similar analysis was also performed for annealed samples. For $T > 100$ K, $\mathbf{b}$ is again found to vary linearly with T. For lower temperatures, the departure from

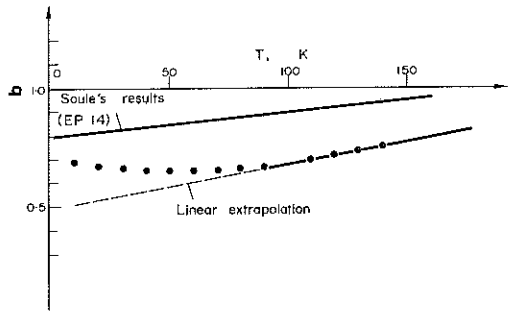

Fig. 4. Mobility ratio $\mathbf{b}$ as a function of temperature for the irradiated sample. The points show the values of $\mathbf{b}$ calculated from the experimental TEP curve using equation (1) with $\mathbf{a} = 1$ and $E_0 = 0{\cdot}01$ eV. In the calculation, we have assumed the absence of phonon-drag. Soule's results for EP14 crystal are shown for reference.

linearity is larger because $|S_{pd}|$ is greater in this case. It, therefore, appears that the choice of $\mathbf{b}(T) = \alpha T + \beta$ for all the samples is reasonable. This is not to suggest that the linearity of $\mathbf{b}(T)$, assumed in the text, is exact, but it is certainly realistic. If it is assumed to be exact, it may involve an overestimation of $|S_{pd}|$ and hence, an underestimation of the concentration of defects. For instance, for the irradiated sample, our analysis gives $n_t = 1{\cdot}16 \times 10^{-4}$, whereas the method of Bochirol and Bonjour gives $n_t = 1{\cdot}4 \times 10^{-4}$.

REFERENCES

1. TAKEZAWA T., TSUZUKU T., ONO A. and HISHIYAMA Y., *Phil. Mag.* **19**, 623 (1969).
2. RASOR N. S., *Nuclear Engineering and Manufacturing N.A.A.*, Downey, California (1955).
3. TAMARIN P. V., SHALYT S. S. and VOLGA V. I., *Fiz. tverd. Tela* **11**, 1725 (1969) (English Transl.: *Soviet Phys. solid State* **11**, 1399 (1969)).
4. JAY-GERIN J. P. and MAYNARD R., *J. low temp. Phys.* **3**, 377 (1970).
5. MOORE A. W., UBBELOHDE A. R. and YOUNG D. A., *Proc. R. Soc. Lond.* **280A**, 153 (1964).
6. DE COMBARIEU A., *Institut International du Froid*, Commission 1, pp. 63–71, Grenoble (1965).
7. SLACK G. A., *Phys. Rev.* **122**, 1451 (1961).
8. BOCHIROL L. and BONJOUR E., *Carbon* **6**, 661 (1968).
9. SIMMONS J. H. W., *Radiation Damage in Graphite*, Pergamon Press, New York (1965).
10. REYNOLDS W. N., Radiation damage in graphite, in *Chemistry and Physics of Carbon*, (Edited by P. L. Walker, Jr.) Vol. 2, Marcel Dekker, New York (1966).
11. KOHN W., *Phys. Rev. Lett.* **2**, 393 (1959).
12. KLEIN C. A., *J. appl. Phys.* **35**, 2947 (1964).
13. SPAIN I. L., UBBELOHDE A. R. and YOUNG D. A., *Phil. Trans. R. Soc. Lond.* **262A**, 345 (1967).
14. BLAKEMORE J. S., Tables of the Fermi-Dirac Integrals, in Appendix B, pp. 346–353, *Semiconductor Statistics*, Pergamon Press, Oxford, London, New York and Paris (1962).
15. COOPER J. D., SMITH J. P., WOORE J. and YOUNG D. A., *J. Phys. C.-Solid St. Phys.* **4**, 442 (1970).
16. BONJOUR E., DOULAT J., MAS P. and GOGGIN P. R., *Radiation Damage in Reactor Material* **II**, 83, IAEA Vienna (1969).
17. SOULE D. E., *Phys. Rev.* **112**, 698 (1958).
18. DREYFUS B. and MAYNARD R., *J. Phys.* **28**, 955 (1967)
19. MAYNARD R., *Thèse de Doctorat Sciences*, Grenoble, France (1967).

CHAPITRE V

ETUDE DES EFFETS THERMOMAGNETIQUES DANS LE GRAPHITE A BASSES TEMPERATURES EN PRESENCE D'UN CHAMP MAGNETIQUE FAIBLE ($H \lesssim 15$ kG).

Ce chapitre est consacré à une étude du pouvoir thermoélectrique, S(H), et du coefficient Nernst-Ettingshausen, $A_{NE}(H)$, du graphite à basses températures et en présence d'un champ magnétique $\vec{H}$ dirigé parallèlement à l'axe c et suffisamment faible ($H \lesssim 15$ kG) pour que l'on puisse négliger l'effet de la quantification des orbites électroniques, ainsi que la variation du niveau de Fermi avec le champ magnétique.

Cette étude a été motivée à l'origine par les expériences de Takezawa, Tsuzuku, Ono et Hishiyama (1971) et de Sugihara, Takezawa, Tsuzuku, Hishiyama et Ono (1972), et par celles de Tamarin, Shalyt et Volga (1969). Takezawa et ses collaborateurs (1971, 1972) ont observé qu'en présence d'un champ magnétique $\vec{H}$ parallèle à l'axe c, l'anomalie de "phonon-drag" du pouvoir thermoélectrique mesuré suivant les plans graphitiques subit un léger changement de position de 40 K à environ 30 K, et surtout un accroissement considérable d'amplitude jusqu'à environ - 80 µV/K pour H = 1.7 kG, et environ - 2000 µV/K pour H = 8 kG (Fig. 17). De leur côté, Tamarin et al. (1969) ont observé que le coefficient Nernst-Ettingshausen présente également un minimum très prononcé à $T_d \approx 30$ K, d'environ - 470 x 10^{-9} V/Gauss K pour H = 1 kG (Figs. 18 et 19).

Très récemment, Takezawa, Mangez, Hewes, Dresselhaus et Tsuzuku (1973) ont réalisé une série de mesures préliminaires du pouvoir thermoélectrique du graphite en présence d'un champ magnétique dans le domaine $0 < H < 105$ kG et dans celui de températures $4.2 < T < 77$ K (Figs. 20 et 21). Ils ont montré que l'effet Nernst-Ettingshausen doit être séparé systématiquement de la tension Seebeck, même dans les échantillons très soigneusement préparés (Dresselhaus 1974). La nécessité de séparer ces deux effets ne fut pas prise en considération dans les mesures antérieures de Takezawa et ses collaborateurs (1971, 1972). D'une manière qualitative, les nouveaux résultats de S(H) confirment les anciens, en ce sens que l'anomalie de "phonon-drag" vers 30 K est fortement augmentée par la présence d'un champ magnétique. Quantitativement, cette augmentation est cependant beaucoup moins marquée que celle observée antérieurement : pour un graphite pyrolytique traité à 3600° C, Takezawa, Mangez, Hewes, Dresselhaus et Tsuzuku (1973) ont en effet obtenu, à T = 30 K, un pouvoir thermoélectrique d'environ - 100 µV/K pour H = 10 kG, et - 350 µV/K pour H = 100 kG (Figs. 20 et 21).

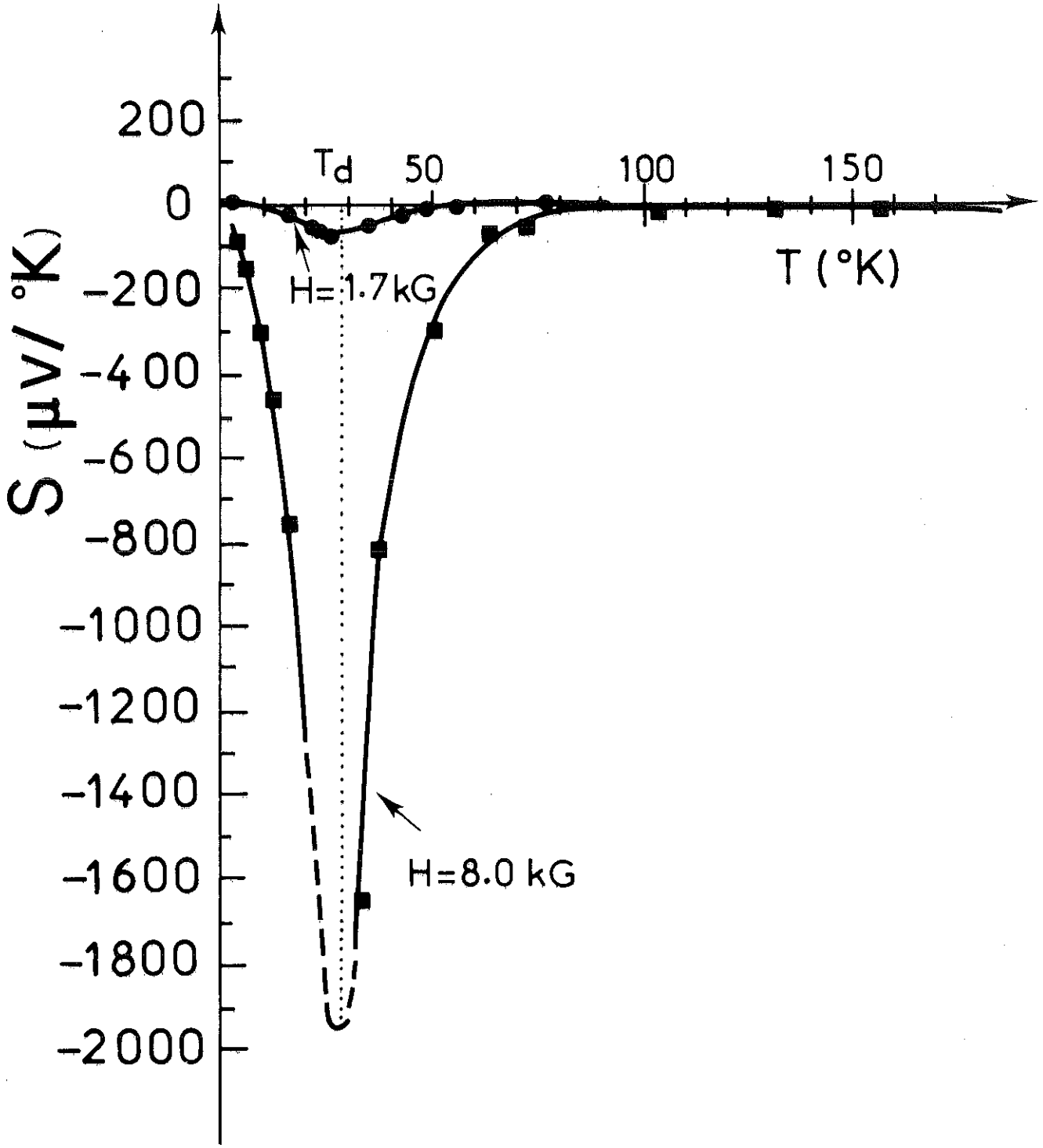
200
0
-200
-400
-600
-800
-1000
-1200
-1400
-1600
-1800
-2000
S (μV/°K)
Td
50
100
150
T (°K)
H=1.7kG
H=8.0 kG

Fig. 17

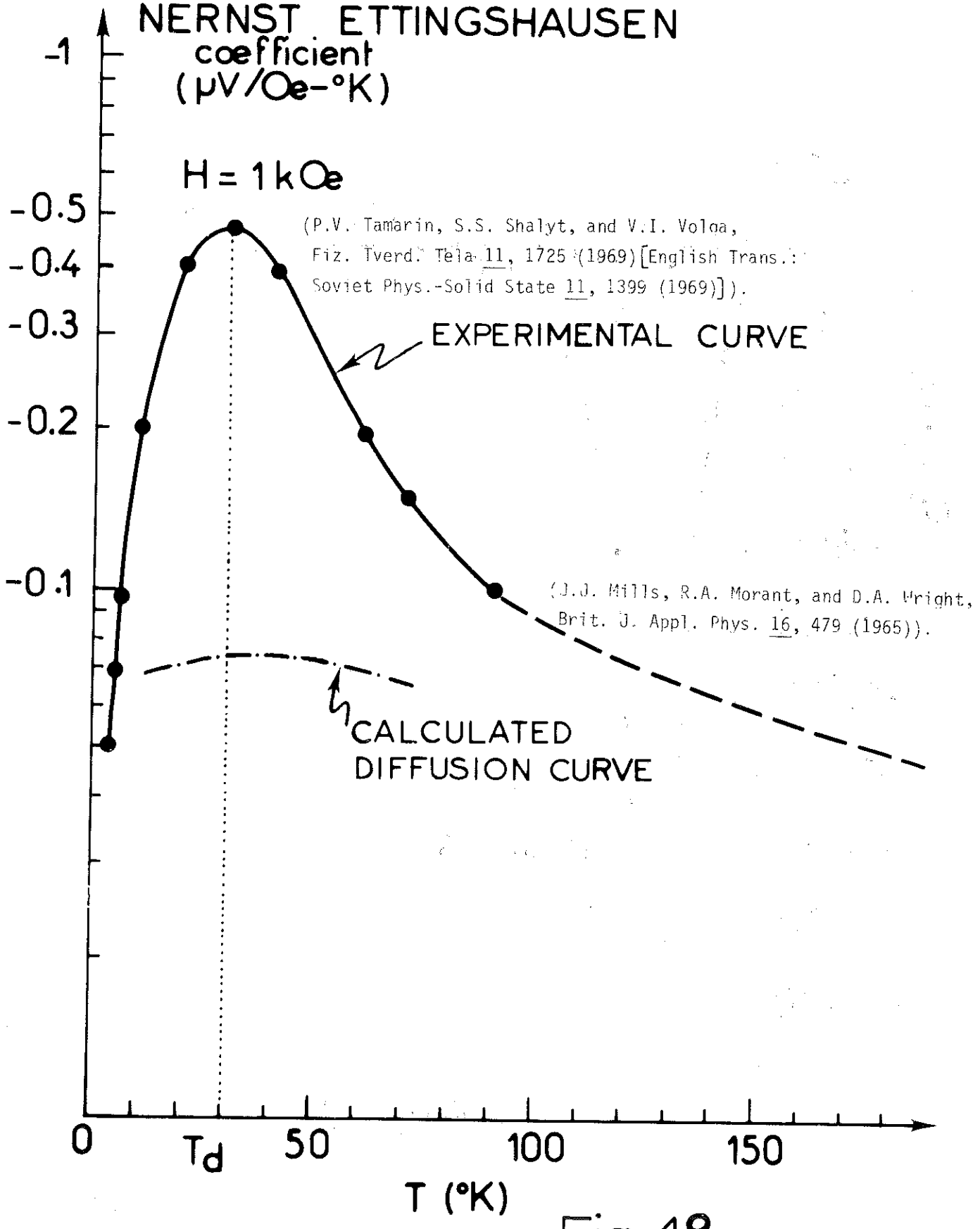
NERNST ETTINGSHAUSEN
coefficient
(μV/Oe-°K)
H = 1 kOe
-1
-0.5
-0.4
-0.3
-0.2
-0.1
(P.V. Tamarin, S.S. Shalyt, and V.I. Volga,
Fiz. Tverd. Tela 11, 1725 (1969) [English Trans.:
Soviet Phys.-Solid State 11, 1399 (1969)]).
EXPERIMENTAL CURVE
(J.J. Mills, R.A. Morant, and D.A. Wright,
Brit. J. Appl. Phys. 16, 479 (1965)).
CALCULATED
DIFFUSION CURVE
0
Td
50
100
150
T (°K)

Fig. 18

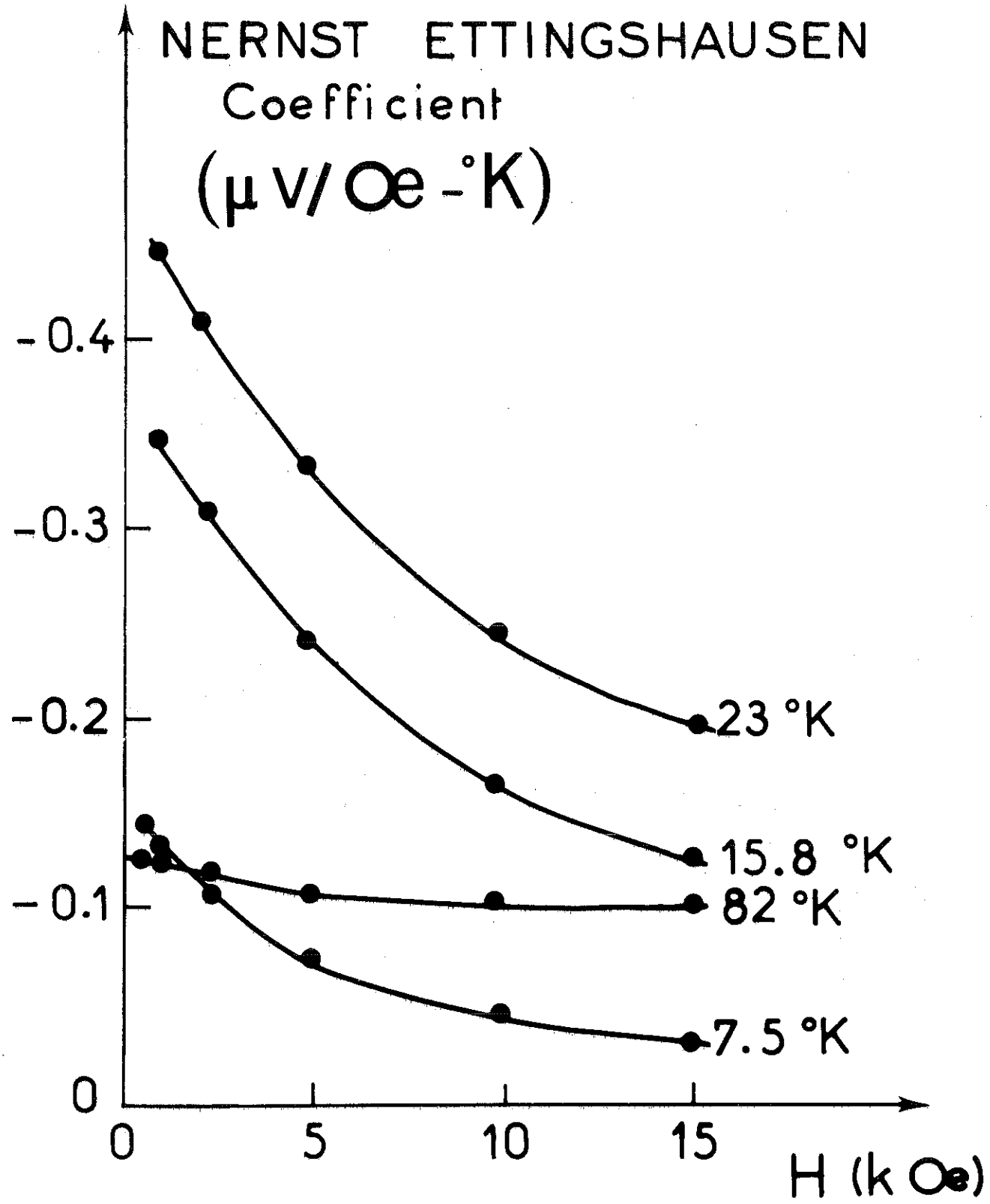
NERNST ETTINGSHAUSEN
Coefficient
(μV/Oe - °K)
-0.4
-0.3
-0.2
-0.1
0
0
5
10
15
H (k Oe)
23 °K
15.8 °K
82 °K
7.5 °K

Fig.19

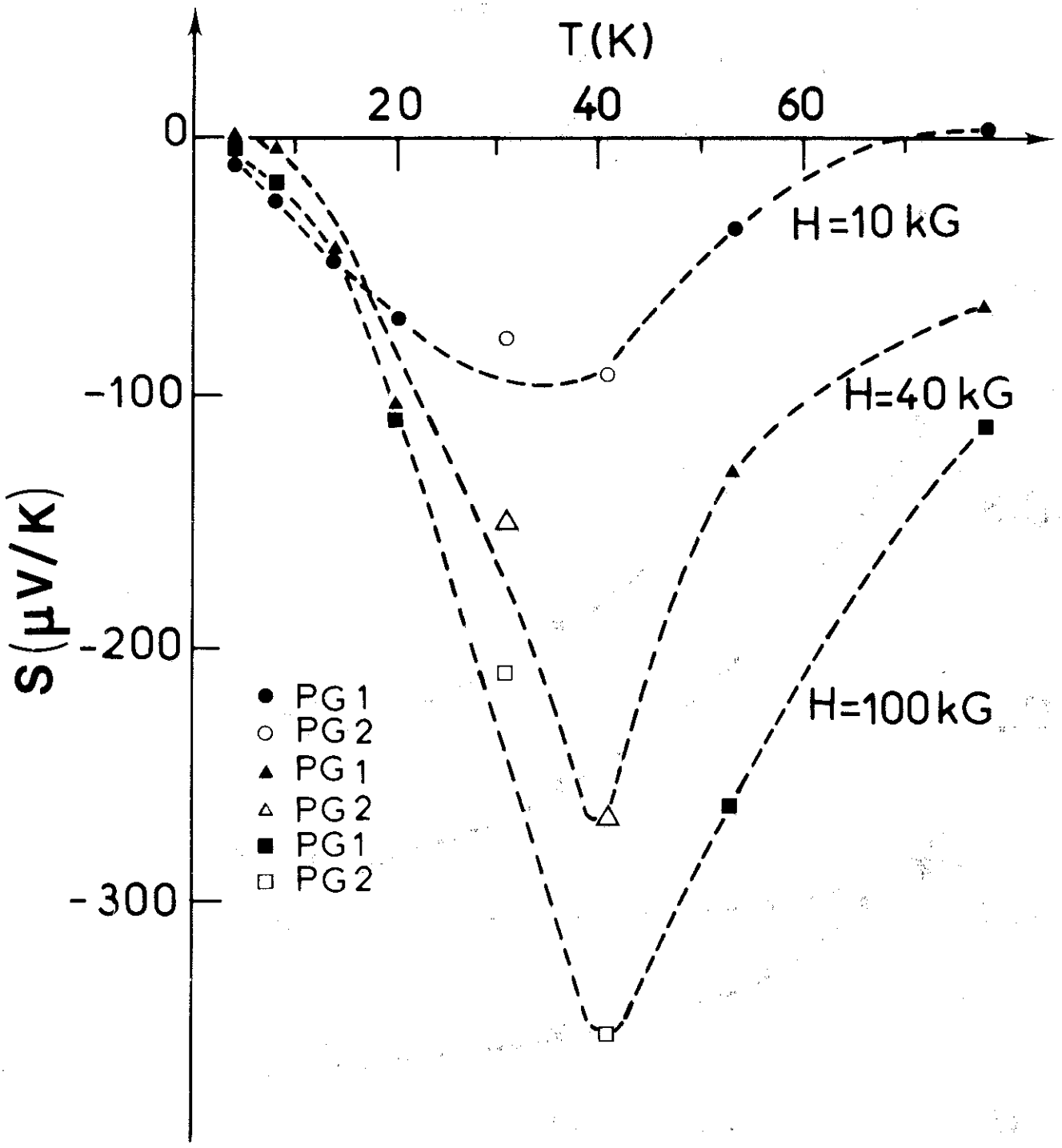
T(K)
20
40
60
0
-100
-200
-300
S(μV/K)
H=10 kG
H=40 kG
H=100 kG
PG 1
PG 2
PG 1
PG 2
PG 1
PG 2

Fig. 20

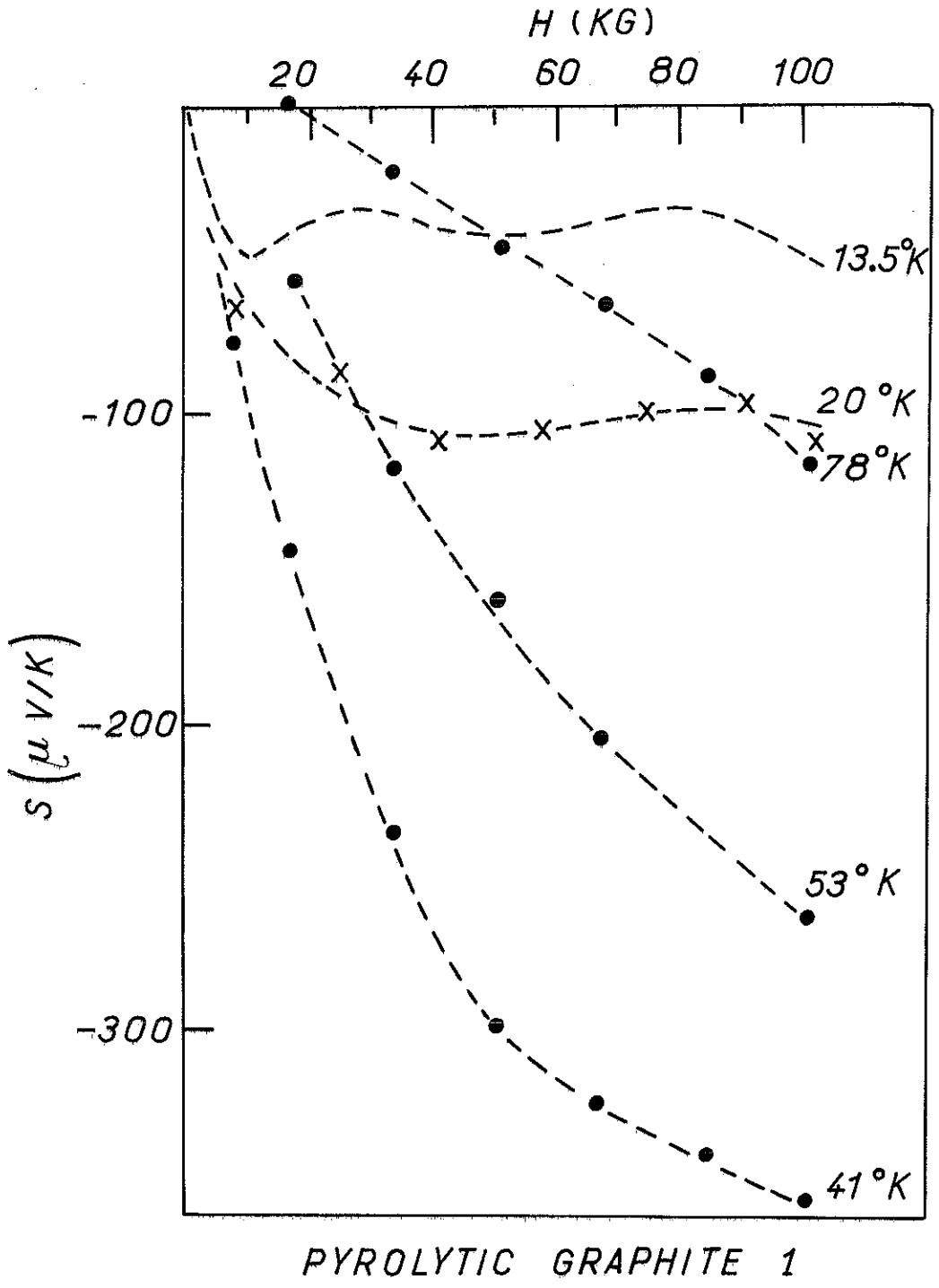
H (KG)
20
40
60
80
100
13.5°K
20 °K
78°K
53° K
41° K
-100
-200
-300
S (μV/K)
PYROLYTIC GRAPHITE 1

Fig. 21

L'analyse présentée dans ce chapitre repose essentiellement sur la théorie de l'effet de "phonon-drag" dans le graphite en l'absence de champ magnétique, que nous avons développéeau chapitre III, et dans laquelle le pouvoir thermoélectrique de "phonon-drag" est étroitement lié à l'anomalie d'écran de Kohn. Nous avons étendu cette théorie au calcul de S(H) et de $A_{NE}(H)$ en champs magnétiques faibles ($H \lesssim 15$ kG). Dans ce cas, le traitement du champ magnétique peut être réalisé avec l'aide des équations de transport de Boltzmann couplées pour les électrons et les phonons (Argyres 1958, Ziman 1965 et Sugihara, Takezawa, Tsuzuku, Hishiyama et Ono 1972). Les expressions de S(H) et de $A_{NE}(H)$ s'écrivent (pour le détail du calcul, voir l'Appendice) :

$$S(H) = \frac{E_x}{\nabla_x T} = \frac{1}{T}\left[\rho_{xx}\,\chi_{xx}(-H) + \rho_{xy}\,\chi_{xy}(-H)\right], \qquad (V\text{-}1)$$

$$A_{NE}(H) = \frac{E_y}{H\nabla_x T} = \frac{1}{TH}\left[\rho_{xx}\,\chi_{xy}(-H) - \rho_{xy}\,\chi_{xx}(-H)\right], \qquad (V\text{-}2)$$

dans l'hypothèse où la direction Oz coïncide avec la direction du champ magnétique appliqué $\vec{H}$ et dans le cas où il existe un gradient de température $\vec{\nabla}T$ suivant la direction Ox. A partir des expressions (V-1) et (V-2), on peut montrer que, pour un échantillon de graphite suffisamment pur et de bonne qualité (tel que $\bar{\mu}H/c \gg 1$, où $\bar{\mu}$ est une mobilité électronique moyenne, H le champ magnétique appliqué et c la vitesse de la lumière), S(H) et $A_{NE}(H)$ s'expriment sensiblement sous la forme :

$$S(H) \approx n|e|c\,R_H\,|S_{ph}(0)|, \qquad (V\text{-}3)$$

$$A_{NE}(H) \approx -\frac{n|e|c}{H^2}\,\rho_{xx}\,|S_{ph}(0)|, \qquad (V\text{-}4)$$

où $n = 2.80 \times 10^{18}$ cm^{-3} est la concentration d'électrons et de trous, $|e|$ la valeur absolue de la charge électronique, $R_H = -\frac{1}{H}\rho_{xy}$ le coefficient Hall, ρ_{xx} la magnétorésistance et $|S_{ph}(0)|$ la somme des valeurs absolues des contributions de "phonon-drag" au pouvoir thermoélectrique en champ magnétique nul dues aux électrons et aux trous. Ainsi, pour un champ magnétique donné, les variations de S(H) et de $A_{NE}(H)$ en fonction de la température doivent refléter l'anomalie de "phonon-drag" de $|S_{ph}(0)|$ (voir chapitre III), puisque les variations thermiques de R_H et de ρ_{xx} sont essentiellement monotones à basses températures.

Plus spécifiquement, puisque $|R_H|$ varie comme T^{-2} et ρ_{xx} comme T^{-1} (Soule 1958), nous avons là l'explication du déplacement vers les plus basses températures ($T_d \approx 30$ K) de l'anomalie de "phonon-drag". Nous avons également une confirmation

directe de l'analyse présentée au chapitre III en ce qui concerne l'interaction phonon-phonon, laquelle ne joue aucun rôle fondamental pour expliquer la décroissance du pouvoir thermoélectrique dans la région de températures $T > T_d$. Nous trouvons en effet une loi de décroissance en T^{-3} dans cette région, puisque $|S_{ph}(0)|$ varie comme T^{-1} par suite de l'affaiblissement du couplage électron-phonon dû à l'élargissement thermique des contours de la surface de Fermi (voir chapitre III). Cette loi reproduit bien l'allure de la courbe expérimentale de Takezawa, Mangez, Hewes, Dresselhaus et Tsuzuku (1973) pour H = 10 kG (Fig. 20). D'autre part, d'après l'équation (V-4), $A_{NE}(H)$ varie comme T^{-2} pour $T > T_d$, ce qui est aussi en accord avec les mesures de Tamarin, Shalyt et Volga (1969) (Fig. 18). Au point de vue quantitatif, nous devons souligner que notre analyse donne un ordre de grandeur de S(H) qui correspond bien à celui trouvé expérimentalement par Takezawa et al. (1973). Comme l'indique l'équation (V-3), S(H) dépend d'une manière très sensible du coefficient Hall R_H, qui peut varier considérablement d'un échantillon de graphite à un autre (Soule 1958, Pacault 1965, Spain, Ubbelohde et Young 1967 et Delhaès 1974). Bien que Takezawa et al. (1973) n'aient pas effectué de mesures d'effet Hall sur leurs échantillons, on peut penser raisonnablement que ces échantillons sont d'une pureté et d'une qualité telles que leurs propriétés doivent être très voisines de celles des monocristaux naturels EP-7 et EP-14 de Soule (1958). Dans cette hypothèse, il est possible d'utiliser les résultats expérimentaux de Soule pour avoir une estimation de R_H en fonction de la température et du champ magnétique. Ainsi, pour H = 10 kG et $T = T_d \approx 30$ K, on peut estimer $R_H \approx -6$ cm^3/C (cristal EP-14). A partir des résultats du chapitre III, $|S_{ph}(0)|$ à $T \approx 30$ K est sensiblement égale à 70 µV/K, ce qui donne pour S(H) une valeur voisine de - 140 µV/K. Cette valeur, qui est évidemment très loin des - 2000 µV/K obtenus par Takezawa et ses collaborateurs (1971, 1972), doit être considérée comme satisfaisante (la valeur expérimentale obtenue par Takezawa et al. (1973) est en effet - 100 µV/K) compte-tenu des hypothèses et simplifications utilisées. Il est intéressant de noter que Takezawa, Mangez, Hewes, Dresselhaus et Tsuzuku (1973) ont observé une dépendance approximativement linéaire (et non quadratique, comme il avait été observé antérieurement) de S(H) en fonction du champ magnétique pour $T < T_d$ et pour H < 10 - 20 kG (Fig. 21). Ce point peut être expliqué à partir de notre analyse. En effet, la variation de S(H) avec H est déterminée essentiellement par la variation de R_H avec H (voir Eq. (V-3)). Si on utilise à nouveau les résultats expérimentaux de Soule (1958) sur les monocristaux naturels EP-7 et EP-14, R_H varie de façon sensiblement linéaire avec H pour $H \gtrsim 3$ kG à 77 K et pour $H \lesssim 10$ kG à 4.2 K. Ces résultats vont donc bien dans le sens d'une dépendance linéaire de S(H) en fonction du champ magnétique appliqué.

En ce qui concerne le coefficient Nernst-Ettingshausen $A_{NE}(H)$, notre analyse donne également un ordre de grandeur en bon accord avec les mesures de Tamarin,

Shalyt et Volga (1969). En effet, pour H = 1 kG et T = $T_d \approx 30$ K, on peut estimer $\rho_{xx} \approx 1.4 \times 10^{-16}$ unités CGS (cristal EP-14), ce qui conduit à une valeur de $A_{NE}(H)$ voisine de - 0.39 µV/Gauss K (la valeur expérimentale correspondante de Tamarin et al. (1969) est sensiblement égale à - 0.47 µV/Gauss K (Fig. 18)). Pour H = 10 kG et T = T_d, on a $\rho_{xx} \approx 62 \times 10^{-16}$ unités CGS (cristal EP-14), ce qui donne $A_{NE}(H) \approx$ - 0.18 µV/Gauss K (la valeur expérimentale est voisine de - 0.24 µV/Gauss K (Fig. 19)). Ainsi, pour un champ magnétique appliqué de 10 kG et à une température de 30 K, il se développe dans l'échantillon une tension Nernst-Ettingshausen d'environ 1800 µV/K, ce qui est évidemment tout à fait considérable comparée à la tension thermoélectrique qui est voisine de 100 µV/K pour ce champ et cette température. Ces estimations confirment donc bien les récents résultats de Takezawa, Mangez, Hewes, Dresselhaus et Tsuzuku (1973).

Il est enfin intéressant de souligner que les expressions obtenues pour S(H) et $A_{NE}(H)$ doivent permettre de déduire, directement de l'expérience, les constantes de couplage électron-phonon et trou-phonon. La connaissance de ces constantes est en effet extrêmement importante, puisque nous savons que l'effet de "phonon-drag" est directement proportionnel à la force du couplage électron-phonon. Nous avons donc là une possibilité qui s'offre à nous de comprendre le délicat problème du signe négatif du pouvoir thermoélectrique du graphite, dans lequel les électrons et les trous sont en étroite compétition.

La présente étude a suscité, au Service des Basses Températures du Centre d'Etudes Nucléaires de Grenoble (Ayache et De Combarieu), des mesures expérimentales systématiques des divers coefficients de transport du graphite, tels que la magnétorésistance, le coefficient Hall, le pouvoir thermoélectrique en absence et en présence d'un champ magnétique, le coefficient Nernst-Ettingshausen, la conductivité thermique, ... Ces mesures, actuellement en cours de réalisation, doivent apporter dans un proche avenir une contribution très importante dans la compréhension des propriétés du graphite.

Low-Temperature Thermomagnetic Effects in Graphite

J. P. JAY-GERIN[1]
Eaton Laboratory, McGill University, Montreal, Quebec

Received April 24, 1972

The low-temperature thermoelectric power (TEP) and the Nernst–Ettingshausen (NE) coefficient of graphite due to phonon drag are studied in the presence of a magnetic field $\boldsymbol{H}$ directed along the c axis and small enough for the quantum-mechanical character of the motion of the carriers to be negligible. Expressions for the TEP and the NE coefficient are obtained on the basis of the theory of Jay-Gerin and Maynard, in which the phonon-drag TEP of graphite in the absence of a magnetic field is linked with the Kohn screening anomaly. The results suggest a method by which information might be obtained about the strength of the electron- and hole–phonon coupling directly from experiment. A satisfactory agreement is found with the measurements of Takezawa, Tsuzuku, Ono, and Hishiyama and of Tamarin, Shalyt, and Volga.

On a étudié le pouvoir thermoélectrique (TEP) et le coefficient Nernst–Ettingshausen (NE) du graphite à basse températures et en présence d'un champ magnétique $\boldsymbol{H}$ dirigé suivant l'axe c et suffisamment faible pour qu'on puisse négliger le caractère quantique du mouvement des porteurs de charge. Des expressions du TEP et du coefficient NE sont obtenues sur la base de la théorie de Jay-Gerin et Maynard, dans laquelle le TEP du graphite, en l'absence de champ magnétique, est étroitement lié à l'anomalie d'écran de Kohn. Les résultats suggèrent une méthode par laquelle la force du couplage électron–phonon et trou–phonon pourrait être déduite directement de l'expérience. Un accord satisfaisant est obtenu avec les mesures de Takezawa, Tsuzuku, Ono et Hishiyama ainsi qu'avec celles de Tamarin, Shalyt et Volga.

[Traduit par le journal]

Canadian Journal of Physics, **50**, 2444 (1972)

I. Introduction

As is now well known, in the absence of a magnetic field the thermoelectric power (TEP) of very well oriented, nearly single-crystal graphite measured along the basal plane direction exhibits a sharp negative dip of about $-20\ \mu$V/K at around 40 K (Rasor 1955; Spain, Ubbelohde, and Young 1967; Takezawa, Tsuzuku, Ono, and Hishiyama 1969; Tamarin, Shalyt, and Volga 1969; de Combarieu quoted in Jay-Gerin and Maynard 1970; Tsuzuku, Takezawa, Hishiyama, and Ono 1972). This low-temperature anomaly in the TEP is attributed to phonon drag.

Recently, Takezawa, Tsuzuku, Ono, and Hishiyama (1971) have shown that, in the presence of a magnetic field $\boldsymbol{H}$ directed along the c axis, the anomalous phonon-drag TEP dip experiences both a slight shift of position from 40 K to near 30 K and a large increase in magnitude to about $-80\ \mu$V/K for $H = 1.7$ kOe, and about $-2000\ \mu$V/K for $H = 8$ kOe. On the other hand, Tamarin, Shalyt, and Volga (1969) reported experimentally that the low-field Nernst–Ettingshausen (NE) coefficient experiences also a sharp minimum of -470×10^{-9} V/Oe K at around 35 K and for $H = 1$ kOe in a pyrolytic graphite specimen heated to 3200 °C. By comparing the experimental and the usual electronic diffusion term values of the NE coefficient, these authors concluded that there was a prominent phonon-drag effect. In addition, it is interesting to note that similar anomalies have already been observed in the magneto-Seebeck and NE effects in other semimetals such as bismuth and antimony (Farag 1968; Red'ko and Shalyt 1968).

Theories for the phonon-drag effect in graphite (Sugihara 1970; Jay-Gerin and Maynard 1970; Sugihara, Takezawa, Tsuzuku, Hishiyama, and Ono 1971, 1972) use essentially the same method relying on the two coupled Boltzmann transport equations for phonons and carriers with a relaxation time approximation for the carriers and on a simplified energy-band model with an ellipsoidal Fermi surface. It must be noted, however, that the physical interpretation of this phenomenon by Jay-Gerin and Maynard on the basis of the enhanced coupling by anisotropy of the Kohn (1959) phonons $\boldsymbol{q} = 2\boldsymbol{k}_F$ with carriers is quite distinct from that by Sugihara and collaborators.

[1]Present address: Centre de Recherches sur les Très Basses Températures, CNRS, B.P. 166, Centre de Tri 38042, Grenoble Cedex, France.

The analysis presented in this paper is based on the theory of Jay-Gerin and Maynard of phonon drag in graphite in zero magnetic field. Our main interest is to extend this previous study to the calculation of both the TEP and the NE coefficient in the presence of a magnetic field. Throughout the paper, we restrict ourselves to magnetic field strengths less than about 15 kOe, so that all quantum-oscillatory effects, as well as the variation of the Fermi energy with magnetic field, are neglected.

II. Phenomenological Formulation

The linear relations between electric current density $\boldsymbol{J}$, electric field $\boldsymbol{E}$, negative temperature gradient $(-\nabla T)$, and heat current density $\boldsymbol{U}$, may be written as the well-known phenomenological transport equations (Ziman 1965)

$$[1] \qquad \begin{cases} \boldsymbol{J} = \sigma \boldsymbol{E} + \beta(-\nabla T) \\ \boldsymbol{U} = \chi \boldsymbol{E} + \kappa(-\nabla T) \end{cases}$$

where the coefficients, actually tensors, satisfy the Onsager relations of the thermodynamics of irreversible processes

$$[2] \qquad \begin{cases} \sigma_{ij}(\boldsymbol{H}) = \sigma_{ji}(-\boldsymbol{H}) \\ T\beta_{ij}(\boldsymbol{H}) = \chi_{ji}(-\boldsymbol{H}) \\ \kappa_{ij}(\boldsymbol{H}) = \kappa_{ji}(-\boldsymbol{H}) \end{cases}$$

Following Sugihara *et al.* (1971), if the temperature gradient lies in the x direction, $\boldsymbol{E} = (E_x, E_y, 0)$ in the basal plane direction, and $\boldsymbol{H} = (0, 0, H)$ in the z direction, the TEP and the NE coefficient are defined by

$$[3] \qquad S(H) = \frac{E_x}{\nabla_x T} = \frac{\sigma_{yy}\chi_{xx}(-H) - \sigma_{xy}\chi_{xy}(-H)}{T(\sigma_{yy}\sigma_{xx} - \sigma_{xy}\sigma_{yx})}$$

$$[4] \qquad A_{\mathrm{NE}}(H) = \frac{E_y}{H\nabla_x T} = \frac{\sigma_{xx}\chi_{xy}(-H) - \sigma_{yx}\chi_{xx}(-H)}{HT(\sigma_{yy}\sigma_{xx} - \sigma_{xy}\sigma_{yx})}$$

For magnetic fields parallel to the high symmetry c axis of graphite

$$[5] \qquad \sigma_{xx} = \sigma_{yy}, \qquad \sigma_{yx} = -\sigma_{xy}$$

and in terms of the magnetoresistivity tensor $\rho = \sigma^{-1}$

$$[6] \qquad \rho_{xx} = \sigma_{xx}/(\sigma_{xx}^2 + \sigma_{xy}^2), \qquad \rho_{xy} = -\sigma_{xy}/(\sigma_{xx}^2 + \sigma_{xy}^2)$$

Using [5] and [6], $S(H)$ and $A_{\mathrm{NE}}(H)$ can be rewritten as follows:

$$[7] \qquad S(H) = (1/T) \times [\rho_{xx}\chi_{xx}(-H) + \rho_{xy}\chi_{xy}(-H)]$$

$$[8] \qquad A_{\mathrm{NE}}(H) = (1/HT) \times [\rho_{xx}\chi_{xy}(-H) - \rho_{xy}\chi_{xx}(-H)]$$

To actually determine the TEP and the NE coefficient it follows from [7] and [8] that we need to know both the magnetoresistivity and Peltier tensor components. However, the low-field galvanomagnetic properties of graphite at low temperatures have been intensively studied from many points of view (Kinchin 1953; Soule 1958; McClure 1956, 1958; Sugihara and Sato 1963; Arkhipov, Kechin, Likhter, and Pospelov 1963; Klein 1964; Ono and Sugihara 1966; Spain, Ubbelohde, and Young 1967), so that in the following we focus our attention essentially on the derivation of the Peltier tensor χ. Using the method of π approach of the thermoelectric problems (Herring, Geballe, and Kunzler 1958) we calculate the heat current density $\boldsymbol{U}$ due to the presence of the electric field $\boldsymbol{E}$ assuming the temperature gradient to be always zero. χ is then determined by the formula $\boldsymbol{U} = \chi \boldsymbol{E}$.

Now, because of the strong carrier-phonon interaction in graphite, $\boldsymbol{U}$ must be considered as the sum of two contributions: $\boldsymbol{U}_{\mathrm{el}}$, the usual electronic diffusion part and $\boldsymbol{U}_{\mathrm{ph}}$, the phonon-drag part. However, at low temperatures and in the presence of high magnetic fields it is well known (Puri 1965; Sugihara 1969; Tamarin, Shalyt, and Volga 1969) that the main contribution to $\boldsymbol{U}$ comes from $\boldsymbol{U}_{\mathrm{ph}}$, $\boldsymbol{U}_{\mathrm{el}}$ making quite a small contribution. Accordingly, in the following we shall ignore $\boldsymbol{U}_{\mathrm{el}}$ and consider only the heat transfer part due to drag.

III. Phonon-Drag Contribution to the Heat Current Density U

We consider the approach to equilibrium of the system of interacting carriers (electrons and

holes) and phonons in graphite in the presence of a small electric field $\boldsymbol{E} \parallel 0x$ and a magnetic field $\boldsymbol{H}$ applied parallel to the c-axis direction, here called $0z$. The usual Boltzmann transport equation for phonons of mode $\boldsymbol{q}j$ gives

$$[9] \qquad \boldsymbol{U}_{\rm ph} = \sum_j (2\pi)^{-3} \int \mathrm{d}\boldsymbol{q}\ \hbar\omega_{\boldsymbol{q}j}\boldsymbol{v}_{\boldsymbol{q}j}\tau_{\rm ph}(\boldsymbol{q}j)(\partial N_{\boldsymbol{q}j}/\partial t)_{\rm carr.}$$

where we have written explicitly the dependence of the integrand on $\boldsymbol{q}j$, $\boldsymbol{q}$ and j being the phonon wave vector and the polarization index respectively. Since we are concerned with low-temperature transport problems in graphite along the basal plane direction, only the longitudinal $j=(l)$ and transverse $j=(t)$ "in-plane" acoustical phonons contribute to carrier scattering, "out-of-plane" acoustical phonons being quite inefficient (Sugihara and Sato 1963; Dreyfus and Maynard 1967). Therefore, $\sum_j$ reduces to a sum over $j=(l)$, (t) "in-plane" phonon modes only. For this class of phonons, the dispersion relation $\omega(\boldsymbol{q})$ is nearly cylindrical (Dreyfus and Maynard 1967). In the present analysis, we assume $\omega = v_j q_\perp$ for all the values of ω, where v_j is the velocity of sound, $q_\perp$ the component of $\boldsymbol{q}$ on the graphitic planes ($q_\perp^2 = q_x^2 + q_y^2$), and $\boldsymbol{v}_{\boldsymbol{q}j} = v_j(\boldsymbol{q}_\perp/q_\perp)$ the phonon group velocity. The phonon-relaxation processes other than those on carriers are described by a relaxation time $\tau_{\rm ph}(\boldsymbol{q}j)$. We assume that $\tau_{\rm ph}(\boldsymbol{q}j)$ is independent of H. Such an expectation is confirmed by low-temperature specific heat measurements in graphite in the presence of magnetic fields up to 60 kOe (Delhaes, Lemerle, and Blondé-Gondé 1971). $(\partial N_{\boldsymbol{q}j}/\partial t)_{\rm carr.}$ is the time rate of change of the phonon distribution $N_{\boldsymbol{q}j}$ as a result of the carrier–phonon scattering processes, and is calculated correct up to the first order in the electric field and the second in the carrier–phonon interaction (Born approximation) within the framework of Jay-Gerin and Maynard (1970) and proceeding as in the zero-field case. The Fermi surfaces of graphite are assumed to be true elongated ellipsoids with energies quadratic in wavenumber (Soule, McClure, and Smith 1964)

$$[10] \qquad \varepsilon(\boldsymbol{k}_\perp, k_z) = \hbar^2\boldsymbol{k}_\perp^2/2m_\perp + \hbar^2 k_z^2/2m_z$$

where $m_\perp$ and m_z are the carrier effective masses perpendicular and parallel to the c axis respectively. We restrict ourselves to magnetic field strengths small enough ($H \lesssim 15$ kOe) to neglect the quantum nature of the motion of the carriers in the magnetic field. In this case the treatment of the magnetic field can thus be achieved in conjunction with the Boltzmann carrier transport equation (Argyres 1958). To solve this equation, use is made of a similar method to that by Sugihara (1970) and by Sugihara *et al.* (1971, 1972), assuming that the approach to equilibrium of the perturbed carrier distribution that arises from the scattering of carriers by point defects and by phonons can be described by a unique energy dependent relaxation time τ (Blatt 1957; Dugdale and Bailyn 1967; Spain 1970). For this model under consideration, the integration of [9] is carried out in a straightforward manner. Remembering that the phonon-drag components of the Peltier tensor χ are defined by $\boldsymbol{U}_{\rm ph} = \chi_{\rm ph}\boldsymbol{E}$, we obtain the following results:

$$[11] \qquad [\chi_{xx}(-H)]_{\rm ph} = \frac{[\chi^{\rm e}_{xy}(-H)]_{\rm ph}}{\mu_{\rm e}H/c} - \frac{[\chi^{\rm h}_{xy}(-H)]_{\rm ph}}{\mu_{\rm h}H/c}$$

and

$$[12] \qquad [\chi_{xy}(-H)]_{\rm ph} = [\chi^{\rm e}_{xy}(-H)]_{\rm ph} + [\chi^{\rm h}_{xy}(-H)]_{\rm ph}$$

where $\mu_{\rm e} = |e|\tau_{\rm e}/m^{\rm e}_\perp$ and $\mu_{\rm h} = |e|\tau_{\rm h}/m^{\rm h}_\perp$ are the electron and hole mobilities respectively. The contribution $[\chi^\lambda_{xy}(-H)]_{\rm ph}$ of the λth carriers (λ = e, h) is given by

$$[13] \qquad [\chi^\lambda_{xy}(-H)]_{\rm ph} = -\frac{Tn_\lambda|e|c}{H[1+(\mu_\lambda H/c)^2]}(\mu_\lambda H/c)^2|S^\lambda_{\rm ph}(0)|$$

where n_λ is the λth-carrier density per unit volume, $|e|$ is the magnitude of the electronic charge,

c is the speed of light, and $|S_{ph}^{\lambda}(0)|$ is the absolute value of the phonon-drag contribution to the TEP in zero magnetic field due to the λth carriers:

$$[14] \qquad |S_{ph}^{\lambda}(0)| = \frac{k_B}{|e|}\frac{1}{2n_\lambda}\sum_j (2\pi c_0 v_j^2)^{-1}\int_0^{\omega_{max.}} \omega\, d\omega\, C_{ph}\left(\frac{\hbar\omega}{k_B T}\right)\left(\frac{\Gamma_\lambda(\omega)}{\Gamma_\lambda(\omega)+1/\tau_{ph}}\right)$$

where the various parameters have the same meaning as in the Jay-Gerin and Maynard (1970) paper.

IV. General Expressions for the TEP and the NE Coefficient and Discussion

Let us return to the eqs. 7 and 8. Using [11]–[13], we find the following expressions for the TEP and the NE coefficient:

$$[15] \qquad S(H) \simeq \frac{n|e|c}{H}\frac{(\bar{\mu}H/c)}{[1+(\bar{\mu}H/c)^2]}\,[HR_H(\bar{\mu}H/c)|S_{ph}(0)| + \rho_{xx}S_{ph}(0)]$$

$$[16] \qquad A_{NE}(H) \simeq \frac{n|e|c}{H^2}\frac{(\bar{\mu}H/c)}{[1+(\bar{\mu}H/c)^2]}\,[-\rho_{xx}(\bar{\mu}H/c)|S_{ph}(0)| + HR_H S_{ph}(0)]$$

where $n = n_e \approx n_h$, $R_H = -\rho_{xy}/H$ is the Hall coefficient, $\bar{\mu} = (\mu_e\mu_h)^{1/2}$ is an average carrier mobility (Soule 1958; Spain, Ubbelohde, and Young 1967), $S_{ph}(0) = -|S_{ph}^{e}(0)| + S_{ph}^{h}(0)$ is the phonon-drag contribution to the TEP in the zero-field case taking electrons and holes into account, and $|S_{ph}(0)| = |S_{ph}^{e}(0)| + S_{ph}^{h}(0)$.

When deriving [15] and [16], we have neglected the electronic diffusion part of the Peltier tensor χ. At low temperatures and in the presence of sufficiently high magnetic fields, this approximation is quite reasonable (Puri 1965; Sugihara 1969) and introduces only a very small error in the above calculations of $S(H)$ and of $A_{NE}(H)$. For instance, Tamarin, Shalyt, and Volga (1969) compared the experimental and "theoretical" (usual diffusion term) values of the NE coefficient at $T = 20$ K for a magnetic field as small as 1 kOe. They found $(A_{NE})_{diff.} \approx -30 \times 10^{-9}$ V/Oe K, whereas $(A_{NE})_{exp.} \approx -400 \times 10^{-9}$ V/Oe K. On the other hand, Sugihara *et al.* (1971) reported the diffusion term of the NE coefficient calculated by Okuyama and Takeya for $H = 1$ kOe as a function of temperature. The magnitude of this term was consistent with the previous numerical estimate of Tamarin, Shalyt, and Volga (1969) and the curve of $(A_{NE})_{diff.}$ vs. T showed a very smooth variation over the entire low-temperature region. Such results confirm our expectation.

It is now worth noting that [15] and [16] turn out to be extremely useful in practice since they provide a convenient way of obtaining information about the electron– and hole–phonon interactions in graphite directly from experiment. Using these formulas, it is not difficult to determine numerically and separately both $|S_{ph}^{e}(0)|$ and $S_{ph}^{h}(0)$, by measuring simultaneously on the *same* sample of graphite the TEP in the absence and in the presence of a magnetic field with the Hall, magneto-resistivity, and NE coefficients. Then, in the light of the theoretical results of Jay-Gerin and Maynard (1970), the coupling constants of the electron– and hole–phonon interactions can readily be deduced. Since the effect of phonon drag is proportional to the strength of the carrier–phonon interaction, the knowledge of these coupling constants is quite important, essentially in providing an opportunity to understand things about the delicate problem of the negative sign of the TEP of graphite, in which the number of holes is equal to the number of electrons. Unfortunately, neither Tamarin, Shalyt, and Volga (1969) nor Takezawa, Tsuzuku, Ono, and Hishiyama (1971) have reported experimental data on R_H and ρ_{xx}. In addition, low-temperature thermal conductivity measurements are also desirable for determining the phonon relaxation time τ_{ph}, which appears in [14]. Consequently, because of this lack of experimental data, it appears not to be possible at the present time to obtain accurate information about the electron– and hole–phonon interactions in graphite from the formulas derived in this paper.

Although a quantitative analysis of the results of Tamarin, Shalyt, and Volga (1969) and of Takezawa, Tsuzuku, Ono, and Hishiyama (1971) requires further experimental studies on the *same*

samples of graphite, let us now turn our attention to the temperature and field dependences of the TEP and of the NE coefficient, as deduced from [15] and [16]. Analysis of Soule's experimental data (Soule 1958) indicates, for the natural graphite single crystal coded EP 14, that $(\bar{\mu}H/c)$ is about equal to 21 at 4.2 K and to 2 at 77 K for a magnetic field strength of 3 kOe. On the other hand, it is well known (Soule 1958; Spain, Ubbelohde, and Young 1967; Spain 1970) that $\bar{\mu}$ decreases with increasing temperature as about $T^{-1.2}$ from 20 K to 500 K, while below about 20 K the curve of $\bar{\mu}$ vs. T flattens somewhat indicating the increasing effect of impurity scattering. Consequently, in the temperature region below about 30 K the inequality $(\bar{\mu}H/c)^2 \gg 1$ appears to be certainly well satisfied for a high-quality graphite crystal. We have, however, to notice at this point that the observations of the de Haas–van Alphen effect (Williamson, Foner, and Dresselhaus 1965) and of related oscillatory variations in the magnetoresistivity (Soule 1958; Soule, McClure, and Smith 1964; Woollam 1971) and in the Hall effect (Soule 1958; Woollam 1971) at 1.1 and 4.2 K show that the quantization becomes important for $H \gtrsim 15$ kOe. In other words, since we have treated the motion of the carriers in the magnetic field in a classical way through the Boltzmann transport equation, the present analysis is correct for magnetic fields fairly strong but certainly less than about 15 kOe. In the case of $(\bar{\mu}H/c)^2 \gg 1$, [15] and [16] reduce to the following expressions:

$$S(H) \simeq n|e|c\left[R_H|S_{ph}(0)| + \frac{\rho_{xx}}{H}\frac{S_{ph}(0)}{(\bar{\mu}H/c)}\right] \quad [17]$$

$$A_{NE}(H) \simeq (n|e|c/H^2)\left[-\rho_{xx}|S_{ph}(0)| + \frac{HR_H S_{ph}(0)}{(\bar{\mu}H/c)}\right] \quad [18]$$

We now discuss the TEP in this low-temperature limit, namely $T \lesssim 30$ K. We first observe from a crude numerical estimate that the dominant contribution to $S(H)$ is given by the first term of [17]. It is easy to see that this term arises from $[\chi_{xy}]_{ph}$. The physical explanation is straightforward and as follows. For a magnetic field $\boldsymbol{H} \parallel 0z$ and an electric field $\boldsymbol{E} \parallel 0x$, electrons and holes mainly drift along the y direction. This carrier flow drags phonons with itself, and thus induces the Peltier heat $(\boldsymbol{U}_{ph})_y$. With the above observations, [17] can be used for explaining the experimental behavior of $S(H)$. Firstly, $S(H)$ is expected to be negative because R_H is negative in the limit under consideration. For instance, for crystal EP 14 at 8 kOe, R_H is changing very rapidly from about -8 cm^3/C at 4.2 K to -0.2 cm^3/C at 77 K (Soule 1958). Secondly, since $|S_{ph}(0)|$ exhibits a sharp maximum as a function of temperature near 40 K (Jay-Gerin and Maynard 1970) and since $|R_H|$ varies as about T^{-2}, the position of the phonon-drag TEP dip will be shifted towards $T_d \approx 30$ K, independently of the magnetic field strength. Finally, for $T < T_d$, $|S_{ph}(0)|$ is expected to vary exponentially with temperature like the Einstein function $C_{ph}(\omega_K/T)$, ω_K being the Kohn phonon frequency (Jay-Gerin and Maynard 1970). Therefore, $|S(H)|$ varies with temperature as $T^{-2}C_{ph}(\omega_K/T)$. On the other hand, $S(H)$ behaves like R_H as a function of magnetic field, and thus shows a H^2 dependence. All these conclusions are supported by the experiments of Takezawa, Tsuzuku, Ono, and Hishiyama (1971).

We now consider the NE coefficient in the same limit of low temperatures. Here, the term arising from $[\chi_{xx}]_{ph}$ in [18] may be neglected, and $A_{NE}(H)$ becomes simply

$$A_{NE}(H) \approx -(n|e|c/H^2)\rho_{xx}|S_{ph}(0)| \quad [19]$$

Equation 19 gives a negative sign for $A_{NE}(H)$ in agreement with the observations of Tamarin, Shalyt, and Volga (1969). According to Soule (1958), ρ_{xx} is found to fall off with increasing temperature as about T^{-1}, $|A_{NE}(H)|$ is thus expected to vary with temperature like $T^{-1}C_{ph}(\omega_K/T)$. Such a behavior predicts a shift of the position of the phonon-drag dip—which arises from $|S_{ph}(0)|$—from 40 K towards lower temperatures. This agrees quite well with the experimental measurements of Tamarin, Shalyt, and Volga (1969), who found a sharp phonon-drag minimum for $A_{NE}(H)$ at a temperature between 30 and 35 K. On the other hand, $A_{NE}(H)$ behaves like ρ_{xx}/H^2

as a function of magnetic field. But, below about 50 K, ρ_{xx} has not a simple field dependence (Soule 1958; Spain, Ubbelohde, and Young 1967). For instance, for Soule's crystal EP 7 at $T = 4.2$ K, ρ_{xx} continuously changes from about a H^2 dependence at low fields to a $H^{0.8}$ dependence at 25 kOe. Accordingly, $A_{NE}(H)$ is expected to vary with magnetic field like H^n, where $-1.2 < n < 0$. Such a variation is in general agreement with the observations of Tamarin, Shalyt, and Volga (1969).

Let us now discuss the behavior of $S(H)$ and of $A_{NE}(H)$ at high temperatures, namely $T > 30$ K. In this temperature region, the previous inequality $(\bar{\mu}H/c)^2 \gg 1$ may no longer be satisfied, and we must go back to [15] and [16] to explain the experimental TEP and NE coefficient measurements. Using the relation

$$\rho_{xx} \simeq \rho_0[1 + (\bar{\mu}H/c)^2] \quad [20]$$

where ρ_0 is the zero-field resistivity, we obtain for the TEP

$$S(H) \simeq n|e|c\left[R_H \frac{(\bar{\mu}H/c)^2}{1 + (\bar{\mu}H/c)^2}|S_{ph}(0)| + \frac{\rho_0}{H}(\bar{\mu}H/c)S_{ph}(0)\right] \quad [21]$$

where $|R_H|$ is going with temperature as about T^{-2} and ρ_0 roughly varies as $T^{1.2}$. According to Jay-Gerin and Maynard (1970), $|S_{ph}(0)|$ behaves like T^{-1} for T above the temperature of the phonon-drag dip as a result of the weakening of the carrier–phonon interaction on account of the thermal smearing of the Fermi surface. Thus, if the limit $(\bar{\mu}H/c)^2 \gg 1$ is assumed to be exact, $|S(H)|$ goes about as T^{-3}. But, as we see from [21], it clearly appears that we may expect a still higher temperature dependence for $S(H)$ above 30 K when this inequality is no longer satisfied. In other words, the behavior of $S(H)$ is linked very sensitively with the magnitude of $(\bar{\mu}H/c)^2$ with respect to unity. What it means, physically, is that the purity and the quality of the sample of graphite used play a prominent role as far as the temperature dependence of $S(H)$ above the temperature of the phonon-drag peak is concerned. Actually, it may be concluded from this analysis that $|S(H)|$ decreases as T^{-m} above 30 K, with $3 < m < 5.5$ depending on the properties of the sample. If the sample is pure and of good quality, $m \to 3$. It should be noted here that Sugihara (1970) and Sugihara *et al.* (1971, 1972) give a T^{-5} temperature dependence for $S(H)$ for $T > 30$ K. Their calculations, however, take the anharmonic phonon–phonon scattering into account for explaining the decrease of $|S_{ph}(0)|$ in this region. We do not believe that the phonon–phonon interaction plays any primary part here. The present study seems to confirm our expectation. Experimentally, Takezawa, Tsuzuku, Ono, and Hishiyama (1971) reported a $\approx T^{-4.3}$ dependence for $|S(H)|$ above 30 K. But, without any information about the quality of their sample, it is difficult to compare their measurements with our results.

Finally, let us turn our attention to the behavior of $A_{NE}(H)$ for $T > 30$ K. Using [20], we obtain from [16]

$$A_{NE}(H) \approx -(n|e|c/H^2)(\bar{\mu}H/c)^2\rho_0|S_{ph}(0)| \quad [22]$$

In deriving [22], we have again neglected the small contribution due to $[\chi_{xx}]_{ph}$. Unlike $S(H)$, the temperature dependence of $A_{NE}(H)$ is quite well determined. We find a $T^{-2.2}$ behavior above the temperature of the phonon-drag dip. As a function of field, $A_{NE}(H)$ varies like ρ_{xx}/H^2. According to Soule (1958), ρ_{xx} behaves like $H^{1.8}$ above 50 K, and thus induces a $H^{-0.2}$ field dependence for $A_{NE}(H)$. These results are in excellent agreement with the measurements of Tamarin, Shalyt, and Volga (1969).

Acknowledgments

The author is grateful to Professor P. R. Wallace for his generous hospitality and for his constant interest in this work. He would like to thank Dr. R. Maynard for suggesting this problem to him and Dr. J. Sanders for a critical reading of the manuscript.

ARGYRES, P. N. 1958. Phys. Rev. **109**, 1115.

ARKHIPOV, R. G., KECHIN, V. V., LIKHTER, A. I., and POSPELOV, YU. A. 1963. Zh. Eksp. Teor. Fiz. **44**, 1964 (Engl. transl.: 1963. Sov. Phys.—JETP, **17**, 1321).

BLATT, F. J. 1957. Solid State Phys. **4**, 199.
DELHAES, P., LEMERLE, M. Y., and BLONDÉ-GONDÉ, G. 1971. C.R. Acad. Sci. Paris, **272**, 1285.
DREYFUS, B. and MAYNARD, R. 1967. J. Phys. **28**, 955.
DUGDALE, J. S. and BAILYN, M. 1967. Phys. Rev. **157**, 485.
FARAG, B. S. 1968. Ph.D. Thesis, The University of Tokyo, Tokyo, Japan.
HERRING, C., GEBALLE, T. H., and KUNZLER, J. E. 1958. Phys. Rev. **111**, 36.
JAY-GERIN, J. P. and MAYNARD, R. 1970. J. Low Temp. Phys. **3**, 377.
KINCHIN, G. H. 1953. Proc. Roy. Soc. (London) A, **217**, 9.
KLEIN, C. A. 1964. J. Appl. Phys. **35**, 2947.
KOHN, W. 1959. Phys. Rev. Lett. **2**, 393.
MCCLURE, J. W. 1956. Phys. Rev. **101**, 1642.
——— 1958. Phys. Rev. **112**, 715.
ONO, S. and SUGIHARA, K. 1966. J. Phys. Soc. Jap. **21**, 861.
PURI, S. M. 1965. Phys. Rev. **139**, A995.
RASOR, N. S. 1955. Nuclear engineering and manufacturing (N.A.A., Downey, California).
RED'KO, N. A. and SHALYT, S. S. 1968. Fiz. Tverd. Tela, **10**, 1557 (Engl. transl.: 1968. Sov. Phys.—Solid State, **10**, 1233).
SOULE, D. E. 1958. Phys. Rev. **112**, 698.
SOULE, D. E., MCCLURE, J. W., and SMITH, L. B. 1964. Phys. Rev. **134**, A453.
SPAIN, I. L. 1970. J. Chem. Phys. **52**, 2763.
SPAIN, I. L., UBBELOHDE, A. R., and YOUNG, D. A. 1967. Phil. Trans. Roy.Soc. (London), **262**, 345.
SUGIHARA, K. 1969. J. Phys. Soc. Jap. **27**, 356.
——— 1970. J. Phys. Soc. Jap. **29**, 1465.
SUGIHARA, K. and SATO, H. 1963. J. Phys. Soc. Jap. **18**, 332.
SUGIHARA, K., TAKEZAWA, T., TSUZUKU, T., HISHIYAMA, Y., and ONO, A. 1971. Proceedings of the Tenth Biennial Conference on Carbon, Bethlehem, Pennsylvania, p. 305.
——— 1972. J. Phys. Chem. Solids. **33**, 1475.
TAMARIN, P. V., SHALYT, S. S., and VOLGA, V. I. 1969. Fiz. Tverd. Tela, **11**, 1725 (Engl. transl.: 1969. Sov. Phys.—Solid State, **11**, 1399).
TAKEZAWA, T., TSUZUKU, T., ONO, A., and HISHIYAMA, Y. 1969. Phil. Mag. **19**, 623.
——— 1971. Phil. Mag. **23**, 1241.
TSUZUKU, T., TAKEZAWA, T., HISHIYAMA, Y., and ONO, A. 1972. Phil. Mag. **25**, 929.
WILLIAMSON, S. J., FONER, S., and DRESSELHAUS, M. S. 1965. Phys. Rev. **140**, A1429.
WOOLLAM, J. A. 1971. Phys. Rev. B, **3**, 1148.
ZIMAN, J. M. 1965. Principles of the theory of solids (Cambridge University Press, Cambridge), p. 194.

APPENDICE

Les équations de transport en présence d'un champ magnétique $\vec{H}$ s'écrivent, d'une manière très générale (Ziman 1965),

$$\vec{E} = \rho\vec{J} + S\,\vec{\nabla}T \qquad (1)$$

$$\vec{U} = \pi\vec{J} - \kappa\,\vec{\nabla}T, \qquad (2)$$

ou encore, sous une forme équivalente,

$$\vec{J} = \sigma\vec{E} - \beta\,\vec{\nabla}T \qquad (3)$$

$$\vec{U} = \chi\vec{E} - \kappa\,\vec{\nabla}T. \qquad (4)$$

Dans ces expressions, $\vec{J}$ désigne la densité de courant électrique, $\vec{E}$ le champ électrique, $\vec{\nabla}T$ le gradient de température et $\vec{U}$ la densité de courant de chaleur. Les divers coefficients $\rho(\vec{H})$ (magnétorésistance), $S(\vec{H})$ (pouvoir thermoélectrique), $\pi(\vec{H})$ (coefficient Peltier), $\kappa(\vec{H})$ (conductivité thermique), $\sigma(\vec{H})$ (magnétoconductivité), $\beta(\vec{H})$ et $\chi(\vec{H})$ sont, en fait, des tenseurs et sont reliés par les relations de Onsager de la thermodynamique des processus irréversibles (Onsager 1931)

$$\rho_{ij}(\vec{H}) = \rho_{ji}(-\vec{H}) \qquad (5)$$

$$\kappa_{ij}(\vec{H}) = \kappa_{ji}(-\vec{H}) \qquad (6)$$

$$S_{ij}(\vec{H}) = \frac{1}{T}\,\pi_{ji}(-\vec{H}), \qquad (7)$$

et

$$\sigma_{ij}(\vec{H}) = \sigma_{ji}(-\vec{H}) \qquad (8)$$

$$T\,\beta_{ij}(\vec{H}) = \chi_{ji}(-\vec{H}). \qquad (9)$$

A partir de la relation (1), l'équation de définition du pouvoir thermoélectrique S s'écrit

$$\vec{E} = S\,\vec{\nabla}T, \qquad (10)$$

avec la condition auxiliaire $\vec{J} = 0$. Supposons que la direction Oz coïncide avec la direction du champ magnétique $\vec{H}$ et considérons le cas particulier où il existe un gradient de température $\vec{\nabla}T$ suivant la direction Ox. L'équation (3) donne alors :

$$J_x = \sigma_{xx} E_x + \sigma_{xy} E_y - \beta_{xx} \nabla_x T \qquad (11)$$

$$J_y = \sigma_{yx} E_x + \sigma_{yy} E_y - \beta_{yx} \nabla_x T \quad , \qquad (12)$$

où E_x et E_y sont les composantes du champ électrique $\vec{E}$, qui apparaît transversalement à $\vec{H}$. La condition de courant électrique nul, $\vec{J} = 0$, signifie à la fois $J_x = 0$, ce qui entraîne la relation

$$\sigma_{xx} \frac{E_x}{\nabla_x T} = - \sigma_{xy} \frac{E_y}{\nabla_x T} + \beta_{xx} \quad , \qquad (13)$$

et $J_y = 0$, ce qui conduit à la relation

$$\frac{E_y}{\nabla_x T} = \frac{\beta_{yx}}{\sigma_{yy}} - \frac{\sigma_{yx}}{\sigma_{yy}} \frac{E_x}{\nabla_x T} \quad . \qquad (14)$$

En éliminant la quantité $\frac{E_y}{\nabla_x T}$ entre les équations (13) et (14), nous obtenons directement l'expression du pouvoir thermoélectrique :

$$S(H) = S_{xx} = \frac{E_x}{\nabla_x T} = \frac{\sigma_{yy}\beta_{xx} - \sigma_{xy}\beta_{yx}}{\sigma_{xx}\sigma_{yy} - \sigma_{xy}\sigma_{yx}} \quad . \qquad (15)$$

Notons qu'en l'absence de champ magnétique, cette expression se réduit à

$$S(0) = \frac{\beta_{xx}(0)}{\sigma_{xx}(0)} \quad ,$$

qui n'est autre que la relation $\frac{1}{T}\left(\frac{U_x}{J_x}\right)_{\vec{\nabla}T \equiv 0}$ rencontrée au chapitre III.

L'effet Nernst-Ettingshausen se manifeste traditionnellement par l'apparition d'un champ électrique normal au gradient de température en présence d'un champ magnétique transverse, en analogie avec la configuration de l'effet Hall. L'équation de définition du coefficient Nernst-Ettingshausen A_{NE} s'écrit

$$\vec{E} = A_{NE}(\vec{H} \wedge \vec{\nabla}T), \qquad (16)$$

avec la condition auxiliaire $\vec{J} = 0$. Considérons à nouveau le cas particulier où $\vec{H}//Oz$ et $\vec{\nabla}T//Ox$. En éliminant la quantité $\frac{E_x}{\nabla_x T}$ entre les équations (13) et (14), nous obtenons immédiatement :

$$A_{NE}(H) = \frac{E_y}{H \nabla_x T} = \frac{\sigma_{xx}\beta_{yx} - \sigma_{yx}\beta_{xx}}{H(\sigma_{xx}\sigma_{yy} - \sigma_{xy}\sigma_{yx})} \quad . \qquad (17)$$

Dans le cas du graphite, pour des champs magnétiques $\vec{H}$ parallèles à l'axe de haute

symétrie c, nous avons les relations supplémentaires :

$$\sigma_{xx} = \sigma_{yy} \ , \tag{18}$$

$$\sigma_{xy} = - \sigma_{yx} \ , \tag{19}$$

et pour le tenseur de magnétorésistivité $\rho = \sigma^{-1}$

$$\rho_{xx} = \frac{\sigma_{xx}}{\sigma_{xx}^2 + \sigma_{xy}^2} \ , \tag{20}$$

$$\rho_{xy} = \frac{- \sigma_{xy}}{\sigma_{xx}^2 + \sigma_{xy}^2} \ . \tag{21}$$

En utilisant les relations (18) - (21) avec la relation (9), nous pouvons réécrire $S(H)$ et $A_{NE}(H)$ sous la forme :

$$S(H) = \frac{1}{T} \left[\rho_{xx}\chi_{xx}(-H) + \rho_{xy}\chi_{xy}(-H)\right] \tag{22}$$

$$A_{NE}(H) = \frac{1}{TH} \left[\rho_{xx}\chi_{xy}(-H) - \rho_{xy}\chi_{xx}(-H)\right] . \tag{23}$$

Il est intéressant de remarquer ici l'avantage que présentent, par rapport aux expressions (15) et (17), les expressions (22) et (23) : en effet, pour les premières, il est nécessaire de considérer simultanément les effets du champ électrique et du gradient de température ("approche-Seebeck"), tandis que pour les secondes, il suffit de résoudre un problème de conduction purement électrique en supposant que le gradient de température est identiquement nul ("approche-Peltier"). Il convient également de noter les propriétés, extrêmement utiles sur le plan expérimental :

$$S(-H) = S(H) \ , \tag{24}$$

$$A_{NE}(-H) = -A_{NE}(H) \ , \tag{25}$$

Celles-ci nous enseignent qu'un renversement du champ magnétique change le signe de la force électromotrice Nernst-Ettingshausen, mais laisse inchangé le signe de la force électromotrice Seebeck.

BIBLIOGRAPHIE

A.M. AFANAS'EV and Yu. KAGAN : Zh. Eksperim. i Teor. Fiz. 43, 1456 (1962) [English transl. : Soviet Phys. - JETP 16, 1030 (1963)].

P.N. ARGYRES : Phys. Rev. 109, 1115 (1958).

R.D. BARNARD : "Thermoelectricity in Metals and Alloys" (Taylor and Francis Ltd., London, 1972).

L. BOCHIROL and E. BONJOUR : Carbon 6, 661 (1968).

H.B.G. CASIMIR : Physica 5, 495 (1938).

A.P. CRACKNELL : "The Fermi Surfaces of Metals" (Taylor and Francis Ltd., London, 1971), p. 74.

A. DE COMBARIEU : J. Physique 28, 951 (1967).

A. DE COMBARIEU : Centre d'Etudes Nucléaires, Grenoble, communication privée.

P. DELHAÈS : Communication privée (1974).

M.S. DRESSELHAUS and J.G. MAVROIDES : IBM J. Res. Develop. 8, 262 (1964).

M.S. DRESSELHAUS : 12th Intern. Conf. on the Physics of Semiconductors (Stuttgart, Fed. Rep. Germany, July 15-19, 1974).

M.S. DRESSELHAUS : Communication privée (1974).

B. DREYFUS et R. MAYNARD : J. Physique 28, 955 (1967).

Le Groupe Français d'Etude des Carbones : "Les Carbones" (Masson et C^{ie}, Paris, 1965), vol. 1.

L. GUREVICH : J. Phys. (Moscow) 9, 477 (1945).

L. GUREVICH : J. Phys. (Moscow) 10, 67 (1946).

R.R. HAERING and S. MROZOWSKI : "Progress in Semiconductors" (Heywood and Company Ltd., London, 1960), vol. 5, p. 273.

C. HERRING : Phys. Rev. 95, 954 (1954).

C. HERRING, T.H. GEBALLE, and J.E. KUNZLER : Phys. Rev. 111, 36 (1958).

T. IWATA, F.E. FUJITA, and H. SUZUKI : J. Phys. Soc. Japan 16, 197 (1961).

M.I. KAGANOV and A.I. SEMENENKO : Zh. Eksperim. i Teor. Fiz. 50, 630 (1966) [English transl. : Soviet Phys. - JETP 23, 419 (1966)].

M.I. KAGANOV and A.I. SEMENENKO : Fiz. Tverd. Tela 9, 1129 (1967) [English transl. : Soviet Phys. - Solid State 9, 884 (1967)].

B.T. KELLY and R. TAYLOR : "The thermal Properties of Graphite", in "Chemistry and Physics of Carbon", edited by P.L. WALKER, Jr. and P.A. THROWER (Marcel Dekker, Inc. New York, 1973), vol. 10, p. 1.

W. KOHN : Phys. Rev. Letters 2, 393 (1959).

K. KOMATSU and T. NAGAMIYA : J. Phys. Soc. Japan 6, 438 (1951).

K. KOMATSU : J. Phys. Soc. Japan 10, 346 (1955).

D.K.C. MAC DONALD : "Thermoelectricity : An Introduction to the Principles" (John Wiley and Sons, New York, 1962).

J.W. Mc CLURE : Phys. Rev. 108, 612 (1957).

J.W. Mc CLURE : Phys. Rev. 119, 606 (1960).

J.W. Mc CLURE and Y. YAFET : "Proceedings of the Fifth Conference on Carbon" (Pergamon Press, New York, 1962), vol. 1, p. 22.

J.W. Mc CLURE : IBM Journal of Research and Development 8, 255 (1964).

J.W. Mc CLURE : J. Phys. Chem. Solids 32, sup. # 1, 127 (1971).

R. MAYNARD : Thèse de Doctorat ès Sciences Physiques, présentée à la Faculté des Sciences de l'Université de Grenoble (1967).
J.J. MILLS, R.A. MORANT, and D.A. WRIGHT : Brit. J. Appl. Phys. 6, 479 (1965).
T. NAGAMIYA and K. KOMATSU : J. Chem. Phys. 22, 1457 (1954).

P. NOZIÈRES : Phys. Rev. 109, 1510 (1958).

S. ONO and K. SUGIHARA : J. Phys. Soc. Japan 21, 861 (1966).

S. ONO and K. SUGIHARA : J. Phys. Soc. Japan 24, 818 (1968).

L. ONSAGER : Phys. Rev. 37, 405 (1931).

L. ONSAGER : Phys. Rev. 38, 2265 (1931).

A. PACAULT : "Propriétés Electroniques des Pyrocarbones", dans "Les Carbones" (Masson et C^{ie}, Paris, 1965), vol. 1, p. 479.

D. PINES : "Elementary Excitations in Solids" (W.A. Benjamin, Inc., New York, Amsterdam, 1964).

N.S. RASOR : Nuclear Engineering and Manufacturing N.A.A., Downey, California (1955).

W.N. REYNOLDS : "Radiation Damage in Graphite" in "Chemistry and Physics of Carbon", edited by P.L. WALKER, Jr. (Marcel Dekker, Inc. New York, 1966), vol. 2, p. 121.

W.N. REYNOLDS : "Physical Properties of Graphite" (Elsevier Publishing Co. Ltd., London, 1968).

D. ROUBY ; Thèse de Doctorat d'Etat, Lyon, 1974.

P.R. SCHROEDER, M.S. DRESSELHAUS, and A. JAVAN : Phys. Rev. Letters 20, 1292 (1968).

M.P. SHARMA, L.G. JOHNSON, and J.W. Mc CLURE : Phys. Rev. B9, 2467 (1974).

J.H.W. SIMMONS : "Radiation Damage in Graphite" (Pergamon Press, New York, 1965).

J.C. SLONCZEWSKI and P.R. WEISS : Phys. Rev. 109, 272 (1958).

D.E. SOULE : Phys. Rev. 112, 698 (1958).

D.E. SOULE, J.W. Mc CLURE, and L.B. SMITH : Phys. Rev. 134, A453 (1964).

I.L. SPAIN, A.R. UBBELOHDE, and D.A. YOUNG : Phil. Trans. Roy. Soc. London 262, 345 (1967).

I.L. SPAIN : "The Electronics Properties of Graphite", in "Chemistry and Physics of Carbon", edited by P.L. WALKER, Jr. and P.A. THROWER (Marcel Dekker, Inc. New York, 1973), vol. 8, p. 1.

K. SUGIHARA and H. SATO : J. Phys. Soc. Japan 18, 332 (1963).

K. SUGIHARA, T. TAKEZAWA, T. TSUZUKU, Y. HISHIYAMA, and A. ONO : J. Phys. Chem. Solids 33, 1475 (1972).

T. TAKEZAWA, T. TSUZUKU, A. ONO, and Y. HISHIYAMA : Phil. Mag. 19, 623 (1969).

T. TAKEZAWA, T. TSUZUKU, A. ONO, and Y. HISHIYAMA : Phil. Mag. 23, 1241 (1971).

T. TAKEZAWA, J.H. MANGEZ, C.R. HEWES, M.S. DRESSELHAUS, and T. TSUZUKU : 1973 March Meeting of the American Physical Society, San Diego, California.

P.V. TAMARIN, S.S. SHALYT, and V.I. VOLGA : Fiz. Tverd. Tela 11, 1725 (1969) [English Transl. : Soviet Phys. - Solid State 11, 1399 (1969)].

P.L. TAYLOR : Phys. Rev. 131, 1995 (1963).

P.L. TAYLOR : "A Quantum Approach to the Solid State" (Prentice-Hall, Inc., Englewood Cliffs, New Jersey, 1970), p. 178.

W.W. TOY, C.R. HEWES, and M.S. DRESSELHAUS : Carbon 11, 575 (1973).

T. TSUZUKU, T. TAKEZAWA, Y. HISHIYAMA, and A. ONO : Phil. Mag. 25, 929 (1972).

P.R. WALLACE : Phys. Rev. 71, 622 (1947).

P.R. WALLACE : Solid State Commun. 4, 521 (1966).

S.J. WILLIAMSON, S. FONER, and M.S. DRESSELHAUS : Phys. Rev. 140, A1429 (1965).

E.J. WOLL and W. KOHN : Phys. Rev. 126, 1693 (1962).

J.M. ZIMAN : Advanc. Phys. 10, 1 (1961).

J.M. ZIMAN : "Principles of the Theory of Solids" (Cambridge University Press, Cambridge, 1965).

PARTIE II

ETUDE DE LA "TRANSITION STATISTIQUE" PAR UN CHAMP MAGNETIQUE INTENSE DANS LES SEMICONDUCTEURS EN REGIME EXTREME QUANTIQUE

RESUME

Le thème central de la seconde partie de ce travail est d'examiner le comportement des électrons de conduction d'un semiconducteur en "régime extrême quantique", c'est-à-dire lorsqu'il ne reste plus qu'un seul niveau de Landau occupé par les électrons en dessous du niveau de Fermi. En régime extrême quantique, la distribution électronique est régie principalement par la position du niveau de Fermi ζ par rapport au bas de la sous-bande de Landau fondamentale $\frac{1}{2}\hbar\omega_c$. Lorsque la "largeur" de la bande remplie ($\zeta - \frac{1}{2}\hbar\omega_c$) devient inférieure à l'épaisseur k_BT du "flou" thermique au niveau de Fermi, la statistique de Fermi-Dirac évolue vers la statistique classique de Maxwell-Boltzmann. A partir de cette idée, nous avons étudié les modifications qui apparaissent, par suite du changement de statistique et de dimensionalité des électrons en champs magnétiques intenses, dans la chaleur spécifique électronique, le coefficient d'effet magnétothermique $(\frac{\partial T}{\partial H})_S$ et les coefficients de transport tels que le pouvoir thermoélectrique (contributions de "diffusion" électronique et de "phonon-drag") et le coefficient Nernst-Ettingshausen.

CHAPITRE I

GAZ D'ELECTRONS "LIBRES"
DANS UN CHAMP MAGNETIQUE INTENSE
A TRES BASSES TEMPERATURES
(TRAITEMENT DE LANDAU)

Les différentes caractéristiques thermodynamiques d'un conducteur -métal ou semiconducteur-, ainsi que ses propriétés de transport, peuvent, sous certaines conditions, être radicalement modifiées à basses températures par l'application d'un champ magnétique intense.

Ces modifications sont la conséquence directe de l'effet de la quantification du mouvement orbital des électrons dans un champ magnétique.

Classiquement, il est bien connu (voir, par exemple, Landau et Lifshitz 1951) qu'un électron de charge e et de masse effective m^*, soumis à un champ magnétique uniforme constant $\vec{H}$ parallèle à l'axe Oz, décrit une hélice dont l'axe est dirigé suivant le champ. La projection du mouvement dans un plan perpendiculaire au champ est un mouvement circulaire de rayon arbitraire et de vitesse angulaire

$$\omega_c = \frac{|e|\,H}{m^*_c} , \qquad (I\text{-}1)$$

la fréquence cyclotron. A ce mouvement périodique en mécanique classique correspond des niveaux d'énergie discrets en mécanique quantique, appelés "niveaux de Landau". En d'autres termes, seuls certains rayons deviennent possibles pour les orbites circulaires électroniques. Les effets de Haas-van Alphen (variation oscillatoire de la susceptibilité magnétique avec l'inverse du champ magnétique) et Shubnikov-de Haas (oscillations de magnétorésistance) donnent une remarquable démonstration de la quantification de Landau des niveaux d'énergie des électrons dans un conducteur en champ magnétique élevé.

Pour décrire le mouvement orbital quantifié d'un électron dans un champ magnétique $\vec{H}$, il est nécessaire d'introduire le potentiel vecteur $\vec{A}$ de $\vec{H}$, tel que $\vec{H} = \overrightarrow{rot}\,\vec{A}$. Considérons le modèle simple d'une bande d'énergie parabolique et isotrope dans l'espace des moments, caractérisée par la masse effective m^* (approximation de masse effective). Un tel modèle est parfaitement approprié dans l'étude des composés III-V semiconducteurs ayant des concentrations suffisamment faibles en électrons. En l'absence de champ magnétique, l'énergie est :

$$E(\vec{p}) = \frac{1}{2\,m^*}\,(p_x^2 + p_y^2 + p_z^2) , \qquad (I\text{-}2)$$

où p_x, p_y et p_z sont les composantes du moment $\vec{p}$ de l'électron. L'Hamiltonien magnétique correspondant $\mathcal{H}$ est donné par (Landau 1930)

$$\mathcal{H} = \frac{1}{2\,m^*}\left(\vec{p} - \frac{e}{c}\vec{A}\right)^2 . \qquad \text{(I-3)}$$

En choisissant le potentiel vecteur $\vec{A}$ du champ uniforme $\vec{H}$ // Oz sous la forme (jauge de Landau)

$$A_x = 0, \quad A_y = Hx, \quad A_z = 0 , \qquad \text{(I-4)}$$

l'Hamiltonien $\mathcal{H}$ devient :

$$\mathcal{H} = \frac{1}{2\,m^*}\left[p_x^2 + (p_y + m^*\omega_c x)^2 + p_z^2\right] , \qquad \text{(I-5)}$$

où ω_c est la fréquence cyclotron définie Eq.(I-1). Pour un cristal de dimensions L_y et L_z respectivement dans les directions Oy et Oz, et de dimension infinie dans la direction Ox, les fonctions propres de $\mathcal{H}$ sont (voir, par exemple, les mises au point de Roth et Argyres 1966, de Slater 1967 et d'Askenazy 1973) :

$$\psi_{n,k_y,k_z}(\vec{r}) = (L_y L_z)^{-\frac{1}{2}}\,\phi_n\left[x - x_o(k_y)\right]\,e^{i(k_y y + k_z z)} , \qquad \text{(I-6)}$$

où k_y et k_z sont les nombres d'onde associés avec les composantes y et z du mouvement de l'électron, n est un nombre quantique qui peut prendre les valeurs 0,1,2,3,..., et $\phi_n\left[x - x_o(k_y)\right]$ sont les fonctions d'onde normalisées d'un oscillateur harmonique à une dimension de fréquence ω_c et centré au point :

$$x_o = -\frac{\hbar}{m^*\omega_c}\,k_y . \qquad \text{(I-7)}$$

Les valeurs propres de $\mathcal{H}$ associées avec les fonctions d'onde $\psi_{n,k_y,k_z}(\vec{r})$ sont :

$$\varepsilon_{n,k_z} = \left(n + \frac{1}{2}\right)\hbar\omega_c + \frac{\hbar^2}{2\,m^*}\,k_z^2 , \qquad \text{(I-8)}$$

où le premier terme est l'énergie quantifiée correspondant au mouvement de l'électron dans le plan xy perpendiculairement à $\vec{H}$ et le second est l'énergie cinétique due au mouvement (libre) de l'électron parallèlement à $\vec{H}$. Ainsi, en présence d'un champ magnétique uniforme, la bande est clivée en une série de sous-bandes unidimensionnelles (sous-bandes de Landau), chaque sous-bande étant identifiée par le nombre quantique "orbital" n. En particulier, à la sous-bande de Landau fondamentale, n = 0, corres-

pond une énergie de l'électron :

$$\epsilon_{0,k_z} = \frac{1}{2}\hbar\omega_c + \frac{\hbar^2}{2\,m^*}k_z^2 \qquad \text{(I-9)}$$

et une fonction d'onde :

$$\psi_{0,k_y,k_z}(\vec{r}) = (L_y L_z)^{-\frac{1}{2}}\,(\pi\, r_c^2)^{-\frac{1}{4}}\, e^{-\frac{1}{2}\left(\frac{x + r_c^2 k_y}{r_c}\right)^2}\, e^{i(k_y y + k_z z)}\,, \qquad \text{(I-10)}$$

où

$$r_c^2 = \frac{\hbar}{m^*\omega_c} = \frac{\hbar c}{|e|\,H} \qquad \text{(I-11)}$$

est le rayon cyclotron classique pour l'électron dans son état fondamental. La nature du spectre électronique en présence d'un champ magnétique est illustrée Figs.(1) et (2).

Chaque sous-bande (niveau) de Landau possède un haut degré de dégénérescence : ceci apparaît clairement dans le fait que l'énergie (Eq.(I-8)) ne dépend pas du nombre quantique k_y. Le nombre d'états dégénérés peut être déterminé en introduisant des conditions aux limites périodiques dans la direction Oy (k_y peut alors prendre toutes les valeurs multiples de $2\pi/L_y$) et en tenant compte du fait que le "centre" de l'oscillateur doit rester à l'intérieur du volume occupé par le cristal (seules sont alors permises les valeurs de k_y telles que $0 \leqslant x_o = (-\hbar k_y/m^*\omega_c) \leqslant L_x$, où L_x est la dimension du cristal dans la direction Ox). Ainsi, pour une énergie donnée ϵ (c'est-à-dire, pour une valeur du nombre quantique n et une de k_z), le nombre total d'états k_y possibles est égal à :

$$\frac{m^*\omega_c}{2\pi\hbar} L_x L_y \,.$$

Ce résultat peut être utilisé pour obtenir l'expression de la densité d'états en présence d'un champ magnétique. Considérons en effet, pour n fixé, l'intervalle de nombre d'onde dk_z, compris entre k_z et k_z+dk_z. En introduisant des conditions aux limites périodiques dans la direction Oz (les valeurs permises de k_z sont alors toutes les valeurs multiples de $2\pi/L_z$), nous trouvons aisément que le nombre d'états électroniques possibles dans l'intervalle dk_z est donné par :

$$\frac{\mathcal{V}}{(2\pi)^2}\,\frac{m^*\omega_c}{\hbar}\,dk_z \,,$$

où $\mathcal{V} = L_x L_y L_z$ est le volume du cristal.

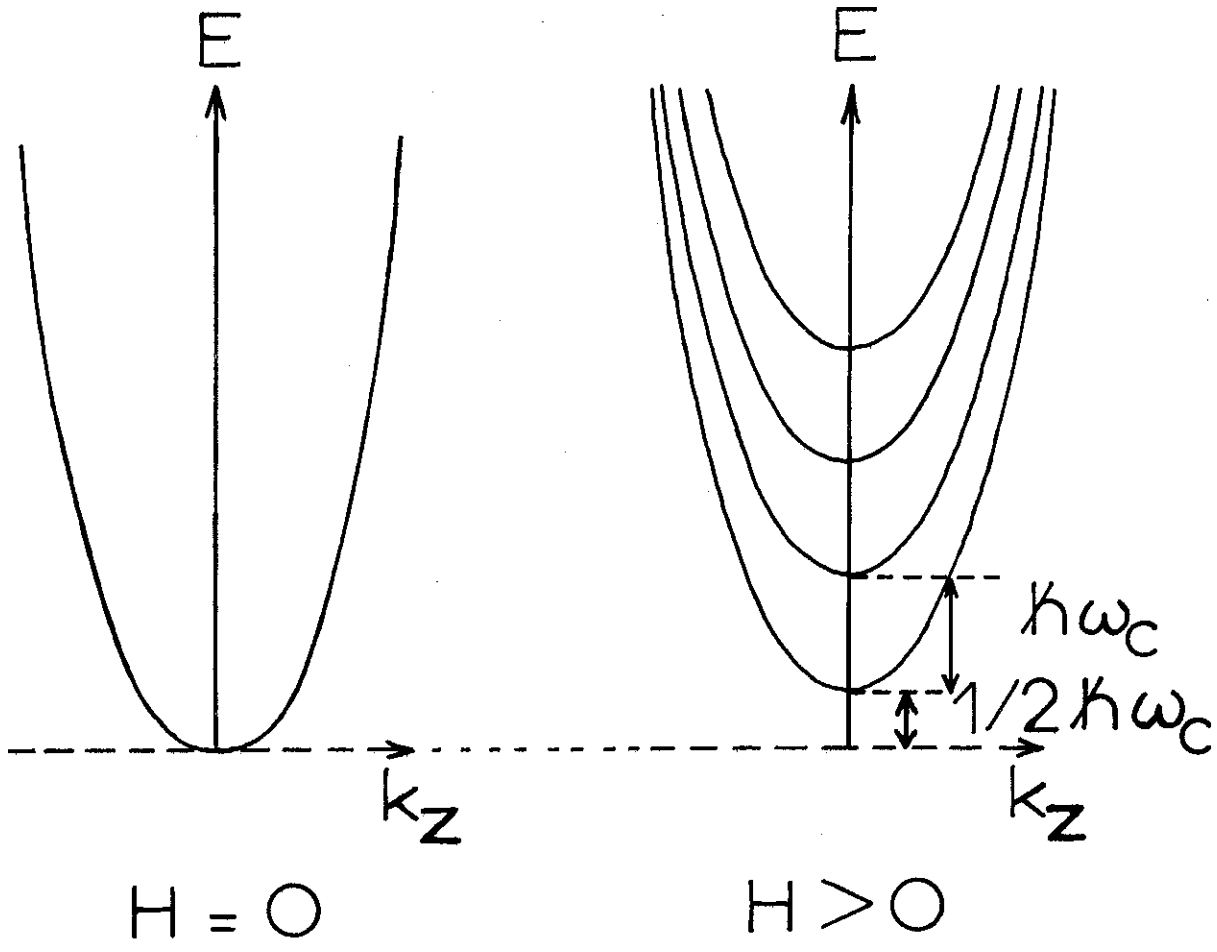

Fig. 1

Sous - bandes de Landau

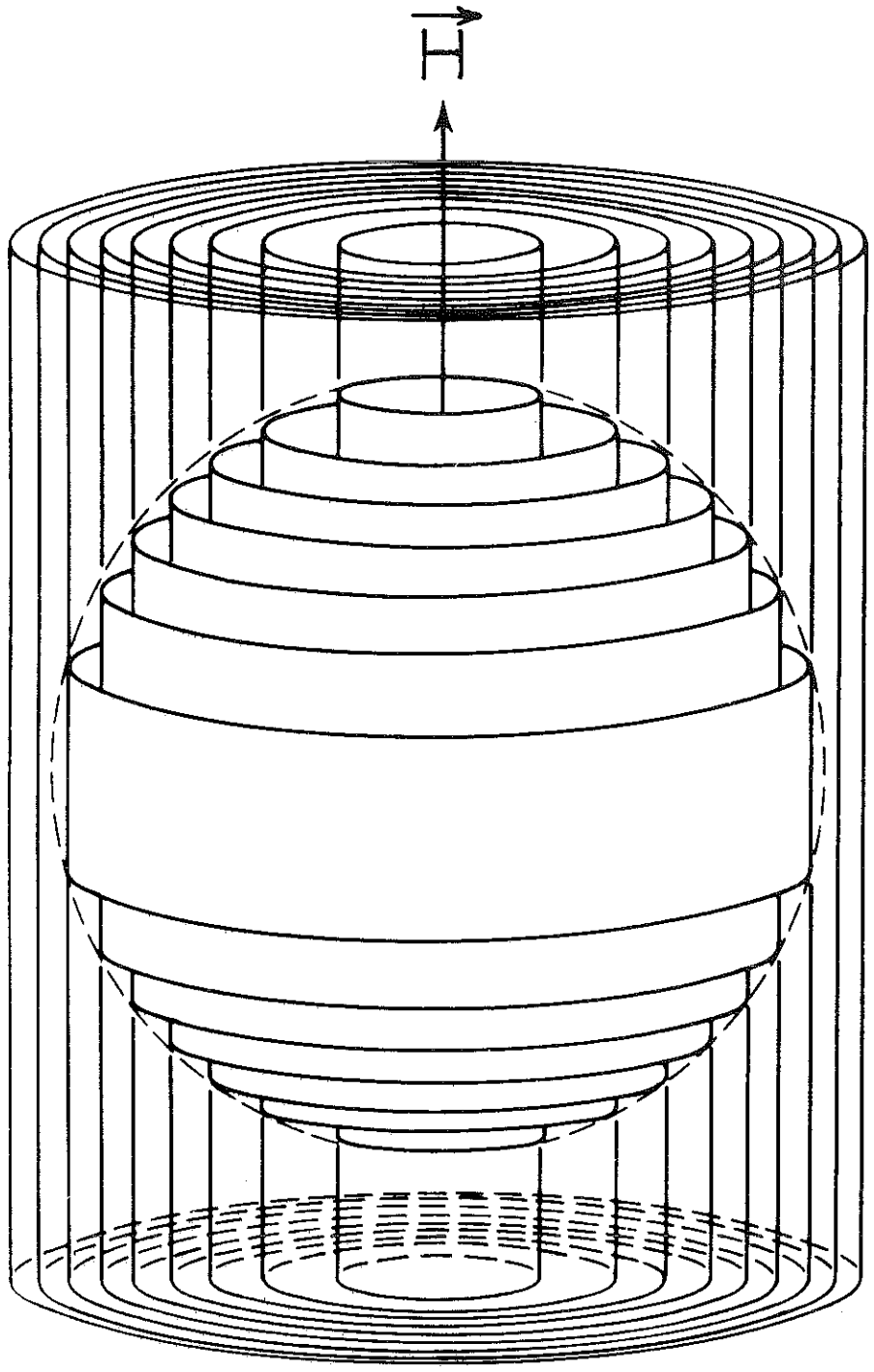

Fig. 2

Magnetic quantization of a spherical constant energy surface in $\vec{k}$-space into discrete, concentric cylinders whose axes are parallel to the magnetic field. The dashed circle represents the Fermi surface.
(From H.M. Rosenberg, "Low Temperature Solid State Physics", p. 352, Oxford University Press, London, 1963).

Le nombre d'états possibles dans l'intervalle d'énergie dε, compris entre ε et ε+dε est alors, pour la sous-bande de Landau n :

$$2 \frac{\mathcal{V}}{(2\pi)^2} \frac{m^* \omega_c}{\hbar} \left(\frac{dk_z}{d\varepsilon}\right) d\varepsilon ,$$

où, compte-tenu de l'équation (I-8),

$$\left(\frac{dk_z}{d\varepsilon}\right) = \frac{1}{2} \left(\frac{2m^*}{\hbar^2}\right)^{1/2} \left[\varepsilon - \left(n+\frac{1}{2}\right) \hbar\omega_c\right]^{-1/2} .$$

En additionnant les contributions de toutes les sous-bandes de Landau n permises, nous obtenons pour la densité d'états $\mathcal{D}(\varepsilon)$ par unité de volume et d'énergie :

$$\mathcal{D}(\varepsilon) = \frac{1}{2} (2\pi)^{-2} \left(\frac{2m^*}{\hbar^2}\right)^{3/2} \hbar\omega_c \sum_{n=0}^{n=m} \left[\varepsilon - \left(n+\frac{1}{2}\right) \hbar\omega_c\right]^{-1/2} , \qquad \text{(I-12)}$$

où m est la valeur maximum de n satisfaisant $\varepsilon - (n+\frac{1}{2})\hbar\omega_c > 0$. L'allure de la fonction $\mathcal{D}(\varepsilon)$ est montrée graphiquement Fig.(3). Nous voyons que $\mathcal{D}(\varepsilon)$ diffère considérablement de la fonction

$$\mathcal{D}_o(\varepsilon) = (2\pi)^{-2} \left(\frac{2m^*}{\hbar^2}\right)^{3/2} \varepsilon^{1/2} ,$$

donnant la densité d'états par unité de volume et d'énergie en l'absence de champ magnétique.

Alors que la variation de $\mathcal{D}_o(\varepsilon)$ en fonction de l'énergie est monotone (loi en $\varepsilon^{1/2}$), la densité d'états $\mathcal{D}(\varepsilon)$ en présence d'un champ magnétique présente une singularité au bas de chaque sous-bande de Landau, c'est-à-dire chaque fois que $\varepsilon = (n + \frac{1}{2}) \hbar\omega_c$. L'origine d'une telle singularité provient essentiellement de la nature unidimensionnelle des ondes longitudinales k_z dont la densité devient grande et varie comme k_z^{-1} lorsque $k_z \to 0$. Tous les effets magnéto-oscillatoires, tels que l'effet de Haas-van Alphen ou l'effet Shubnikov-de Haas, reposent fondamentalement sur ce comportement singulier de la densité d'états en fonction du champ magnétique appliqué H. Dans tout le développement qui précède, nous avons ignoré la dégénérescence supplémentaire due au spin de l'électron. Naturellement, dans un champ magnétique suffisamment intense, cette dégénérescence est levée : chaque niveau de Landau se clive en deux sous-niveaux, séparés l'un de l'autre par une énergie

$$g \mu_B H,$$

où g est le facteur de Landé de l'électron (Cardona 1963), $\mu_B = |e| \hbar / 2 m_o c$ le magnéton de Bohr et m_o la masse de l'électron libre (Fig.4).

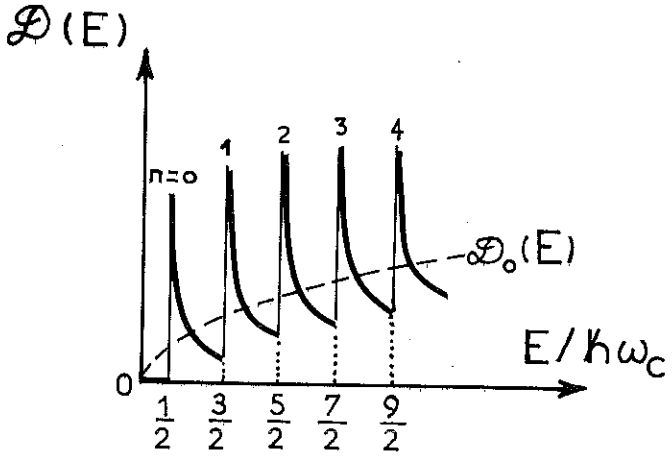

Fig. 3

Density of states for no magnetic field, $\mathscr{D}_0(E)$, and for $H \neq 0$, $\mathscr{D}(E)$. The number of each Landau level is given in the figure.

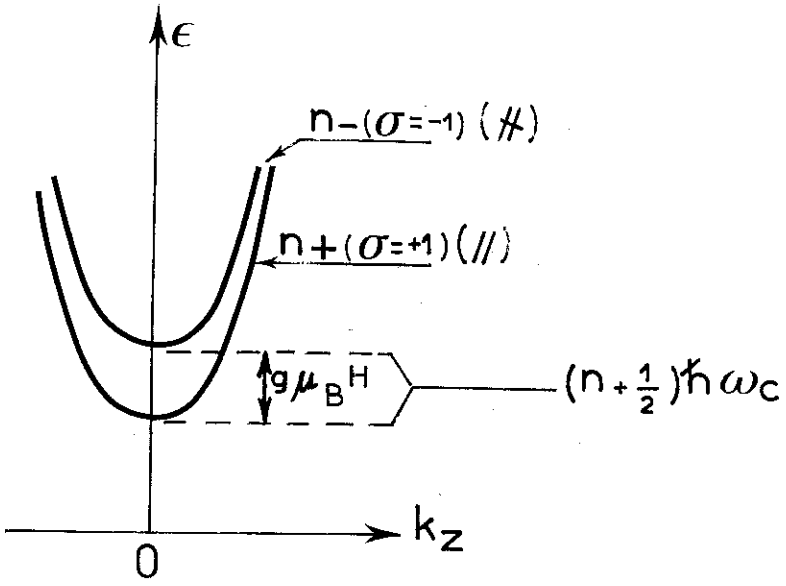

Fig. 4

Effect of electron spin.

L'expression pour les valeurs propres de l'énergie (Eq.(I-8)), incluant l'effet de spin de l'électron, s'écrit :

$$\varepsilon_{n,k_z,\sigma} = \left(n + \frac{1}{2}\right) \hbar\omega_c + \frac{\hbar^2 k_z^2}{2m^*} - \frac{1}{2} g \mu_B \sigma H , \qquad \text{(I-13)}$$

où $\sigma = \pm 1$ correspond aux deux orientations possibles de spin, parallèle et antiparallèle au champ magnétique appliqué.

L'équation (I-13) peut être réécrite sous une forme plus compacte :

$$\varepsilon_{n,k_z,\sigma} = \left[n + \frac{1}{2}(1 - \gamma\sigma)\right] \hbar\omega_c + \frac{\hbar^2 k_z^2}{2m^*} , \qquad \text{(I-14)}$$

où $\gamma = g(m^*/2m_o)$. Pour se fixer les idées, on peut noter les valeurs $|\gamma| = 0.33$ pour l'antimoniure d'indium type n ($g = -44$) et $\gamma = 0.013$ pour l'arséniure de gallium type n ($g = 0.32$) (Roth et Argyres 1966). La densité d'états par unité de volume et d'énergie pour la sous-bande de Landau n et le spin σ devient :

$$\mathcal{D}_{n,\sigma}(\varepsilon) = \frac{1}{2} (2\pi)^{-2} \left(\frac{2m^*}{\hbar^2}\right)^{3/2} \hbar\omega_c \left\{\varepsilon - \left[n + \frac{1}{2}(1 - \gamma\sigma)\right] \hbar\omega_c\right\}^{-1/2} .$$

La densité d'états électroniques totale, incluant le spin de l'électron, est alors obtenue en sommant sur n et σ :

$$\mathcal{D}(\varepsilon) = \sum_{n,\sigma} \mathcal{D}_{n,\sigma}(\varepsilon) .$$

DEFINITION DES DOMAINES QUANTIQUE, ULTRA-QUANTIQUE ET HYPER-QUANTIQUE. POSSIBILITE D'UNE "TRANSFORMATION STATISTIQUE" PAR UN CHAMP MAGNETIQUE INTENSE

Selon l'intensité du champ magnétique appliqué, il est possible de définir trois domaines bien distincts, à savoir le domaine quantique, le domaine ultra-quantique et le domaine hyper-quantique.

Le "domaine quantique" correspond à des champs magnétiques suffisamment forts, tels que les conditions suivantes :

$$\omega_c \tau >> 1 ,$$

où τ est le temps de vie moyen d'un électron entre deux chocs consécutifs, et

$$k_B T << \hbar\omega_c < \zeta ,$$

où ζ est l'énergie de Fermi, sont réalisées. Ces conditions appellent naturellement quelques commentaires. En effet, nous avons jusqu'ici envisagé uniquement le cas d'une température nulle T = 0 K et d'un libre parcours moyen électronique infini, où le concept de niveaux d'énergie de l'électron a une signification rigoureuse. En fait, dans tous les systèmes réels, il existe des collisions entre les électrons et divers types de diffuseurs. Ces collisions conduisent à une indétermination dans l'énergie des états stationnaires ou, en d'autres termes, à un élargissement des niveaux de Landau d'une quantité de l'ordre de $\frac{\hbar}{\tau}$, d'après le principe d'Heisenberg. Il est évident que la quantification des orbites électroniques en niveaux de Landau ne peut être observée que si $\hbar\omega_c >> \frac{\hbar}{\tau}$ (ce qui équivaut à $\omega_c\tau >> 1$), c'est-à-dire si la "distance" entre les divers niveaux de Landau excède largement l'épaisseur d'un niveau. Physiquement, cela signifie que l'électron effectue plusieurs révolutions autour du champ magnétique avant d'être diffusé. La température joue également un rôle fondamental dans l'observation de la quantification des orbites électroniques. Il est en effet nécessaire que l'intervalle d'énergie séparant deux niveaux de Landau voisins, à savoir $\hbar\omega_c$, soit très supérieur à la largeur du "flou thermique" au niveau de Fermi, qui est de l'ordre de $k_B T$. Evidemment, l'inégalité $\hbar\omega_c >> k_B T$ en résulte. Cette dernière condition, compte-tenu des champs magnétiques utilisables actuellement, n'est ordinairement satisfaite qu'à très basses températures (4 K, ou plus basse température). Dans un tel domaine de températures, le gaz d'électrons est dégénéré ($k_B T << \zeta$), et l'occupation statistique des diverses sous-bandes de Landau situées au-dessous du niveau de Fermi ($\zeta > \hbar\omega_c$) est gouvernée par la fonction de distribution de Fermi-Dirac.

Si l'on augmente progressivement le champ magnétique appliqué, les niveaux de Landau franchissent un à un le niveau de Fermi, occasionnant à chaque passage une singularité dans la densité d'états. Une telle situation se reflète par des effets oscillatoires dans les propriétés thermodynamiques et cinétiques, tels que l'effet de Haas-van Alphen ou l'effet Shubnikov-de Haas. Pour un champ magnétique suffisamment intense, il arrive un moment où tous les niveaux de Landau ont franchi le niveau de Fermi, excepté le dernier. Pourvu que la température soit suffisamment basse, tous les électrons s'accommodent alors dans le plus bas niveau de Landau avec le nombre quantique n = 0. Ce régime, pour lequel $\omega_c\tau >> 1$, $\hbar\omega_c >> k_B T$ et $\frac{3}{2}\hbar\omega_c > \zeta$, est appelé "régime extrême quantique". Evidemment, dans ce régime, tous les effets oscillatoires dont nous avons parlé ci-dessus disparaissent, et les diverses caractéristiques thermodynamiques et cinétiques du conducteur évoluent de façon monotone en fonction du champ magnétique. A titre indicatif, dans les matériaux semiconducteurs comme, par exemple, Ga As ou In Sb, avec des concentrations d'électrons suffisamment faibles,

disons de l'ordre de quelques 10^{16} cm^{-3}, le régime extrême quantique est atteint à très basses températures ($\lesssim$ 4 K) pour des champs magnétiques typiquement de l'ordre de 50 ou 100 kG. La figure 5 illustre la nature du spectre électronique dans le régime extrême quantique.

Nous devons maintenant noter une remarque d'intérêt fondamental pour la suite de notre étude : en régime extrême quantique, la distribution électronique est régie principalement par la position du niveau de Fermi ζ par rapport au bas de la sous-bande de Landau fondamentale $\frac{1}{2}\hbar\omega_c$. Une telle remarque nous amène à définir les domaines ultra et hyper-quantiques. Nous parlons de "domaine ultra-quantique" lorsque, en régime extrême quantique, la distribution électronique obéit à la statistique de Fermi-Dirac. Ceci est réalisé tant que l'inégalité $\zeta - \frac{1}{2}\hbar\omega_c \gg k_BT$ est satisfaite ou, en d'autres termes, tant que la "largeur" de la bande remplie excède l'épaisseur k_BT du "flou thermique" au niveau de Fermi. Si nous augmentons alors l'intensité du champ magnétique appliqué, l'ensemble des électrons est conduit progressivement vers le niveau de Fermi. On peut montrer en effet qu'à champ magnétique croissant, la "distance" qui sépare le bas de la sous-bande de Landau fondamentale $n = 0$ du niveau de Fermi décroît très rapidement comme $1/H^2$ (voir, par exemple, Roth et Argyres 1966 et Askenazy 1973). Il est dès lors facile de concevoir à la limite, en champs magnétiques très intenses, que le bas du niveau de Landau $n = 0$ s'approche si près du niveau de Fermi que la condition $\zeta - \frac{1}{2}\hbar\omega_c \gg k_BT$ n'est plus réalisée. Dans ce cas, le comportement du conducteur devient celui d'un conducteur non-dégénéré. C'est ce domaine de champs magnétiques, dans lequel le gaz d'électrons obéit effectivement à la statistique de Maxwell-Boltzmann, qui correspond au "domaine hyper-quantique" (Askenazy 1973).

Un champ magnétique peut donc transformer, en régime extrême quantique, la distribution dégénérée $\zeta - \frac{1}{2}\hbar\omega_c \gg k_BT$ en une distribution non-dégénérée $\zeta - \frac{1}{2}\hbar\omega_c \lesssim k_BT$. Le passage de la statistique de Fermi-Dirac à la statistique de Maxwell-Boltzmann commence dès que le bas de la sous-bande de Landau fondamentale $n = 0$ s'approche de la région du "flou thermique" ($\sim k_BT$) au niveau de Fermi. Ainsi, à champ magnétique croissant, l'ensemble des électrons se trouve amené progressivement dans le régime de statistique non-dégénéré. L'état statistique du conducteur peut être considéré comme totalement non-dégénéré lorsque l'énergie cinétique moyenne des électrons (repérée par rapport au bas de la sous-bande de Landau $n = 0$) le long de la direction du champ magnétique appliqué devient de l'ordre de $\frac{1}{2}k_BT$. En d'autres termes, le système peut être considéré comme totalement non-dégénéré dès que la dynamique du gaz d'électrons devient identique à celle d'un gaz non-dégénéré quasi-unidimensionnel. Expérimentalement, la "transformation statistique" (dégénéré en non-dégénéré) a été observée pour la première fois par Askenazy, Ulmet et Léotin

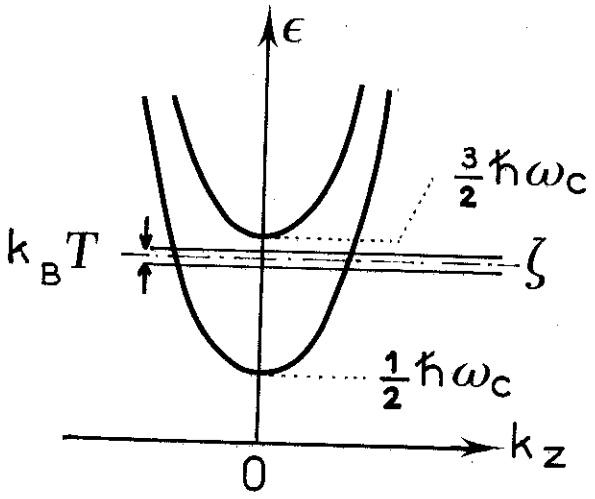

Fig. 5

Energy level diagram of electrons in the extreme quantum region.
(The effect of spin is neglected).

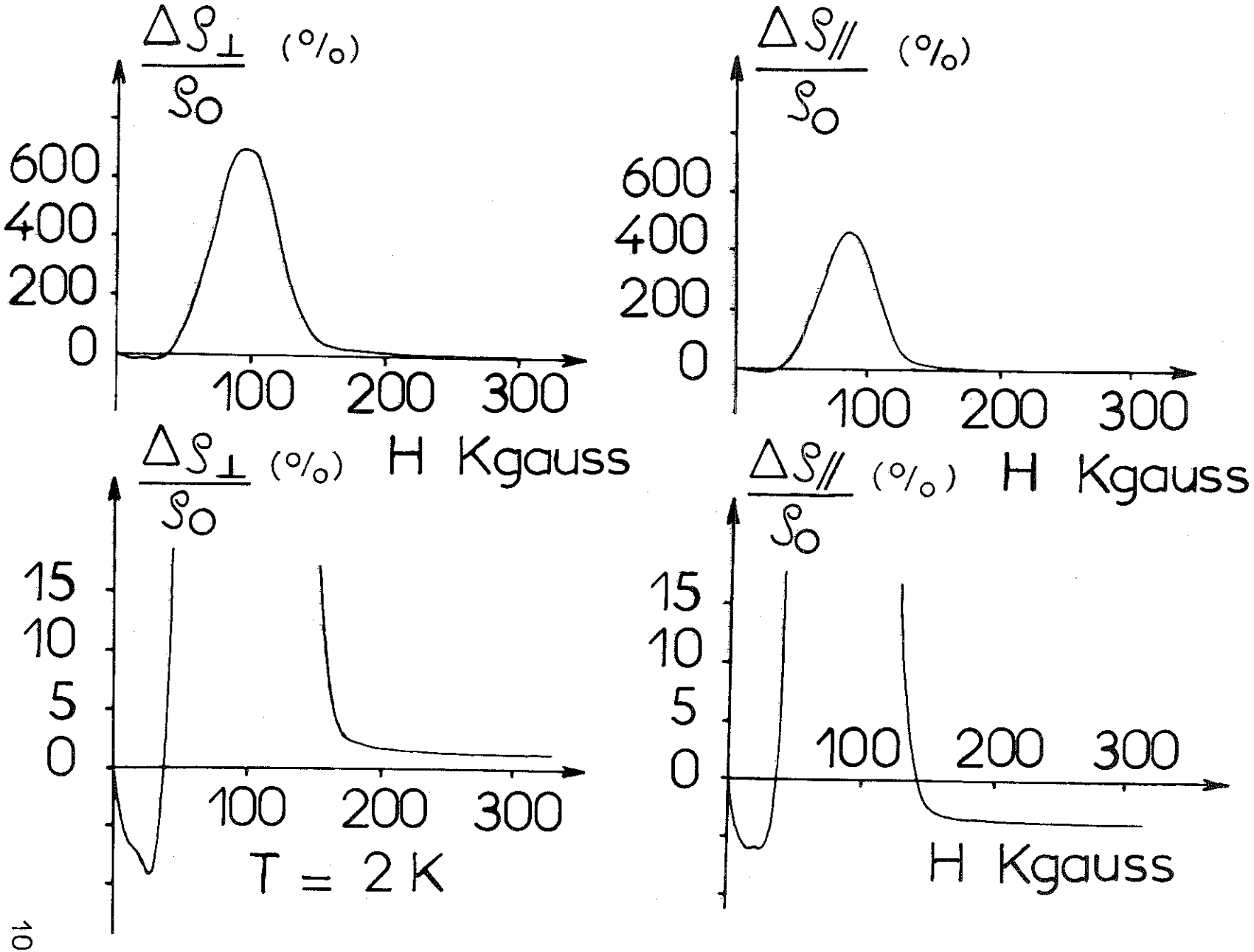

Fig. 6 Magnétorésistance transverse et longitudinale du GaAs, $N = 3.8 \times 10^{16}$ cm^{-3}.
(D'après S. Askenazy, J.P. Ulmet et J. Léotin, Solid State Commun. 7, 989 (1969)).

(1969) dans la magnétorésistance longitudinale ($\rho_{//}$) et transverse ($\rho_{\perp}$) d'un échantillon d'arséniure de gallium (Ga As) de type n, avec une concentration d'électrons de 3.8×10^{16} cm^{-3}, à T = 2 K. En utilisant un champ magnétique pulsé de 400 kG, ces auteurs ont mis en évidence, lorsque le gaz d'électrons passe d'un état dégénéré à un état non-dégénéré, une "oscillation" géante de $\rho_{//}$ et $\rho_{\perp}$ commençant vers 30 kG, atteignant un maximum vers 90 kG et décroissant rapidement vers une valeur négative relativement faible et variant lentement à environ 150 kG (Fig. 6).

EFFET DE L'ELARGISSEMENT DES NIVEAUX DE LANDAU DÛ AUX COLLISIONS. TEMPERATURE DE DINGLE

Comme nous l'avons mentionné précédemment, l'effet des collisions conduit à une indétermination dans l'énergie des états stationnaires électroniques, c'est-à-dire à un élargissement des niveaux d'énergie de Landau. Si τ est le temps de vie moyen d'un électron entre deux collisions consécutives, l'incertitude correspondante sur l'énergie est, d'après le principe d'Heisenberg, $\Gamma \sim \frac{\hbar}{\tau}$ (Fig. 7).

Evidemment, cet élargissement des niveaux de Landau dû aux collisions peut entraîner une modification profonde de la courbe de la densité d'états $\mathscr{D}(\varepsilon)$: suivant que $\hbar\omega_c \gg \Gamma$ ($\omega_c\tau \gg 1$) ou que $\hbar\omega_c \gtrsim \Gamma$ ($\omega_c\tau \gtrsim 1$), les singularités de $\mathscr{D}(\varepsilon)$, en $1/\left[\varepsilon - (n + \frac{1}{2})\hbar\omega_c\right]^{1/2}$ (voir Eq. (I-12)), s'amortissent, et $\mathscr{D}(\varepsilon)$ se transforme en une courbe présentant une série de maximums plus ou moins marqués (Roth et Argyres 1966, Landwehr 1969 et Askenazy 1973). En particulier, dans le cas où $\hbar\omega_c \lesssim \Gamma$, les divers niveaux d'énergie se recouvrent les uns les autres, et le caractère quasi-périodique de la densité d'états disparaît totalement (Fig. 8).

L'effet des collisions électroniques sur la densité d'états est obtenu simplement en supposant que l'élargissement de chaque niveau de Landau peut être décrit par une fonction de distribution de forme Lorentzienne, paramètrée par le "temps de collision" τ. Ce traitement, de nature essentiellement phénoménologique, a été formulé à l'origine par Dingle (1952) dans le cas d'un gaz d'électrons libres, pour étudier l'influence des impuretés sur l'amplitude de la composante oscillatoire de la susceptibilité diamagnétique des métaux (effet de Haas-van Alphen). Il a ensuite été étendu par Williamson, Foner et Smith (1964), en utilisant la méthode de Lifshitz et Kosevich (1955), au cas d'une surface de Fermi de géométrie arbitraire. Plus récemment, une étude rigoureuse de l'influence des collisions électroniques sur l'effet de Haas-van Alphen, ne nécessitant aucun recours à l'attribution phénoménologique additionnelle d'une fonction de distribution spécifique pour décrire chaque niveau de Landau, a été développée par Brailsford (1966). Notons enfin les travaux

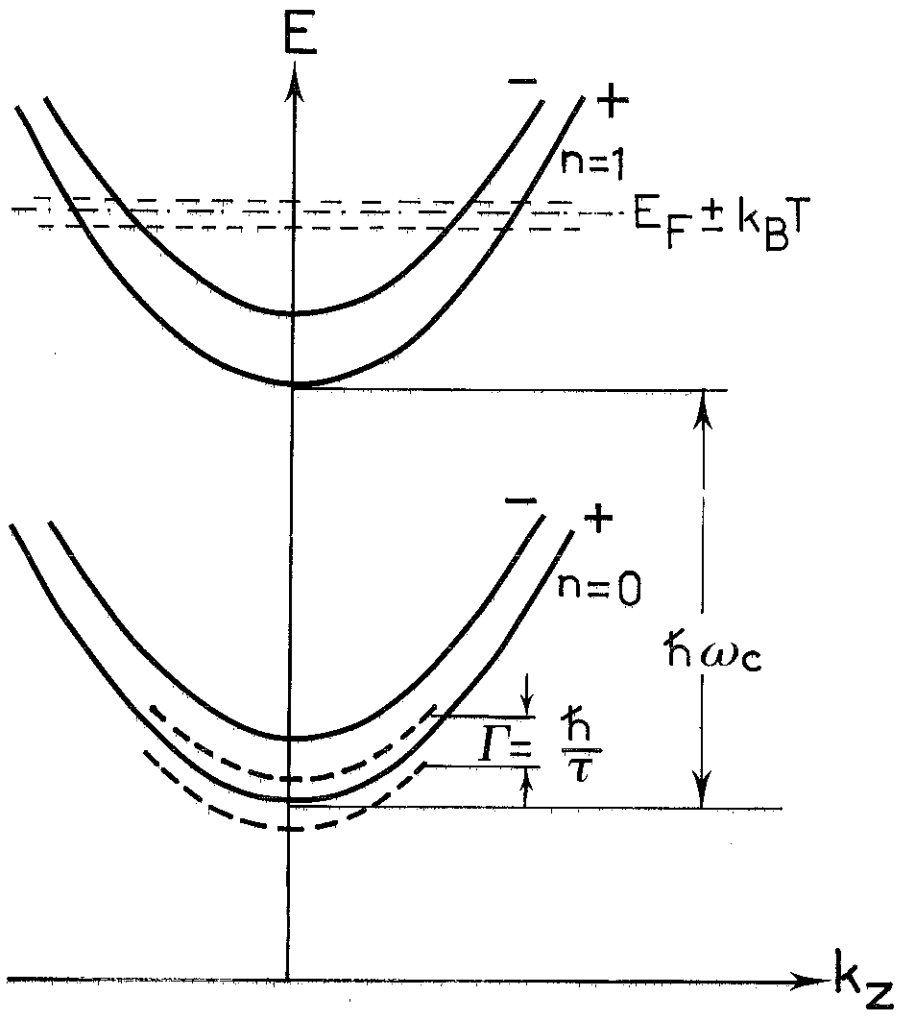

Fig. 7

Niveaux de Landau et énergie de Fermi, compte-tenu de l'élargissement dû aux collisions et du flou thermique

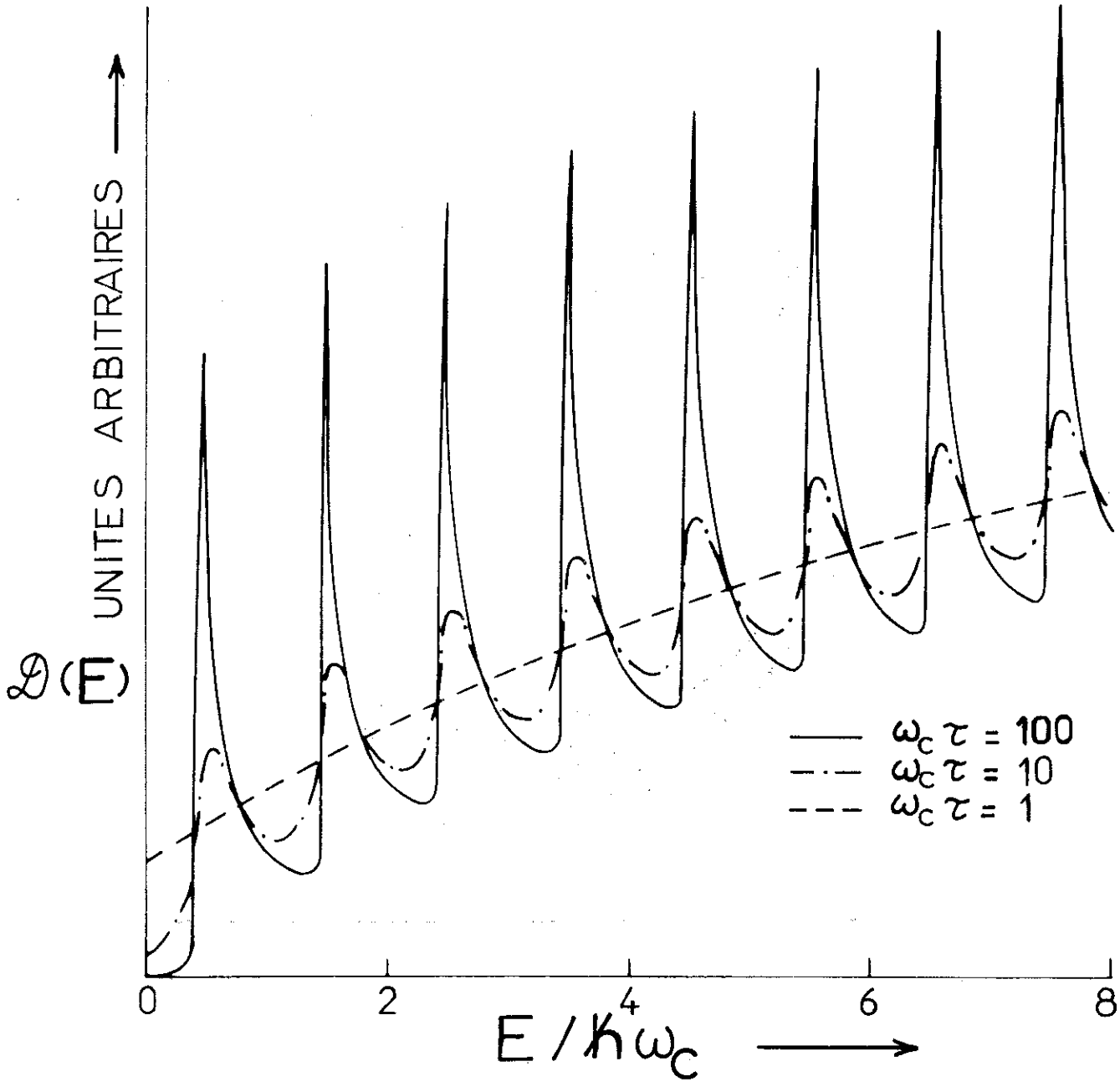

Fig. 8

Amortissement des singularités de la densité d'état.
(D'après G. Landwehr, "Physics of Solids in Intense Magnetic Fields", p. 415 (Plenum Press, New York, 1969)).

de Kubo, Miyake et Hashitsume (1965), qui ont donné une description détaillée de l'effet des collisions sur les propriétés de transport (essentiellement sur les composantes transverse et longitudinale du tenseur de conductivité électrique) dans le domaine des champs magnétiques intenses ($\hbar\omega_c >> k_B T$, $\hbar\omega_c \gtrsim \zeta$).

Un des principaux résultats obtenus par Dingle (1952), Williamson et al. (1964) et Brailsford (1965) est, qu'en première approximation, les collisions donnent un effet global sensiblement identique à une augmentation apparente de température, généralement appelée la "température de Dingle", $T_D = \hbar/2\pi k_B \tau = \Gamma/2\pi k_B$. En d'autres termes, l'influence des collisions électroniques dans la détermination de la densité d'états réelle peut être obtenue simplement en utilisant la densité d'états non-perturbée en l'absence d'impuretés et une fonction de distribution thermique caractérisée par une température "effective" plus élevée $T^* = T + T_D$. Ceci revient donc à assimiler l'amortissement des singularités de $\mathcal{D}(\varepsilon)$ dû aux collisions, à un élargissement thermique équivalent des bords de la distribution de Fermi (voir, par exemple, les mises au point de Landwehr 1969 et d'Abrikosov 1972).

Ainsi, toutes les considérations envisagées dans ce chapitre peuvent encore être appliquées, lorsque l'on veut rendre compte de l'influence des collisions, simplement en remplaçant T par la température "effective" T^*. Plus précisément, en ce qui concerne la "transition statistique" en régime extrême quantique, le passage de la distribution de Fermi-Dirac à celle de Maxwell-Boltzmann sous l'action d'un champ magnétique intense, doit s'affirmer dès que la condition $\zeta - \frac{1}{2}\hbar\omega_c \lesssim k_B T^*$ est réalisée. Autrement dit, sous l'influence des collisions, la "transition statistique" est gouvernée, non plus par T, mais par la température "effective" T^*, toute autre chose restant par ailleurs inchangée.

Dans toute la suite de ce travail, nous avons négligé l'effet de l'élargissement des niveaux de Landau, et considéré des matériaux semiconducteurs de pureté et de qualité suffisantes pour que l'inégalité $\omega_c \tau >> 1$ soit vérifiée dans tous les cas.

CHAPITRE II

ETUDE DE LA CHALEUR SPECIFIQUE ET DU COEFFICIENT MAGNETOTHERMIQUE D'UN SEMICONDUCTEUR EN REGIME EXTREME QUANTIQUE

Dans ce chapitre, nous présentons une analyse détaillée et quantitative de la chaleur spécifique électronique et du coefficient magnétothermique d'un semiconducteur en régime extrême quantique, en nous attachant tout particulièrement à l'étude des effets dus à la "transition statistique" (dégénéré en non-dégénéré) (voir chapitre I).

Dans la théorie développée ici, nous supposons que le matériau semiconducteur (nous avons pris, à titre d'exemple, l'arséniure de gallium de type n) est de pureté suffisante pour que soit réalisée la condition $\omega_c \tau >> 1$, où ω_c est la fréquence cyclotron et τ le temps de relaxation électronique. Dans cette limite, nous savons que la quantification de Landau est préservée malgré les collisions des électrons avec le réseau (voir chapitre I). D'autre part, nous utilisons, dans cette étude, la théorie des électrons "libres" avec l'approximation de la masse effective dans laquelle les électrons ont une masse effective m^* et un facteur de Landé g. La surface de Fermi de Ga As est très sensiblement sphérique, et aux concentrations suffisamment faibles d'électrons que nous considérons ici ($\lesssim 10^{16}$ cm^{-3}), la bande de conduction est approximativement parabolique. Ga As est également approprié pour l'étude des phénomènes en régime extrême quantique, car la masse de l'électron est pratiquement indépendante de l'intensité du champ magnétique appliqué jusqu'à environ 400 kG (Askenazy, Ulmet et Léotin 1969). Malgré la petite masse effective ($m^* \simeq 0.07\ m_o$, où m_o est la masse de l'électron libre) et le très faible facteur de Landé ($g \simeq 0.32$) des électrons de conduction dans Ga As, nous tenons compte dans les calculs de l'effet de clivage de spin. Ce dernier point mérite évidemment une certaine attention, en ce sens que, dans les matériaux impurs, cet effet peut être masqué par l'élargissement des niveaux de Landau dû aux collisions (voir chapitre I). Nous supposons enfin qu'en régime extrême quantique, la concentration électronique ne dépend pas de la température et que le matériau considéré est suffisamment dopé pour ne pas offrir de gel de porteur par le champ magnétique. Ces deux hypothèses ont été vérifiées expérimentalement : (1) Wilson, Love et Miller (1968) n'ont trouvé aucune dépendance en température du coefficient Hall entre 4 et 0.4 K dans un échantillon d'antimoniure d'indium de type n avec une concentration électronique de 2.6×10^{15} cm^{-3} ; (2) Amirkhanov, Bashirov et Mollaev (1971) ont étudié l'effet de gel de porteur dans Ga As en champs magnétiques pulsés jusqu'à 300 kG et dans le domaine de température

entre 4.2 et 77 K, en utilisant des mesures du coefficient Hall. Leurs résultats indiquent que l'effet de gel de porteur n'intervient pas dans les conditions envisagées dans la présente étude pour des champs inférieurs à environ 200 kG.

Le calcul de la chaleur spécifique électronique C_H^e à champ magnétique constant et du coefficient magnétothermique $(\frac{\partial T}{\partial H})_S$ (variation différentielle de température avec le champ magnétique à entropie S constante) est réalisé simplement à partir de l'énergie libre de Helmholtz F(H) du gaz d'électrons, en s'appuyant sur les relations thermodynamiques suivantes :

$$S = (-\frac{\partial F(H)}{\partial T}) \quad , \tag{II-1}$$

$$C_H^e = T(\frac{\partial S}{\partial T})_H = -T(\frac{\partial^2 F(H)}{\partial T^2})_H \quad , \tag{II-2}$$

$$(\frac{\partial T}{\partial H})_S = -\frac{T}{C_H}(\frac{\partial M}{\partial T})_H \quad \text{(relation de Maxwell)} \tag{II-3}$$

où M est l'aimantation, définie par :

$$M = (-\frac{\partial F(H)}{\partial H}) \quad , \tag{II-4}$$

$$(\frac{\partial M}{\partial T})_H = \frac{\partial}{\partial T}(-\frac{\partial F(H)}{\partial H}) = \frac{\partial}{\partial H}(-\frac{\partial F(H)}{\partial T}) = (\frac{\partial S}{\partial H})_T \tag{II-5}$$

et $C_H = C_H^\ell + C_H^e$ (C_H^ℓ est la chaleur spécifique du réseau et C_H^e celle des électrons) est la chaleur spécifique totale à champ magnétique constant de l'échantillon étudié. L'expression de F(H) utilisée dans le calcul est établie dans l'Appendice A.

Les principaux résultats obtenus pour C_H^e et $(\frac{\partial T}{\partial H})_S$ peuvent se résumer ainsi :

(1) C_H^e, chaleur spécifique électronique

Dans le domaine ultra-quantique, lorsque le système d'électrons est fortement dégénéré, la relation habituelle de la chaleur spécifique électronique en termes de densité d'états au niveau de Fermi, $\mathcal{D}(\zeta)$, s'applique :

$$C_H^e = \frac{1}{3}\pi^2 k_B^2 \mathcal{D}(\zeta)\, T \quad , \tag{II-6}$$

où $\mathcal{D}(\zeta)$ est donnée par :

$$\mathcal{D}(\zeta) = \frac{1}{4\pi^2}(\frac{2m^*}{\hbar^2})^{3/2} \frac{\hbar\omega_c}{\sqrt{\zeta - \frac{1}{2}\hbar\omega_c}} \quad . \tag{II-7}$$

Lorsque, à champ magnétique croissant, le bas de la sous-bande de Landau fondamentale n = 0 s'approche à quelques ($k_B T$) du niveau de Fermi, la chaleur spécifique augmente considérablement en raison de l'accroissement de la densité d'états effective.

Avec l'apparition de la non-dégénérescence, C_H^e atteint une valeur maximum, puis décroît très lentement vers la valeur classique $\frac{1}{2} N k_B$, une fois que le système est devenu complètement non-dégénéré (N est le nombre total d'électrons et k_B la constante de Boltzmann). Ce résultat est raisonnable, puisque la quantification de Landau empêche les degrés de liberté, perpendiculaires au champ magnétique, de contribuer à la chaleur spécifique. D'autre part, les électrons deviennent non-dégénérés par rapport au mouvement dans la direction du champ. Ils simulent donc un gaz non-dégénéré unidimensionnel.

Si l'on tient compte du clivage de spin du niveau de Landau fondamental n = 0, il s'introduit une contribution supplémentaire (analogue à un effet Schottky) qui double approximativement le maximum de la chaleur spécifique. Un tel effet peut néanmoins être masqué par l'élargissement des niveaux dans les échantillons impurs.

Nous devons insister ici sur le fait que le terme électronique à la chaleur spécifique, bien que très petit par rapport au terme de réseau, n'en est pas moins détectable expérimentalement à très basses températures, même pour les faibles concentrations envisagées dans ce travail ($\sim 10^{16}$ électrons par cm^3). En effet, les mesures de chaleur spécifique de Cetas, Tilford et Swenson (1968) sur certains composés III-V semiconducteurs, tels que Ga As, Ga Sb, In As et In Sb, en champ magnétique nul et dans l'intervalle de température 1-30 K, indiquent, dans tous les cas, la présence d'une contribution électronique aux plus basses températures. De plus, nous avons effectué récemment des mesures de chaleur spécifique en champ nul, d'effet Hall et de résistivité entre 0.3 et 4 K, sur un échantillon d'antimoniure de gallium de type p ayant une concentration nette de trous voisine de 4×10^{15} cm^{-3}. L'analyse des résultats montre clairement l'existence d'une contribution à la chaleur spécifique d'origine électronique (voir le détail de cette étude dans l'Appendice B).

En d'autres termes, la "transition statistique" devrait pouvoir être révélée expérimentalement par une mesure de chaleur spécifique à très basses températures et en champs magnétiques intenses.

(2) $(\frac{\partial T}{\partial H})_S$, coefficient magnétothermique

En régime extrême quantique, lorsque l'on ignore l'effet de clivage de spin du niveau de Landau fondamental n = 0, le coefficient magnétothermique $(\frac{\partial T}{\partial H})_S$ est donné par :

$$\left(\frac{\partial T}{\partial H}\right)_S = - \frac{T}{C_H} \left(\frac{\partial M_d}{\partial T}\right)_H , \qquad \text{(II-8)}$$

où M_d est l'aimantation due au diamagnétisme de Landau-Peierls et où $\left(\frac{\partial M_d}{\partial T}\right)_H$ est relié simplement à la chaleur spécifique électronique C_H^e par l'équation :

$$\left(\frac{\partial M_d}{\partial T}\right)_H = \frac{2\, C_H^e}{H} , \qquad \text{(II-9)}$$

$\left(\frac{\partial T}{\partial H}\right)_S$ est donc négatif et sa variation avec le champ magnétique est sensiblement donnée par le rapport C_H^e/H, puisque, aux températures considérées ici (0.5-2 K), la chaleur spécifique totale $C_H = C_H^\ell + C_H^e$ est essentiellement dominée par la contribution du réseau et, par suite, indépendante du champ. A partir de ce résultat et compte-tenu des résultats précédents concernant C_H^e, on en déduit immédiatement une variation dramatique de $\left(\frac{\partial T}{\partial H}\right)_S$ en fonction du champ magnétique, lors de la "transition statistique" : le passage de la distribution électronique de l'état dégénéré à l'état non-dégénéré, à champ magnétique croissant, se manifeste par un minimum négatif très marqué de $\left(\frac{\partial T}{\partial H}\right)_S$. A titre indicatif, pour l'arséniure de gallium de type n avec 1.2×10^{16} électrons par cm^3, à T = 0.5 K, ce minimum atteint environ -3×10^{-6} K/Gauss pour un champ magnétique de l'ordre de 50 kG. Un tel effet devrait pouvoir être détecté par les techniques expérimentales actuelles. Il est également intéressant de noter qu'une mesure du produit $H\left(\frac{\partial T}{\partial H}\right)_S$ en fonction du champ magnétique pourrait être employée pour obtenir la variation de la chaleur spécifique électronique C_H^e avec H (voir Eqs.(II-8) et (II-9)).

Le clivage de spin du niveau de Landau fondamental n = 0 ne modifie pas sensiblement l'amplitude de l'anomalie de $\left(\frac{\partial T}{\partial H}\right)_S$ précitée. Il introduit cependant une contribution positive supplémentaire, donnée par

$$\left(\frac{\partial T}{\partial H}\right)_S^{spin} = - \frac{T}{C_H} \left(\frac{\partial M_p}{\partial T}\right)_H , \qquad \text{(II-10)}$$

où M_p, qui est l'aimantation due au paramagnétisme de Pauli, reflète l'alignement des spins de tous les électrons libres, lorsque le bas de la branche de spin supérieure franchit le niveau de Fermi . Cette contribution supplémentaire

produit, dans la région de la "transition statistique", un maximum prononcé de $\left(\frac{\partial T}{\partial H}\right)_S$ aux plus basses températures. Cet effet est dû à la rapide variation de M_p en fonction de la température dans cette région. Evidemment, si la concentration en électrons augmente, le champ requis pour obtenir l'alignement des spins augmente également : avec les champs magnétiques utilisables présentement, la concentration électronique doit rester, dans tous les cas, inférieure à quelques 10^{16} cm^{-3} pour que l'effet soit observable. Là encore, il convient de noter que l'élargissement des niveaux dû aux collisions dans les matériaux impurs peut masquer complètement un tel effet.

Journal of Low Temperature Physics, Vol. 7, No. 5/6, 1972

Low-Temperature Specific Heat of a Semiconductor in a Strong Magnetic Field

J. P. Jay-Gerin* and P. R. Wallace

McGill University, Montreal, Canada

(Received December 2, 1971)

We calculate the electronic specific heat of a semiconductor (GaAs) at very low temperatures when subjected to a magnetic field strong enough to make the electron distribution nondegenerate. The transition to nondegeneracy is characterized by a large and rapid increase in the specific heat. For large fields the value approaches that of a one-dimensional nondegenerate gas, after first exceeding this value. Zeeman splitting, even with a very small g factor (0.32), almost doubles the maximum in the specific heat as a function of field.

1. INTRODUCTION

It has been shown by Askenazy *et al.*[1] that a sample of GaAs with 3.8×10^{16} carriers at 2 K experiences a large increase in both longitudinal and transverse resistivity starting at ≈ 50 kG, reaching a maximum at ≈ 100 kG, and decreasing again to a relatively small and slowly varying value by about 150 kG. This behavior is associated with the transition to nondegeneracy which takes place when the lowest Landau level is pushed up towards, and ultimately past, the Fermi level. The resistance decreases strongly as the electron distribution becomes nondegenerate.

Our aim is to show that the change in the electron distribution manifested in this experiment is also characterized by a rapid rise in the electronic specific heat. As the lowest Landau level approaches within a few times kT of the Fermi level, the specific heat rises rapidly to a maximum, then decreases toward the value $\frac{1}{2}Nk_B$, where N is the number of carriers. This is reasonable, since the degrees of freedom perpendicular to the magnetic field are inhibited from contributing to the specific heat by Landau quantization.

*On leave from Centre de Recherches sur les Très Basses Températures, Grenoble, France.

On the other hand, the electrons become nondegenerate with respect to motion along the field. Thus, they simulate a one-dimensional nondegenerate gas.

Though Askenazy claims that Zeeman splitting may be ignored because of the small value of the g factor (0.32), we note that, in the region of interest, the spin splitting may be equal to or greater than kT. When this is the case, the specific heat at maximum may be approximately doubled by virtue of the spin splitting.* The curve of C_v vs. H also tends to flatten somewhat as the bottom of the upper spin band passes through the Fermi level μ, before rising again to its peak. This "knee" in the curve becomes more pronounced as the temperature is raised.

We note that the specific heat of GaAs has been measured in the absence of a magnetic field, in a sample with $N \approx 2 \times 10^{18}\,\mathrm{cm}^{-3}$ and at temperatures between 1 and 30 K by Cetas, Tilford, and Swenson.[2] They are able to distinguish clearly an electronic component. We have used their results to estimate the lattice specific heat, assumed to obey a T^3 law; it is also assumed that it will not vary significantly with magnetic field.

von Piesbergen[3] has measured the specific heat above 12 K; he finds quite good conformity to a T^3 law up to 30–40 K.

Two possible complications deserve attention. First, is there a danger that the high magnetic fields envisaged will in some degree freeze out the carriers? Amirkhanov, Bashirov, and Mollaev[4] have studied magnetic freeze out in GaAs in pulsed fields up to 300 kG and in the temperature range from 4.2 to 77 K, using Hall coefficient measurements. Their results suggest that freeze out is not likely to take place under the conditions envisaged in this paper for fields below ≈ 200 kG, and even then would not be a large effect. If one uses higher carrier concentrations than that which we have chosen for illustrative purposes ($N = 1.2 \times 10^{16}\,\mathrm{cm}^{-3}$), the rise in specific heat will take place at higher fields; however, the effect of higher carrier concentrations in inhibiting freeze out is expected to be greater than the effect of the increased fields in stimulating it.

The second question concerns the possibility of a substantial decrease in carrier density with decreasing temperature. However, in the temperature range below that considered by Askenazy (2 K) it seems unlikely that carriers are produced by thermal excitation. Rather, it seems probable that the electrons are effectively conducting independently of temperature. We note that a similar situation has been surmised by Wilson, Love, and Miller[5] in galvanomagnetic experiments in InSb down to 0.3 K; they found no evidence of the existence of an excitation energy.

*Askenazy has observed, however, [private communication] that this effect may be masked by level broadening in impure samples.

2. CALCULATION OF THE SPECIFIC HEAT

In fields large enough that only the $n = 0$ Landau level is occupied, the energy of the electrons is

$$U = \frac{1}{4\pi^2 r_c^2}\left(\frac{2m^*}{\hbar^2}\right)^{1/2} \sum_\sigma \int \frac{Ef(E)}{[E - \frac{1}{2}\hbar\omega_c(1 + \gamma\sigma)]^{1/2}}\, dE \tag{1}$$

where m^* is the effective mass, r_c is the radius of cyclotron orbit equal to $(\hbar c/eH)^{1/2}$, σ is the spin (equal to ± 1), $\gamma = |g|(m^*/2m_0)$, ω_c is the cyclotron frequency equal to eH/m^*c, $f(E)$ is the Fermi distribution function, and $\beta = 1/k_B T$. Introducing

$$\beta[E - \tfrac{1}{2}\hbar\omega_c(1 + \gamma\sigma)] = x \qquad \beta[\mu - \tfrac{1}{2}\hbar\omega_c(1 + \gamma\sigma)] = \xi_\sigma \tag{2}$$

we may write, omitting the term $\frac{1}{2}\hbar\omega_c N$,

$$U = \frac{A}{2\beta^{3/2}}\left[\sum_\sigma \mathscr{F}_{1/2}(\xi_\sigma) + \hbar\omega_c\gamma\beta \sum_\sigma \sigma\mathscr{F}_{-1/2}(\xi_\sigma)\right] \tag{3}$$

where the $\mathscr{F}$'s are the functions defined by Blakemore:[6]

$$\mathscr{F}_j(\xi) = [1/\Gamma(j + 1)] \int_0^\infty \{x^j\, dx/[e^{(x-\xi)} + 1]\} \tag{4}$$

The constant A is $(1/4\pi^2 r_c^2)(2m^*\pi/\hbar^2)^{1/2}$. These functions satisfy the condition

$$\mathscr{F}_j' = \mathscr{F}_{j-1}$$

It is useful to define $\mathscr{F}_{-3/2} = \mathscr{F}'_{-1/2}$ (primes indicate derivatives with respect to ξ).

We shall also introduce

$$R = \tfrac{1}{2}\hbar\omega_c\gamma\beta \tag{5}$$

which is half the ratio of the spin splitting to the thermal energy.

The specific heat is now given by

$$C_v = \partial U/\partial T = -k_B\beta^2(\partial U/\partial\beta) \tag{6}$$

We note that

$$\partial\xi_\sigma/\partial\beta = M - (1/\beta)R\sigma \tag{7}$$

where

$$M = \mu - \tfrac{1}{2}\hbar\omega_c + \beta(\partial\mu/\partial\beta) \tag{8}$$

We may then directly calculate C_v in the form

$$C_v = (Ak_B/\beta^{1/2})[\tfrac{3}{4}S_1 - \tfrac{1}{2}S_{-1}\beta M + R\Delta_{-1} - R\Delta_{-3}\beta M + R^2 S_{-3}] \tag{9}$$

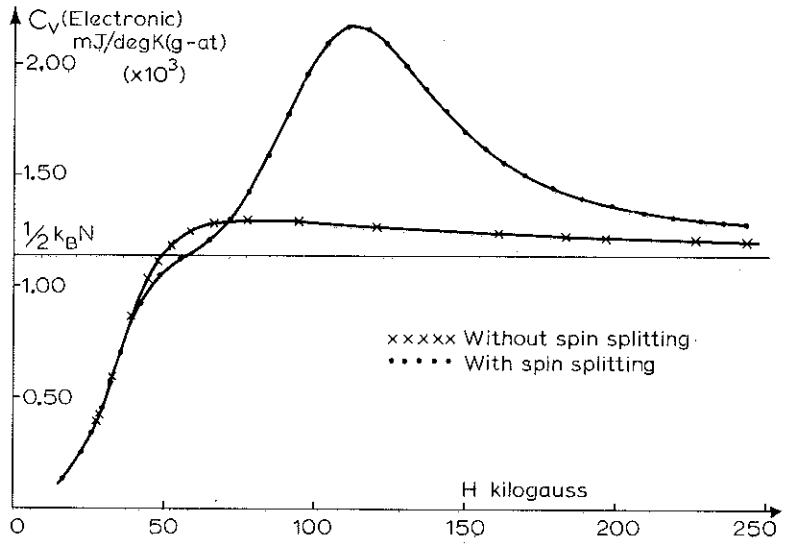

Fig. 1. Specific heat, as a function of magnetic field, calculated with and without spin splitting for GaAs with $N = 1.2 \times 10^{16}$ cm^{-3} carriers, and at a temperature of $T = 0.5$ K, $g = 0.32$, and $m^* = 0.07m_0$ (m_0 is the electron mass). The lattice specific heat at this temperature is 0.0061 mJ/deg · g · at. The one-dimensional "classical" value $(1/2)Nk_B$ is shown for reference.

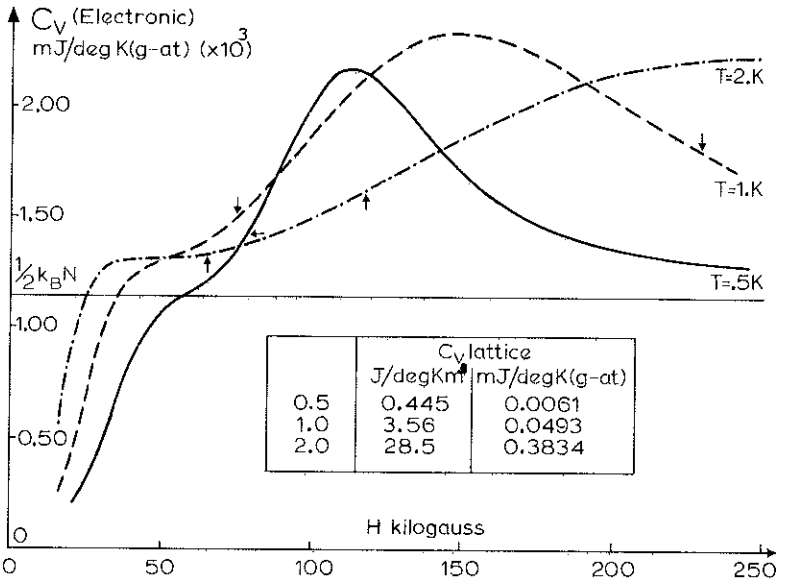

Fig. 2. Electronic specific heat vs. temperature at $T = 0.5$, 1.0, and 2.0 K. The three arrows to the left indicate the fields at which the bottom of the upper spin band coincides with the Fermi energy. The two arrows to the right show the same for the *lower* spin band. The value for 0.5 K does not fall in the range of fields shown. Parameters as in Fig. 1.

where

$$S_p = \sum_\sigma \mathscr{F}_{p/2}(\xi_\sigma) \tag{10}$$

and

$$\Delta_p = \sum_\sigma \sigma \mathscr{F}_{p/2}(\xi_\sigma) \tag{11}$$

The quantity M can be eliminated by differentiating the equation which determines the Fermi level μ,

$$N = (A/\beta^{1/2}) \sum_\sigma \mathscr{F}_{-1/2}(\xi_\sigma)$$

to get

$$\beta M = [1/(S_{-3})][\tfrac{1}{2}S_{-1} + R\Delta_{-3}] \tag{12}$$

Substituting this into (9) gives

$$C_v = (Ak_B/\beta^{1/2}S_{-3})[\tfrac{1}{4}(3S_1S_{-3} - S_{-1}^2) + R(\Delta_{-1}S_{-3} - S_{-1}\Delta_{-3}) + R^2(S_{-3}^2 - \Delta_{-3}^2)] \tag{13}$$

It is easily shown that

$$\Delta_{-1}S_{-3} - S_{-1}\Delta_{-3} = 2[\mathscr{F}_{-1/2}(\xi_+)\mathscr{F}_{-3/2}(\xi_-) - \mathscr{F}_{-3/2}(\xi_+)\mathscr{F}_{-1/2}(\xi_-)] \tag{14}$$

and

$$S_{-3}^2 - \Delta_{-3}^2 = 4\mathscr{F}_{-3/2}(\xi_+)\mathscr{F}_{-3/2}(\xi_-) \tag{15}$$

When the bottom of the upper spin band coincides with μ,

$$\xi_+ = 0 \qquad \xi_- = 2R$$

When the same happens to the bottom of the *lower* spin band,

$$\xi_- = 0 \qquad \xi_+ = -2R$$

When the spin splitting is neglected, $R \to 0$ and only the first term in (13) survives. In GaAs ($g = 0.32$)

$$R = 1.07 \times 10^{-2}(H/T)$$

where H is in kilogauss and T in degrees. Thus, at $H = 100$ kG, $T = 1$ K, $R \approx 1$.

Figure 1 shows the difference in the specific heat calculated with and without spin splitting for $N = 1.2 \times 10^{16}$ carriers, at a temperature of 0.5 K.

In Fig. 2 we illustrate the difference in the effect of spin splitting at the temperatures 0.5, 1, and 2 K. The variation of C_v with H is seen to vary strikingly with temperature in this range.

3. LOW-FIELD AND HIGH-FIELD LIMITS

In the regime in which only the $n = 0$ levels are occupied, but the system is still strongly degenerate, the familiar formula for the specific heat in terms of density of states still applies:

$$C_v = \tfrac{1}{3}\pi^2 k_B^2 T \mathcal{N}(\mu) \tag{16}$$

The density of states in this case is given by

$$\mathcal{N}(\mu) = (A\beta^{1/2}/\pi^{1/2})\{[1/(\xi_+)^{1/2}] + [1/(\xi_-)^{1/2}]\} \tag{17}$$

which increases as the bottom of the upper spin band approaches the Fermi level.

Figure 3 shows the variation of the Fermi level with respect to the bottoms of the two spin bands. The horizontal line corresponds to the lower of these bands, the sloping one to the upper. For reference, we have indicated the point at which the energy difference between them corresponds to $k_B T$ at 1 K. In fact, for GaAs,

$$2R = 2.14 \times 10^{-2} H(kG)/T \tag{18}$$

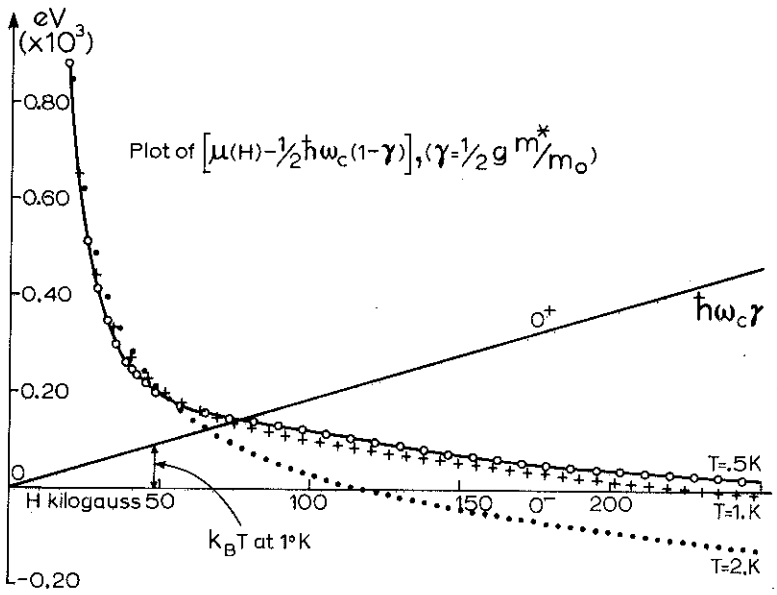

Fig. 3. Plot of Fermi level vs. H in kilogauss for $N = 1.2 \times 10^{16}$ cm^{-3} and temperatures of 0.5, 1.0, and 2.0 K. 0^+, 0^- designate, on the same scale, the energies at the bottoms of the two spin bands. $k_B T$ at 1 K is shown for reference.

We see that at 1°K the first critical field is at ≈ 75 kG and the second at ≈ 230 kG. At the lower, effectively all the electrons associated with one spin have become nondegenerate; but because the splitting is only $\approx 1.5k_BT$ a substantial proportion of those of the other spin have also.

The intermediate region is rather complicated, though the general behavior of the C_v–H curve can be understood. With increasing field, not only is the density of states increasing, but more and more electrons are being driven into the region of nondegenerate statistics.

Once the system has become completely nondegenerate, explicit and rather simple forms for the specific heat again become possible. In this regime, we may write, to a good approximation,

$$\mathscr{F}_j(\xi) \approx e^{-|\xi|} - [1/2^{j+1}]\, e^{-2|\xi|} \tag{19}$$

In fact, only ξ_- contributes appreciably, since

$$|\xi_+| = |\xi_-| + 2R$$

and R is substantially larger than unity.

The Fermi level is determined by

$$N = (A/\beta^{1/2})\{e^{-|\xi_-|} - [1/(2)^{1/2}]\, e^{-2|\xi_-|}\} \tag{20}$$

Using (19), the R-independent term, which gives the result *without* spin splitting, is

$$C_v' = (Ak_B/\beta^{1/2})(e^{-|\xi|}/2)[1 - (3\sqrt{2}/8)\, e^{-|\xi|}] \tag{21}$$

From (20) and (21)

$$\begin{aligned} C_v' &= \tfrac{1}{2}Nk_B[1 + (\sqrt{2}/8)\, e^{-|\xi|}] \\ &\approx \tfrac{1}{2}Nk_B[1 + (\pi^2/2)(N\hbar c/eH)(\hbar^2/\pi m^* k_B T)^{1/2}] \end{aligned} \tag{22}$$

Thus, the asymptotic value tends towards the one-dimensional "classical" value, the variation going as $1/H$ and $1/T^{1/2}$.

When we take account of spin splitting, however, the remaining terms, while ultimately going to zero as e^{-2R}, may be quite appreciable in the intermediate region because of the R and R^2 multiplying factors. From (14) and (15) we observe that these terms contribute only by virtue of the presence of some electrons of opposite spin.

Designating by $C_v^{(s)}$ the spin splitting contribution to specific heat, if we keep only terms to the first order in e^{-2R} and to the second order in $e^{-|\xi_-|} = e^{-\xi}$, we get

$$\begin{aligned} C_v^{(s)} &= (Ak_B/\beta^{1/2}S_{-3})\, e^{-2\xi-2R}[-\sqrt{2}R\, e^{-\xi} + 4R^2(1 - \sqrt{2}\, e^{-\xi})] \\ &\approx Nk_B\, e^{-2R}(4R^2 - \sqrt{2}R\, e^{-\xi}) \end{aligned}$$

by virtue of (20). The second term in the bracket is approximately

$$-\sqrt{2}R(N\beta^{1/2}/A) \approx -(\hbar^2/\pi m^* k_B T)^{3/2} 2\pi^3 \gamma N = -\lambda \tag{23}$$

and is thus independent of H.

Thus the additional contribution which must be added to C_v' [Eq. (21)] to give the whole specific heat is

$$C_v^{(s)} = Nk_B(4R^2 - \lambda)\, e^{-2R} \tag{24}$$

It is easily verified that this contribution is diminishing in the whole region of complete nondegeneracy. It is, however, as seen from Fig. 2, not a small contribution. On the other hand, it ultimately decreases exponentially with H, while the excess over the "classical" value of the contribution which is not dependent on spin merely decreases as $1/H$.

ACKNOWLEDGMENTS

We wish to acknowledge the assistance of the National Research Council of Canada in the form of a research grant to one of us (P.R.W.). We also wish to thank Dr. O. P. Gupta for useful discussions and assistance with the computer program.

REFERENCES

1. S. Askenazy, J.-P. Ulmet, and J. Léotin, *Solid State Commun.* **7**, 989 (1969).
2. T. C. Cetas, C. R. Tilford, and C. A. Swenson, *Phys. Rev.* **174**, 835 (1968).
3. V. von Piesbergen, *Z. Naturforsch.* **18a**, 141 (1963).
4. Kh. I. Amirkhanov, R. I. Bashirov, and A. Yu. Mollaev, *Fiz. Tverd. Tela* **13**, 849 (1971) [English trans., *Soviet Phys.—Solid State* **13**, 701 (1971)].
5. J. H. Wilson, W. F. Love, and S. C. Miller, *Phys. Rev.* **165**, 923 (1968).
6. J. S. Blakemore, *Semiconductor Statistics* (Pergamon Press, Oxford, 1962), p. 346.

THE MAGNETOTHERMAL EFFECT IN SEMICONDUCTORS IN STRONG MAGNETIC FIELDS

J.P. JAY-GERIN and A. BRIGGS

Centre de Recherches sur les Très Basses Températures, C.N.R.S.,
B.P. 166 Centre de Tri, 38042 Grenoble-Cédex, FRANCE.

ABSTRACT

We have calculated the adiabatic differential temperature change, $(\frac{\partial T}{\partial H})_S$, of a semiconductor at very low temperatures when subjected to a magnetic field strong enough to make the electron distribution non-degenerate. The transition to non-degeneracy is characterized by a sharp negative dip in $(\frac{\partial T}{\partial H})_S$. Zeeman splitting may greatly modify the variation of $(\frac{\partial T}{\partial H})_S$ as a function of field. The results are illustrated with numerical calculations for Ga As with electron concentrations of 1.2×10^{16} cm^{-3} and 3.8×10^{16} cm^{-3}.

RESUME

Nous avons calculé la variation différentielle de température avec le champ magnétique à entropie constante, $(\frac{\partial T}{\partial H})_S$, d'un semiconducteur à très basses températures, soumis à un champ magnétique suffisamment intense pour induire la distribution électronique à un état non-dégénéré. La transition vers la non-dégénérescence est caractérisée par un minimum négatif très marqué de $(\frac{\partial T}{\partial H})_S$. L'effet du clivage de spin peut modifier profondément la variation de $(\frac{\partial T}{\partial H})_S$ en fonction du champ. Les résultats sont illustrés par des calculs numériques pour l'arséniure de gallium avec des concentrations de 1.2×10^{16} et 3.8×10^{16} électrons par cm^3.

I. INTRODUCTION

Experiments on magnetothermal effects measure the adiabatic variation of temperature of a sample as the magnetic field is changed. The most well-known example of the effect is the adiabatic demagnetisation of a paramagnetic salt, which, until recently, was the sole method of obtaining temperature below 0.1 K. Other examples of the magnetothermal effect exist. In particular, the oscillatory magnetothermal effect[1], which is related to the oscillatory variation of the free energy of a system of electrons in a magnetic field, is of interest as a tool for exploring the Fermi surface and for measuring spin-splittings in situations where the Fermi energy does not change greatly with magnetic field. The quantity frequently measured in this type of experiment is the magnetothermal coefficient $(\frac{\partial T}{\partial H})_S$. The sensitivity is such that variations in this quantity of 10^{-8} K/gauss^{-1} at 0.5 K may be detected. Measurements of the effect have hitherto been made in various metals and semimetals[2], but, so far no attempt seems to have been made to investigate the effect in semiconductors.

The behaviour of electrons in a solid is profoundly modified by the application of a magnetic field. Due to the effects of quantisation, the energy level structure (ignoring spin-splitting) consists of a set of magnetic sub-bands (Landau levels) separated in energy by $\hbar\omega_c$ (ω_c cyclotron frequency). Since the density of states is discontinuous at the bottom of each of these sub-bands, the free energy is a periodic function of the inverse magnetic field. Properties related to it, such as the magnetisation and the magnetothermal coefficient, reflect this periodic behaviour and, as noted above, may be used at low temperatures to study the Fermi surface. However, as the magnetic field is increased, the electrons become concentrated in fewer and fewer Landau levels, the effects of spin-splitting become apparent

and, eventually, the region of oscillatory behaviour is surpassed and only the lowest, n = 0, level is occupied. This is the extreme quantum region, which while the electron distribution is still degenerate is referred to as the ultra-quantum region. When, as the magnetic field is increased further, the n = 0 level is pushed towards, and finally past, the Fermi level, a transition from the degenerate to a non-degenerate electron system occurs[3,4]: the so-called hyper-quantum region is reached.

Experimentally, the extreme quantum region occurs for magnetic fields sufficiently strong and temperatures sufficiently low that $\hbar\omega_c >> k_B T$ and $\frac{3}{2}\hbar\omega_c >> \mu$, where $k_B T$ is the thermal energy of a typical conduction electron, and μ the Fermi energy. For a metal such as sodium this region is attained in fields of the order of 2000 KG, but in a lightly doped semiconductor, the region may be attained in a field of 100 KG, which is well within the range of those presently available. In fact the transition to the hyper-quantum region has so far only been observed experimentally in the transverse and longitudinal magnetoresistance of Ga As with an electron concentration of 3.8×10^{16} cm^{-3} for fields between 30 and 150 KG at 2 K[5].

In the work reported here we have calculated, under certain simplifying assumptions, $(\frac{\partial T}{\partial H})_S$ for a semiconductor in the extreme quantum region. The aim of this calculation was twofold : to determine whether the change in the electron distribution could be observed in a magnetothermal experiment, and to examine the effects of the Zeeman splitting of the n = 0 Landau level.

II. CALCULATION of $(\frac{\partial T}{\partial H})_S$

The adiabatic differential temperature change $(\frac{\partial T}{\partial H})_S$ is given by

$$(\frac{\partial T}{\partial H})_S = - \frac{T}{C_H} (\frac{\partial M}{\partial T})_H , \qquad (1)$$

where M is the magnetisation, T the absolute temperature, H the magnetic field strength, S the entropy, and C_H ($=C_H^e+C_H^\ell$, where C_H^e is the electron heat capacity and C_H^ℓ is the lattice heat capacity) the total heat capacity at constant H. C_H^ℓ has been assumed to obey a T^3 law in the range of temperature of interest[6], and to be independent of H. By reformulating Eq.(1) in terms of the Helmholtz free-energy F(H) of the system of electrons per unit volume, we obtain

$$\left(\frac{\partial M}{\partial T}\right)_H = \frac{\partial}{\partial T}\left(-\frac{\partial F(H)}{\partial H}\right) = \frac{\partial}{\partial H}\left(-\frac{\partial F(H)}{\partial T}\right) , \qquad (2)$$

$$C_H^e = T\,\frac{\partial}{\partial T}\left(-\frac{\partial F(H)}{\partial T}\right) . \qquad (3)$$

In the extreme quantum region and for a parabolic band of effective mass m^*, F(H) can be written in the form[7]

$$F(H) = N\left(\mu - k_B T\,\frac{S_+}{S_1}\right) , \qquad (4)$$

where

$$S_+ = \sum_\sigma \mathcal{F}_{1/2}(\xi_\sigma) \ , \ S_1 = \sum_\sigma \mathcal{F}_{-1/2}(\xi_\sigma) , \qquad (5)$$

$$\xi_\sigma = \frac{1}{k_B T}\left[\mu - \frac{1}{2}\hbar\omega_c(1-\gamma\sigma)\right] , \qquad (6)$$

$\omega_c = \dfrac{|e|\,H}{m^*c}$ is the cyclotron frequency, $|e|$ is the magnitude of the electron charge, $\gamma = g(m^*/2m_o)$, g is the spectroscopic Landé factor of the conduction electrons, m_o is the free-electron mass, σ is the spin (equal to ± 1), and the $\mathcal{F}$'s are the Fermi-Dirac fundions defined by[8]

$$\mathcal{F}_j(\xi) = \frac{1}{\Gamma(j+1)} \int_0^\infty \frac{x^j\, dx}{e^{(x-\xi)}+1} \,. \tag{7}$$

These functions satisfy the condition $\mathcal{F}_j' = \mathcal{F}_{j-1}$ (prime indicates derivative with respect to ξ). The equation which determines the Fermi level μ is

$$N = A(k_B T)^{1/2} S_1 \,, \tag{8}$$

where N is the total number of electrons per unit volume,

$$A = \frac{1}{4\pi^2 r_c^2} \left(\frac{2m^* \pi}{\hbar^2}\right)^{1/2} \,, \tag{9}$$

and $r_c = (\hbar c/|e|H)^{1/2}$ is the cyclotron radius for the electron in its ground state.

Using Eqs.(1)-(9), the final expression for $\left(\frac{\partial T}{\partial H}\right)_S$ is

$$\left(\frac{\partial T}{\partial H}\right)_S = - \frac{A(k_B T)^{3/2}\left[\frac{1}{2}\left(3S_+ - \frac{S_1^2}{S_3}\right) - \frac{1}{2}R\left(\Delta_1 - \frac{S_1\Delta_3}{S_3}\right) - R^2\left(S_3 - \frac{\Delta_3^2}{S_3}\right)\right]}{H\left\{C_H^{\ell} + A\, k_B (k_B T)^{1/2}\left[\frac{1}{4}\left(3S_+ - \frac{S_1^2}{S_3}\right) - R\left(\Delta_1 - \frac{S_1\Delta_3}{S_3}\right) + R^2\left(S_3 - \frac{\Delta_3^2}{S_3}\right)\right]\right\}} \,, \tag{10}$$

where

$$S_3 = \sum_\sigma \mathcal{F}_{-3/2}(\xi_\sigma) \,, \quad \Delta_1 = \sum_\sigma \sigma \mathcal{F}_{-1/2}(\xi_\sigma) \,, \quad \Delta_3 = \sum_\sigma \sigma \mathcal{F}_{-3/2}(\xi_\sigma) \,,$$

and $R = \frac{1}{2}(\hbar\omega_c \gamma / k_B T)$ is half the ratio of the spin splitting to the thermal energy. When the effects of spin-splitting are neglected, $R \to 0$. We have assumed in deriving Eq.(10) that the electron concentration is independent of magnetic field and temperature[9]. Magnetic freeze-out of the carriers may occur in high magnetic fields. The results of Amirkhanov, Bashirov, and

Mollaev[10] for Ga As in fields up to 300 KG suggest, however, that freeze-out is unlikely to take place for the concentrations which we have chosen in fields below 200 KG. A variation of the concentration with temperature implies that the carriers are produced by thermal excitation. It is unlikely that this is the case at the low temperatures needed to observe the effects discussed here.

III. NUMERICAL RESULTS FOR Ga As

Since Ga As has been shown to be a suitable material for studying effects in the extreme quantum limit[5], a numerical calculation has been made for this material. The behaviour of $(\frac{\partial T}{\partial H})_S$ as a function of magnetic field was investigated for two electron concentrations at various temperatures.

For Ga As, $g \approx 0.32$, $m^* = 0.07\ m_o$, and hence $R = 1.07 \times 10^{-2}\ (\frac{H}{T})$, where H is in kilogauss and T in degrees. Thus, for H = 100 KG and T = 0.5 K, $R \approx 2$.

Figure (1) shows the difference in the variation of $(\frac{\partial T}{\partial H})_S$ with magnetic field, both with and without spin splitting for a concentration of $N = 1.2 \times 10^{16}\ cm^{-3}$ electrons, at temperatures of 0.5, 1, and 2 K. The variation of $(\frac{\partial T}{\partial H})_S$ with H is seen to vary strikingly with temperature in this range.

In Fig.(2), we illustrate the difference in $(\frac{\partial T}{\partial H})_S$ calculated with and without spin splitting for two different electron concentrations, $N = 1.2 \times 10^{16}\ cm^{-3}$ and $N = 3.8 \times 10^{16}\ cm^{-3}$, at a temperature of 1 K.

Figure (3) shows the variation of $(\frac{\partial T}{\partial H})_S$ with magnetic field, both with and without spin splitting for a concentration of $N = 1.2 \times 10^{16}\ cm^{-3}$ electrons, at a temperature of 0.5 K, neglecting the lattice contribution to the total heat capacity ($C_H^{\ell} = 0$). In this case, it is easy to see from

Eq.(10) that, in the absence of spin splitting, $(\frac{\partial T}{\partial H})_S$ simply reduces to

$$(\frac{\partial T}{\partial H})_S = - \frac{2T}{H} . \qquad (11)$$

From these plots, we note :

(1) The transition to non-degeneracy in the electron distribution, which takes place when the bottom of the $\underline{n}$ = 0 Landau level (in the absence of spin effects) approaches within a few ($k_B T$) of the Fermi level, has a large effect on the variation of $(\frac{\partial T}{\partial H})_S$ with magnetic field. The curve of $(\frac{\partial T}{\partial H})_S$ vs. H exhibits a sharp negative dip as the electron distribution becomes non-degenerate. Such an effect should be detected at temperatures below 1 K by present experimental techniques.

(2) Spin splitting does not greatly change the depth of this anomalous dip, but produces a marked maximum in $(\frac{\partial T}{\partial H})_S$ at the lowest temperatures. The latter effect reflects the alignment of the spins of all the free electrons as the bottom of the upper spin branch of the $\underline{n}$ = 0 Landau band is pushed through the Fermi level[11]. As the electron concentration is increased, the field required for alignment of the spins also increases : with the magnetic fields presently available, the electron concentration must be less than a few times 10^{16} cm^{-3} for this effect to be observable.

IV. DISCUSSION

It is clear from Eq.(1) that the detailed behaviour of the quantity $(\frac{\partial T}{\partial H})_S$ is essentially controlled by two effects : (1) the variation of the

total heat capacity C_H with magnetic field and (2) the competition between the temperature derivatives of the diamagnetic $(\frac{\partial M_d}{\partial T})_H$ and the paramagnetic $(\frac{\partial M_p}{\partial T})_H$ contributions to the magnetisation M.

When the spin splitting is ignored, it is easily shown that

$$(\frac{\partial M_d}{\partial T})_H = \frac{2\, C_H^e}{H} > 0 \,, \tag{12}$$

and

$$(\frac{\partial T}{\partial H})_S = - \frac{2T}{H} (\frac{C_H^e}{C_H}) \,. \tag{13}$$

Here, C_H^e is given by

$$C_H^e = \frac{A}{2} k_B (k_B T)^{1/2} \left\{ 3\, \mathcal{F}_{1/2}(\xi) - \frac{[\mathcal{F}_{-1/2}(\xi)]^2}{\mathcal{F}_{-3/2}(\xi)} \right\}, \tag{14}$$

with $\xi = \dfrac{\mu - \frac{1}{2}\hbar\omega_c}{k_B T}$.

According to the results of Ref.(9), the general behaviour of the C_H^e-H curve is quite well understood : (1) in the region in which only the $\underline{n} = 0$ Landau level is occupied, but the system is still strongly degenerate, the electronic specific heat increases rapidly with increasing H, as a result of the rapid increase of the density of states ; (2) with the onset of non-degeneracy, C_H^e reaches a maximum value, then decreases very slowly towards the value $\frac{1}{2} N k_B$, once the system has become completely non-degenerate. Therefore, it follows from Eq.(12) that, as the lowest Landau level approaches within a few $(k_B T)$ of the Fermi level, $(\frac{\partial M_d}{\partial T})_H$ rises rapidly to a maximum, and then decreases as about 1/H. Now, for the temperatures under consideration, $C_H = C_H^{\ell} + C_H^e$ is essentially dominated by the lattice contribution, and is thus approximately independent of field. According to Eqs.(12) and (13), it follows that $(\frac{\partial T}{\partial H})_S$ is negative, and its variation with magnetic field is just the opposite

of that of $(\frac{\partial M_d}{\partial T})_H$ (dashed curves in Figs.(1) and (2)). It is finally worth noting that a measurement of the product $H(\frac{\partial T}{\partial H})_S$ as a function of magnetic field could be used to obtain the variation of the electronic specific heat C_H^e with H.

When the spin splitting is taken into account, we must consider, in addition to $(\frac{\partial M_d}{\partial T})_H$, the temperature derivative of the paramagnetic contribution $(\frac{\partial M_p}{\partial T})_H$ to the magnetisation M. In this case, the behaviour of $(\frac{\partial T}{\partial H})_S$ results from the competition between these two quantities. In fact, we have from Eq.(10)

$$(\frac{\partial M_p}{\partial T})_H = - \frac{A\, k_B (k_B T)^{1/2}}{2H} R \left[(\Delta_1 - \frac{\Delta_3 S_1}{S_3}) + 2R\, (S_3 - \frac{\Delta_3^2}{S_3}) \right] < 0 \quad . \qquad (15)$$

This quantity, which is nearly zero in the region of strong degeneracy, decreases to a negative minimum value as the bottom of the upper spin band of the $\underline{n} = 0$ Landau level passes through the Fermi level. It ultimately increases with H as the electron gas becomes non-degenerate. Obviously, the change of sign of $(\frac{\partial T}{\partial H})_S$ at 0.5 K reflects the fact that over a certain range of fields around 100 KG, there exists a paramagnetic contribution to the magnetisation for which $\left|(\frac{\partial M_p}{\partial T})_H\right| > (\frac{\partial M_d}{\partial T})_H$. This does not imply, however, that the semiconductor is paramagnetic in this range of fields. In fact, according to Ref.(10), the magnetisation M is given by

$$M = A\, k_B (k_B T)^{1/2} (\frac{T}{H}) \left[S_+ - \frac{1}{2}(\frac{\hbar\omega_c}{k_B T})\, S_1 + R\, \Delta_1 \right] , \qquad (16)$$

where the first two terms represent the Landau-Peierls diamagnetism and the last term the Pauli paramagnetism. Using Eq.(16), it is easy to show that $|M_d/M_p| \sim 100$ at T = 0.5 K, H = 100 KG, and N = 1.2×10^{16} cm^{-3}.

Finally, it should be noted that the results of Eq.(10) regarding

the effects of spin splitting actually hold for sufficiently pure samples and very low temperatures. In effect, if there exist collisions between the electrons and various kinds of scatterers, or if the temperature is raised, then either the broadening of the Landau energy levels or the thermal smearing of the Fermi level may become greater than the spin splitting, and therefore mask the corresponding spin effects. Obviously, Eq.(13) holds in thesesituations.

V. CONCLUSIONS

We have shown that the magnetothermal coefficient of a semiconductor varies dramatically in the extreme quantum region.

The transition to non-degeneracy is characterised by a sharp negative dip, which may be greatly modified by the Zeeman splitting. A very small paramagnetic contribution to the total magnetisation is sufficient to change the sign of the coefficient. The effects of the splitting may, however, be masked by impurity effects.

A numerical calculation for Ga As shows that the effect could be measured below 1 K by present experimental techniques. In addition, the electronic specific heat in a magnetic field could be obtained directly from a measurement of $H(\frac{\partial T}{\partial H})_S$ as a function of field.

REFERENCES

(1) J.E. KUNZLER, F.S. HSU, and W.S. BOYLE
Phys. Rev., 128, 1084 (1962).

(2) B. Mc COMBE and G. SEIDEL
Phys. Rev., 155, 633 (1967).

(3) L.M. ROTH and P.N. ARGYRES, in : "Semiconductors and Semimetals", Vol. 1, p. 159, Academic Press, New York (1966).

(4) E.N. ADAMS and T.D. HOLSTEIN
J. Phys. Chem. Solids, 10, 254 (1959).

(5) S. ASKENAZY, J.P. ULMET, and J. LÉOTIN
Solid State Commun., 7, 989 (1969).

(6) T.C. CETAS, C.R. TILFORD, and C.A. SWENSON
Phys. Rev., 174, 835 (1968).

(7) J.-P. JAY-GERIN
J. Phys. Chem. Solids, 35, 61 (1974).

(8) J.S. BLAKEMORE, in : "Semiconductor Statistics", Appendix B, p. 346. Pergamon Press, Oxford (1962).

(9) J.-P. JAY-GERIN and P.R. WALLACE
J. Low Temp. Phys., 7, 525 (1972).

(10) Kh. I. AMIRKHANOV, R.I. BASHIROV, and A.Yu. MOLLAEV

Fiz. Tverd. Tela, 13, 849 (1971).

[English transl. : Soviet Phys. - Solid State, 13, 701 (1971)]

(11) P.R. WALLACE and O.P. GUPTA

Phys. Stat. Solidi, 50, 619 (1972).

FIGURE CAPTIONS

Figure (1) : $(\frac{\partial T}{\partial H})_S$ as a function of magnetic field at T = 0.5, 1 and 2 K. The three arrows to the left indicate the fields at which the bottom of the upper spin band coincides with the Fermi level. The two arrows to the right show the same for the lower spin band. The value for 0.5 K does not fall in the range of fields shown.

Figure (2) : $(\frac{\partial T}{\partial H})_S$ vs. magnetic field for two different electron concentrations, $N = 1.2 \times 10^{16}$ cm^{-3} and $N = 3.8 \times 10^{16}$ cm^{-3}, at T = 1 K. The two arrows indicate the fields at which the bottom of the upper spin band coincides with the Fermi level.

Figure (3) : $(\frac{\partial T}{\partial H})_S$, as a function of magnetic field, calculated with (g=0.32) and without spin splitting for Ga As with $N = 1.2 \times 10^{16}$ cm^{-3} electrons, at a temperature of T = 0,5 K, assuming C_H^{ℓ} (lattice heat capacity) = 0. The arrow indicates the field at which the bottom of the upper spin band coincides with the Fermi energy.

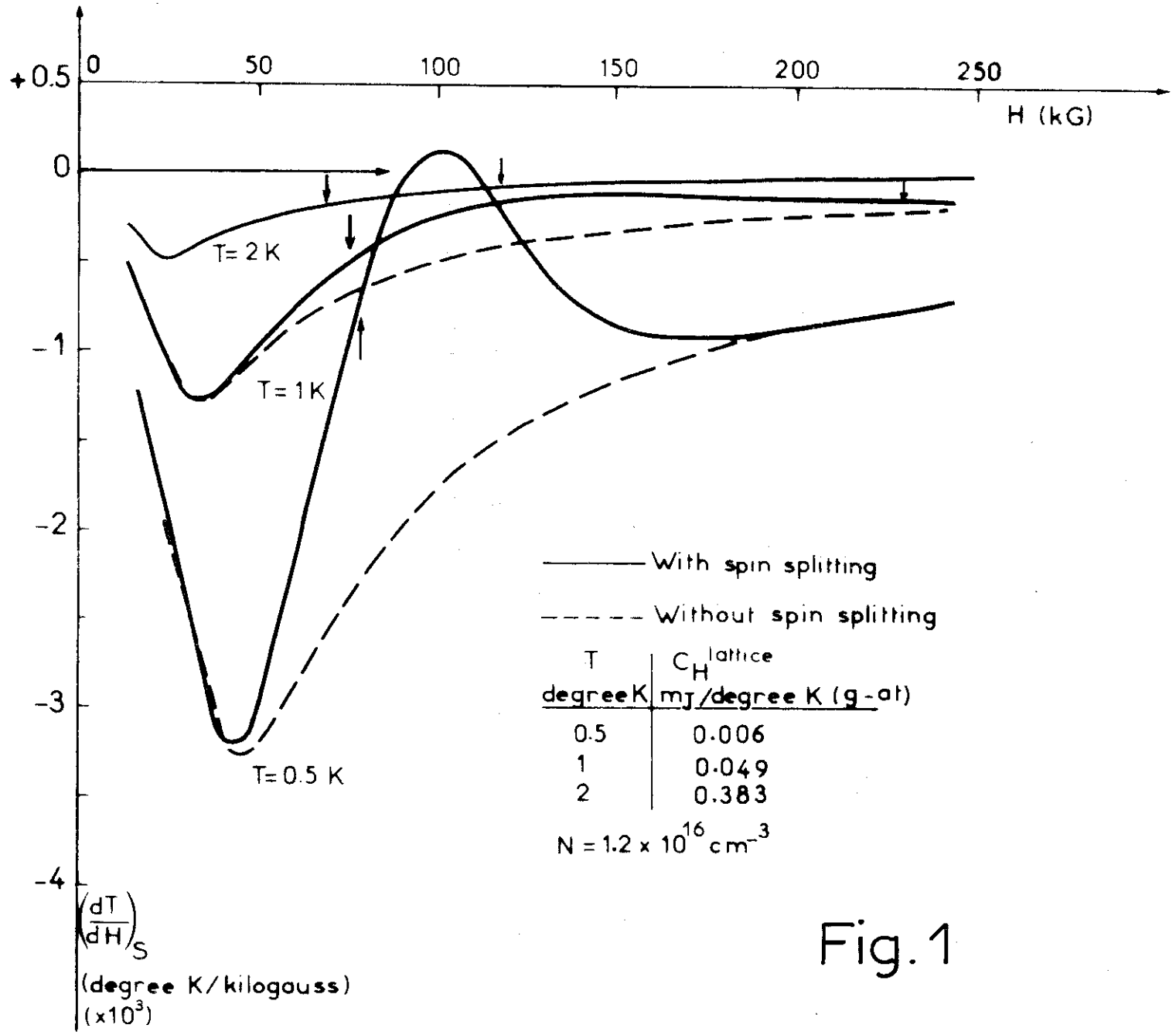

T degree K	$C_H^{lattice}$ mJ/degree K (g-at)
0.5	0.006
1	0.049
2	0.383

$N = 1.2 \times 10^{16}\ cm^{-3}$

Fig. 1

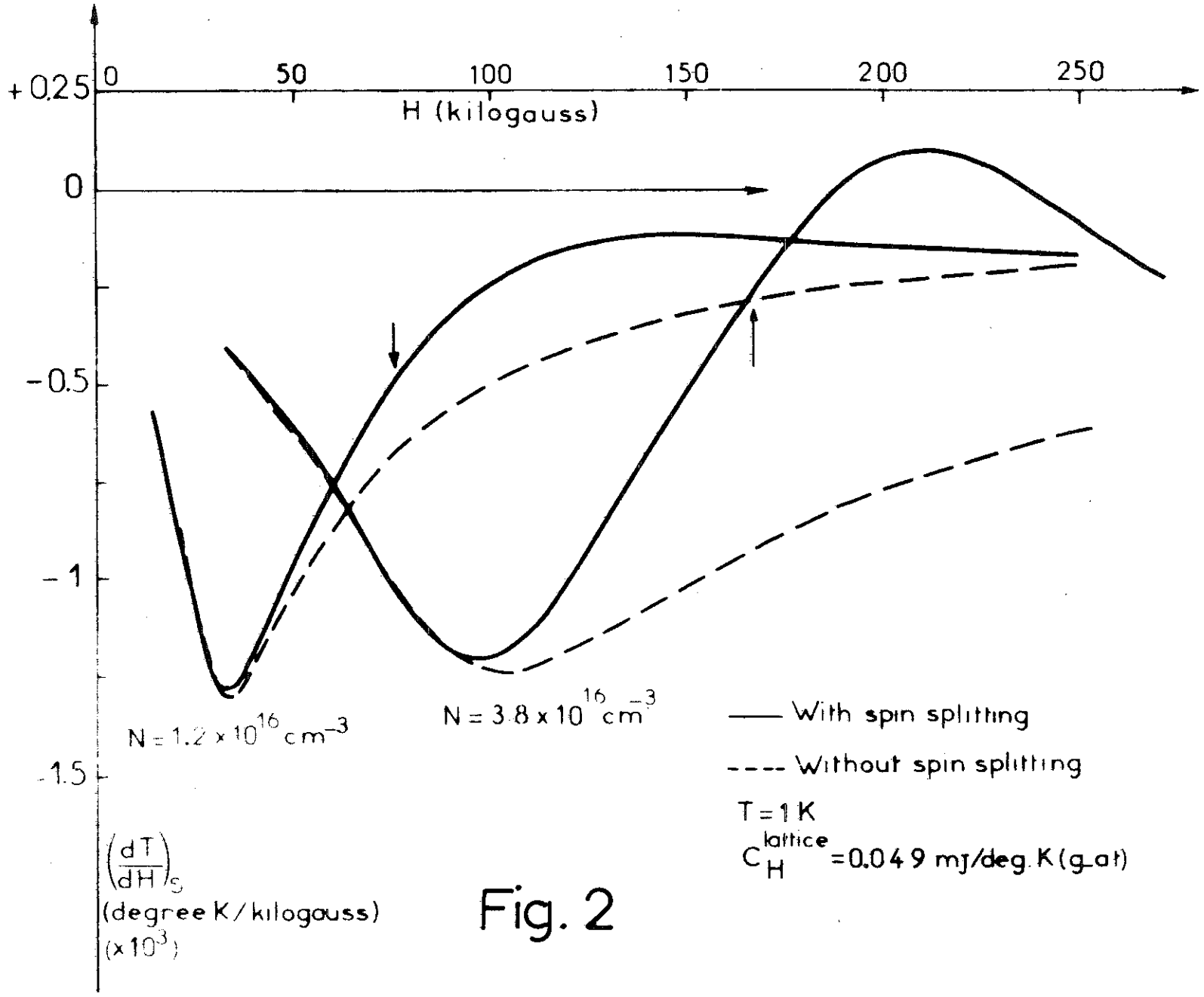
+0.25
0
-0.5
-1
-1.5
0
50
100
150
200
250
H (kilogauss)
N = 1.2 x 10^16 cm^-3
N = 3.8 x 10^16 cm^-3
With spin splitting
Without spin splitting
T = 1 K
C_H^lattice = 0.049 mj/deg.K (g-at)
(dT/dH)_S
(degree K / kilogauss)
(x 10^3)

Fig. 2

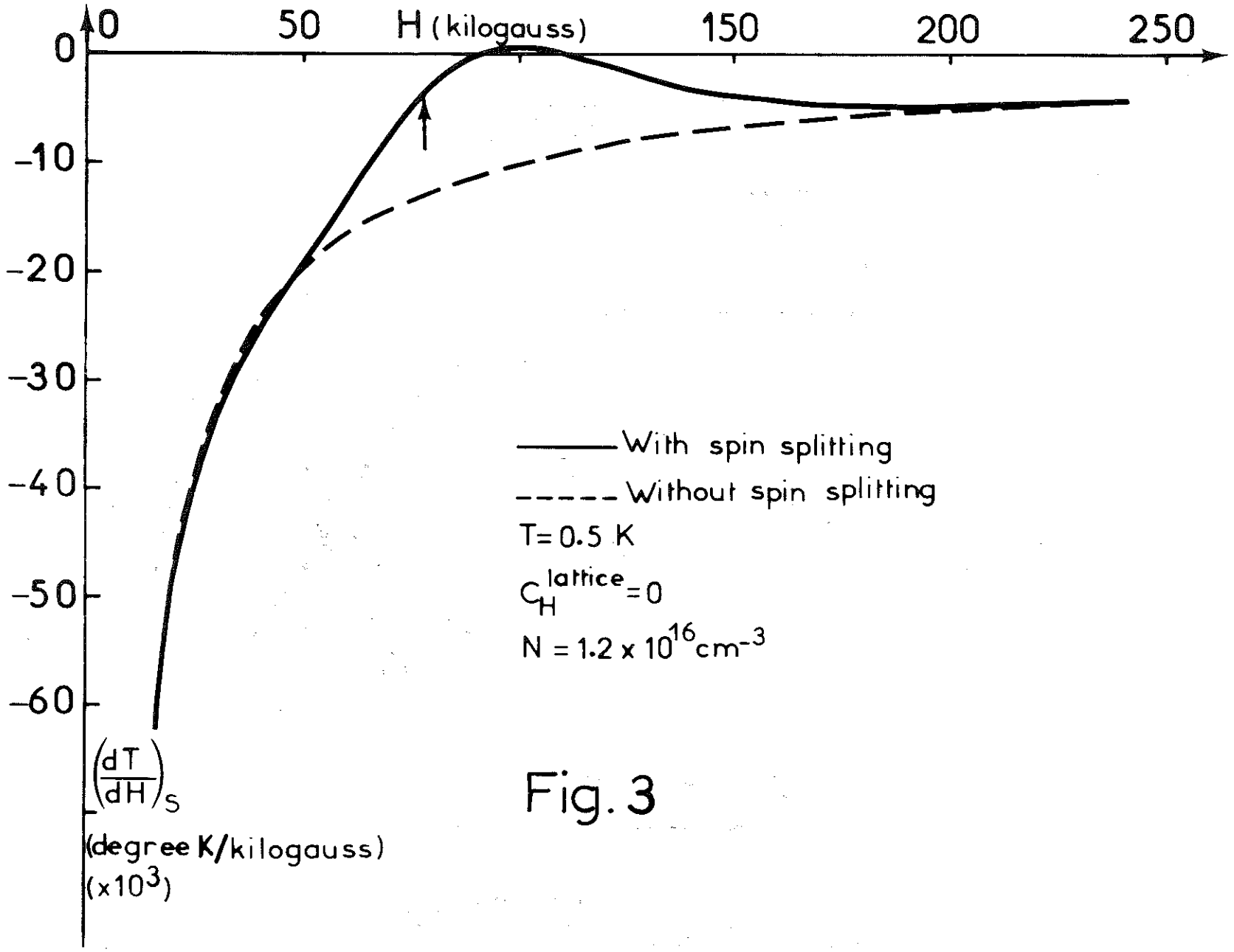
0
50
H (kilogauss)
150
200
250
0
-10
-20
-30
-40
-50
-60
With spin splitting
Without spin splitting
T= 0.5 K
$C_H^{lattice} = 0$
$N = 1.2 \times 10^{16} cm^{-3}$
$\left(\frac{dT}{dH}\right)_S$
(degree K/kilogauss)
$(\times 10^3)$

Fig. 3

CHAPITRE III

ETUDE DES EFFETS THERMOMAGNETIQUES (POUVOIR THERMOELECTRIQUE ET COEFFICIENT NERNST-ETTINGSHAUSEN) DANS UN SEMICONDUCTEUR EN REGIME EXTREME QUANTIQUE

Ce chapitre est consacré à une étude théorique des propriétés de transport thermomagnétiques (effets magnéto-Seebeck et Nernst-Ettingshausen) d'un semiconducteur en régime extrême quantique, quand tous les électrons de la bande de conduction sont concentrés dans le plus bas niveau de Landau n = 0. Dans le calcul développé ici, la distribution électronique est dégénérée ou non-dégénérée, suivant l'intensité du champ magnétique appliqué. L'intérêt principal de ce travail est d'examiner l'effet de la "transition statistique" (dégénéré en non-dégénéré), qui se produit dans le gaz d'électrons lorsque le bas du niveau de Landau fondamental n = 0 s'approche à quelques ($k_B T$) du niveau de Fermi (voir chapitre I), sur les variations du pouvoir thermoélectrique S(H) et du coefficient Nernst-Ettingshausen $A_{NE}(H)$.

Nous supposons, comme dans les chapitres précédents que l'échantillon est de qualité et de pureté suffisantes pour que soit satisfaite la condition $\omega_c \tau >> 1$, où ω_c est la fréquence cyclotron et τ le temps de relaxation des électrons. D'autre part, nous considérons le modèle simple d'un semiconducteur isotrope, avec une bande d'énergie parabolique de masse effective m^*. Un tel modèle décrit convenablement la situation pour des concentrations en électrons suffisamment faibles.

Dans la théorie présentée ici, nous utilisons l'"approche Peltier" des phénomènes de transport thermomagnétiques, due à Herring (Herring 1954, Herring, Geballe et Kunzler 1958 et 1959 et Gurevich et Nedlin 1962) (voir, également, Partie I, chapitre III) : nous calculons la densité de courant de chaleur Peltier $\vec{U}$ créé par la présence d'un champ électrique $\vec{E}$, dans des conditions isothermes. Compte-tenu de l'interaction électron-phonon, $\vec{U}$ est la somme de deux contributions : $\vec{U} = \vec{U_e} + \vec{U_p}$, où $\vec{U_e}$ est le flux de chaleur transportée par les électrons eux-mêmes (contribution de "diffusion électronique") et $\vec{U_p}$ le flux de chaleur transportée par le système de phonons, lequel est entraîné par les électrons (contribution de "phonon-drag").

La considération du mouvement électronique, en présence d'un champ électrique $\vec{E}$ // Ox ($\vec{E}$ = (E,0,0)) et d'un champ magnétique $\vec{H}$ // Oz ($\vec{H}$ = (0,0,H)) croisés, nous enseigne que les électrons se déplacent principalement le long de la direction Oy avec une vitesse moyenne $\overline{v_y}$ égale à la vitesse de Hall (voir, par exemple, Kahn et Frederikse 1959 et Landau et Lifshitz 1962). Aux faibles concentrations d'impuretés que nous envisageons dans ce travail, $\overline{v_y}$ est, en effet, beaucoup plus grand que

la vitesse électronique moyenne $\overline{v_x}$ parallèle au champ électrique $\vec{E}$. Ceci vient du fait que le flux de courant dans la direction Ox, J_x, est produit et augmenté par les collisions des électrons avec le réseau, alors que la composante y du courant, J_y, est entièrement déterminée par les champs électrique et magnétique eux-mêmes, indépendamment des paramètres de collisions électroniques. Dans l'ensemble de cette étude, nous nous plaçons délibérément à l'approximation d'ordre zéro par rapport aux collisions électroniques. Cette approximation, bien qu'élémentaire, décrit convenablement la situation dans le cas d'un semiconducteur à très basses températures, soumis à des champs magnétiques suffisamment intenses pour que la condition $\omega_c\tau >> 1$ soit réalisée. Dans le cadre de cette approximation, nous avons alors $\overline{v_x} = 0$ et $\overline{v_y} = -\frac{cE}{H}$, où E et H sont respectivement les intensités des champs électrique et magnétique et c la vitesse de la lumière. En d'autres termes, le courant électrique est exactement le long de la direction Oy. Ce flux d'électrons donne naissance au flux de chaleur Peltier $(U_e)_y$ dans la direction Oy. D'autre part, par suite du couplage électron-phonon, le flux d'électrons entraîne avec lui le système de phonons, qui induit, à son tour, le flux de chaleur Peltier $(U_p)_y$ dans la direction Oy. A partir de la relation de définition du coefficient Peltier π,

$$\vec{U} = \pi \vec{J} \ , \qquad (\vec{\nabla} T \equiv 0) \tag{III-1}$$

où $\vec{J}$ est la densité de courant électrique, nous avons :

$$(\pi_{e,p})_{yy}(H) = \frac{(U_{e,p})_y}{J_y} \ , \quad \vec{H} = (0,0,H) \tag{III-2}$$

les indices e et p désignant respectivement les contributions de "diffusion électronique" et de "phonon-drag".

D'après les relations de Kelvin-Onsager de la thermodynamique des processus irréversibles, nous obtenons :

$$\begin{aligned} S_{e,p} = (S_{e,p})_{yy}(H) &= \frac{1}{T}(\pi_{e,p})_{yy}(-H) \\ &= \frac{1}{T}\frac{(U_{e,p})_y}{E}\rho_{xy}(H) \end{aligned} \tag{III-3}$$

pour les composantes de "diffusion électronique" (S_e) et de "phonon-drag" (S_p) du pouvoir thermoélectrique transverse S(H). $\rho_{xy}(H)$ est ici l'élément du tenseur de magnétorésistance, donné par (Beer 1963) :

$$\rho_{xy}(H) = -\frac{1}{\sigma_{xy}(H)} \quad , \quad |\sigma_{xy}| >> |\sigma_{xx}|$$

$$= -\frac{H}{N\,e\,c} \quad , \quad \vec{H} = (0,0,H) \qquad \text{(III-4)}$$

où N est le nombre total d'électrons par unité de volume et e(<0) leur charge.

Les composantes de "diffusion électronique" (A_{NE}^{e}) et de "phonon-drag" (A_{NE}^{p}) du coefficient Nernst-Ettingshausen transverse $A_{NE}(H)$ s'écrivent (voir Partie I, Appendice) :

$$A_{NE}^{e,p} = \frac{1}{H\,T}\,\frac{(U_{e,p})_y}{E}\,\rho_{xx}(H) \quad , \qquad \text{(III-5)}$$

où ρ_{xx} est l'élément du tenseur de magnétorésistance, donné par (Roth et Argyres 1966) :

$$\rho_{xx}(H) = \rho_{\perp} = \frac{\sigma_{xx}}{\sigma_{xx}^2 + \sigma_{xy}^2} \approx \frac{\sigma_{xx}}{(\sigma_{xy})^2} \quad , \ \vec{H} = (0,0,H)$$

$$\approx \left(\frac{H}{Nec}\right)^2 \sigma_{xx} \quad . \qquad \text{(III-6)}$$

1) Pouvoir thermoélectrique de "diffusion électronique" S_e

A l'approximation d'ordre zéro par rapport aux collisions, nous négligeons complètement la conversion irréversible d'énergie électronique en chaleur par les collisions avec le réseau. Nous pouvons donc en quelque sorte supposer des conditions de quasi-équilibre, et par conséquent regarder le processus comme réversible (Mac Donald 1962, Obraztsov 1965 et Woollam 1971). Nous avons alors, à partir de l'équation (III-3) :

$$S_e = \frac{S}{N\,e} \quad , \qquad \text{(III-7)}$$

où S est l'entropie du gaz d'électrons par unité de volume, donnée par (voir chapitre II) :

$$S = -\frac{\partial F(H)}{\partial T} \quad , \qquad \text{(III-8)}$$

où F(H) est l'énergie libre de Helmholtz du système d'électrons par unité de volume (voir Appendice A).

Les relations (III-7) et (III-8) montrent clairement qu'en champs magnéti-

ques suffisamment intenses, tels que $\omega_c\tau >> 1$, le pouvoir thermoélectrique de "diffusion électronique" S_e peut être obtenu directement à partir de la seule connaissance de la concentration d'électrons et de la structure de bandes, en ignorant les paramètres de collisions électroniques (Zawadzki 1974).

Les principaux résultats obtenus concernant S_e se résument ainsi :

(i) Dans le domaine ultra-quantique, lorsque le gaz d'électrons est fortement dégénéré, S_e s'exprime en termes de la densité d'états au niveau de Fermi $\mathcal{D}(\zeta)$ par la relation habituelle, valable en l'absence de collisions (Mac Donald 1962 et Ziman 1960):

$$S_e = \frac{k_B}{e} \frac{\pi^2}{3} k_B T \frac{\mathcal{D}(\zeta)}{N} \quad , \qquad \text{(III-9)}$$

où $\mathcal{D}(\zeta)$ est donnée par (en ignorant les effets de spin) :

$$\mathcal{D}(\zeta) = \frac{1}{4\pi^2} \left(\frac{2m^*}{\hbar^2}\right)^{3/2} \frac{\hbar\omega_c}{\sqrt{\zeta - \frac{1}{2}\hbar\omega_c}} \quad . \qquad \text{(III-10)}$$

(ii) La "transition statistique" (dégénéré en non-dégénéré), qui s'opère dans la distribution électronique quand le bas de la bande de Landau fondamentale n = 0 s'approche à quelques ($k_B T$) du niveau de Fermi, a un effet important sur la variation de S_e en fonction du champ magnétique appliqué. Cet effet se manifeste par une augmentation considérable de $|S_e|$, qui résulte essentiellement de la rapide augmentation de la densité d'états effective au niveau de Fermi, lors du passage de la distribution électronique vers le régime non-dégénéré.

(iii) Le clivage de spin du niveau de Landau fondamental n = 0 peut modifier et réduire appréciablement $|S_e|$ en fonction du champ magnétique. Lorsque l'on tient compte de cet effet, la courbe $|S_e|(H)$ croît rapidement vers un maximum, s'aplatit quelque peu quand le bas de la branche supérieure de spin franchit le niveau de Fermi, puis croît à nouveau de façon monotone avec H. Comme l'indique clairement l'équation (III-7), liant S_e à l'entropie du gaz électronique, une telle variation reflète l'alignement des spins de tous les électrons libres. Cet effet peut néanmoins être masqué par l'élargissement des niveaux dans les échantillons impurs.

2) Pouvoir thermoélectrique de "phonon-drag" S_p

En ce qui concerne le calcul du flux de chaleur Peltier $\vec{U}_p$ transportée par le système de phonons dans le cristal en présence de champs magnétique $\vec{H}$ // Oz et

électrique $\vec{E}$ // Ox constants croisés, l'équation de transport de Boltzmann pour les phonons donne :

$$\vec{U}_p = \sum_{\vec{q},j} \hbar\omega_{\vec{q}j}\, \vec{v}_{\vec{q}j}\, \tau_p(\vec{q}j) \left[\frac{\partial N_{\vec{q}j}}{\partial t}\right]_{e\text{-}p} , \qquad \text{(III-11)}$$

où $\vec{q}$ et j représentent respectivement le vecteur d'onde de phonon et l'indice de polarisation. Dans le domaine des très basses températures qui nous concerne ici, seuls contribuent à la sommation sur $\vec{q}$ les modes de vibration acoustiques de grande longueur d'onde. Pour ces modes, nous adoptons la relation de dispersion $\omega_{\vec{q}j}=s_j q$, où s_j est la vitesse du son et q le module de $\vec{q}$. La vitesse de groupe d'un phonon d'énergie $\hbar\omega_{\vec{q}j}$ est alors $\vec{v}_{\vec{q}j} = s_j(\vec{q}/q)$. D'autre part, puisque les surfaces d'énergie constante électroniques sont isotropes, seuls les phonons longitudinaux peuvent intéragir avec les électrons, et les deux branches transverses du spectre de phonons sont inefficaces dans le processus de "phonon-drag". Il s'ensuit que la sommation sur j, dans l'équation (III-11), se réduit simplement à la contribution de la branche acoustique longitudinale. τ_p est un temps de relaxation qui décrit la diffusion des phonons par les bords de l'échantillon, les impuretés et les autres phonons, à l'exception des électrons. A températures suffisamment basses, seule la diffusion des phonons par les limites du cristal est importante, et τ_p peut être considéré comme indépendant de q et T (Casimir 1938). Nous supposons également que τ_p n'est pas affecté par la présence du champ magnétique (Puri 1965). $(\partial N_{\vec{q}j}/\partial t)_{e\text{-}p}$ représente enfin le taux de variation de la fonction de distribution de phonons dû aux processus de collisions électron-phonon.

A partir des équations (III-3), (III-4) et (III-11), nous obtenons une expression pour S_p, moyennant les hypothèses suivantes : (1) tous les électrons dans la bande de conduction sont concentrés dans le niveau de Landau fondamental n = 0 (régime extrême quantique), le gaz électronique pouvant être dégénéré ou non-dégénéré suivant la force du champ magnétique ; (2) le nombre quantique n = 0 ne change pas lors de la collision d'un électron par un phonon ; (3) l'interaction électron-phonon est traitée à l'aide du potentiel de déformation ; (4) l'effet de clivage de spin peut être ignoré. L'expression finale, qui est valable au premier ordre en champ électrique (notons ici que le calcul des niveaux d'énergie d'un électron en présence d'un champ électrique $\vec{E}$ // Ox et d'un champ magnétique $\vec{H}$ // Oz constants croisés est développé à l'Appendice C) et au second ordre dans le couplage électron-phonon (approximation de Born au premier ordre), est donnée par :

$$S_p = \frac{k_B}{e}\, \frac{1}{4\pi^2 N}\, \left(\frac{k_B T}{\hbar s}\right)^3 \int_0^{\Theta_D/T} dx\, x^2\, \mathcal{C}_p(x)\, I_p(x) , \qquad \text{(III-12)}$$

où $\frac{k_B}{|e|} = 86.2\ \mu V/K$, N est la concentration d'électrons, Θ_D la température de Debye, $\mathcal{C}_p(x) = x^2\, e^x/(e^x-1)^2$ la fonction d'Einstein, $x = \hbar sq/k_BT$,

$$I_p(x) = \int_0^1 (1-\mu^2)\ \left(\frac{\Gamma(x,\mu)}{\Gamma(x,\mu) + \frac{1}{\tau_p}}\right) \qquad \text{(III-13)}$$

mesure l'efficacité d'"entraînement" dans le processus de "phonon-drag", c'est-à-dire la fréquence relative des collisions phonon (q)-électron par rapport à l'ensemble des collisions auxquelles les phonons (q) peuvent participer, $\mu = \cos\theta$, θ étant l'angle entre la direction $\vec{q}$ et l'axe Oz,

$$\Gamma(\vec{q}) = \Gamma(q,\mu)$$

$$= \frac{A(q)\ e^{\frac{1}{2}r_c^2\, q^2\, \mu^2}}{|\mu|\left[\mathrm{Cosh}\left(\frac{m^*\, s^2}{2k_BT\ \mu^2} + \frac{q^2\mu^2}{4\ q_T^2} - \xi\right) + \mathrm{Cosh}\left(\frac{1}{2}\frac{\hbar sq}{k_BT}\right)\right]}\ , \qquad \text{(III-14)}$$

est l'inverse du temps de relaxation électron-phonon, $r_c = (\hbar c/|e|H)^{1/2}$ le rayon de l'orbite cyclotron, $q_T = (2m^*\, k_BT/\hbar^2)^{1/2}$ le vecteur d'onde thermique électronique, $\xi = \frac{1}{k_BT}\left(\zeta - \frac{1}{2}\hbar\omega_c\right)$,

$$A(q) = \frac{m^*\, C^2}{2\,\pi\,\hbar^2\, d\, s\, r_c^2}\ e^{-\frac{1}{2}r_c^2\, q^2}\ \mathrm{Sinh}\left(\frac{1}{2}\frac{\hbar sq}{k_BT}\right)\ , \qquad \text{(III-15)}$$

C la constante de couplage par potentiel de déformation et d la densité du cristal.

Les principaux résultats obtenus concernant S_p peuvent se résumer ainsi:

(i) A T donnée, $|S_p|$ croît considérablement avec le champ magnétique en régime extrême quantique, beaucoup plus vite que la composante de "diffusion électronique" $|S_e|$. A la température de l'hélium liquide, S_p fournit la contribution dominante au pouvoir thermoélectrique total $S = S_e + S_p$. En champs magnétiques intenses, la courbe $|S_p|(H)$ tend à se saturer. Cette tendance à la saturation est davantage prononcée lorsque la température diminue. Un tel comportement est étroitement lié avec le changement de statistique (dégénéré en non-dégénéré) qui s'opère dans la distribution électronique, lorsque le bas de la bande de Landau fondamentale n = 0 s'approche à (k_BT) près du niveau de Fermi.

(ii) A H donné, $|S_p|$ décroît très rapidement avec T aux plus basses températures (approximativement comme T^3 (voir Eq. (III-12)). A très basses températures (disons,

par exemple, 0.5 K), S_p devient quasiment négligeable comparé au terme de "diffusion électronique" S_e, qui décroît aussi avec T, mais bien moins vite. Compte-tenu des résultats précédents concernant le calcul de S_e dans la limite extrême quantique, l'étude du pouvoir thermoélectrique en régime extrême quantique et à très basses températures, devrait permettre d'obtenir des renseignements complémentaires sur la structure de bandes des semiconducteurs.

(iii) La diffusion des phonons sur les limites de l'échantillon (diffusion de type Casimir) peut modifier considérablement l'amplitude et la variation de $|S_p|$ en fonction de H. Le pouvoir thermoélectrique de "phonon-drag" est particulièrement sensible aux dimensions et à la forme de l'échantillon en régime extrême quantique.

(iv) Les collisions phonon-phonon réduisent $|S_p|$ aux plus hautes températures. Typiquement, à H fixé, la courbe $|S_p|(T)$, après une croissance initiale rapide, passe par un maximum, puis décroît lentement. Ici encore, l'étude du pouvoir thermoélectrique en régime extrême quantique devrait être à même de constituer un outil intéressant pour l'analyse des interactions phonon-phonon dans les semiconducteurs.

3) Coefficient Nernst-Ettingshausen A_{NE}

A températures suffisamment basses et en champs magnétiques suffisamment intenses, nous pouvons, dans une bonne approximation, négliger la chaleur Peltier d'origine purement électronique devant la contribution due à l'effet de "phonon-drag". Nous avons alors ($\omega_c\tau \gg 1$) (voir Eqs. (III-3) et (III-5)):

$$S(H) \simeq S_p = \frac{1}{T} \frac{(U_p)_y}{E} \rho_{xy}(H) \qquad \text{(III-16)}$$

et

$$A_{NE}(H) \simeq A_{NE}^p = \frac{1}{HT} \frac{(U_p)_y}{E} \rho_{xx}(H) \ . \qquad \text{(III-17)}$$

En combinant les équations (III-16) et (III-17), et en utilisant les relations (III-4) et (III-6), nous obtenons

$$A_{NE}(H) \simeq - \frac{N e c}{H^2} S(H) \quad \rho_\perp \ . \qquad \text{(III-18)}$$

Puisque le pouvoir thermoélectrique S(H) en régime extrême quantique varie de manière sensiblement monotone avec le champ magnétique appliqué, $A_{NE}(H)$ doit refléter l'anomalie "géante" de $\rho_\perp$ en fonction de H à la "transition statistique", lorsque le bas de la bande de Landau n = 0 s'approche à quelques ($k_B T$) du niveau de Fermi (voir chapitre I).

Solid State Communications, Vol. 14, pp. 831–834, 1974. Pergamon Press. Printed in Great Britain

MAGNETIC FIELD DEPENDENCE OF THE THERMOELECTRIC POWER OF n – TYPE GALLIUM ARSENIDE IN THE EXTREME QUANTUM LIMIT*

J.P. Jay-Gerin†

Centre de Recherches sur les Très Basses Températures, C.N.R.S., B.P. 166 Centre de Tri, 38042 Grenoble-Cédex, France

(*Received* 23 *October* 1973 *by J.L. Olsen*)

The effect of the quantization of the electron energy levels in a strong transverse magnetic field H on the low-temperature thermoelectric power (TEP) S of a high-purity isotropic semiconductor (n – type gallium arsenide GaAs) is investigated theoretically. The "electron-diffusion" (S_e) and "phonon-drag" (S_p) components of $S(=S_e+S_p)$ are calculated in the extreme quantum limit, when all the electrons in the conduction band are concentrated in the lowest Landau level. The transition to nondegeneracy, which takes place when the bottom of the lowest Landau level is driven through the Fermi level, has a large effect on the variations of S_e and S_p with magnetic field. The results are illustrated with numerical calculations for n – type GaAs at 4.2 K with $1.2 \times 10^{16}\,\mathrm{cm}^{-3}$ electrons.

1. INTRODUCTION

ASKENAZY *et al.*[1] measured the longitudinal ($\rho_\parallel$) and transverse ($\rho_\perp$) magnetoresistance at $T = 2$ K of a sample of n – type gallium arsenide (GaAs) with $N = 3.8 \times 10^{16}\,\mathrm{cm}^{-3}$ electrons. They found that, after a large and rapid increase in the range 30–90 kG, the magnetoresistance curve turned over and decreased rapidly above ≈ 90 kG, going to a relatively small and slowly varying negative value by about 150 kG. This anomaly they associated with the transition from degenerate to non-degenerate statistics as the bottom of the lowest Landau level approaches the Fermi level.

In this work, we wish to study, under certain simplifying assumptions, the thermoelectric power (TEP) S of a semiconductor (GaAs) at very low temperatures when subjected to a transverse magnetic field sufficiently strong that all the conduction electrons are condensed into the lowest Landau cylinder. This regime, in which $\hbar\omega_c \gg k_B T, \zeta$, where $\hbar\omega_c$ is the Landau level spacing, $k_B T$ the thermal energy, and ζ the Fermi energy, is what we call the 'extreme quantum limit'. The main object of our work is to show that the change in the electron distribution manifested in (1) has also a large effect on the variation of S as a function of magnetic field. For this purpose, the electron gas may be either degenerate or nondegenerate, depending on the strength of the applied transverse magnetic field H. In the theory presented here, we assume the sample of sufficiently high purity such that $\omega_c \tau \gg 1$, where $\omega_c = |e|H/m^* c$ is the cyclotron frequency and τ the electron relaxation time. In this limit, the Landau quantization is preserved in spite of the collisions of the electrons with the lattice. GaAs is chosen because of its very small spectroscopic g – factor ($g \approx 0.32$), so that Zeeman splitting can be ignored. In addition, a simple parabolic energy band with isotropic effective mass m^* is assumed. This adequately describes the situation at sufficiently low electron concentrations.

As is well known,[2–4] the total TEP of a semiconductor at low temperatures and in the presence of

* A part of this work was performed at the Eaton Electronics Research Laboratory, McGill University, Montreal, Canada.

† Also at Centre d'Etudes Nucléaires de Grenoble, B.P. 85, 38041, Grenoble, France.

high quantizing magnetic fields is accounted for by the sum of two contributions: $S = S_e + S_p$, where S_e represents the 'electron-diffusion' contribution, and S_p represents the 'phonon-drag' contribution. At low electron concentrations, S_e and S_p can be calculated independently of each other, and discussed separately.[2] We report here the results of the calculation of S_e and S_p in the extreme quantum limit, examine separately their variation as a function of magnetic field, and then give the major conclusions obtained by this study. The details of the calculation will be presented elsewhere.

2. THE 'ELECTRON-DIFFUSION' CONTRIBUTION S_e

We consider the electron transport phenomena in the presence of a vanishingly small electric field **E** directed along the x axis and of a strong quantizing magnetic field **H** directed along the z axis, under isothermal conditions $\nabla T \equiv 0$ (π – approach method to thermoelectric and thermomagnetic problems).[2] Confining the discussion to the zeroth-order approximation with respect to scattering (this adequately describes the situation in the particular case of a high-purity semiconductor at very low temperatures in sufficiently strong magnetic fields such that $\omega_c \tau \gg 1$), we can write the 'electron-diffusion' thermopower, S_e, in the form[5]

$$S_e = (S_e)_{yy}(H) = \frac{\alpha(H)}{Ne}, \qquad (1)$$

where N is the total number of electrons per unit volume, e their charge, and $\alpha(H)$ is the entropy of the system of electrons per unit volume given by

$$\alpha(H) = -\frac{\partial F(H)}{\partial T}, \qquad (2)$$

where $F(H)$ is the Helmholtz free-energy of the system per unit volume. Equation (1) shows that S_e can be calculated accurately from the only knowledge of the electron concentration and of the band structure, irrespectively of the electron scattering parameters. Neglecting the effect of spin splitting (in GaAs, the g – factor is considerably lower than unity), $F(H)$ can be expressed, for the parabolic band model in the extreme quantum limit where all the conducting electrons are localized in the ground oscillator state with the quantum number $n = 0$, as

$$F(H) = N\left[\zeta - k_B T \frac{\mathcal{F}_{1/2}(\mathfrak{E})}{\mathcal{F}_{-1/2}(\mathfrak{E})}\right], \qquad (3)$$

where ζ is the energy of the Fermi level, which is a rapidly varying function of magnetic field,[5,6] the $\mathcal{F}$'s are the Fermi–Dirac integrals defined by,[7,8] k_B is Boltzmann's constant, and

$$\mathfrak{E} = \frac{1}{k_B T}\left(\zeta - \frac{1}{2}\hbar\omega_c\right). \qquad (4)$$

By differentiating $F(H)$ with respect to temperature T, and by assuming that, in the very low temperature range we consider here, the electrons are effectively conducting independently of T,[9] we find

$$S_e = \frac{k_B}{e}\left(\frac{3}{2}\frac{\mathcal{F}_{1/2}(\mathfrak{E})}{\mathcal{F}_{-1/2}(\mathfrak{E})} - \mathfrak{E}\right). \qquad (5)$$

3. THE 'PHONON-DRAG' CONTRIBUTION S_p

Consideration of the electronic motion in the presence of crossed electric (**E** // Ox) and magnetic (**H** // Oz) fields shows that the electrons mainly drift along the y direction with a mean velocity $\bar{v}_y$ equal to the Hall velocity.[10] At the low impurity concentrations we are concerned with in this paper, $\bar{v}_y$ is indeed much greater than the mean electron velocity $\bar{v}_x$ parallel to the electric field **E**. This follows from the fact that the current flow in the x direction, J_x, is precisely produced and enhanced by the collisions of the electrons with the lattice, whereas the y component, J_y, can be regarded as entirely determined by the electric and magnetic fields, and therefore, as independent of the electron-scattering parameters. In the zeroth-order approximation with respect to scattering, $\bar{v}_x = 0$ and $\bar{v}_y = -cE/H$, where c is the speed of light, and E and H are the strengths of the electric and magnetic fields, respectively. In other words, the net electric current is exactly along the y direction in this limit. Now, because of the electron-phonon interaction, this directed flow of electrons drags phonons with it, inducing a Peltier heat flux $(U_p)_y$ in the y direction. The 'phonon-drag' thermopower, S_p, can then be written as

$$S_p = (S_p)_{yy}(H) = \frac{1}{T}\frac{(U_p)_y}{E}\rho_{xy}(H), \qquad \mathbf{H} = (0, 0, H) \qquad (6)$$

where $\rho_{xy}(H)$ is the element of the magnetoresistivity tensor given by[11]

$$\rho_{xy}(H) = -\frac{H}{Nec} . \quad (7)$$

The usual steady-state Boltzmann transport equation for phonons of mode $\mathbf{q}, j$ leads to

$$\mathbf{U}_p = \sum_j (2\pi)^{-3} \int d^3q \, \hbar\omega_{\mathbf{q}j} \, \mathbf{v}_{qj} \, \tau_p \left(\frac{\partial N_{\mathbf{q}j}}{\partial t}\right)_{e-p} \quad (8)$$

where $\mathbf{q}$ and j are the phonon wave vector and the polarization index, respectively. Since the electron constant energy surfaces are assumed to be isotropic, only the longitudinal phonons can scatter the electrons, and the two transverse branches of the phonon spectrum are ineffective in the phonon-drag phenomenon. Therefore, the summation over j, in equation (8), simply reduces to the contribution of the longitudinal branch. On the other hand, in the very low temperature range we consider here, only the long-wavelength acoustic modes of vibration contribute. For these modes, we take the dispersion relation to be $\omega_{\mathbf{q}} = sq$, where s is the sound velocity, q is the magnitude of $\mathbf{q}$, and $\mathbf{v}_{\mathbf{q}} = s(\mathbf{q}/q)$ is the group velocity of a phonon of energy $\hbar\omega_{\mathbf{q}}$. The phonon-relaxation processes other than those on electrons (that is to say boundary scattering, isotope and point defect scattering, and phonon-phonon scattering) are described by a total relaxation time τ_p. However, at sufficiently low temperatures, boundary scattering of phonons dominates, and τ_p is independent of q or T. τ_p is also assumed to be independent of magnetic field.[3] Finally, $(\partial N_{\mathbf{q}}/\partial t)_{e-p}$ is the net time rate of change of the phonon distribution function $N_{\mathbf{q}}$ due to the electron–phonon scattering processes.

An expression for S_p can be obtained, assuming that (i) all the electrons are in the $n = 0$ Landau level (extreme quantum limit), (ii) the quantum number $n = 0$ does not change during scattering (because of insufficient energy exchange between the electrons and the phonon system), (iii) the scattering is due to the deformation potential (in the strong-field region, it is quite reasonable to neglect the scattering due to the piezoelectric mode), and (iv) the effect of spin splitting is neglected. The final result, which is correct only to the first order in the electric field (we are principally concerned here with vanishingly small electric fields) and to the second order in the electron–phonon interaction (first Born approximation), is as follows[12]

$$S_p = \frac{k_B}{e} \frac{1}{4\pi^2 N} \left(\frac{k_B T}{\hbar s}\right)^3 \int_0^{\Theta_D/T} dx \, x^2 \, \mathcal{C}_p(x) I_p(x), \quad (9)$$

where $k_B/|e| = 86.2$ μV/deg, Θ_D is the Debye temperature, $\mathcal{C}_p(x) = x^2 e^x/(e^x - 1)^2$ is the Einstein function, $x = \hbar sq/k_B T$,

$$I_p(x) = \int_0^1 (1 - z^2) \left(\frac{\Gamma(x, z)}{\Gamma(x, z) + (1/\tau_p)}\right) dz. \quad (10)$$

Here, $z = \cos\theta$, θ being the angle between the $\mathbf{q}$ direction and the direction of the z axis,

$$\Gamma(x, z) = A(x) \frac{\exp\left[\frac{1}{2} r_c^2 \left(\frac{k_B T}{\hbar s}\right)^2 x^2 z^2\right]}{|z| \left[\cosh\left(\frac{x}{2}\right) + \cosh\left(\frac{m^* s^2}{2k_B T z^2} + \frac{k_B T x^2 z^2}{8m^* s^2} - \mathfrak{S}\right)\right]} \quad (11)$$

is the phonon absorption coefficient due to the electron-phonon interaction, $r_c = (\hbar c/|e|H)^{1/2}$ is the radius of cyclotron orbit, and

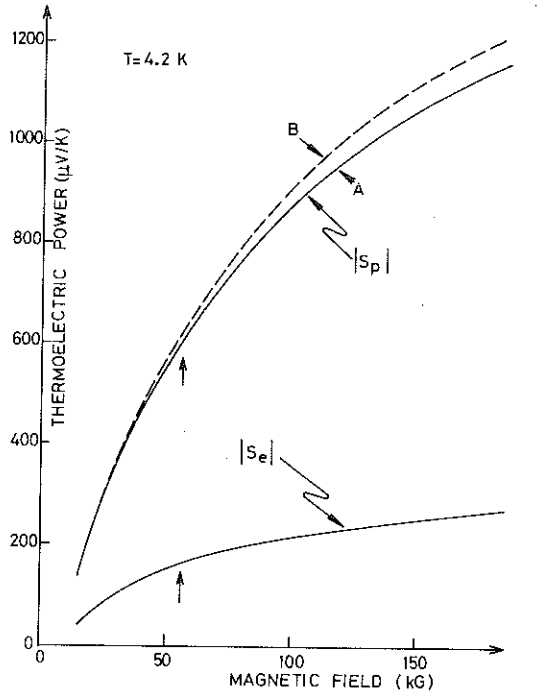

FIG. 1. 'Electron-Diffusion' TEP, $|S_e|$, and 'phonon-drag' TEP (curves A and B), $|S_p|$, as a function of magnetic field H for n-type GaAs with $N = 1.2 \times 10^{16}$ cm^{-3} electrons at $T = 4.2$ K. The two arrows indicate the field (≈ 56 kG) at which the bottom of the $n = 0$ Landau band coincides with the Fermi energy. Curve A is calculated, assuming (14): $1/\tau_p = \tau_B^{-1} + \tau_{pt}^{-1} + \tau_{3ph}^{-1}$, where $\tau_B^{-1} = 0.60 \times 10^6$ sec^{-1} is the boundary inverse relaxation time, $\tau_{pt}^{-1} = A\omega^4$ with $A = 0.46 \times 10^{-44}$ sec^3 is the inverse relaxation time for the scattering due to isotopes, point defects, etc., and $\tau_{3ph}^{-1} = B\omega^2 T^3$ with $B = 5 \times 10^{-22}$ sec/deg^3 is the three-phonon inverse relaxation time. Curve B is calculated, assuming $1/\tau_p = \tau_B^{-1}$ ($\tau_B^{-1} = 0.60 \times 10^6$ sec^{-1}).

$$A(x) = \frac{C^2}{4\pi d s r_c^2}\left(\frac{2m^*}{\hbar^2}\right)\exp\left[-\frac{1}{2}r_c^2\left(\frac{k_B T}{\hbar s}\right)^2 x^2\right]\sinh\left(\frac{x}{2}\right) \tag{12}$$

where C is the deformation potential constant, and d is the density of the crystal.

4. NUMERICAL RESULTS AND CONCLUSION

Figure 1 shows the variations of $|S_e|$ and $|S_p|$ with magnetic field, as obtained by numerical evaluation of equations (5) and (9), for n-type gallium arsenide ($N = 1.2 \times 10^{16}$ cm^{-3} electrons) at liquid helium temperature $T = 4.2$ K. The numerical values of physical parameters for this material are: $m^* = 0.07\, m_0$ (m_0 = free-electron mass), $s = 5.24 \times 10^5$ cm/sec, $d = 5.31$ g/cm^3, $\Theta_D = 345$ K, and $C = 7.0$ eV.[13] We can draw the following major conclusions: (i) The change in the electron distribution, which takes place at ≈ 56 kG, has a large effect on the variation of S_e and S_p with magnetic field. This effect is essentially characterized by a large and rapid increase in both $|S_e|$ and $|S_p|$. (ii) Unlike $\rho_{\perp}$ and $\rho_{\parallel}$, no anomalous behavior occurs at the transition to non-degeneracy. (iii) For large magnetic fields, $|S_e|$ and $|S_p|$ increase monotonically with H, although the rate of increase of $|S_e|$ is much slower than that of $|S_p|$. Finally (iv), in the extreme quantum limit, $|S_p|$, which is large compared to $|S_e|$, makes the dominant contribution to the total TEP $S = S_e + S_p$.

Acknowledgments – The author wishes to thank Professor P.R. Wallace, Dr. O.P. Gupta, and Professor J.D.N. Cheeke for a number of stimulating discussions. He also wishes to thank Dr. J. Texeira for assistance with the computer program.

REFERENCES

1. ASKENAZY S., ULMET J.P. and LÉOTIN J., *Solid State Commun.* 7, 989 (1969).
2. HERRING C., GEBALLE T.H. and KUNZLER J.E., *Phys. Rev.* **111**, 36 (1958).
3. PURI S.M., *Phys. Rev.* **139**, A995 (1965).
4. ZYRYANOV P.S. and GUSEVA G.I., *Usp. Fiz. Nauk* **95**, 565 (1968). (English transl.: *Soviet Physics-Uspekhi* **11**, 538 (1969)).
5. JAY-GERIN J.P., *J. Phys. Chem. Solids* **35**, 81 (1974).
6. WALLACE P.R. and GUPTA O.P., *Phys. Status Solidi* **50**, 619 (1972).
7. BLAKEMORE J.S., *Semiconductor Statistics* Appendix B, p. 346 Pergamon Press, Oxford (1962).
8. STONER E.C., *Phil. Mag.* **21**, 145 (1936).
9. JAY-GERIN J.P. and WALLACE P.R., *J. Low Temp. Phys.* 7, 525 (1972).
10. LANDAU L.D. and LIFSHITZ E.M., *The Classical Theory of Fields*, p. 62 Pergamon Press, Oxford, London, Paris, Frankfurt, (1962).
11. BEER A.C., *Solid State Physics*, Vol. 4, p. 96. (edited by SEITZ F. and TURNBULL D). Academic Press, New York and London, (1963).
12. JAY-GERIN J.P., (to be published).
13. RODE D.L., *Phys. Rev.* **B2**, 1012 (1970).
14. HOLLAND M.G., *Phys. Rev.* **134**, A 471 (1964).

L'effet de la quantification des niveaux d'énergie électroniques dans un fort champ magnétique transverse H sur le pouvoir thermoélectrique (TEP) S, à basse température, d'un semiconducteur isotrope et de haute pureté (Arséniure de Gallium GaAs de type n) est étudié théoriquement. Les composantes de 'diffusion électronique' (S_e) et de 'phonon-drag' (S_p) de S ($= S_e + S_p$) sont calculées dans la limite extreme quantique, quand tous les électrons dans la bande de conduction sont concentrés dans le plus bas niveau de Landau. La transition statistique (dégénéré en non dégénéré), qui s'opère quand le bas du niveau de Landau fondamental franchit le niveau de Fermi, a un effet important sur les variations de S_e et de S_p avec le champ magnétique. Les résultats sont illustrés par des calculs numériques pour GaAs de type n à 4.2 K avec 1.2×10^{16} électrons par cm^3.

J. Phys. Chem. Solids, 1974, Vol. 35, pp. 81–87. Pergamon Press. Printed in Great Britain

THERMOELECTRIC POWER OF SEMICONDUCTORS IN THE EXTREME QUANTUM LIMIT—I
THE 'ELECTRON-DIFFUSION' CONTRIBUTION

J. P. JAY-GERIN*
Centre de Recherches sur les Très Basses Températures, C.N.R.S., B.P. 166 Centre de Tri, 38042 Grenoble-Cédex, France

(*Received* 11 *August* 1972; *in revised form* 15 *June* 1973)

Abstract—A study is made of the effect of the quantization of the electron energy levels in a strong magnetic field on the 'electron-diffusion' contribution, S_e, of the transverse thermoelectric power of a high-purity isotropic semiconductor (n-type gallium arsenide GaAs) in the extreme quantum limit, when all the carriers in the conduction band are in the lowest Landau level. A theoretical expression for S_e is derived, taking into account of spin splitting. The sign of S_e is either positive or negative, depending on the sign of the conducting carriers. The transition to nondegeneracy, which takes place when the lowest Landau level is driven through the Fermi level, has a large effect on the variation of S_e with magnetic field. This effect is characterized by a large and rapid increase in $|S_e|$. Spin splitting effects, even with a small effective mass ($m^* = 0{\cdot}07m_0$, where m_0 is the free-electron mass) and a very small g-factor ($g \simeq 0{\cdot}32$), greatly modify and reduce $|S_e|$ as a function of field. For large fields, $|S_e|$ increases monotonically with H. Calculations are carried out for n-type GaAs at $T = 0{\cdot}5$°K with $N = 1{\cdot}2 \times 10^{16}$ cm^{-3} carriers.

1. INTRODUCTION

In the presence of a magnetic field, the energy levels of the charge carriers in a crystal are quantized. When the magnetic field strength is changed, a shift of these quantized Landau levels relative to the Fermi level takes place. Now, when the magnetic field applied to the crystal is sufficiently strong, all except the lowest of the Landau levels may have crossed over the Fermi level. Therefore, provided that the temperature is sufficiently low, all the charge carriers are concentrated in their lowest Landau level with the quantum number $n = 0$. This regime, in which $\hbar\omega_c \gg k_B T, \zeta$, where $\hbar\omega_c$ is the Landau level spacing, $k_B T$ the thermal energy, and ζ the Fermi energy, is what we shall call the 'extreme quantum limit'. If the strength of the magnetic field is increased further, the energy separation between the bottom of the $n = 0$ Landau level and the Fermi level diminishes. Therefore, with increasing magnetic field, the charge carriers are progressively drawn up to the Fermi level. Let H_{cr} be the value of the magnetic field for which the bottom of the $n = 0$ Landau level coincides with the Fermi level. Evidently, H_{cr} is defined by

$$\tfrac{1}{2}\hbar\omega_c^{cr} = \zeta \quad \text{with} \quad \omega_c^{cr} = \frac{|e| H_{cr}}{m^* c},$$

where c is the speed of light, and $|e|$ and m^* are the magnitude of the charge and the effective mass of a carrier, respectively.

A situation of theoretical as well as of experimental interest occurs at $H = H_{cr}$. In fact, at $H = H_{cr}$, a transition is induced in the crystal from a degenerate carrier state, in which the carrier gas obeys Fermi–Dirac statistics, to a nondegenerate one, in which the carrier gas obeys Maxwell–Boltzmann statistics [1, 2]. However, this change in the carrier distribution does not take place immediately after the lowest Landau level has passed through the Fermi level. In fact, the transition to nondegeneracy begins as soon as the bottom of the $n = 0$ Landau level approaches within a few times $k_B T$ of the Fermi level [3]. With increasing magnetic field, more and more carriers are progressively driven into the region of non-degenerate statistics. Actually, the carrier gas may be considered as completely nondegenerate when the mean kinetic energy of the carriers along the direction of the magnetic field becomes of the order of $(1/2)k_B T$ (quasi-one-dimensional non-degenerate gas [4]).

Experimentally, the transition to nondegeneracy was observed for the first time by Askenazy, Ulmet and Léotin [5] in the behaviour of both the longitudinal ($\rho_\parallel$) and the transverse ($\rho_\perp$) magnetoresistivity of a sample of n-type gallium arsenide (GaAs), a III–V semiconductor, with $N = 3{\cdot}8 \times 10^{16}$ cm^{-3} charge carriers at $T = 2$°K. As the carrier gas passes

*A part of this work was performed at the Eaton Electronics Research Laboratory, McGill University, Montreal, Canada.

from a degenerate state to a non-degenerate one with increasing magnetic field, the magnetoresistance shows a giant peak starting at $\approx$ 30 kG, reaching a maximum at $\approx$ 90 kG, and decreasing again to a relatively small and slowly varying negative value by about 150 kG.

On an intuitive basis, we may expect that the change in the carrier distribution manifested in this experiment appreciably affects the thermoelectric properties of a semiconductor. It is our aim in this present paper and its sequel [6] to present, under certain simplifying assumptions, a detailed and quantitative calculation of the transverse thermoelectric power (TEP) of a semiconductor in the extreme quantum limit. A part of this work has recently been published in the form of a short communication [7]. As is well known [8–10], the TEP of a semiconductor at low temperatures and in high quantizing magnetic fields is accounted for by the sum of two contributions: $S = S_e + S_p$, where S_e is the 'electron-diffusion' contribution, and S_p is the 'phonon-drag' contribution. At low carrier concentrations, S_e and S_p can be computed independently of each other and discussed separately [8]. For convenience, we leave for our forthcoming paper [6] the task of studying the contribution due to phonon drag, and present in this first paper a detailed analysis of the 'electron-diffusion' contribution S_e. In the theory presented here, the carrier gas may be either degenerate or nondegenerate, depending on the strength of the applied magnetic field. Precisely, our main interest has been the effect of the change in the carrier distribution, which takes place when the bottom of the $n = 0$ Landau level is driven through the Fermi level, on the variation of S_e with magnetic field. On the other hand, it is assumed in the following that the sample is of sufficiently high purity, so that $\omega_c\tau \gg 1$, where ω_c is the cyclotron frequency and τ the carrier relaxation time. In this limit, the Landau quantization is preserved in spite of the collisions of the carriers with the lattice. In addition, we have restricted our calculations to an isotropic semiconductor (n-type gallium arsenide) with a simple parabolic band of effective mass m^*. This adequately describes the situation at sufficiently low carrier concentrations. In spite of the small effective mass ($m^* = 0{\cdot}07m_0$, where m_0 is the free-electron mass) and the very small spectroscopic g-factor ($g \approx 0{\cdot}32$) of the conduction carriers in n-type GaAs, the effects of spin splitting are also taken into account in the calculation.

It should finally be mentioned that several prior treatments of the transverse thermal e.m.f. (S_e) in strong quantizing magnetic fields have been carried out, but each of these treatments was somewhat specialized. Obraztsov [11] calculated the thermal e.m.f. of a standard band semiconductor in a strong magnetic field for which the condition $\omega_c\tau \gg 1$ is satisfied. He derived expressions for S_e for certain limiting cases: (i) 'quantum limit' ($\hbar\omega_c \gg k_BT$ and $(3/2)\hbar\omega_c \gg \zeta$), (ii) 'strong degeneration in the quantum limit' and (iii) 'absence of degeneration in the quantum limit'. However, he did not draw extensive physical conclusions from his formulae. In addition, the effects of splitting of the Landau levels due to spin were not taken into account in the calculation. Ansel'm and Tarkhanyan [12] also calculated the transverse thermal e.m.f. in a strong quantizing magnetic field in an n-indium antimonide (InSb) type semiconductor, allowing for nonparabolicity of the conduction band and electron spin. However, they restricted their calculation to the limiting case of electrons subject to classical Maxwell–Boltzmann statistics (i.e. non-degenerate regime).

2. CALCULATION OF S_e

In the presence of a static magnetic field **H**, the linear relations between electric current density **J**, electric field **E**, temperature gradient ∇T, and heat current density **U**, may be written as the well-known phenomenological transport equations [13]

$$\left.\begin{aligned}\mathbf{E} &= \rho\cdot\mathbf{J} + S\cdot\nabla T\\ \mathbf{U} &= \pi\cdot\mathbf{J} - \kappa\cdot\nabla T\end{aligned}\right\} \tag{1}$$

where all the coefficients, actually tensors, are functions of **H**. In these expressions, ρ is the electrical resistivity tensor, κ is the thermal conductivity tensor, S is the thermoelectric-power (TEP) tensor, and π is the Peltier tensor. These transport coefficients are not independent, but are related by the Onsager relations of the thermodynamics of irreversible processes

$$\left.\begin{aligned}\rho_{ij}(\mathbf{H}) &= \rho_{ji}(-\mathbf{H})\\ \kappa_{ij}(\mathbf{H}) &= \kappa_{ji}(-\mathbf{H})\end{aligned}\right\} \tag{2}$$

and

$$S_{ij}(\mathbf{H}) = \frac{1}{T}\pi_{ji}(-\mathbf{H}) \tag{3}$$

a relation known as the Kelvin relation.

In what follows, we are concerned ourselves with the study of the TEP in a strong quantizing magnetic field. According to equation (1), the defining

equation for S is given by:

$$\mathbf{E} = S \cdot \nabla T \tag{4}$$

with the auxiliary condition that $\mathbf{J} = 0$. However, to calculate S directly from equation (4), we need to consider the effects of the electric field and the temperature gradient simultaneously. As was pointed out by Herring *et al.*[8], Puri[9], and Gurevich and Nedlin[14], we can eliminate the necessity of incorporating a spatially varying temperature in the theory of thermoelectric phenomena, by using the Kelvin relation. In effect, equation (3) provides a very convenient way of calculating the TEP. Instead of a direct calculation of S, we may first determine the Peltier coefficient π from the solution of an electrical conduction problem assuming the temperature gradient to be always zero. Putting $\nabla T = 0$ in equation (1), we have

$$\mathbf{U} = \pi \cdot \mathbf{J} \tag{5}$$

with

$$\mathbf{J} = \sigma \cdot \mathbf{E} \tag{6}$$

where $\sigma = \rho^{-1}$ is the magnetoconductivity tensor. The TEP is then easily obtained using Kelvin's relation. This method of computing S from π is usually known as the π-approach method[8].

Let us now apply this convenient way of solving thermoelectric transport problems to the particular case of a high-purity isotropic semiconductor at very low temperatures when subjected to a strong magnetic field $\mathbf{H} = (0, 0, H)$ directed along the z axis and to a vanishingly small electric field $\mathbf{E} = (E, 0, 0)$ directed along the x axis. According to equations (5) and (6), the procedure is to calculate the heat current density $\mathbf{U}$ in an electrical conduction process in the presence of $\mathbf{E}$ under isothermal conditions. Now, because of the electron–phonon interaction, $\mathbf{U}$ consists of two parts, namely, $\mathbf{U} = \mathbf{U}_e + \mathbf{U}_p$, where $\mathbf{U}_e$ represents the heat flux carried by the charge carriers and $\mathbf{U}_p$ is the heat flux carried by the phonon system[8]. However, as we are interested in this present paper in the purely electron-diffusion part of the TEP, we shall only consider in the following the heat transfer due to the charge carriers themselves, leaving for our forthcoming paper[6] the task of studying the problem of phonon drag.

Consideration of the electronic motion in the presence of crossed electric ($\mathbf{E} \| Ox$) and magnetic ($\mathbf{H} \| O_z$) fields shows that carriers mainly drift along the y direction with a mean velocity $\overline{v_y}$ equal to the Hall velocity[15]. At the low impurity concentrations we are concerned with in this paper, $\overline{v_y}$ is in effect much greater than the mean carrier velocity $\overline{v_x}$ parallel to the electric field $\mathbf{E}$. This follows from the fact that the current flow in the x direction, J_x, is precisely produced and enhanced by the collisions of the carriers with the lattice, whereas the y component of the current, J_y, can be regarded as entirely determined by the electric and the magnetic fields and therefore, as independent of the carrier-scattering parameters[16]. In the following, we deliberately confine the discussion to the zeroth-order approximation with respect to scattering. This approximation, though elementary, adequately describes the situation in the particular case of a high-purity semiconductor at very low temperatures in the presence of sufficiently strong magnetic fields, such that $\omega_c \tau \gg 1$, where $\omega_c = |e|H/m^* c$ is the cyclotron frequency and τ the relaxation time of the charge carriers. Under these conditions, it follows easily then that $\overline{v_x} = 0$ and $\overline{v_y} = -cE/H$. Here, E and H are the strengths of the electric and the magnetic fields respectively, and c is the speed of light. In other words, the net electric current is exactly along the y direction. This directed flow of carriers causes, in its turn, a Peltier heat flux $(U_e)_y$ in the y direction. According to equation (5), the electron–diffusion contribution π_e of the transverse Peltier coefficient (irrespectively of the phonon-drag phenomenon) is given by:

$$[\pi_e]_{yy}(H) = \frac{(U_e)_y}{J_y}, \quad \mathbf{H} = (0, 0, H). \tag{7}$$

Then, using the Kelvin relation (3) with the aid of equations (2), (6) and (7), and assuming the crystal to be isotropic in the absence of a magnetic field, we straightforwardly get for the transverse electron–diffusion TEP

$$S_e = [S_e]_{yy}(H) = \frac{1}{T}[\pi_e]_{yy}(-H)$$

$$= \frac{1}{T}\frac{(U_e)_y}{E}\rho_{xy}(H), \quad \mathbf{H} = (0, 0, H). \tag{8}$$

Here, $\rho_{xy}(H)$ is the element of the magnetoresistivity tensor given by[17]

$$\rho_{xy}(H) = -\frac{1}{\sigma_{xy}(H)}; \quad |\sigma_{xy}| \gg |\sigma_{xx}|$$

$$= -\frac{H}{Nec}, \quad \mathbf{H} = (0, 0, H) \tag{9}$$

where N is the total number of carriers per unit

volume, and e their charge ($e < 0$ for electrons, $e > 0$ for holes).

Now, since we are concerned here with the zeroth-order approximation with respect to scattering, there is no irreversible conversion of electronic energy into heat by collisions with the lattice. Following MacDonald[18], it thus seems very natural to assume some sort of quasi-equilibrium conditions, and therefore to regard the process as reversible. Accordingly, by applying the thermodynamics of reversible processes, we then readily find from equations (8) and (9):

$$S_e = \frac{\alpha(H)}{Ne} \tag{10}$$

where $\alpha(H)$ is the entropy of the system of carriers per unit volume given by

$$\alpha(H) = -\frac{\partial F(H)}{\partial T} \tag{11}$$

where $F(H)$ is the Helmholtz free-energy of the system per unit volume. Equation (10), which we have obtained here in a quite simple way, says that S_e in the zeroth-order approximation with respect to scattering is the ratio of the 'entropy per carrier' to the carrier charge. This result was first obtained by Obraztsov[11] in the case of a standard electron spectrum, taking account of the diamagnetism of conduction electrons. Tséndin and Éfros[19] showed, on the other hand, that the same formula (10) also applies in the case of Kane-type semiconductors. Actually, this formula clearly shows that in a sufficiently strong magnetic field, such that $\omega_c\tau \gg 1$, the purely electron–diffusion contribution S_e of the transverse TEP can be calculated accurately from the only knowledge of the carrier concentration and the band structure, irrespectively of the carrier scattering parameters. Putting equation (11) into equation (10) gives

$$S_e = -\frac{1}{Ne}\frac{\partial F(H)}{\partial T}, \tag{12}$$

and the calculation of S_e reduces to determining the Helmholtz free-energy $F(H)$.

In the extreme quantum limit where only the $n = 0$ Landau levels contribute, $F(H)$ can be written in the form[20]

$$F(H) = N\zeta - \sum_\sigma \int \mathscr{Z}_\sigma(\epsilon) f(\epsilon)\, \mathrm{d}\epsilon \tag{13}$$

with

$$\mathscr{Z}_\sigma(\epsilon) = \int_0^\epsilon D_\sigma(\epsilon)\, \mathrm{d}\epsilon. \tag{14}$$

Here, $f(\epsilon)$ is the Fermi–Dirac distribution function, which expresses the probability of occupation of a given state of energy, designated by ϵ, $D_\sigma(\epsilon)$ is the one-particle density of states per unit volume and energy corresponding to the direction of spin σ and ζ is the energy of the Fermi level, which is determined by the usual condition

$$N = \sum_\sigma \int D_\sigma(\epsilon) f(\epsilon)\, \mathrm{d}\epsilon \tag{15}$$

where N is the total number of carriers per unit volume.

For a parabolic band of effective mass m^*,

$$\epsilon = \frac{1}{2}\hbar\omega_c + \frac{\hbar^2 k_z^2}{2m^*} - \frac{1}{2} g\mu_B \sigma H \quad \mathbf{H} = (0, 0, H) \tag{16}$$

where $\mu_B = e\hbar/2m_0c$ is the Bohr magneton, $\sigma = \pm 1$, g is the effective g-factor of the charge carriers, and m_0 is the free-electron mass. The densities of states of the two spins are then given by

$$D_\sigma(\epsilon) = \frac{1}{4\pi^2 r_c^2}\left(\frac{2m^*}{\hbar^2}\right)^{1/2}\left[\epsilon - \frac{1}{2}\hbar\omega_c(1-\gamma\sigma)\right]^{-1/2} \tag{17}$$

where $r_c = (\hbar c/|e|H)^{1/2}$ is the radius of cyclotron orbit and $\gamma = g(m^*/2m_0)$.

Following the lines of the previous work by Jay-Gerin and Wallace[4] and using equations (13)–(17), we may straightforwardly calculate $F(H)$ in the form:

$$F(H) = N\left(\zeta - k_B T \frac{S_+}{S_1}\right) \tag{18}$$

where

$$N = \frac{1}{4\pi^{3/2} r_c^2}\left(\frac{2m^*}{\hbar^2}\right)^{1/2} (k_B T)^{1/2} S_1,$$

$$S_+ = \sum_\sigma \mathscr{F}_{1/2}(\xi_\sigma),$$

$$S_1 = \sum_\sigma \mathscr{F}_{-1/2}(\xi_\sigma),$$

$$\xi_\sigma = \frac{1}{k_B T}\left[\zeta - \frac{1}{2}\hbar\omega_c(1-\gamma\sigma)\right], \tag{19}$$

and the $\mathscr{F}$'s are the Fermi–Dirac integrals defined by[21, 22]

$$\mathscr{F}_j(\xi) = \frac{1}{\Gamma(j+1)}\int_0^\infty \frac{x^j\, \mathrm{d}x}{e^{(x-\xi)}+1}. \tag{20}$$

By differentiating $F(H)$ with respect to temperature T and by assuming that the charge carriers are

effectively conducting independently of T[4], we finally obtain according to equation (12):

$$S_e = \frac{k_B}{e}\left[\frac{3}{2}\frac{S_+}{S_1} - \frac{(\zeta - \frac{1}{2}\hbar\omega_c)}{k_B T} - R\frac{\Delta_1}{S_1}\right] \tag{21}$$

where

$$R = \frac{1}{2}\frac{\hbar\omega_c\gamma}{k_B T} \tag{22}$$

is half the ratio of the spin splitting to the thermal energy, and

$$\Delta_1 = \sum_\sigma \sigma \mathscr{F}_{-1/2}(\xi_\sigma). \tag{23}$$

When the effects of the spin splitting are neglected, $R \to 0$ and only the first two terms of equation (21) survive. In this case, equation (21) thus reduces to the following expression

$$S_e = \frac{k_B}{e}\left[\frac{3}{2}\frac{\mathscr{F}_{1/2}(\xi)}{\mathscr{F}_{-1/2}(\xi)} - \xi\right] \tag{24}$$

where

$$\xi = \frac{\zeta - \frac{1}{2}\hbar\omega_c}{k_B T}. \tag{25}$$

Equation (24) was previously obtained by Obraztsov[11].

3. NUMERICAL RESULTS FOR GaAs AND DISCUSSION

Numerical calculations of S_e were carried out for n-type gallium arsenide with $N = 1{\cdot}2 \times 10^{16}\,\mathrm{cm}^{-3}$ electrons at a temperature $T = 0{\cdot}5°\mathrm{K}$. It is easy to see from equations (21) and (24) that the actual sign of S_e is the same as the sign of the conducting carriers. For the case of n-type GaAs we are concerned with here, S_e is thus negative. In Fig. 1, we show the difference in the magnetic field dependence of $|S_e|$ calculated with and without spin splitting. Even with a small effective mass ($m^* = 0{\cdot}07\,m_0$) and a very small g-factor ($g \approx 0{\cdot}32$), the variation of $|S_e|$ with H is seen to be greatly modified by virtue of the spin splitting. When we take into account of this effect, the curve of $|S_e|$ vs H begins to increase rapidly to a maximum, then flattens somewhat as the bottom of the upper spin band passes through the Fermi level ζ, before rising again with increasing field. For large fields, $|S_e|$ increases monotonically with H. It should be noted, however, that the results of equation (21) concerning the spin splitting effects actually hold for sufficiently pure samples and very low temperatures. In effect, if there exist collisions between the charge carriers and various kinds of scatterers, or

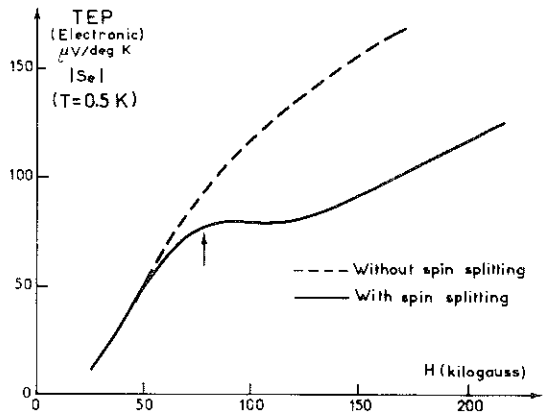

Fig. 1. 'Electron-diffusion' TEP, $|S_e|$, as a function of magnetic field H, calculated with and without spin splitting for n-type gallium arsenide (GaAs) with $N = 1{\cdot}2 \times 10^{16}\,\mathrm{cm}^{-3}$ electrons, $g = 0{\cdot}32$, $m^* = 0{\cdot}07\,m_0$, and at a temperature of $T = 0{\cdot}5°\mathrm{K}$. The arrow indicates the field at which the bottom of the *upper* spin band coincides with the Fermi energy. The value for the *lower* spin band does not fall in the range of fields shown.

if the temperature is raised, then either the broadening of the Landau energy levels or the thermal smearing of the Fermi level may become greater than the spin splitting, and therefore mask the corresponding spin effect. Obviously, equation (24) holds in this latter case[7].

In Fig. 2, we have plotted the variation of the Fermi level ζ as a function of field. In the strong-field extreme quantum limit, ζ is seen to be a rapidly

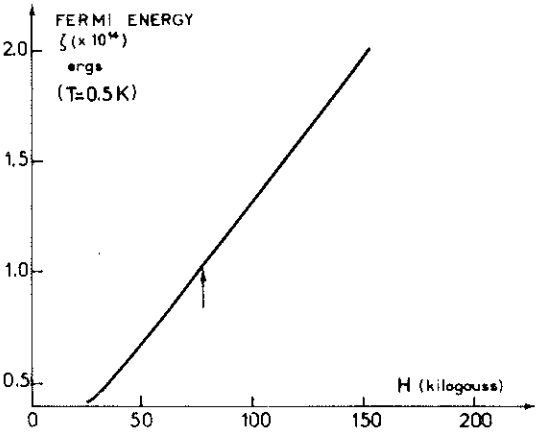

Fig. 2. Plot of the Fermi level ζ as a function of magnetic field H in kilogauss for n-type gallium arsenide with $N = 1{\cdot}2 \times 10^{16}\,\mathrm{cm}^{-3}$ electrons and at a temperature of $T = 0{\cdot}5°\mathrm{K}$. The arrow indicates the field at which the bottom of the *upper* spin band coincides with the Fermi energy. The value for the *lower* spin band does not fall in the range of fields shown.

varying function of the magnetic field strength [4, 20]. Now, for completeness, let us discuss the two following limit cases.

(a) *Strong degeneracy*

In the limit of extreme degeneracy, the Fermi–Dirac functions can be replaced by asymptotic forms due to Sommerfeld and others [21, 22]. In particular,

$$\mathscr{F}_{1/2}(\xi) \approx \frac{4}{3\sqrt{\pi}}\xi^{3/2}\left(1+\frac{\pi^2}{8\xi^2}+\cdots\right) \qquad (26)$$

and

$$\mathscr{F}_{-1/2}(\xi) \approx \frac{2}{\sqrt{\pi}}\xi^{1/2}\left(1-\frac{\pi^2}{24\xi^2}+\cdots\right), \quad \xi \gg 1. \qquad (27)$$

In the regime in which only the $n = 0$ Landau levels are occupied, but the system is still strongly degenerate, equation (21) becomes in terms of density of states at the Fermi level:

$$S_e \approx \frac{k_B}{e}\frac{\pi^2}{3}k_BT\frac{D(\zeta)}{N} \qquad (28)$$

which is, as expected, proportional to the absolute temperature T. Equation (28) is the familiar formula for the electron-diffusion TEP in the zeroth-order approximation with respect to scattering [23, 24]. The density of states in this case is given by

$$D(\zeta) = \frac{1}{4\pi^2 r_c^2}\left(\frac{2m^*}{\hbar^2}\right)^{1/2}(k_BT)^{-1/2}\left[\frac{1}{(\xi_+)^{1/2}}+\frac{1}{(\xi_-)^{1/2}}\right], \qquad (29)$$

which strongly increases as the bottom of the upper spin band approaches the Fermi level.

(b) *Limit of 'classical' statistics*

With increasing field, not only is the density of states increasing, but more and more electrons are being driven into the region of non-degenerate statistics. When the system has become completely nondegenerate, then explicit and rather simple forms for the electron-diffusion TEP again become possible. In this regime, we may write, to a good approximation [4, 21],

$$\mathscr{F}_{1/2}(\xi) \approx e^{-|\xi|}-\frac{1}{2\sqrt{2}}e^{-2|\xi|}\cdots \qquad (30)$$

$$\mathscr{F}_{-1/2}(\xi) \approx e^{-|\xi|}-\frac{1}{\sqrt{2}}e^{-2|\xi|}\cdots, \quad \xi \ll 0. \qquad (31)$$

In fact, only ξ_+ contributes appreciably, since

$$|\xi_-| = |\xi_+| + 2R \qquad (32)$$

and R is substantially larger than unity. Actually, for GaAs ($g \approx 0{\cdot}32$)

$$R = 1{\cdot}07\times10^{-2}\left(\frac{H}{T}\right)$$

where H is in kilogauss and T in degrees. Thus, at $H = 140$ kG, T = 0·5°K, $R \approx 3$.

Using equations (30), (31) and (32), and keeping only terms to the first order in e^{-2R} and to the second order in $e^{-|\xi_+|} = e^{-\eta}$, we get from equations (19) and (23):

$$S_+ = e^{-\eta}\left(1-\frac{1}{2\sqrt{2}}e^{-\eta}+e^{-2R}\right), \qquad (33)$$

$$S_1 = e^{-\eta}\left(1-\frac{1}{\sqrt{2}}e^{-\eta}+e^{-2R}\right), \qquad (34)$$

and

$$\Delta_1 = e^{-\eta}\left(1-\frac{1}{\sqrt{2}}e^{-\eta}-e^{-2R}\right). \qquad (35)$$

On the other hand, by virtue of equations (19) and (34), we have approximately

$$e^{-\eta} \approx 2\sqrt{2}\pi^2 N\frac{\hbar c}{|e|H}\left(\frac{\hbar^2}{\pi m^* k_BT}\right)^{1/2}. \qquad (36)$$

With the aid of equations (33)–(36), we then get from equation (21) the following asymptotic value of the electron-diffusion TEP in the region of non-degenerate statistics:

$$S_e = S_e' + S_e^{(s)} \qquad (37)$$

where

$$S_e' \approx \frac{k_B}{e}\left[\frac{3}{2}+\frac{1}{2}\frac{\hbar\omega_c}{k_BT}-\frac{\zeta}{k_BT}+\frac{3\pi^2}{2}N\frac{\hbar c}{|e|H}\times\left(\frac{\hbar^2}{\pi m^* k_BT}\right)^{1/2}\cdots\right] \qquad (38)$$

gives the result without spin splitting, and

$$S_e^{(s)} \approx \frac{k_B}{e}\left[-R(1-2e^{-2R})+\lambda e^{-2R}\cdots\right] \qquad (39)$$

is the additional contribution when we take account of spin splitting. Here,

$$\lambda = \sqrt{2}Re^{-\eta} \approx 2\pi^3\gamma N\left(\frac{\hbar^2}{\pi m^* k_BT}\right)^{3/2} \qquad (40)$$

is independent of H.

Equations (38) and (39) agree with the previous results of Obraztsov [11] and of Ansel'm and Tarkhanyan [12].

Acknowledgements—The author wishes to thank Prof. P. R. Wallace, Dr. O. P. Gupta and Dr. J. D. N. Cheeke for a number of fruitful and stimulating discussions. He would also like to thank Prof. C. Herring for his comments on the manuscript.

REFERENCES

1. Roth L. M. and Argyres P. N., *Semiconductors and Semimetals*, Vol. 1, p. 159. Academic Press, New York (1966).
2. Adams E. N. and Holstein T. D., *J. Phys. Chem. Solids* **10**, 254 (1959).
3. Askenazy S., In: *New Developments in Semiconductors* (Edited by P. R. Wallace, R. Harris and M. J. Zuckermann), p. 365. Noordhoff, Netherlands (1973).
4. Jay-Gerin J. P. and Wallace P. R., *J. low-temp. Phys.* **7**, 523 (1972).
5. Askenazy S., Ulmet J. P. and Léotin J., *Solid State Commun.* **7**, 989 (1969).
6. Jay-Gerin J. P., (to be published).
7. Jay-Gerin J. P., Paper presented at the 13th International Conference on Low Temperature Physics, University of Colorado, Boulder, U.S.A. (1972).
8. Herring C., Geballe T. H. and Kunzler J. E., *Phys. Rev.* **111**, 36 (1958).
9. Puri S. M., *Phys. Rev.* **139**, A995 (1965).
10. Zyryanov P. S. and Guseva G. I., *Usp. Fiz. Nauk*. **95**, 565 (1968) (English transl.: *Soviet Phys.-Usp.* **11**, 538 (1969)).
11. Obraztsov Yu. N., *Fiz. tverd. Tela* **7**, 573 (1965) (English transl.: *Soviet Phys-solid St.* **7**, 455 (1965)).
12. Ansel'm A. I. and Tarkhanyan R. G., *Fiz. tverd. Tela* **6**, 3357 (1964) (English transl.: *Soviet Phys.-solid St.* **6**, 2685 (1965)).
13. Ziman J. M., *Principles of the Theory of Solids*, p. 194. Cambridge University Press, Cambridge (1965).
14. Gurevich L. É. and Nedlin G. M., *Fiz. tverd. Tela* **3**, 2779 (1961) (English transl.: *Soviet Phys.-solid St.* **3**, 2029 (1962)).
15. Landau L. D. and Lifshitz E. M., *The Classical Theory of Fields*, p. 62. Pergamon Press, Oxford (1962).
16. Bastin A., Lewiner C., Betbeder-Matibet O. and Nozieres P., *J. Phys. Chem. Solids* **32**, 1811 (1971). In this paper entitled, Quantum Oscillations of the Hall Effect of a Fermion Gas with Random Impurity Scattering, a detailed analysis of the static electrical conductivity tensor of an electron gas in the presence of a magnetic field has been derived in the case of scattering by spinless random impurities, assuming a δ-function scattering potential, and using a Green's function method. It is shown that a correction to the usual Hall effect, which is linear in the impurity concentration, exists. However, this correction does not significantly affect our results, and consequently has been neglected.
17. Beer A. C., In: *Solid State Physics* (Edited by F. Seitz and D. Turnbull), Vol. 4, p. 96. Academic Press, New York (1963).
18. MacDonald D. K. C., *Thermoelectricity: an Introduction to the Principles*, p. 9. Wiley, New York (1962).
19. Tséndin K. D. and Éfros A. L., *Fiz. tverd. Tela* **8**, 378 (1966) (English transl.: *Soviet Phys.-solid St.* **8**, 306 (1966)).
20. Wallace P. R. and Gupta O. P., *Phys. Status Solidi* **50b**, 619 (1972).
21. Blakemore J. S., *Semiconductor Statistics*. Appendix B, p. 346. Pergamon Press, Oxford (1962).
22. Stoner E. C., *Phil. Mag.* **21**, 145 (1936).
23. Ziman J. M., *Principles of the Theory of Solids*, p. 203. Cambridge University Press, Cambridge (1965).
24. MacDonald D. K. C., *Thermoelectricity: An Introduction to the Principles*, p. 46. Wiley, New York (1962).

THERMOELECTRIC POWER OF SEMICONDUCTORS IN THE EXTREME QUANTUM LIMIT. II. THE "PHONON-DRAG" CONTRIBUTION*

by

J.P. JAY-GERIN†

(Centre de Recherches sur les Très Basses Températures, C.N.R.S., B.P. 166 - Centre de Tri, 38042 GRENOBLE-CEDEX, France).

Physical Review B (1975).

* A part of this work was performed at the Eaton Electronics Research Laboratory, Mc Gill University, MONTREAL, Canada.

† Also at Centre d'Etudes Nucléaires de Grenoble, Service des Basses Températures, B.P. 85 - Centre de Tri, 38041 GRENOBLE-CEDEX, France.

ABSTRACT

In this paper, we develop a study of the effect of the quantization of the electron energy levels in a strong magnetic field H on the "phonon-drag" contribution, S_p, of the transverse thermoelectric power of a high-purity isotropic semiconductor (n - type gallium arsenide GaAs) in the extreme quantum limit. A theoretical expression for S_p is derived, assuming that (i) all the electrons in the conduction band are accommodated in the n = 0 Landau level (extreme quantum limit), (ii) the quantum number n = 0 does not change during scattering (because of insufficient energy exchange between the electrons and the phonon system), (iii) the electron-phonon interaction occurs through the deformation-potential scattering (in the strong-field region, the scattering via the piezoelectric-coupling mechanism can be ignored), and (iv) the effect of spin splitting is neglected. The results, which are valid to the the first order in the electric field and to the second order in the electron-phonon interaction (first Born approximation), show that the transition to non-degeneracy in the electron distribution, which takes place when the bottom of the lowest Landau level approaches within a few ($k_B T$) of the Fermi level at very low temperatures, has a large effect on the variation of S_p with magnetic field. The curves of $|S_p|$ vs. H at first rise very rapidly with increasing H, and then tend to saturate as the electron distribution becomes non-degenerate. This tendency to saturate is more and more pronounced as the temperature is decreased. Numerical calculations are carried out for n - type GaAs with an electron concentration of 1.2×10^{16} cm^{-3}.

I. INTRODUCTION

In the range of low temperatures, it is well known that the total thermoelectric power (TEP) of a semiconductor can be divided into two parts. The first is due to the normal tendency of the electrons to diffuse through the crystal when a temperature gradient is present. The second is connected with the fact that the temperature gradient in the lattice produces a phonon current, which drags electrons with it as a result of the electron-phonon interaction. The first is the usual "electron-diffusion" part of the TEP, and the second is the so-called "phonon-drag" thermopower[1-3]. In semiconducting materials with sufficiently small electron concentrations, these two parts can be computed independently of each other and discussed separately[4,5], so the total TEP, S, may be written as

$$S = S_e + S_p, \tag{1}$$

where the subscripts e and p are used for "electron-diffusion" and for "phonon-drag", respectively.

In the absence of a magnetic field, the electrons occupy Bloch states in the conduction band. Upon application of a sufficiently high magnetic field, the energies of the electrons become quantized in a plane perpendicular to the magnetic field, and remain quasi-continuous in the direction of field.

This quantization of the electronic orbital motion normal to the applied magnetic field destroys the Bloch scheme of classifying the states and results in the formation of semi-discrete energy levels, the well-known "Landau levels", in the electronic band structure.

The presence of such a semi-discrete energy spectrum for the electrons may, under certain circumstances, greatly alter the behaviour of the thermoelectric transport properties of a semiconductor. For instance, Puri and Geballe[6] measured the thermoelectric power, S, of n-type indium antimonide (In Sb) in the presence of high transverse magnetic fields of up to 100 kG in the temperature range from 7 to 80 K. They found that as long as the magnetic field is in the classical region ($\hbar\omega_c \ll k_BT$, where $\hbar\omega_c$ is the Landau-level spacing and k_BT is the thermal energy of a typical conduction electron), the "phonon-drag" component S_p is very small and lies within the uncertainty in measurements. On the other hand, however, in higher magnetic fields, in the quantum region ($\hbar\omega_c \gg k_BT$), when it becomes possible for quantization to play an essential role in the transport properties, the "phonon-drag" TEP increases very rapidly with magnetic field, much more rapidly than the "electron-diffusion" component S_e, and makes the dominant contribution to the total TEP, S, at the lower end of the temperature range. Actually, for In Sb, a "phonon-drag" component of about 10 000 microvolts per degree was obtained at 10 K and in a field of

100 kG. An extensive survey of the subject can be found in the review article by Zyryanov and Guseva[7].

A case of particular physical interest is that of the extreme quantum limit. The term of "extreme quantum limit" is often used to refer to semiconductors in magnetic fields sufficiently strong (typically 50 or 100 kG) and at temperatures sufficiently low (4 K or lower temperature), so that $\hbar\omega_c \gg k_B T$ and $\frac{3}{2}\hbar\omega_c \gg \zeta$, where ζ denotes the Fermi energy. Here, all except the lowest of the quantized Landau levels have crossed over the Fermi level, and all the conduction electrons are accommodated in their lowest Landau level, which is characterized by the oscillator quantum number $n = 0$. The transverse magnetic motion is frozen out and only the one-dimensional longitudinal motion along the direction of the magnetic field remains[8]. Obviously, the well-known de Haas-van Alphen effect (the oscillatory dependence of magnetic susceptibility on reciprocal magnetic field intensity) or the related oscillatory effects in transport phenomena (magnetoresistivity, Hall coefficient, thermoelectric power, for instance) disappear in this limit. Now, if the strength of the applied magnetic field is increased further, the energy separation between the bottom of the $n = 0$ Landau level and the Fermi level diminishes. Therefore, with increasing magnetic field, the electrons are progressively drawn up to the Fermi level. At a certain critical value H_{cr} of the magnetic field, the bottom of the $n = 0$ Landau level coincides with the Fermi level. Evidently, H_{cr} is defined by the condition

$$\frac{1}{2}\hbar\omega_c^{cr} = \zeta, \text{ with } \omega_c^{cr} = \frac{|e|\, H_{cr}}{m^* c} \quad . \tag{2}$$

Here, ω_c denotes the cyclotron frequency, c is the velocity of light, and $|e|$ and m^* are the magnitude of the charge and the effective mass of an electron, respectively. A situation of theoretical as well as of experimental importance occurs at $H = H_{cr}$. In fact, when $H = H_{cr}$, a transition is induced in the crystal from a degenerate electron state, in which the electron gas obeys Fermi-Dirac statistics, to a non-degenerate one, in which the electron gas obeys Maxwell-Boltzmann statistics[9,10]. However, such a change in the electron distribution does not take place immediately after the lowest Landau level has passed through the Fermi level. In fact, the transition to non-degeneracy begins as soon as the bottom of the $n = 0$ Landau level approaches within a few $k_B T$ of the Fermi level[11]. With increasing magnetic field, more and more electrons are progressively driven into the region of non-degenerate statistics. Actually, the electron gas may be considered as completely non-degenerate as soon as the mean kinetic energy of the electrons along the direction of the applied magnetic field becomes of the order of $\frac{1}{2} k_B T$ (quasi-one-dimensional non-degenerate gas)[8]. The transition to non-degeneracy was observed experimentally for the first time by Askenazy, Ulmet, and Léotin[12] in the behavior of both the longitu-

dinal ($\rho_{//}$) and transverse ($\rho_{\perp}$) magnetoresistance of a sample of n-type gallium arsenide (Ga As) with N = 3.8 x 10^{16} cm^{-3} electrons at T = 2 K. They found that, as the electron gas passes from a degenerate to a non-degenerate state with increasing magnetic field, the magnetoresistance curve shows a giant peak starting at $\approx$ 30 kG, reaching a maximum at $\approx$ 90 kG, and decreasing again rapidly to a relatively small and slowly varying negative value by about 150 kG.

On an intuitive basis, we may expect that the change in the electron distribution manifested in this experiment has also a profound effect on the thermoelectric properties of a semiconductor. It is the subject of this research to present, under certain simplifying assumptions, a detailed and quantitative study of the transverse TEP of a semiconductor throughout the extreme quantum limit. In particular, our main interest has been to examine the effect of the transition to non-degeneracy on the variation of S as a function of magnetic field. A part of this work has recently been published in the form of a short communication[13]. We have also reported in a separate paper[14] the detailed analysis of the "electron-diffusion" contribution, S_e, of the transverse TEP of a high-purity isotropic semiconductor (n-type Ga As) in the extreme quantum limit. In the present paper, we now wish to focus our attention to the detailed analysis of the "phonon-drag" contribution, S_p. As in our previous paper[14], it is assumed in the theory developed here that the sample is of sufficiently high purity so that $\omega_c \tau >> 1$, where τ is the electron relaxation time. In this limit, the Landau quantization is preserved in spite of the collisions of the electrons with the lattice. On the other hand, we have restricted our calculations to the case of an isotropic semiconductor (n-type Ga As) with a simple parabolic energy band of effective mass m^*. This adequately describes the situation at sufficiently small electron concentrations. Finally, the effect of spin splitting is neglected in the calculation (in Ga As the spectroscopic g-factor is very small, $g \approx 0.32$[10]).

II. CALCULATION OF S_p

Let us consider the approach to equilibrium of the system of interacting electrons and phonons in a high-purity isotropic semiconductor at very low temperatures in the presence of a strong quantizing magnetic field $\vec{H}$ = (0, 0, H) directed along the z axis and of a vanishingly small electric field $\vec{E}$ = (E, 0, 0) directed along the x axis, under isothermal conditions $\vec{\nabla}T \equiv 0$ (π - approach method to thermoelectric and thermomagnetic problems)[4,5]. The "phonon-drag" contribution, S_p, of the transverse TEP (irrespectively of the "electron-diffusion" phenomenon) can be written as ($\omega_c \tau >> 1$)[14]

$$S_p = \left[S_p\right]_{yy}(H) = \frac{1}{T}\,\frac{(U_p)_y}{E}\,\rho_{xy}(H), \qquad (3)$$

$$\vec{H} = (0, 0, H).$$

Here, $(U_p)_y$ is the y component of the Peltier heat flux carried by the phonon system, as a result of the electron-phonon interaction, T is the absolute temperature, E and H are the strengths of the electric and magnetic fields, respectively, and $\rho_{xy}(H)$ is the element of the magnetoresistivity tensor given by[15]

$$\rho_{xy}(H) = -\frac{H}{N e c}, \qquad (4)$$

where N is the total number of electrons per unit volume, and e their charge ($e < 0$ for electrons).

Regarding the calculation of the energy flux carried by the phonon system in the crystal under the presence of crossed electric ($\vec{E}$ // Ox) and magnetic ($\vec{H}$ // Oz) fields, the usual steady-state Boltzmann transport equation for phonons of mode $\vec{q}j$ gives

$$\vec{U}_p = \sum_j (2\pi)^{-3} \int d^3q\ \hbar\omega_{\vec{q}j}\ \vec{v}_{\vec{q}j}\ \tau_p(\vec{q}j) \left[\frac{\partial N_{\vec{q}j}}{\partial t}\right]_{e\text{-}p}, \qquad (5)$$

where we have written explicitly the dependence of the integrand on $\vec{q}j$, $\vec{q}$ and j being the phonon wave vector and the polarization index, respectively. In the very-low-temperature range we are concerned with in the present study, only the lowest frequencies in the phonon spectrum contribute. For these long-wavelength acoustic modes of vibration, we can take the dispersion relation to be $\omega_{\vec{q}j} = s_j\, q$, where s_j is the velocity of sound, q is the magnitude of $\vec{q}$, and $\vec{v}_{\vec{q}j} = s_j\,(\vec{q}/q)$ is the group velocity of a phonon of energy $\hbar\omega_{\vec{q}j}$. However, since the electron constant energy surfaces are assumed to be isotropic, only the longitudinal phonons can interact with the electrons, and the two transverse branches of the phonon spectrum are ineffective in the "phonon-drag" phenomenon. Therefore, the summation over j, in Eq.(5), simply reduces to the contribution of the longitudinal acoustic branch. In the following, we shall drop the index j. The phonon-relaxation processes other than those on electrons, namely boundary scattering, isotope and point defect scattering, and phonon-phonon scattering, are described by a total relaxation time $\tau_p(\vec{q})$. At sufficiently low temperatures, however, only scattering of phonons by crystal boundaries is important. In this case, τ_p is essentially determined by the dimensions of the crystal, and can then be regarded as independent of q and T. In addition, it is also assumed that τ_p is not affected by the presence of the magnetic field[16]. Finally, $\left[\partial N_{\vec{q}}/\partial t\right]_{e\text{-}p}$

denotes the net time rate of change of the phonon distribution function $N_{\vec{q}}$ due to the electron-phonon scattering processes.

The basic Hamiltonian of the combined system of interacting electrons and phonons can be written as the sum of three terms

$$\mathcal{H} = H_e + H_p + H_{e-p}. \tag{6}$$

Here, H_e is the unperturbed Hamiltonian of the electron gas in the presence of crossed static electric ($\vec{E}$ // Ox) and magnetic ($\vec{H}$ // Oz) fields. In second-quantized form, H_e is given by

$$H_e = \sum_\alpha E_\alpha \, c_\alpha^+ \, c_\alpha, \tag{7}$$

where the c_α^+ and c_α act to create and annihilate an electron in the quantized Landau state $\alpha = (n, k_y, k_z)$. For a parabolic band of effective mass m^*, the one-particle energy E_α is

$$E_\alpha = \varepsilon_\alpha^\circ - eE\, x_\circ(k_y) + \frac{1}{2} m^* \left(\frac{cE}{H}\right)^2, \tag{8}$$

where

$$\varepsilon_\alpha^\circ = \left(n + \frac{1}{2}\right) \hbar\omega_c + \frac{\hbar^2 k_z^2}{2 m^*} \tag{9}$$

is the energy eigenvalue when there is no electric field (E = 0). Here, the Landau magnetic quantum number n is a positive integer or zero, k_y and k_z are the wave numbers associated with the y and z coordinates, and $\omega_c = |e| H/m^* c$ is the cyclotron frequency. The second term in Eq.(8) represents the mean potential energy in the electric field $\vec{E}$ // Ox of the Landau state centred at

$$x_\circ (k_y) = \frac{c}{eH} \left(\hbar k_y + m^* \frac{cE}{H}\right). \tag{10}$$

Finally, the last term in Eq.(8), $\frac{1}{2} m^* (cE/H)^2$, denotes the kinetic energy associated with the "drift" of the electrons along the y direction. In fact, this term is directly related, in the zeroth-order approximation with respect to scattering, to the well-known classical result that an electron in the presence of crossed constant electric ($\vec{E}$ // Ox) and magnetic ($\vec{H}$ // Oz) fields moves, on the average, in the y direction with a drift velocity equal to the Hall velocity $(-cE/H)$[14]. The one-particle eigenfunction $\psi_\alpha(\vec{r})$ associated with E_α is given by

$$\psi_\alpha(\vec{r}) = \frac{1}{\sqrt{L_y L_z}} e^{i(k_y y + k_z z)} \phi_n [x - x_o(k_y)], \tag{11}$$

where $\phi_n[x - x_o(k_y)]$ is the normalized wave function for a simple harmonic oscillator of frequency ω_c in its n th excited state and oscillating in the x direction about the point $x_o(k_y)$, and L_y, L_z are the linear dimensions of the crystal corresponding to the y and z coordinates, respectively. H_p is the Hamiltonian of the system of phonons. In terms of phonon creation and annihilation operators $b^+_{\vec{q}}$ and $b_{\vec{q}}$, H_p is given by

$$H_p = \sum_{\vec{q}} \hbar\omega_{\vec{q}} \left(b^+_{\vec{q}} b_{\vec{q}} + \frac{1}{2}\right). \tag{12}$$

Finally, H_{e-p} is the Hamiltonian of electron-phonon interaction, which may be expressed in second quantized form as[17]

$$H_{e-p} = \sum_{\alpha\alpha',\vec{q}} \gamma_{\alpha'\alpha}(\vec{q})\, c^+_{\alpha'} c_\alpha \left(b_{\vec{q}} + b^+_{-\vec{q}}\right), \tag{13}$$

where $\gamma_{\alpha'\alpha}(\vec{q})$ is the matrix element for the scattering of an electron from a state α to a state α' with either absorption of a phonon of momentum $\hbar\vec{q}$ or emission of a phonon of momentum $-\hbar\vec{q}$.

Now, as a consequence of the electron-phonon interaction, the quantized Landau states are unstable. Let $P^{(em)}_{\vec{q}}(\alpha' \to \alpha)$ denote the transition probability per unit time for an electron to be scattered from α' to α with the emission of a phonon of mode $\vec{q}$. By first-order perturbation theory (Born approximation), it is

$$P^{(em)}_{\vec{q}}(\alpha' \to \alpha) = \frac{2\pi}{\hbar} (N_{\vec{q}} + 1) \left|\gamma_{\alpha'\alpha}(\vec{q})\right|^2 \delta(E_{\alpha'} - E_\alpha - \hbar\omega_{\vec{q}}). \tag{14}$$

Similarly, the transition probability per unit time $P^{(abs)}_{\vec{q}}(\alpha \to \alpha')$ for an electron to go from α to α' with the absorption of a phonon of mode $\vec{q}$ is

$$P^{(abs)}_{\vec{q}}(\alpha \to \alpha') = \frac{2\pi}{\hbar} N_{\vec{q}} \left|\gamma_{\alpha'\alpha}(\vec{q})\right|^2 \delta(E_{\alpha'} - E_\alpha - \hbar\omega_{\vec{q}}). \tag{15}$$

Combining emission and absorption, we obtain for the net time rate of change of the phonon distribution function $N_{\vec{q}}$ due to the electron-phonon interaction :

$$\left[\frac{\partial N_{\vec{q}}}{\partial t}\right]_{e-p} = \sum_{\alpha\alpha'} \left\{ P^{(em)}_{\vec{q}}(\alpha' \to \alpha)\, f_{\alpha'} \left[1 - f_\alpha\right] - P^{(abs)}_{\vec{q}}(\alpha \to \alpha')\, f_\alpha \left[1 - f_{\alpha'}\right] \right\}$$

$$= \frac{2\pi}{\hbar} \sum_{\alpha\alpha'} \left|\gamma_{\alpha'\alpha}(\vec{q})\right|^2 \delta(E_{\alpha'} - E_\alpha - \hbar\omega_{\vec{q}}) \left[N_{\vec{q}}(f_{\alpha'} - f_\alpha) + f_{\alpha'}(1 - f_\alpha)\right]. \tag{16}$$

Here, f_α denotes the probability for a state α to be occupied by an electron. Evidently, in the absence of external electric field ($E = 0$), f_α is identical with the usual equilibrium Fermi-Dirac distribution function

$$f_\alpha^\circ = f^\circ(\varepsilon_\alpha^\circ) = \left[e^{\frac{(\varepsilon_\alpha^\circ - \zeta)}{k_B T}} + 1 \right]^{-1}, \tag{17}$$

where ε_α° is given by Eq.(9), and ζ is the Fermi energy. Now, in the case where an external electric field is present ($E \neq 0$), the electron system is described by a non-equilibrium stationary state, and the electron distribution function f_α becomes essentially a non-equilibrium one. As is well known in the theory of nonlinear galvanomagnetic effects in semiconductors[18-20], such a non-equilibrium state of electrons can be described by a Fermi-Dirac distribution function with an "effective" electron temperature $T_e(E)$, which exceeds the lattice temperature T and which is proportional to the square of the magnitude of the electric field through a relation of the form

$$T_e(E) = T(1 + \lambda E^2), \tag{18}$$

where λ is a constant independent of E. (It is precisely this heating of the electron gas that gives rise, at sufficiently high electric fields, to the so-called "warm" or "hot" electron effects in semiconductors). It must be borne in mind, however, that we are principally concerned in the present study with the limiting case of vanishingly small electric fields. Moreover, we wish to calculate $\left[\partial N_{\vec{q}}/\partial t\right]_{e\text{-}p}$ correct only up to terms linear in E. Under these conditions, it can easily be shown from the above considerations that f_α is identical, up to terms of order E^2, with its thermodynamic equilibrium value f_α°, as given in Eq.(17).

To proceed, we next assume, as is usually done in linear transport theory, that the steady-state phonon distribution does not depart very far from equilibrium. Accordingly, we write

$$N_{\vec{q}} = N^\circ(\hbar\omega_{\vec{q}}) + g_{\vec{q}}, \quad \left|g_{\vec{q}}\right| << N^\circ(\hbar\omega_{\vec{q}}), \tag{19}$$

where

$$N^\circ(\hbar\omega_{\vec{q}}) = \left[e^{\frac{\hbar\omega_{\vec{q}}}{k_B T}} - 1 \right]^{-1} \tag{20}$$

is the thermal equilibrium phonon distribution function. From Eq.(5), it is then clear that

$$\left[\frac{\partial N_{\vec{q}}}{\partial t}\right]_{e\text{-}p} = \frac{g_{\vec{q}}}{\tau_p} \quad . \tag{21}$$

Combining this last equation with Eqs.(16), (17), (19), and (20), and solving the resulting equation for $g_{\vec{q}}$, the "out-of-balance" of the steady-state phonon distribution function, we get

$$g_{\vec{q}} = \left[N^\circ(\hbar\omega^*_{\vec{q}}) - N^\circ(\hbar\omega_{\vec{q}})\right] \left(\frac{\Gamma(\vec{q})}{\Gamma(\vec{q}) + 1/\tau_p}\right) , \tag{22}$$

where

$$\Gamma(\vec{q}) = \frac{2\pi}{\hbar} \sum_{\alpha\alpha'} \left|\gamma_{\alpha'\alpha}(\vec{q})\right|^2 \delta(E_{\alpha'} - E_\alpha - \hbar\omega_{\vec{q}}) (f^\circ_\alpha - f^\circ_{\alpha'}) \tag{23}$$

is the phonon absorption coefficient due to the electron-phonon interaction(inverse electronic phonon lifetime), and $\omega^*_{\vec{q}}$ is the Doppler shifted phonon frequency given by

$$\begin{aligned} \omega^*_{\vec{q}} &= \omega_{\vec{q}} + \left(\frac{cE}{H}\right) q_y \\ &= \omega_{\vec{q}} \left[1 + \left(\frac{cE}{sH}\right)\left(\frac{q_y}{q}\right)\right] , \end{aligned} \tag{24}$$

where q_y $(= k'_y - k_y)$ is the y component of the phonon wave vector $\vec{q}$ which is involved in the transition $\alpha \to \alpha'$, and s is the velocity of sound.

As we limit ourselves to phenomena linear in the electric field E, we may expand the difference $\left[N^\circ(\hbar\omega^*_{\vec{q}}) - N^\circ(\hbar\omega_{\vec{q}})\right]$ in Eq.(22) to the first order in E, by making use of Eq.(24). Doing this, we obtain

$$N^\circ(\hbar\omega^*_{\vec{q}}) - N^\circ(\hbar\omega_{\vec{q}}) \approx -\left(\frac{cE}{H}\right)\hbar q_y \frac{k_B T}{(\hbar\omega_{\vec{q}})^2} \mathcal{C}_p\left(\frac{\hbar\omega_{\vec{q}}}{k_B T}\right) , \tag{25}$$

where $\mathcal{C}_p(x) = x^2 e^x/(e^x - 1)^2$ is the well-known Einstein function.

We can now collect factors and obtain a formula for the total Peltier heat flux $\vec{U}_p$ carried by the phonon system, in consequence of the electron-phonon interaction. From Eqs.(5), (21), (22), and (25), it follows that

$$\vec{U}_p = -\left(\frac{cE}{H}\right)\frac{k_B T}{8\pi^3} \int d^3q \left(\frac{\vec{q}}{q^2}\right) q_y \mathcal{C}_p\left(\frac{\hbar\omega_{\vec{q}}}{k_B T}\right) \frac{\Gamma(\vec{q})}{\Gamma(\vec{q}) + 1/\tau_p} \quad . \tag{26}$$

Further progress with Eq.(28) depends on the explicit form of $\Gamma(\vec{q})$. Accordingly, we now turn our attention to the evaluation of Eq.(23). For this purpose, we need the electron-phonon-interaction matrix element $\gamma_{\alpha'\alpha}(\vec{q})$. This is easily found to be[21,19]

$$\gamma_{\alpha'\alpha}(\vec{q}) = C(q)\, J_{n'n}(k_y', q_x, k_y)\, \delta_{k_y', k_y + q_y}\, \delta_{k_z', k_z + q_z} \tag{27}$$

where

$$J_{n'n}(k_y', q_x, k_y) = \int_{-\infty}^{+\infty} dx\, \phi_{n'}[x - x_o(k_y')]\, e^{iq_x x}\, \phi_n[x - x_o(k_y)] , \tag{28}$$

and $C(q)$ denotes the strength of the electron-phonon interaction. Substituting Eq.(27) into Eq.(23), and with the aid of Eqs.(8), (9), (17), and (24), we find

$$\Gamma(\vec{q}) = 2\left(\frac{2\pi}{\hbar}\right)|C(q)|^2 \sum_{n,n'} \sum_{k_y,k_z} \left|J_{n'n}(k_y + q_y, q_x, k_y)\right|^2$$

$$\times\, \delta(\varepsilon^{\circ}_{n',k_z+q_z} - \varepsilon^{\circ}_{n,k_z} - \hbar\omega^{*}_{\vec{q}}) \left[f^{\circ}(\varepsilon^{\circ}_{n,k_z}) - f^{\circ}(\varepsilon^{\circ}_{n',k_z+q_z})\right] , \tag{29}$$

the factor 2 taking account of the spin. Note that, in obtaining this result, the summations over k_y' and k_z' were readily evaluated with the Kronecker deltas.
Now, for the case of a semiconductor in the extreme quantum limit, the magnetic field is so large and the temperature is so low that (1) all the electrons in the conduction band are concentrated in the ground oscillator state with $n = 0$, and (2) the magnetic quantum number n does not change during the scattering, because the available thermal energy is insufficient to raise an electron to an excited oscillator state. In other words, this means that $n = 0$ for both the initial and final states in Eq.(29). In that case, the appropriate matrix element is[22]

$$\left|J_{oo}(k_y + q_y, q_x, k_y)\right|^2 = e^{-r_c^2 q_\perp^2/2} , \tag{30}$$

where $q_\perp = (q_x^2 + q_y^2)^{1/2}$ is the component of the phonon wave vector directed normal to the magnetic field, and $r_c = (\hbar c/|e|H)^{1/2}$ is the cyclotron radius for the electron in its ground state. As an immediate consequence, and in the limit where the volume of the crystal $\mathcal{V} = L_x L_y L_z$ becomes infinite, the summation over k_y and k_z in Eq.(29) can simply be transformed to an integral over k_z, in accordance with the relation

$$\sum_{k_y,k_z} \cdots \rightarrow \frac{\mathcal{V}}{4\pi^2 r_c^2} \int_{-\infty}^{+\infty} dk_z \cdots . \tag{31}$$

Substituting Eqs.(30) and (31) into Eq.(29), and making use of Eqs.(9) and (17), and of the well-known identity $\delta[at] = |a|^{-1}\delta[t]$, the integration over k_z is easily performed, and we obtain

$$\Gamma(\vec{q}) = \frac{\mathcal{P}}{\pi r_c^2} \frac{m^* |C(q)|^2}{\hbar^3 |q_z|} e^{-\frac{1}{2} r_c^2 q_\perp^2} \left[f^\circ(\varepsilon) - f^\circ(\varepsilon + \hbar\omega^*_{\vec{q}}) \right] , \qquad (32)$$

where

$$\varepsilon = \frac{1}{2}\hbar\omega_c + \frac{\hbar^2}{2m^*}\left(\frac{m^*\omega^*_{\vec{q}}}{\hbar q_z} - \frac{q_z}{2}\right)^2 , \qquad (33)$$

$$f^\circ(\varepsilon) - f^\circ(\varepsilon+\hbar\omega^*_{\vec{q}}) = f^\circ(u + \zeta - \frac{1}{2}\hbar\omega^*_{\vec{q}}) - f^\circ(u + \zeta + \frac{1}{2}\hbar\omega^*_{\vec{q}})$$

$$= \frac{\sinh\left(\frac{1}{2}\frac{\hbar\omega^*_{\vec{q}}}{k_B T}\right)}{\cosh\left(\frac{u}{k_B T}\right) + \cosh\left(\frac{1}{2}\frac{\hbar\omega^*_{\vec{q}}}{k_B T}\right)} , \qquad (34)$$

and

$$u = \left\{ \frac{1}{2}\hbar\omega_c + \frac{\hbar^2}{2m^*}\left[\left(\frac{m^*\omega^*_{\vec{q}}}{\hbar q_z}\right)^2 + \frac{q_z^2}{4} \right] \right\} - \zeta , \qquad (35)$$

At this point, we are in a position to complete the evaluation of $\Gamma(\vec{q})$ explicitly. As we are interested only in effects at high H which are linear in E, we can make the following two approximations :

(1) For transport phenomena linear in the electric field E, we may neglect the dependency of $\omega^*_{\vec{q}}$ on E and set simply

$$\omega^*_{\vec{q}} \approx \omega_{\vec{q}} = s\,q \qquad (36)$$

in the calculations which follow. According to Eq.(24), this requires $(cE/H) \ll s(q/q_y)$. This condition is certainly well satisfied in the limit of the vanishingly small electric fields with which we are concerned in this paper. Moreover, this agrees well with the results of Kazarinov and Skobov[18] and of Calecki[19], who have shown that the non-linearities in E associated with a heating of the electron gas occur when $(cE/H) > s$.

(2) The form of C(q) to be used depends upon the mode of coupling between the electrons and acoustic phonons. In the region of low temperatures, the electron-phonon interaction occurs essentially through two types of scattering : (i) piezoelectric scattering and (ii) deformation-potential scattering. However, for the high magnetic fields with which we are concerned here, the scattering via the piezoelectric-coupling mechanism ($|C(q)|^2 = D/q$, where D is the coupling constant) becomes less probable because it is discriminated against. This follows from the fact that in the extreme quantum limit the wave vector of phonons that contribute most to electron-

phonon scattering continuously increases with the magnetic field ($q \sim 1/r_c = (|e|\,H/\hbar c)^{1/2}$)[23]. Puri[16] and Puri and Geballe[24] have confirmed experimentally (in the case of In Sb) this prediction. Indeed, their results show that the high-field phonon-drag is not affected to any appreciable degree by piezoelectric scattering. Taking these remarks into account, we may therefore neglect the piezoelectric mode of scattering completely, and assume that the electron-phonon interaction occurs entirely through the usual deformation-potential-coupling mechanism. In that case, we have[10]

$$|C(q)|^2 = \frac{\hbar\, C^2\, q}{2\, d\, \vartheta_s} \quad , \tag{37}$$

where C is the deformation-potential constant and d is the mass density of the crystal.

Having made these approximations, it is now a simple matter to write down an explicit formula for $\Gamma(\vec{q})$. In fact, introducing spherical polar coordinates ($q_z = q\cos\theta$, and $q_\perp = q\sin\theta$, where θ is the angle between the $\vec{q}$ direction and the direction of the z axis), and combining Eqs.(32) and (34)-(37), we obtain the result

$$\Gamma(\vec{q}) = \Gamma(q,\ \mu = \cos\theta) = \frac{A(q)\, e^{\frac{1}{2} r_c^2\, q^2\, \mu^2}}{|\mu| \left[\mathrm{Cosh}\left(\frac{m^* s^2}{2 k_B T\, \mu^2} + \frac{q^2\, \mu^2}{4\, q_T^2} - \xi\right) + \mathrm{Cosh}\left(\frac{1}{2}\frac{\hbar s q}{k_B T}\right)\right]} \quad , \tag{38}$$

where

$$A(q) = \frac{m^* C^2}{2\,\pi\,\hbar^2\, d\, s\, r_c^2}\, e^{-\frac{1}{2} r_c^2\, q^2}\, \mathrm{Sinh}\left(\frac{1}{2}\frac{\hbar s q}{k_B T}\right) \quad , \tag{39}$$

$q_T = (2m^* k_B T / \hbar^2)^{1/2}$ is the thermal de Broglie wave vector for the electrons, and

$$\xi = \frac{1}{k_B T}\left(\zeta - \frac{1}{2}\hbar\omega_c\right). \tag{40}$$

We can now collect factors and obtain the final expression for the "phonon-drag" contribution, S_p, of the transverse TEP. Introducing the dimensionless integration variable $x = \hbar s q / k_B T$, and substituting Eqs.(4), (26), and (38) into Eq.(3), we obtain, after some calculations,

$$S_p = \frac{k_B}{e}\, \frac{1}{6\,\pi^2\, N} \left(\frac{k_B T}{\hbar s}\right)^3 \int_0^{x_{max} = \Theta_D/T} dx\, x^2\, \mathcal{C}_p(x)\, I_p(x) \quad , \tag{41}$$

where $k_B/|e| = 86.2$ microvolts per degree, $\Theta_D = \hbar s q_{max}/k_B$ is the Debye temperature,

and

$$I_p(x) = \frac{3}{2}\int_0^1 d\mu\,(1-\mu^2)\left(\frac{\Gamma(x,\mu)}{\Gamma(x,\mu)+1/\tau_p}\right) . \qquad (42)$$

As is clearly seen from Eq.(42), the quantity $I_p(x)$ [or, $I_p(q)$] to which S_p is proportional reflects the efficiency of the "drag" (that is to say, the fraction of phonon (q) - electron collisions to <u>all</u> phonon (q) collisions), and hence plays a role of major importance in the determination of the "phonon-drag" TEP. It is worth noting here that $I_p(q)$, as given by Eq.(42), is just a suitable average value of the quantity $\Gamma(\vec{q})/(\Gamma(\vec{q})+1/\tau_p)$ over the phonon constant-energy surface $\omega_{\vec{q}} = sq =$ constant, defined by[25]

$$I_p(q) = \left[I_p\right]_{yy}(q)$$
$$= \int_{\omega_{\vec{q}}=\text{ constant}} \frac{dS}{|\vec{v}_{\vec{q}}|}\,(\vec{v}_{\vec{q}})_y\,(\vec{v}_{\vec{q}})_y\left(\frac{\Gamma(\vec{q})}{\Gamma(\vec{q})+1/\tau_p}\right) \Big/ \int_{\omega_{\vec{q}}=\text{ constant}} \frac{dS}{|\vec{v}_{\vec{q}}|}\,(\vec{v}_{\vec{q}})_y\,(\vec{v}_{\vec{q}})_y \quad , \qquad (43)$$

where the weighting factor for averaging, $dS\left[(\vec{v}_{\vec{q}})_y\right]^2 / |\vec{v}_{\vec{q}}|$, represents the effective number of phonons in the <u>y</u> direction, parallel to the net electric current[14] ($|\vec{v}_{\vec{q}}|$ is the velocity of sound <u>s</u>, and dS is the element of area on the constant-energy surface in $\vec{q}$ space). Actually, since the quantity $\Gamma(\vec{q})/(\Gamma(\vec{q})+1/\tau_p)$ can only take values between 0 and 1, this directly implies from Eqs.(42) and (43) that $I_p(q)$ lies between 0 and 1, depending on the magnitude of $\Gamma(\vec{q})$ compared with $1/\tau_p$. If $\Gamma(\vec{q}) \ll 1/\tau_p$, $I_p(q) \to 0$; in this case, phonon momentum is transferred to the lattice with greater probability than to the electron system, and there is no appreciable "phonon-drag" contribution of the TEP. On the other hand, if $\Gamma(\vec{q}) \gg 1/\tau_p$, $I_p(q) \to 1$; in that case, phonon momentum is imparted predominantly to the conduction electrons, and the "phonon-drag" TEP takes its maximum value appropriate to the temperature under consideration.

III. NUMERICAL RESULTS FOR Ga As

In order to have a quantitative estimate of the above theoretical results, some numerical calculations have been carried out for the case of <u>n</u>-type gallium arsenide with an electron concentration $N = 1.2 \times 10^{16}$ cm^{-3}. The numerical values of the physical parameters for this material are : $m^* = 0.07\ m_o$, where m_o is the free-electron mass, $s = 5.24 \times 10^5$ cm/sec, $d = 5.31$ g/cm^3, $\Theta_D = 345$ K, and $C = 7.0$ eV[26]. An advantage with <u>n</u>-Ga As is that it is known to be a very high-mobility material, so that the

extreme quantum limit can easily be attained at low temperatures for relatively low magnetic fields. In addition, because of the very small spectroscopic g-factor ($g \approx 0.32$) of the conduction electrons, the effect of spin splitting can be ignored.

All the calculations have been performed under the following two assumptions : (1) the electron concentration does not change with the temperature[8], and (2) no magnetic "freeze out" of the conduction electrons occurs[8]. The main results of our calculations are :

(1) $|S_p|$ increases very rapidly with the magnetic field in the extreme quantum limit, much more rapidly than the "electron-diffusion" contribution, $|S_e|$. This is illustrated in Fig. (1), which shows the variation of $|S_p|$ as a function of magnetic field at liquid helium temperature T = 4.2 K, for two different phonon relaxation times[27] : (a) $1/\tau_p = \tau_B^{-1} + \tau_{pt}^{-1} + \tau_{3ph}^{-1}$, where $\tau_B^{-1} = 0.60 \times 10^6$ sec^{-1} is the boundary inverse relaxation time, $\tau_{pt}^{-1} = A\omega^4$, with $A = 0.46 \times 10^{-44}$ sec^3, is the inverse relaxation time for the scattering due to isotopes, point defects, etc., and $\tau_{3ph}^{-1} = B\omega^2T^3$, with $B = 5 \times 10^{-22}$ sec/deg^3, is the three-phonon inverse relaxation time (solid curve marked A), and (b) $1/\tau_p = \tau_B^{-1}$ (dashed curve marked B). It is apparent from the figure that only the boundary scattering of phonons is important at 4.2 K, the other phonon--relaxation processes being relatively ineffective. The plot of $|S_e|$, the "electron--diffusion" TEP, as a function of H at T = 4.2 K is also shown on the same figure for reference [14]. As we can see, at liquid helium temperature, S_p makes the dominant contribution to the total thermoelectric power. All these features are in general agreement with the experimental results of Puri and Geballe in n-In Sb[6].

(2) Boundary scattering of the phonons greatly modifies both the magnitude and the variation of $|S_p|$ as a function of magnetic field. This is illustrated in Fig. (2), where we show the dependence of $|S_p|$ upon H at T = 4.2 K for different values of the boundary-scattering inverse relaxation time τ_B^{-1}, ranging from 0.10×10^6 sec^{-1} to 120×10^6 sec^{-1}. As we can see, $|S_p|$ decreases very strongly with increasing τ_B^{-1}, while the initial rise of the $|S_p|$-versus-H curve, at the lower end of the magnetic-field range, is gradually more and more pronounced. In fact, for $\tau_B^{-1} = 0.10 \times 10^6$ sec^{-1}, the curve of $|S_p|(H)$ rises approximately as $H^{1.4}$ with increasing H between 15.6 and 23.3 kG, while for $\tau_B^{-1} = 120 \times 10^6$ sec^{-1}, $|S_p|$ increases approximately as $H^{4.1}$ in the same magnetic-field range. Since τ_B^{-1} is essentially determined by the dimensions of the specimen through the relation $\tau_B^{-1} = s/L$, where s is the velocity of sound and L is a suitable boundary scattering length[28], the scattering of the phonons by the boundaries of the specimen makes the "phonon-drag" TEP especially sensitive to the size and shape of the specimen in the extreme quantum limit. This "size effect", which has been confirmed experimentally in n-type germanium[29] and in n-type

InSb[6], was discussed in detail by Herring[4].

(3) The variation of $|S_p|$ with H varies strikingly with temperature. This is shown in fig. (3), where $|S_p|$ is plotted as a function of magnetic field at the temperatures 2, 3, 4.2, and 5 K. The curves of $|S_p|$ vs. H at first rise rapidly as H is increased, and then tend to saturate at higher fields. This tendency to saturate, which is more and more pronounced as the temperature is decreased, arises as a result of the transition from degenerate to non-degenerate statistics, as we shall see in the next section. In addition, $|S_p|$ decreases very rapidly with decreasing T at the lowest temperatures. This result, which is essentially due to the presence of the term T^3 in the expression of S_p [Eq. (41)] is also apparent from fig. (4), which shows the temperature dependence of $|S_p|$ between 1 and 10 K, for different values of the magnetic field strength, 17.5, 30, and 80 kG. Accordingly, it is to be expected that, at very low temperatures (e.g., 0.5 K), the "phonon-drag" contribution to the TEP will become increasingly negligible compared with the "electron-diffusion" contribution, $|S_e|$, which also decreases with decreasing temperature, but much more slowly. The latter point is illustrated in fig. (5), where we have plotted, for comparison, the variation of $|S_e|$ with H at the temperatures 0.5, 2, 3, and 5 K[14]. Since the purely electronic TEP, in the extreme quantum limit, can be determined completely from the electron concentration and the band structure, irrespectively of the electron scattering parameters[14], an immediate consequence is that the study of the transverse TEP, in the extreme quantum limit and in the range of very low temperatures, should be a valuable tool for getting an additional information about the band structure of semiconductors[30].

(4) Unlike the transverse ($\rho_\perp$) and longitudinal ($\rho_{//}$) magnetoresistance[12], no "anomalous" behaviour occurs in the variation of $|S_p|$ with magnetic field during the transition from degenerate to non-degenerate statistics. This result can be understood quite readily from the fact that the anomalous behaviour in the magnetoresistance is intimately linked with the screening effect of ionized impurities due to the onset of non-degeneracy in the electron distribution, as the lowest $n = 0$ Landau level approaches within a few times k_BT of the Fermi level[11,31]. On the contrary, the "phonon-drag" TEP, in the extreme quantum limit, is independent of electron scattering other than that on acoustical phonons, and thus is not affected by the presence of ionized impurities[16]. This only holds in the case of transverse fields, i.e., crossed electric and magnetic fields, and follows from the fact that the current flow in the direction of the electric field is caused and moreover enhanced by the collisions themselves.

(5) Phonon-phonon scattering modifies $|S_p|$ at high temperatures. This is shown in fig. (4), where $|S_p|$, calculated with and without phonon-phonon scatte-

ring, is plotted as a function of temperature for three different values of magnetic field. As we can see, the results indicate that, above about 5 K, the (full) curves of $|S_p|$ vs. T, calculated with $1/\tau_p = 0.60 \times 10^6 + 1.35\ T^4\ x^4 + 8.57\ T^5\ x^2\ sec^{-1}$ [see the caption of Fig. (1)], depart from the (dashed) curves of $|S_p|$ vs. T, calculated with $1/\tau_p = 0.60 \times 10^6\ sec^{-1}$ (boundary scattering only), go through a maximum value, which shifts towerds higher temperatures as the magnetic field is increased, and then decrease with further increase of T. Such a behaviour, at high temperatures, is essentially controlled by the mechanism of phonon-phonon scattering. Therefore, it clearly appears that the "phonon-drag" TEP in the extreme quantum limit should provide a valuable tool for learning things about phonon-phonon interactions in semiconductors[4,5,16]. However, we must mention that in the numerical calculation of the curves of $|S_p|$ vs. T presented in Fig. (4), the electron concentration $N = 1.2 \times 10^{16}\ cm^{-3}$ has been taken as a constant for all temperatures. The latter point deserves careful attention, because such an assumption is unlikely to be valid for T above 10 K. Experimentally, Hall coefficient measurements in the temperature range below 10 K should be made in all cases.

IV. DISCUSSION

It is clear from Figs. (1), (2) and (3) that, after a large and rapid initial rise, the $|S_p|$-H curves tend to saturate as the field is increased. This tendency to saturate is seen to depend strikingly on temperature [Fig. (3)]. As it was mentioned above, such a behaviour is associated with the change in the electron distribution which takes place as the $\underline{n} = 0$ Landau level approaches the Fermi level. It is worth noting that the curves of $|S_p|$ vs. T, at given H, in Fig. (4), which behave in approximately the same way, can also be understood on the basis of the transition to non-degeneracy in the electron distribution. In order to examine this point in more detail, we have made a series of drawings to show more clearly what is happening. In Fig. (6), we have plotted the so-called "critical field", H_{cr}, which corresponds to the transition from degenerate to non-degenerate statistics [Eq. (2)], as a function of temperature between 1 and 10 K. In the calculation, we have made the assumption that the electron concentration, N, does not change with temperature in this range[8]. As we can see, H_{cr} strongly depends upon temperature; the lower the temperature, the larger the value of H_{cr}. For example, let us confine our attention to the case where T = 4.2 K. For this temperature, $H_{cr} \simeq 56.4$ kG [Fig. (6)]. It is of interest to see the variation of the quantity $\xi = (\zeta - \frac{1}{2}\hbar\omega_c)/k_BT$ [Eq. (40)] as a function of magnetic field in the extreme quantum limit. This is shown in Fig. (7). The reason of such an interest is that ξ gives at once a clear indication, showing whether the electron gas is degene-

rate or non-degenerate. In fact, ξ behaves very differently in the two regions. In the region in which only the $\underline{n} = 0$ Landau level is occupied, but the system is still strongly degenerate, ξ is much larger than unity. With increasing magnetic field, the curve of ξ vs. H falls sharply until the onset of non-degeneracy in the electron distribution occurs ($\xi \gtrsim 1$, H $\sim$ 30-40 kG) [Fig. (7)]. Once the system has become non-degenerate, the curve of ξ shows a marked lessening of slope, and then continues to decrease, but rather slowly, with increasing H. Actually, throughout the non-degenerate region, $|\xi| \lesssim 1$. Let us now return to Eq. (41). It is clear that, as far as the magnetic field dependence of the "phonon-drag" TEP is concerned, the quantity with which we are especially interested is $I_p(x = \hbar sq/k_B T)$. Indeed, I_p is the only factor in the expression of S_p which effectively depends on the magnetic field. As was mentioned above, $I_p(x)$ gives the efficiency of the "drag", that is, the fraction of phonon (q)-electron collisions to all phonon (q) collisions [Eqs. (42) and (43)]. In Fig. (8), we have plotted I_p vs. x at T = 4.2 K for different values of the magnetic field intensity, and for $1/\tau_p = \tau_B^{-1} + \tau_{pt}^{-1} + \tau_{3ph}^{-1}$ as in Fig. (1). For a given H, the curve of I_p vs. x is seen to rise sharply from zero (at x = 0) to a maximum (at x $\sim$ 0.8) of about 0.75-0.93, and then decrease more or less rapidly to zero for $x \gtrsim 0.8$, depending critically on the value of H. In the regime of strong degeneracy (below 30-40 kG), the maximum of $I_p(x)$ at x $\sim$ 0.8 increases very rapidly with increasing H, then becomes gradually broader and broader, and finally tends to stabilize around the value 0.93 as the onset of non-degeneracy is approached. Above this maximum, we note that I_p decreases steeply to zero with increasing x. Now, in the regime of complete non-degeneracy (that is to say, above 30-40 kG), the entire region of the maximum of $I_p(x)$ (say, for $x \lesssim 1.5$) remains practically unchanged as the field is increased, while the decrease of I_p to zero, for $x \gtrsim 1.5$, becomes slower and slower. According to Eqs. (42) and (43), it is clear that, since the relaxation time τ_p of the phonons is assumed to be unaltered by the presence of the magnetic field[16], the variation of $I_p(x)$ with H is essentially controlled by the field dependence of $\Gamma(\vec{q})$, the phonon absorption coefficient due to the electron-phonon interaction [Eqs. (32)-(40)]. To see what actually happens, we write :

$$\Gamma(\vec{q}) \propto H \frac{q}{|q_z|} \; e^{-\frac{1}{2} r_c^2 q_\perp^2} \left[f^\circ(\varepsilon) - f^\circ(\varepsilon + \hbar\omega_q^{\rightarrow}) \right] , \qquad (44)$$

showing how $\Gamma(\vec{q})$ depends on $\vec{q} = (q_\perp, q_z)$, the magnetic field H, and the temperature T. As before, f° is the equilibrium Fermi-Dirac distribution function, which is defined in Eq. (17),

$$r_c^2 = (\hbar c/|e|H), \quad \omega_{\vec{q}} = s\,q \quad [\text{Eq. (36)}],$$

$$\varepsilon = \frac{1}{2}\hbar\omega_c + \frac{\hbar^2}{2m^*}\left(\frac{q_z}{2} - \frac{m^*\omega_{\vec{q}}}{\hbar q_z}\right)^2 \quad \text{[Eq. (33)]} \quad ,$$

$$\varepsilon + \hbar\omega_{\vec{q}} = \frac{1}{2}\hbar\omega_c + \frac{h^2}{2m^*}\left(\frac{q_z}{2} + \frac{m^*\omega_{\vec{q}}}{\hbar q_z}\right)^2 \quad , \text{ and the Fermi factor}$$

$\left[f^\circ(\varepsilon) - f^\circ(\varepsilon+\hbar\omega_{\vec{q}})\right]$ is given by [Eq. (34)]

$$f^\circ(\varepsilon) - f^\circ(\varepsilon+\hbar\omega_{\vec{q}}) = \mathrm{Sinh}\left(\frac{1}{2}\frac{\hbar\omega_{\vec{q}}}{k_BT}\right) \Big/ \left[\mathrm{Cosh}\left(\frac{u}{k_BT}\right) + \mathrm{Cosh}\left(\frac{1}{2}\frac{\hbar\omega_{\vec{q}}}{k_BT}\right)\right], \tag{45}$$

with [Eq. (35)]

$$-\frac{u}{k_BT} = \xi - \frac{\left[\frac{q_z^2}{4} + \left(\frac{m^*\omega_{\vec{q}}}{\hbar q_z}\right)^2\right]}{q_T^2} \quad , \tag{46}$$

where $\xi = (\zeta - \frac{1}{2}\hbar\omega_c)/k_BT$ [Eq.(40)], and $q_T^2 = 2m^*k_BT/\hbar^2$ is the thermal electron wavevector. As we can see from Eqs. (44)-(46), the q_z dependence of $\Gamma(\vec{q})$ is rather complicated. However, we can get a little orientation on the problem by remarking that, if we neglect the inelasticity in the electron-phonon interaction, which arises from the finite phonon energy, we find that $\Gamma(\vec{q})$ increases like $|q_z|^{-1}$ as $q_z \to 0$. The source of this singularity is the one-dimensional nature of the electron gas in the extreme quantum limit. It is worth noting here that the divergence arising from the factor $|q_z|^{-1}$ in Eq. (44) is removed owing to the term $\mathrm{Cosh}(u/k_BT)$, which appears in Eq.(45). In fact, the factor $\omega_{\vec{q}}$ in Eq.(46) arises from the effect of the inelasticity in the electron-phonon interaction[9,32]. Because of the $|q_z|^{-1}$ factor in the expression for the inverse electronic phonon lifetime, most of the contribution to $\Gamma(\vec{q})$ arises for sufficiently small q_z, and therefore, we can replace $q_\perp$ by q in Eq.(44). With this modification, the exponential term in Eq.(44), which is essentially unimportant for small q, plays a major role when its argument exceeds unity, that is, when $q \gtrsim \sqrt{2}/r_c \approx 1.74 \times 10^5 \sqrt{H}\ \mathrm{cm}^{-1}$, or, correspondingly, when $x = \hbar sq/k_BT \gtrsim 6.98 \times 10^{-1}\ (\sqrt{H}/T)$, where H is the field in kilogauss and T in degrees. Numerically, for T = 4.2 K, this gives $x \gtrsim 0.80$ at H = 23.3 kG, $x \gtrsim 1.25$ at H = 56.4 kG, and $x \gtrsim 1.76$ at H = 112.3 kG. Now, to understand completely the behaviour of $\Gamma(\vec{q})$, we must examine the Fermi factor $\left[f^\circ(\varepsilon) - f^\circ(\varepsilon+\hbar\omega_{\vec{q}})\right]$. According to Eq.(45), we see that for small x (say, for $x < 1$), the Fermi factor is proportional to x. Departures from this proportionality evidently occurs as soon as $x \gtrsim 1$. To illustrate this, we have plotted in Fig.(9) the quantity $\left[f^\circ(\varepsilon) - f^\circ(\varepsilon+\hbar\omega_{\vec{q}})\right]$, as given by Eq.(45), against $x = \hbar sq/k_BT$, with the quantity (u/k_BT) as a parameter. In the calculation, (u/k_BT) is simply taken to be a constant as a

function of q, and is further identified with ξ [see Eq.(46)]. Such an assumption is not so unreasonable, since ξ essentially dominates the variation of the quantity (u/k_BT). Using this assumption, and with the aid of Fig.(7), we have indicated on the curves, for T = 4.2 K, the values of the magnetic field which correspond to the values chosen for the parameter (u/k_BT). According to the results presented in Fig.(9), and to the above considerations, we can draw, at this point, several conclusions regarding the behaviour of $\Gamma(\vec{q})$:

(i) For given T and H, $\Gamma(\vec{q})$ behaves essentially like $q\, e^{-\frac{1}{2}r_c^2q^2}$ as a function of q. For small q, $\Gamma(\vec{q})$ increases linearly with q, then goes through a maximum value for $q \approx q_m = 1/r_c \approx 1.23 \times 10^5 \sqrt{H}$ cm^{-1}, or, correspondingly, for $x = \hbar sq/k_BT \approx x_m \approx 4.94 \times 10^{-1}$ $(\sqrt{H}/T)$, and finally decreases exponentially for large q. Numerically, for T = 4.2 K, we get $x_m \approx 0.57$ at H = 23.3 kG, $x_m \approx 0.88$ at H = 56.4 kG, and $x_m \approx 1.25$ at H = 112.3 kG. However, the position of this maximum can slightly be shifted towards either larger (at H = 15.8, 18.4, and 23.3 kG, for instance) or smaller (at H = 33.2 kG, and higher) values of q (or x), as a result of the departures from linearity of the Fermi factor as a function of q (or x) [see Fig.(9), and Eqs.(45) and (46)].

(ii) For given T and q, $\Gamma(\vec{q})$ behaves in two different ways as a function of magnetic field, depending on whether the electron gas is degenerate or non-degenerate. In the region of strong degeneracy (below 30-40 kG, for T = 4.2 K), the Fermi factor, which varies as $1/[\mathrm{Cosh}(u/k_BT) + \mathrm{Cosh}(x/2)]$ [Eqs.(45) and (46)], increases very rapidly with increasing H [see Fig.(9), for instance], due to the extremely rapid change of ξ in this region [see Fig.(7)]. Accordingly, $\Gamma(\vec{q})$ increases very rapidly with H, essentially as $H\, e^{-1/2\, r_c^2q^2} / [\mathrm{Cosh}(u/k_BT) + \mathrm{Cosh}(x/2)]$. The variation with H of the maximum of $\Gamma(\vec{q})$, at $q \approx q_m = 1/r_c$, is thus very nearly $Hx_m/[\mathrm{Cosh}(u/k_BT)+\mathrm{Cosh}(x_m/2)]$. Here, the factor H arises from the density of states which increases linearly with magnetic field in the extreme quantum limit. It is worth noting that, as H increases, the Fermi energy ζ also increases. In fact, ζ strongly depends on magnetic field in the extreme quantum limit[14,33]. In Fig.(10), we have plotted the variation of ζ as a function of H for n-Ga As with $N = 1.2 \times 10^{16}$ cm^{-3} electrons at T = 4.2 K. Evidently, since ζ increases with H, the effective average q of the phonon modes to which the electrons deliver their crystal momentum also increases. This excitation of larger q values can clearly be seen in Fig.(8). The behaviour of $\Gamma(\vec{q})$ as a function of H radically changes as the system becomes non-degenerate (that is, above 30-40 kG for T = 4.2 K). This is essentially due to the fact that the Fermi factor is a slowly varying function of H in this region [see Fig.(9), for instance]. Specifically, such a result clearly arises because of the rather slow variation of ξ with H [see Fig.(7)], once the system

has become non-degenerate. For $\xi = 0$, i.e., for $H = H_{cr} \approx 56.4$ kG at $T = 4.2$ K, the Fermi factor goes through a maximum value, and then begins to decrease progressively for $H > H_{cr}$. It is precisely this decrease of the Fermi factor in the region of non-degeneracy which counteracts the effect of increase of the factor $H\, e^{-r_c^2 q^2/2}$, and thus gives rise to a saturation of $\Gamma(\vec{q})$. Evidently, this saturation is more pronounced for the small values of q, especially for $q \approx q_m = 1/r_c$, which corresponds to the maximum of $\Gamma(\vec{q})$. For the sake of illustration, and in order to show all the features we have just obtained before, we have plotted in Fig. (11), for the temperature $T = 4.2$ K, the quantity defined by

$$\Gamma(x=\hbar sq/k_B T) = \int_{\omega_{\vec{q}} = \text{ constant}} \frac{dS}{|\vec{v}_{\vec{q}}|} (\vec{v}_{\vec{q}})_y \, (\vec{v}_{\vec{q}})_y \, \Gamma(\vec{q}) \; / \int_{\omega_{\vec{q}} = \text{ constant}} \frac{dS}{|\vec{v}_{\vec{q}}|} (\vec{v}_{\vec{q}})_y \, (\vec{v}_{\vec{q}})_y$$

$$= \frac{3}{2} \int_0^1 d\mu \, (1 - \mu^2) \, \Gamma(x,\mu) \quad , \qquad (47)$$

where the notations are the same as in Eqs. (38)-(43). $\Gamma(x)$ is nothing else but a suitable average value of $\Gamma(\vec{q})$ over the phonon constant-energy surface $\omega_{\vec{q}} = sq = \text{constant}$[25] [see Eqs. (42) and (43)]. The variation of $I_p(x)$ with both x and H [see Fig. (8)] can be deduced from the above considerations and from the results presented in Fig. (11), and in consequence the behaviour of the "phonon-drag" TEP, $|S_p|$, as a function of H [Figs. (1)-(3)] can be understood.

(iii) The effect of temperature on $\Gamma(\vec{q})$ can also be understood. As we have said before, for given T and H, $\Gamma(\vec{q})$ behaves essentially like $q\, e^{-r_c^2 q^2/2}$. This function exhibits a marked maximum at $x = \hbar sq/k_B T \approx x_m \approx 4.94 \times 10^{-1} (\sqrt{H}/T)$. Accordingly, for a fixed H, increasing T shifts the maximum of $\Gamma(\vec{q})$ towards smaller and smaller values of x (or q), and vice versa. For example, for $H = 17.5$ kG, we have $x_m \approx 1.03$ at $T = 2$ K, $x_m \approx 0.69$ at $T = 3$ K, $x_m \approx 0.41$ at $T = 5$ K, and $x_m \approx 0.26$ at $T = 8$ K. On the other hand, for a fixed H, it is clear from Eqs. (44)-(46) that the magnitude of the maximum of $\Gamma(\vec{q})$ as a function of temperature is essentially controlled by the quantity $x_m \,/\, [\text{Cosh}(u/k_B T) + \text{Cosh}(x_m/2)]$. Two cases have to be considered, depending upon whether the system is degenerate or non-degenerate. To see what actually happens, we have plotted in Fig. (12) the variation of the quantity $\xi = (\zeta - \frac{1}{2}\hbar\omega_c)/k_B T$ [Eq. (40)] as a function of T in the extreme quantum limit, for both $H = 17.5$ kG (degenerate regime) and $H = 80$ kG (non-degenerate regime). As we can see, for $H = 17.5$ kG, ξ is large as compared to unity and decreases rapidly with increasing T. On the contrary, for $H = 80$ kG, ξ is small and decreases very slowly with increase of T. Evidently, such a dif-

ference in the variation of ξ as a function of T leads to a different behaviour of the quantity $(u/k_B T)$ [Eq. (46)]. However, it is difficult to know accurately this quantity $(u/k_B T)$, because of the presence of the factor $[q_z^2/4 + (m\omega_q/\hbar q_z)^2]$ / q_T^2 , which plays a role of increasing importance as the temperature is lowered. To get a definite answer, we have carried out a numerical calculation of $\Gamma(x = \hbar sq/k_B T)$, as given in Eq. (47), for the two values of the magnetic field H = 17.5 kG and H = 80 kG, and for different values of temperature. This is shown in Fig. (13). As we can see, for H = 17.5 kG, the maximum of $\Gamma(x)$ is nearly independent of T, whereas, for H = 80 kG, it roughly decreases as T^{-1}. By taking into account the preceeding considerations and the results presented in Fig. (13), the temperature dependence of the "phonon-drag" TEP [see Eqs. (41) and (42)], $|S_p|$, can be understood [Figs. (3) and (4)].

ACKNOWLEDGMENTS

The author wishes to thank Prof. P.R. Wallace, Dr. O.P. Gupta, Prof. J.D.N. Cheeke, Prof. R. Maynard, and Dr. A. Briggs for a number of stimulating discussions. He also wishes to thank Dr. J. Teixeira for assistance with the computer program.

September 1974.

REFERENCES

1. D.K.C. MAC DONALD,
"Thermoelectricity : an introduction to the principles" (John Wiley and Sons, Inc., New York, London, 1962).

2. R.D. BARNARD,
"Thermoelectricity in Metals and Alloys" (Taylor and Francis Ltd, London, 1972).

3. R.P. HUEBENER,
in "Solid State Physics", edited by H. EHRENREICH, F. SEITZ, and D. TURNBULL (Academic Press, New York and London, 1972), Vol. 27, p. 63.

4. C. HERRING,
Phys. Rev. 96, 1163 (1954).

5. C. HERRING, T.H. GEBALLE, and J.E. KUNZLER,
Phys. Rev. 111, 36 (1958).

6. S.M. PURI and T.H. GEBALLE,
Phys. Rev. 136, A1767 (1964).

7. P.S. ZYRYANOV and G.I. GUSEVA,
Usp. Fiz. Nauk 95, 565 (1968) [English transl. : Soviet Physics - Uspekhi 11, 538 (1969)].

8. J.P. JAY-GERIN and P.R. WALLACE,
J. Low Temp. Phys. 7, 525 (1972).

9. E.N. ADAMS and T.D. HOLSTEIN,
J. Phys. Chem. Solids 10, 254 (1959).

10. L.M. ROTH and P.N. ARGYRES,
in "Semiconductors and Semimetals", edited by R.K. WILLARDSON and A.C. BEER (Academic Press, New York and London, 1966), Vol. 1, p. 159.

11. S. ASKENAZY,
in "New Developments in Semiconductors", edited by P.R. WALLACE, R. HARRIS, and M.J. ZUCKERMANN (Noordhoff, Leyden, The Netherlands, 1973), p. 331.

12. S. ASKENAZY, J.P. ULMET, and J. LÉOTIN,
Solid State Commun. 7, 989 (1969).

13. J.P. JAY-GERIN,
Solid State Commun. 14, 831 (1974).

14. J.P. JAY-GERIN,
J. Phys. Chem. Solids 35, 81 (1974).

15. A.C. BEER,
in "Solid State Physics", edited by F. SEITZ and D. TURNBULL (Academic Press, New York and London, 1963), Vol. 4, p. 96.

16. S.M. PURI,
Phys. Rev. 139, A995 (1965).

17. D. PINES,
"Elementary Excitations in Solids" (W.A. Benjamin, Inc., New York, Amsterdam, 1964), p. 257.

18. R.F. KAZARINOV and V.G. SKOBOV,
Zh. Eksp. Teor. Fiz. 42, 1047 (1962) [English transl. : Soviet Physics - JETP 15, 726 (1962)].

19. D. CALECKI,
J. Phys. Chem. Solids 32, 1835 (1971).

20. A.M. ZLOBIN and P.S. ZYRYANOV,
Usp. Fiz. Nauk 104, 353 (1971) [English transl. : Soviet Physics - Uspekhi 14, 379 (1972)].

21. P.N. ARGYRES,
Phys. Rev. 109, 1115 (1958).

22. P.N. ARGYRES and E.N. ADAMS,
Phys. Rev. 104, 900 (1956).

23. L.É. GUREVICH and G.M. NEDLIN,
Fiz. Tverd. Tela 3, 2779 (1961) [English transl. : Soviet Physics - Solid State 3, 2029 (1962)].

24. S.M. PURI and T.H. GEBALLE,
in "Semiconductors and Semimetals", edited by R.K. WILLARDSON and A.C. BEER (Academic Press, New York and London, 1966), Vol. 1, p. 203.

25. J.P. JAY-GERIN and R. MAYNARD,
J. Low Temp. Phys. 3, 377 (1970).

26. D.L. RODE,
Phys. Rev. B 2, 1012 (1970).

27. M.G. HOLLAND,
Phys. Rev. 134, A471 (1964).

28. H.B.G. CASIMIR
Physica, 5, 495 (1938).

29. T.H. GEBALLE,
Phys. Rev., 92, 857 (1953).

30. W. ZAWADZKI,
Advanc. Phys., 23, 435 (1974).

31. P.R. WALLACE,
J. Phys. C : Solid State Phys., 7, 1136 (1974).

32. D.R. CASSIDAY and H.N. SPECTOR,
J. Phys. Chem. Solids, 35, 957 (1974).

33. P.R. WALLACE and O.P. GUPTA,
Phys. Status Solidi (b), 50 , 612 (1972).

FIGURE CAPTIONS

Figure (1) : "Phonon-drag" TEP (curves A and B), $|S_p|$, as a function of magnetic field H for n-type Ga As with N = 1.2×10^{16} cm^{-3} electrons at T = 4.2 K. Curve A is calculated, assuming[27] : $1/\tau_p = \tau_B^{-1} + \tau_{pt}^{-1} + \tau_{3ph}^{-1}$, where $\tau_B^{-1} = 0.60 \times 10^6$ sec^{-1} is the boundary inverse relaxation time, $\tau_{pt}^{-1} = A\omega^4$ with A = 0.48×10^{-44} sec^3 is the inverse relaxation time for the scattering due to isotopes, point defects, etc., and $\tau_{3ph}^{-1} = B\omega^2T^3$ with B = 5×10^{-22} sec/deg^3 is the three-phonon inverse relaxation time. Curve B is calculated, assuming $1/\tau_p = \tau_B^{-1} = 0.60 \times 10^6$ sec^{-1}. The "electron-diffusion" TEP, $|S_e|$, as a function of H for n-type Ga As with N = 1.2×10^{16} cm^{-3} electrons at T = 4.2 K is shown for reference[14]. The two arrows indicate the field ($\approx$ 56.4 kG) at which the bottom of the n = 0 Landau band coincides with the Fermi level.

Figure (2) : Plot of $|S_p|$ against magnetic field for n-type Ga As with N = 1.2×10^{16} cm^{-3} electrons at T = 4.2 K, and for different values of the phonon relaxation time $1/\tau_p = \tau_B^{-1} = 0.10 \times 10^6$, 0.60×10^6, 1.20×10^6, 12×10^6, and 120×10^6 sec^{-1}. The arrows indicate the field ($\approx$ 56.4 kG) at which the bottom of the n = 0 Landau band coincides with the Fermi level.

Figure (3) : "Phonon-drag" TEP, $|S_p|$, as a function of magnetic field H at T = 2, 3, 4.2, and 5 K. The curves are calculated, assuming $1/\tau_p = \tau_B^{-1} + \tau_{pt}^{-1} + \tau_{3ph}^{-1}$, with τ_B^{-1}, τ_{pt}^{-1}, and τ_{3ph}^{-1} as in Fig.(1). The arrows indicate the fields at which the bottom of the n = 0 Landau band coincides with the Fermi level.

Figure (4) : Plot of $|S_p|$ against temperature for n-type Ga As with N = 1.2×10^{16} cm^{-3} electrons, and for H = 17.5, 30, and 80 kG. The solid curves are for $1/\tau_p = \tau_B^{-1} + \tau_{pt}^{-1} + \tau_{3ph}^{-1}$, with τ_B^{-1}, τ_{pt}^{-1}, and τ_{3ph}^{-1} as in Fig.(1), while the broken curves are for $1/\tau_p = \tau_B^{-1}$.

Figure (5) : "Electron-diffusion" TEP, $|S_e|$, as a function of magnetic field H for n-type Ga As with N = 1.2×10^{16} cm^{-3} electrons at the temperatures 0.5, 2, 3, and 5 K. The curves are calculated from the results of Ref.(14), not taking account of spin splitting (g-factor = 0).

Figure (6) : Plot of the "critical field", H_{cr}, against temperature for n-type Ga As with $N = 1.2 \times 10^{16}$ cm^{-3} electrons. The curve is calculated under the assumption that the electron concentration does not change with temperature[8].

Figure (7) : Plot of $\xi = (\zeta - \frac{1}{2}\hbar\omega_c)/k_BT$ against magnetic field in the extreme quantum limit for n-type Ga As with $N = 1.2 \times 10^{16}$ cm^{-3} electrons at $T = 4.2$ K.

Figure (8) : The efficiency of the "drag", I_p, as a function of $x = \hbar\omega_{\vec{q}}/k_BT$ for different values of the magnetic field strength, and at a temperature of 4.2 K. The curves are calculated, assuming $1/\tau_p = \tau_B^{-1} + \tau_{pt}^{-1} + \tau_{3ph}^{-1}$, with τ_B^{-1}, τ_{pt}^{-1}, and τ_{3ph}^{-1} as in the caption of Fig.(1).

Figure (9) : Plot of the Fermi factor $\left[f^\circ(\varepsilon) - f^\circ(\varepsilon+\hbar\omega_{\vec{q}})\right]$, as given by Eq.(45), against $x = \hbar\omega_{\vec{q}}/k_BT$, for different values of the quantity (u/k_BT). The calculation is performed assuming that (u/k_BT) is a constant as a function of x, and can further be identified with ξ [Eq.(40)]. In this respect, we have indicated, for $T = 4.2$ K, the values of the magnetic field which correspond to the values chosen for the quantity (u/k_BT).

Figure (10) : Plot of the Fermi level, $\zeta = k_BT_F$, as a function of magnetic field H in the extreme quantum limit for n-Ga As with $N = 1.2 \times 10^{16}$ cm^{-3} electrons, and at $T = 4.2$ K. The arrow indicates the field ($\approx$ 56.4 kG) at which the bottom of the $n = 0$ Landau level coincides with the Fermi energy.

Figure (11) : The inverse electronic phonon lifetime $\Gamma(x = \hbar\omega_{\vec{q}}/k_BT, H)$ according to Eq.(47), as a function of x, for different values of the magnetic field strength, and at $T = 4.2$ K. $1/\tau_p = \tau_B^{-1} + \tau_{pt}^{-1} + \tau_{3ph}^{-1}$, with τ_B^{-1}, τ_{pt}^{-1}, and τ_{3ph}^{-1} as in the caption of Fig.(1), is also shown at $T = 4.2$ K for reference (broken curve).

Figure (12) : Plot of $\xi = (\zeta - \frac{1}{2}\hbar\omega_c)/k_BT$ against temperature in the extreme quantum limit for n-type Ga As with $N = 1.2 \times 10^{16}$ cm^{-3} electrons, and for two different values of the magnetic field, H = 17.5 kG and H = 80 kG. The effect of spin splitting is ignored in the calculation.

Figure (13) : The inverse electronic phonon lifetime $\Gamma(x = \hbar\omega_{\vec{q}}/k_B T, T)$ according to Eq.(47), as a function of x, for different values of the temperature, and for two different values of the magnetic field, H = 17.5 kG (degenerate regime) and H = 80 kG (non-degenerate regime).

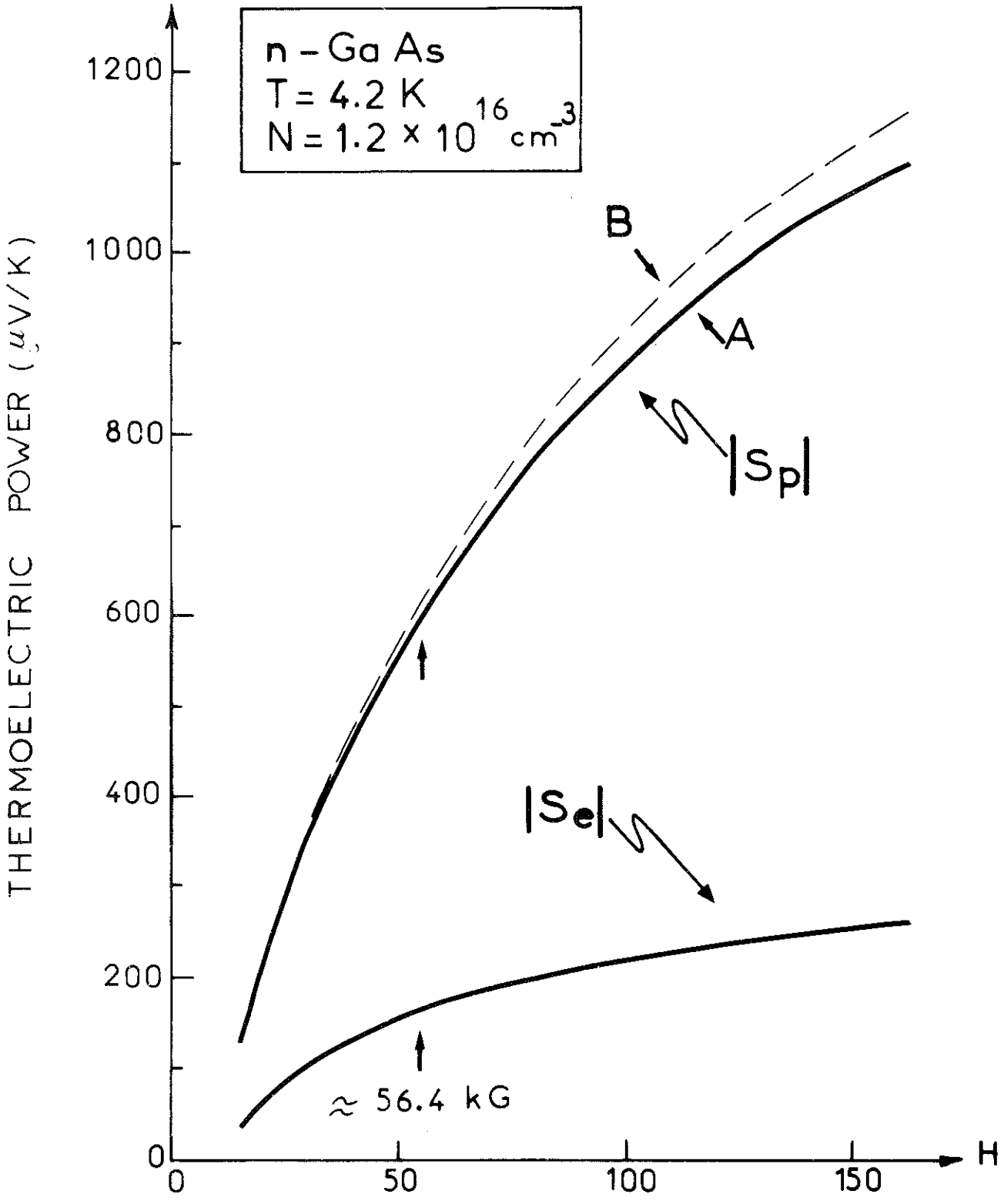
n - Ga As
T = 4.2 K
N = 1.2 × 10^16 cm^-3
B
A
|Sp|
|Se|
≈ 56.4 kG
THERMOELECTRIC POWER (μV/K)
MAGNETIC FIELD (kG)
H
0
200
400
600
800
1000
1200
0
50
100
150

Fig.1

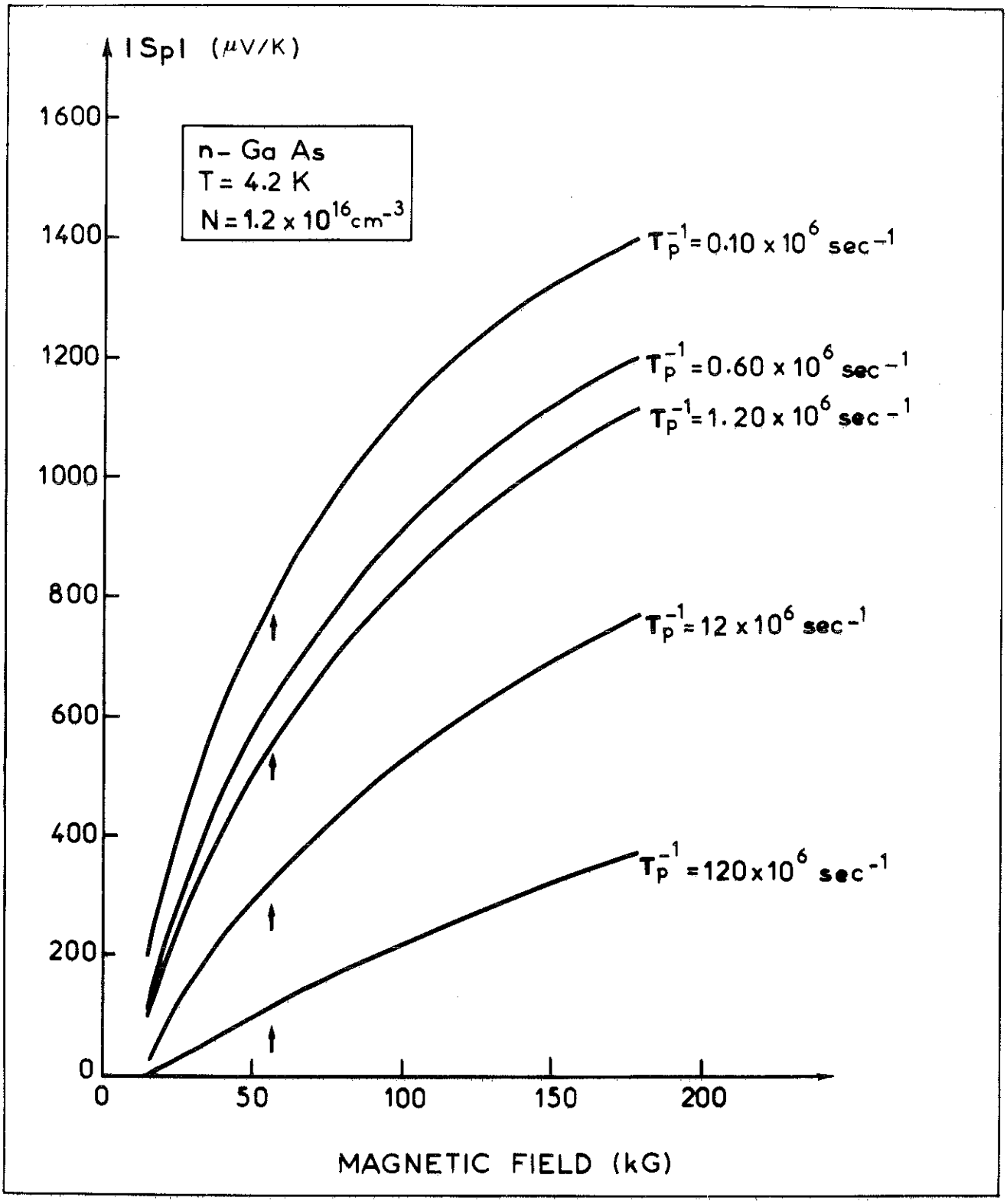
|Sp| (μV/K)
1600
1400
1200
1000
800
600
400
200
0
n- Ga As
T = 4.2 K
N = 1.2 x 10^16 cm^-3
T_p^-1 = 0.10 x 10^6 sec^-1
T_p^-1 = 0.60 x 10^6 sec^-1
T_p^-1 = 1.20 x 10^6 sec^-1
T_p^-1 = 12 x 10^6 sec^-1
T_p^-1 = 120 x 10^6 sec^-1
0
50
100
150
200
MAGNETIC FIELD (kG)

Fig. 2

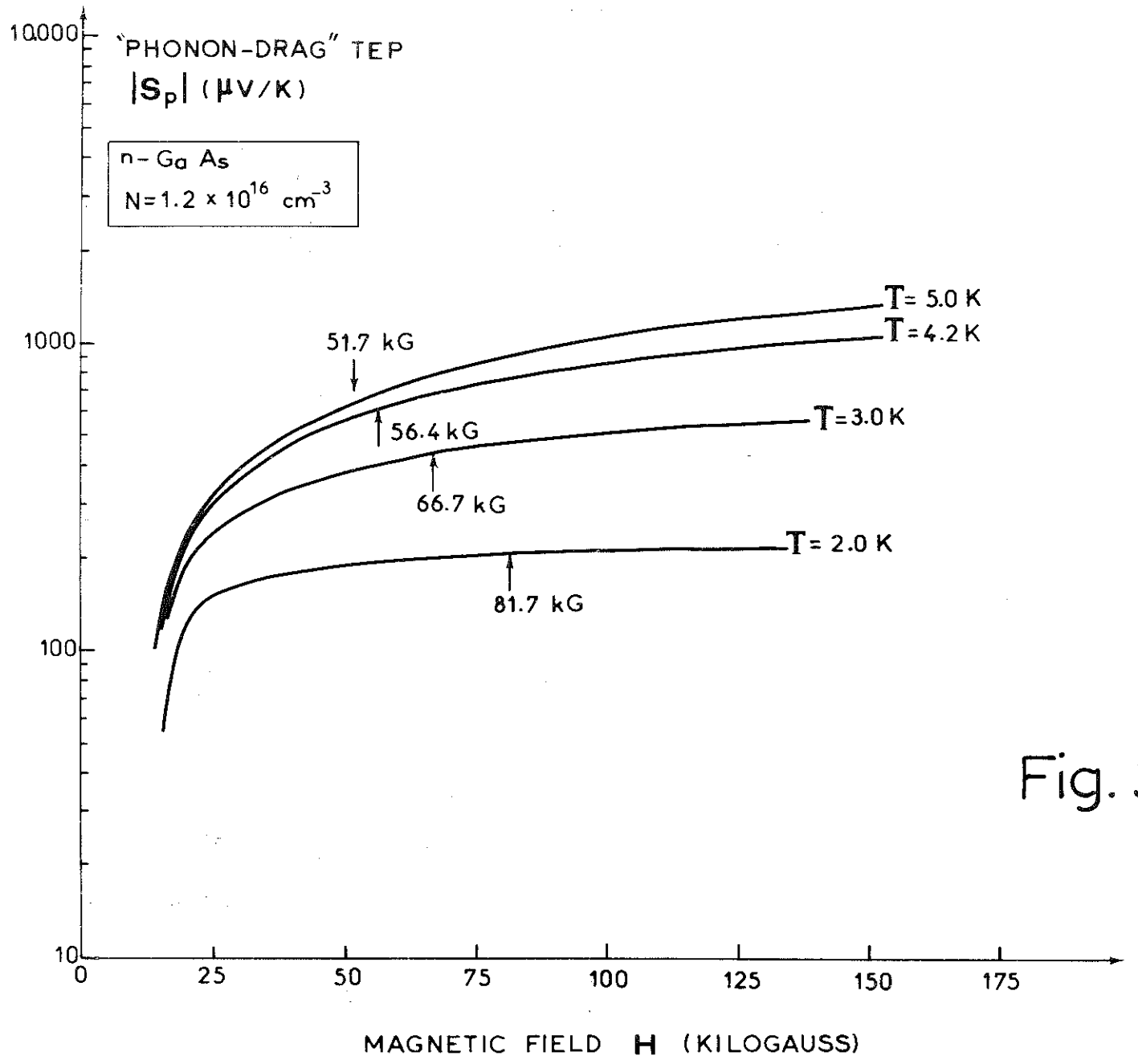
10.000
1000
100
10
"PHONON-DRAG" TEP
$|S_p|$ (μV/K)
n - Ga As
N = 1.2 x 10^{16} cm^{-3}
T = 5.0 K
T = 4.2 K
T = 3.0 K
T = 2.0 K
51.7 kG
56.4 kG
66.7 kG
81.7 kG
0
25
50
75
100
125
150
175
MAGNETIC FIELD H (KILOGAUSS)

Fig. 3

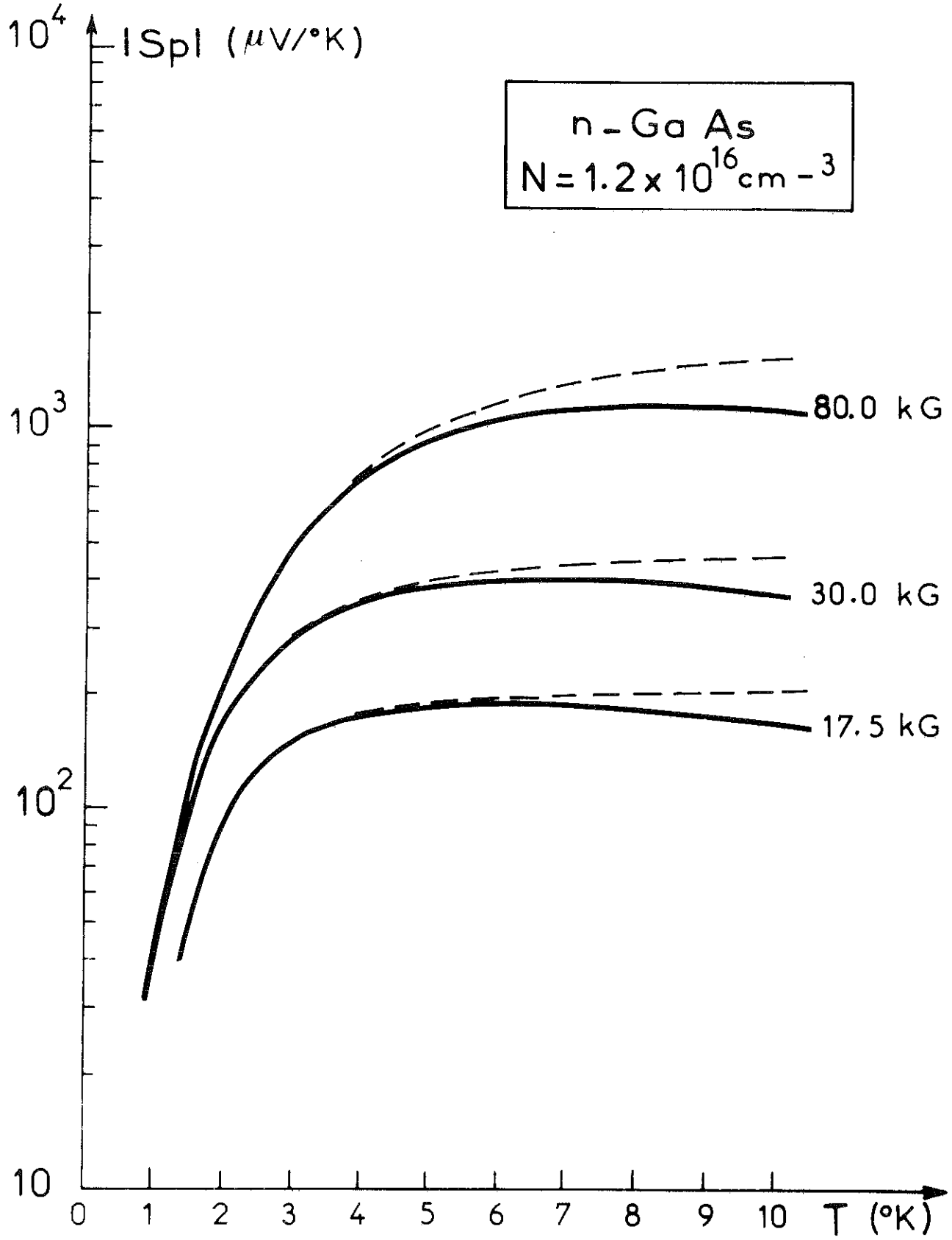
10^4
ISpI (μV/°K)
n - Ga As
N = 1.2 x 10^{16} cm $^{-3}$
10^3
80.0 kG
30.0 kG
17.5 kG
10^2
10
0
1
2
3
4
5
6
7
8
9
10
T (°K)

Fig. 4

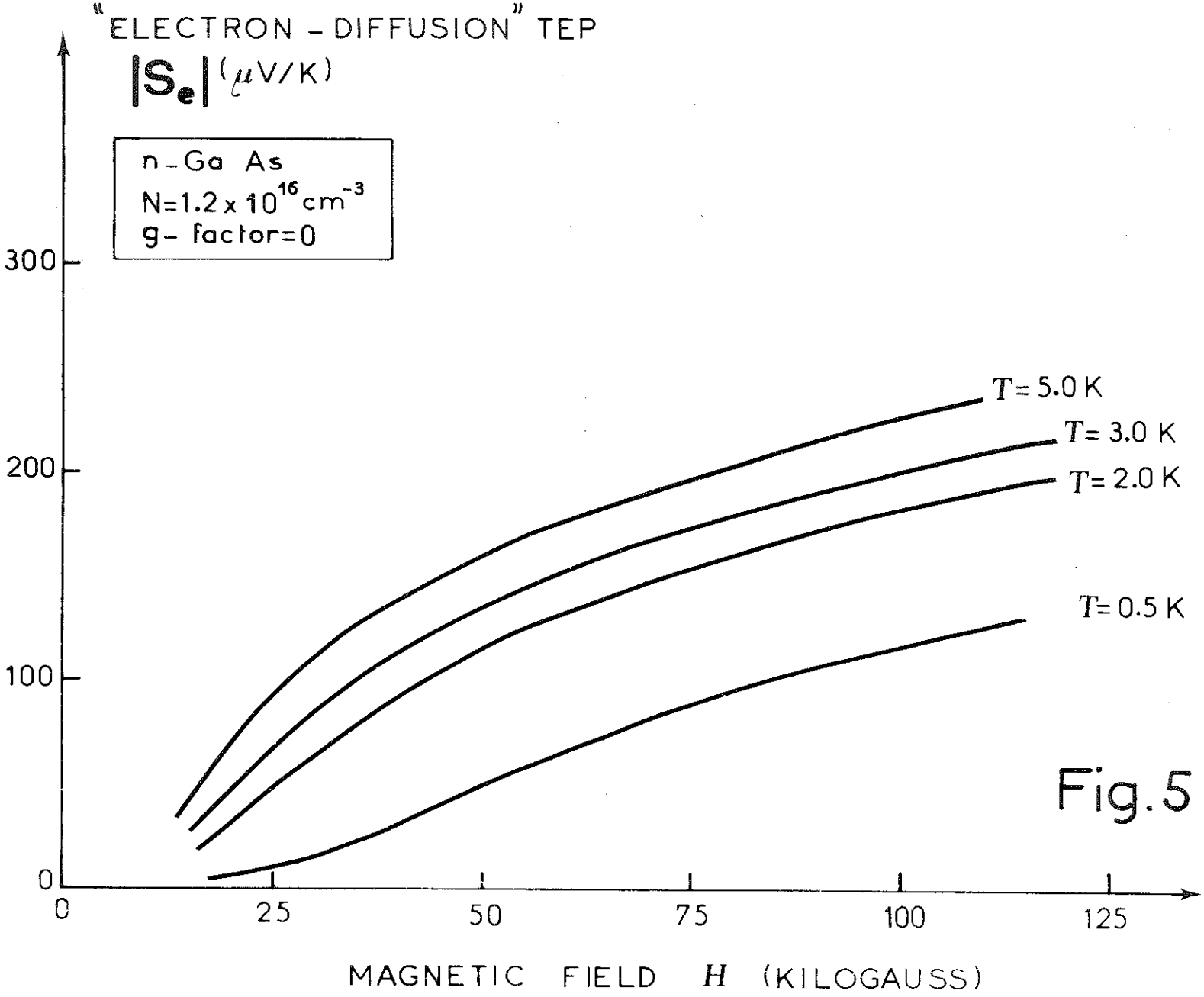
"ELECTRON - DIFFUSION" TEP
$|S_e|$ (μV/K)
n - Ga As
N=1.2 x 10^{16} cm^{-3}
g - factor=0
300
200
100
0
T= 5.0 K
T= 3.0 K
T= 2.0 K
T= 0.5 K
0
25
50
75
100
125
MAGNETIC FIELD H (KILOGAUSS)

Fig. 5

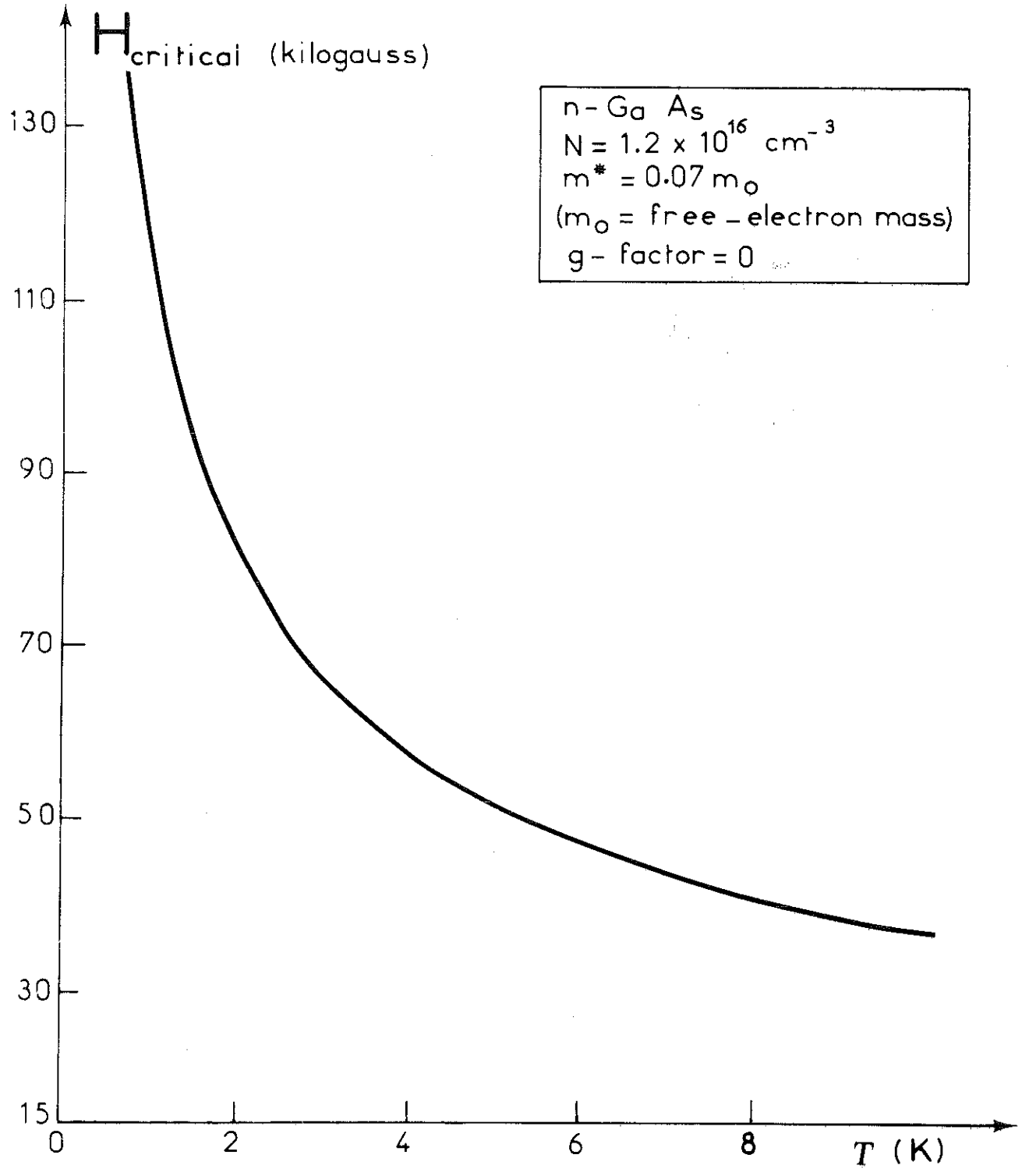
H critical (kilogauss)
n - Ga As
N = 1.2 x 10^16 cm^-3
m* = 0.07 m_o
(m_o = free - electron mass)
g - factor = 0
130
110
90
70
50
30
15
0
2
4
6
8
T (K)

Fig. 6

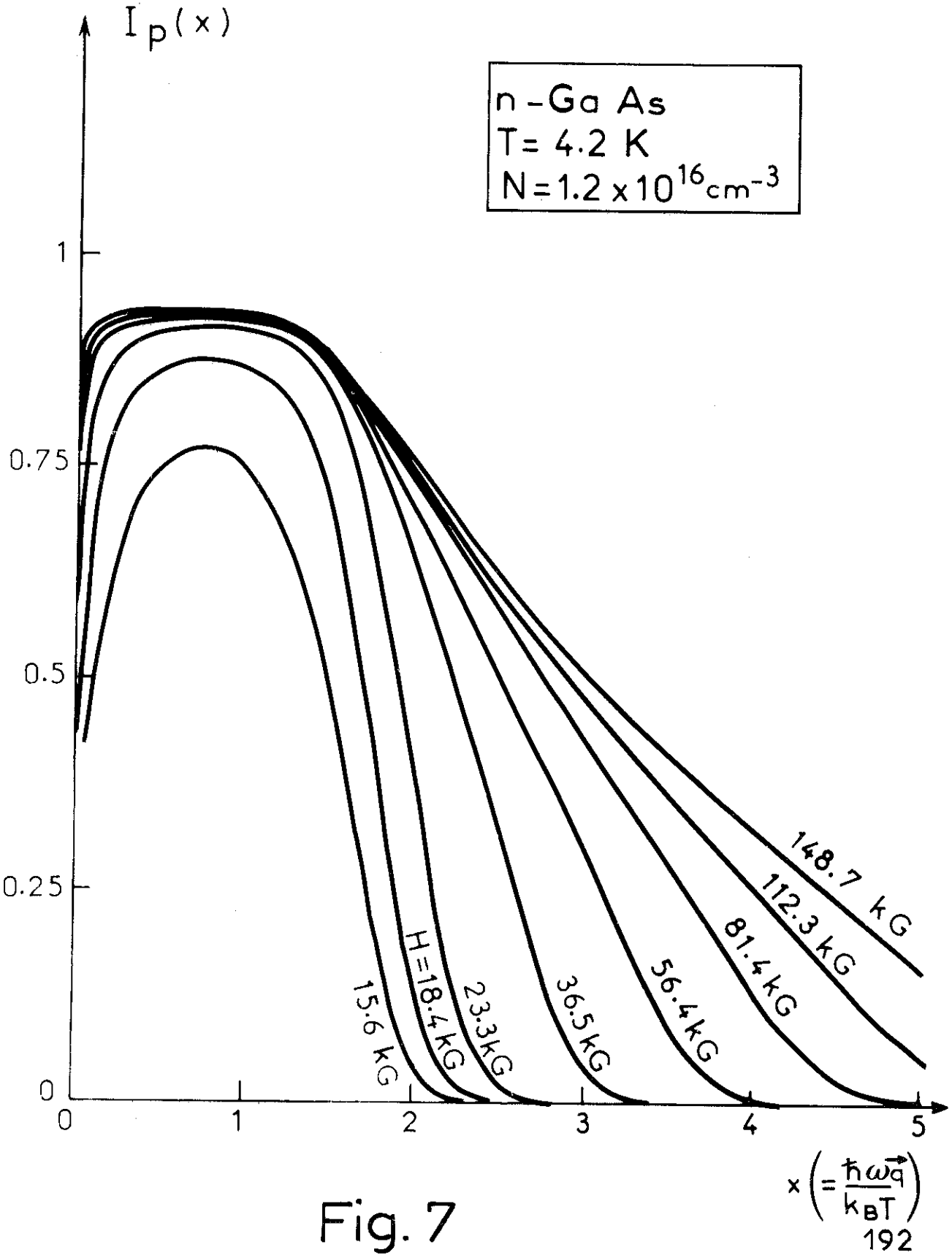
$I_p(x)$
n-Ga As
T= 4.2 K
N=1.2 x 10^{16} cm^{-3}
1
0.75
0.5
0.25
0
0
1
2
3
4
5
148.7 kG
112.3 kG
81.4 kG
56.4 kG
36.5 kG
H=18.4 kG
23.3kG
15.6 kG
$x\left(=\frac{\hbar\omega\vec{q}}{k_BT}\right)$

Fig. 7

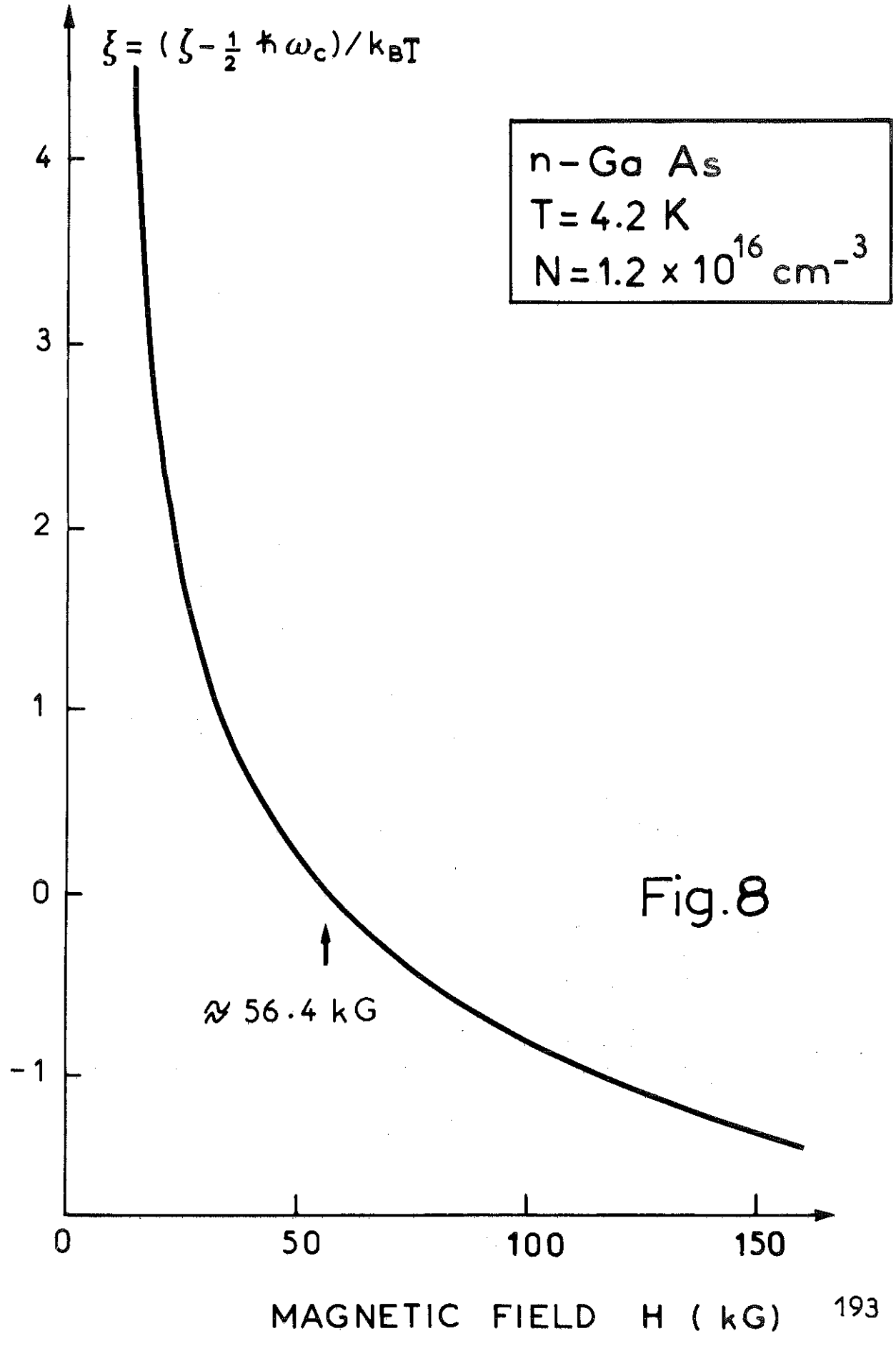
$\xi = (\zeta - \frac{1}{2}\hbar\omega_c)/k_BT$
n-Ga As
T = 4.2 K
N = 1.2 x 10^{16} cm^{-3}
4
3
2
1
0
-1
≈ 56.4 kG
0
50
100
150
MAGNETIC FIELD H (kG)

Fig.8

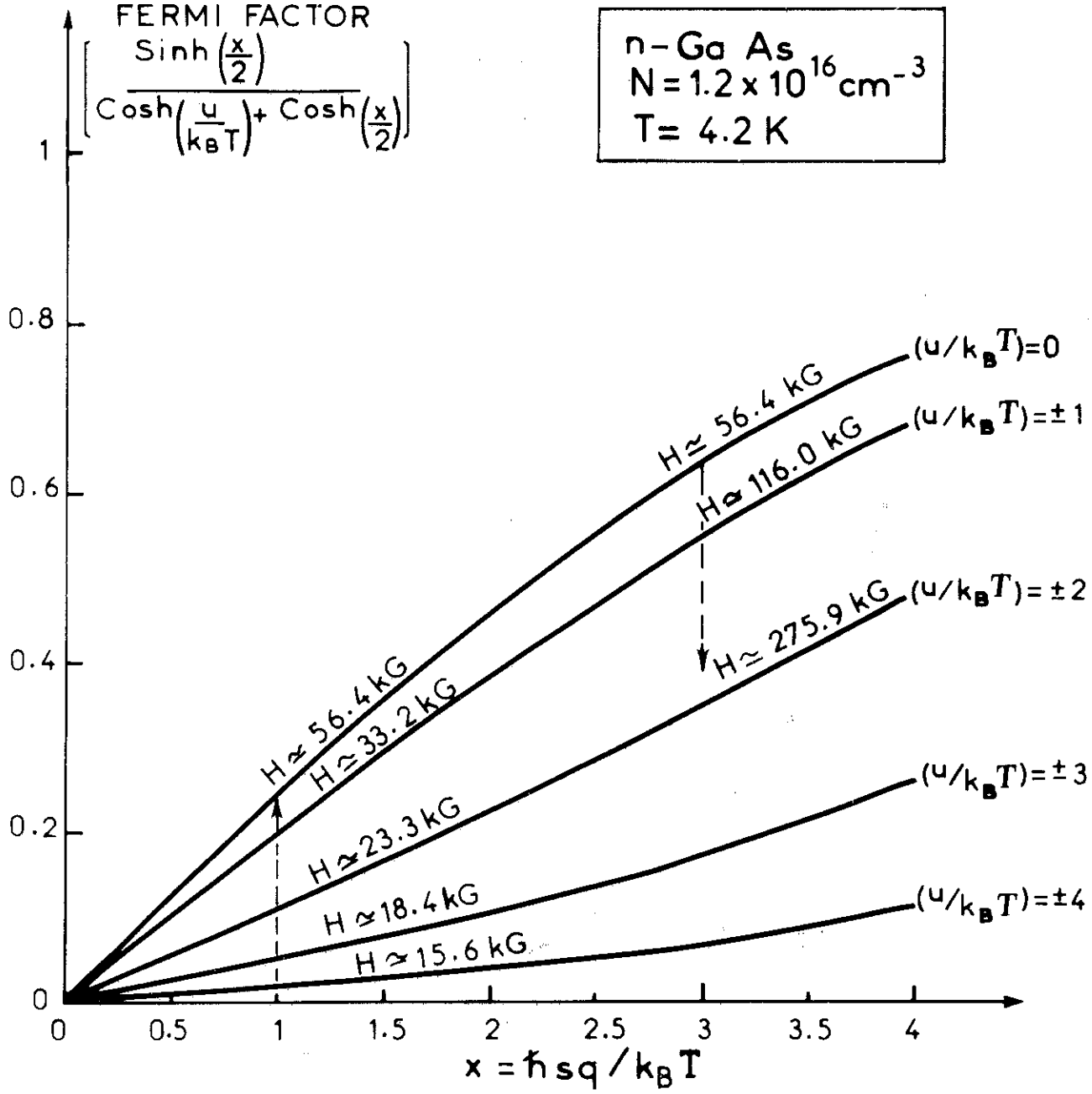
FERMI FACTOR
$\left[\frac{\sinh\left(\frac{x}{2}\right)}{\cosh\left(\frac{u}{k_BT}\right)+\cosh\left(\frac{x}{2}\right)}\right]$
n-Ga As
N = 1.2 x 10^16 cm^-3
T = 4.2 K
1
0.8
0.6
0.4
0.2
0
0
0.5
1
1.5
2
2.5
3
3.5
4
x = ħ sq / k_B T
(u/k_BT)=0
(u/k_BT)=±1
(u/k_BT)=±2
(u/k_BT)=±3
(u/k_BT)=±4
H≃ 56.4 kG
H≃ 116.0 kG
H≃ 275.9 kG
H≃56.4kG
H≃33.2kG
H≃23.3kG
H≃18.4kG
H≃15.6kG

Fig. 9

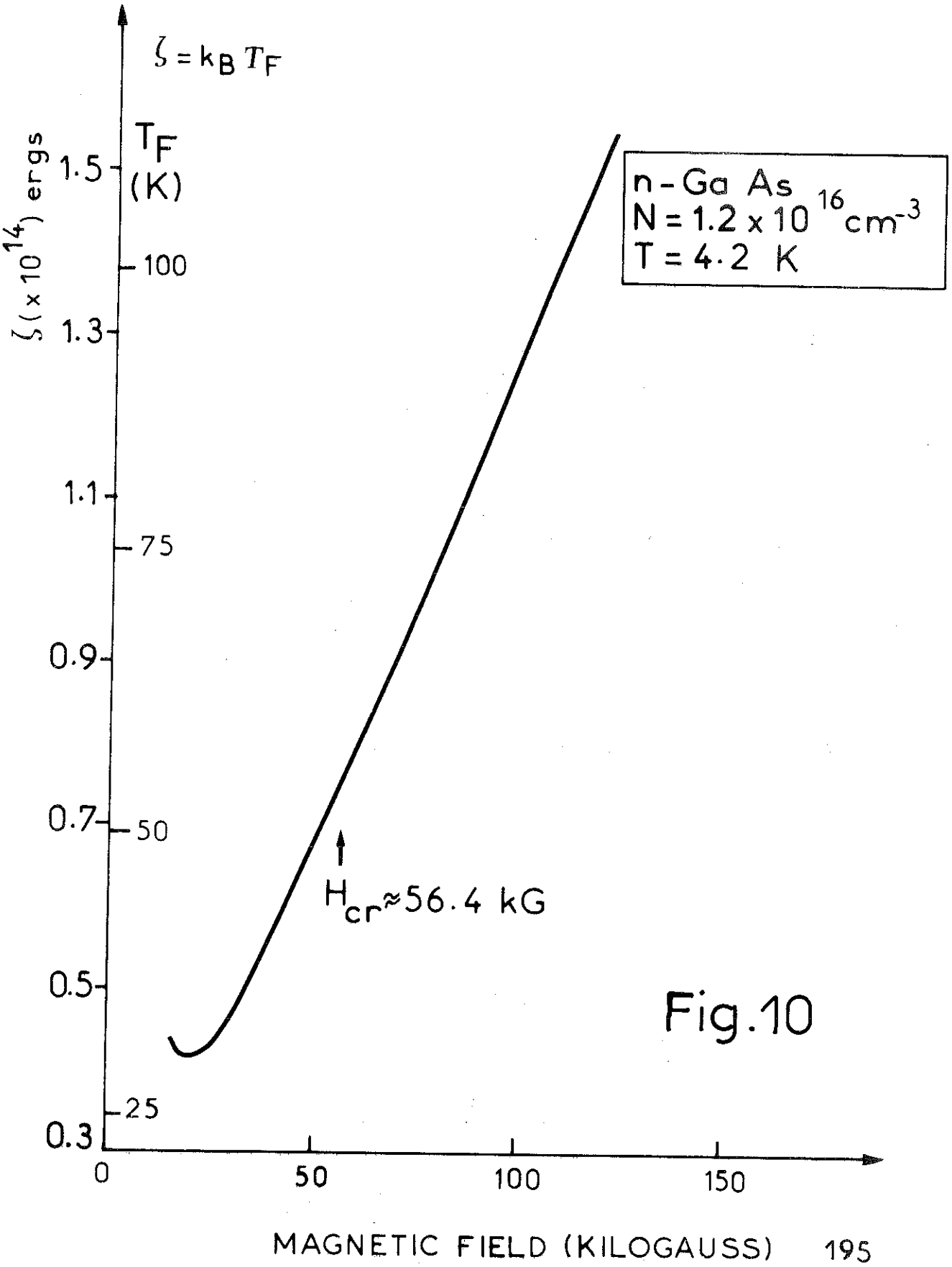
$\zeta = k_B T_F$
T_F (K)
ζ ($\times 10^{14}$) ergs
1.5
100
1.3
1.1
75
0.9
0.7
50
0.5
25
0.3
n-Ga As
N = 1.2 x 10 ^{16} cm^{-3}
T = 4·2 K
$H_{cr} \approx 56.4$ kG
0
50
100
150
MAGNETIC FIELD (KILOGAUSS)

Fig.10

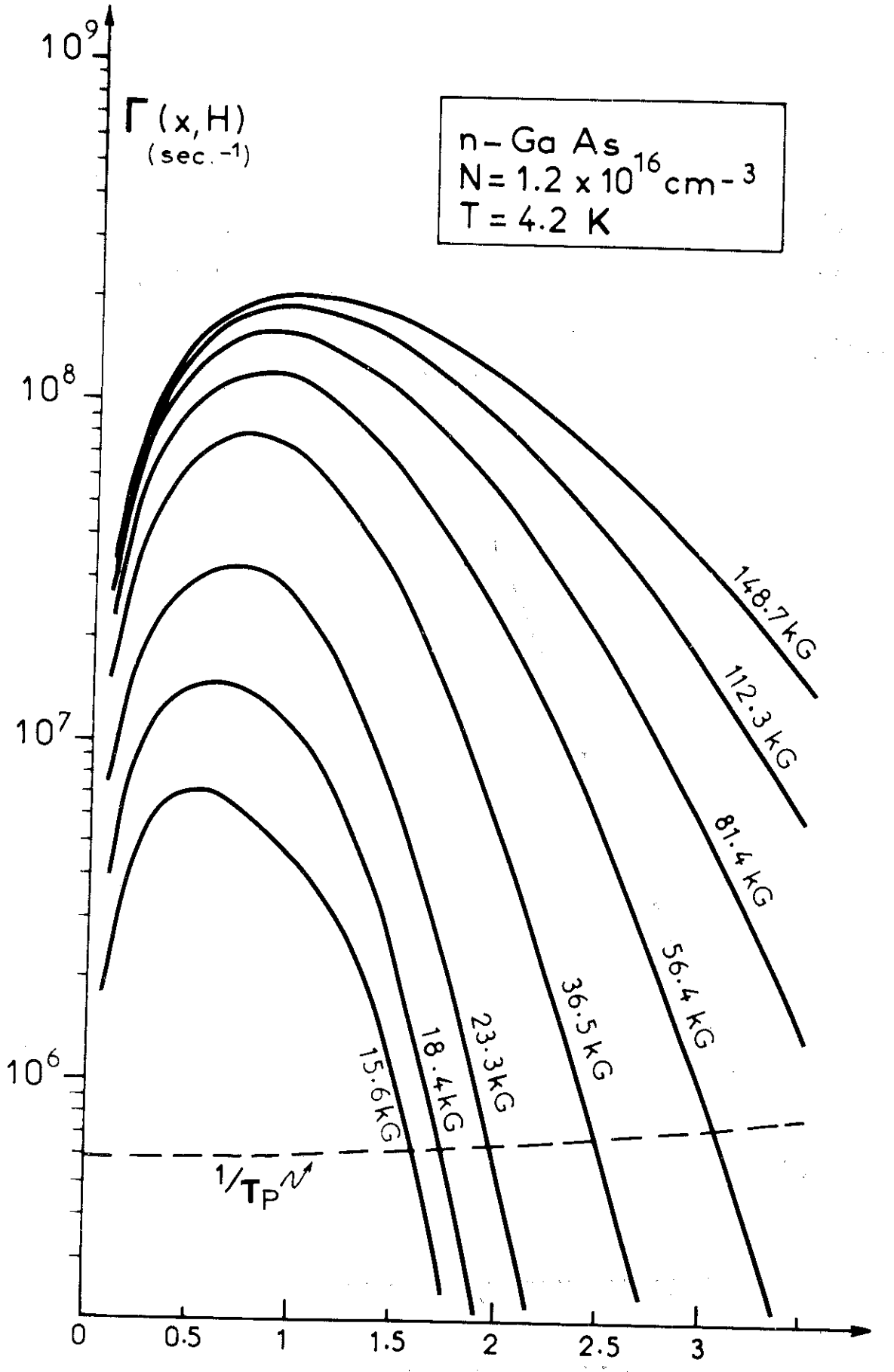
10^9
$\Gamma(x,H)$
(sec.$^{-1}$)
n – Ga As
N = 1.2 x 10^{16} cm^{-3}
T = 4.2 K
10^8
10^7
10^6
148.7 kG
112.3 kG
81.4 kG
56.4 kG
36.5 kG
23.3 kG
18.4 kG
15.6 kG
$1/\tau_P$
0
0.5
1
1.5
2
2.5
3
$x = \hbar sq / k_B T$

Fig. 11

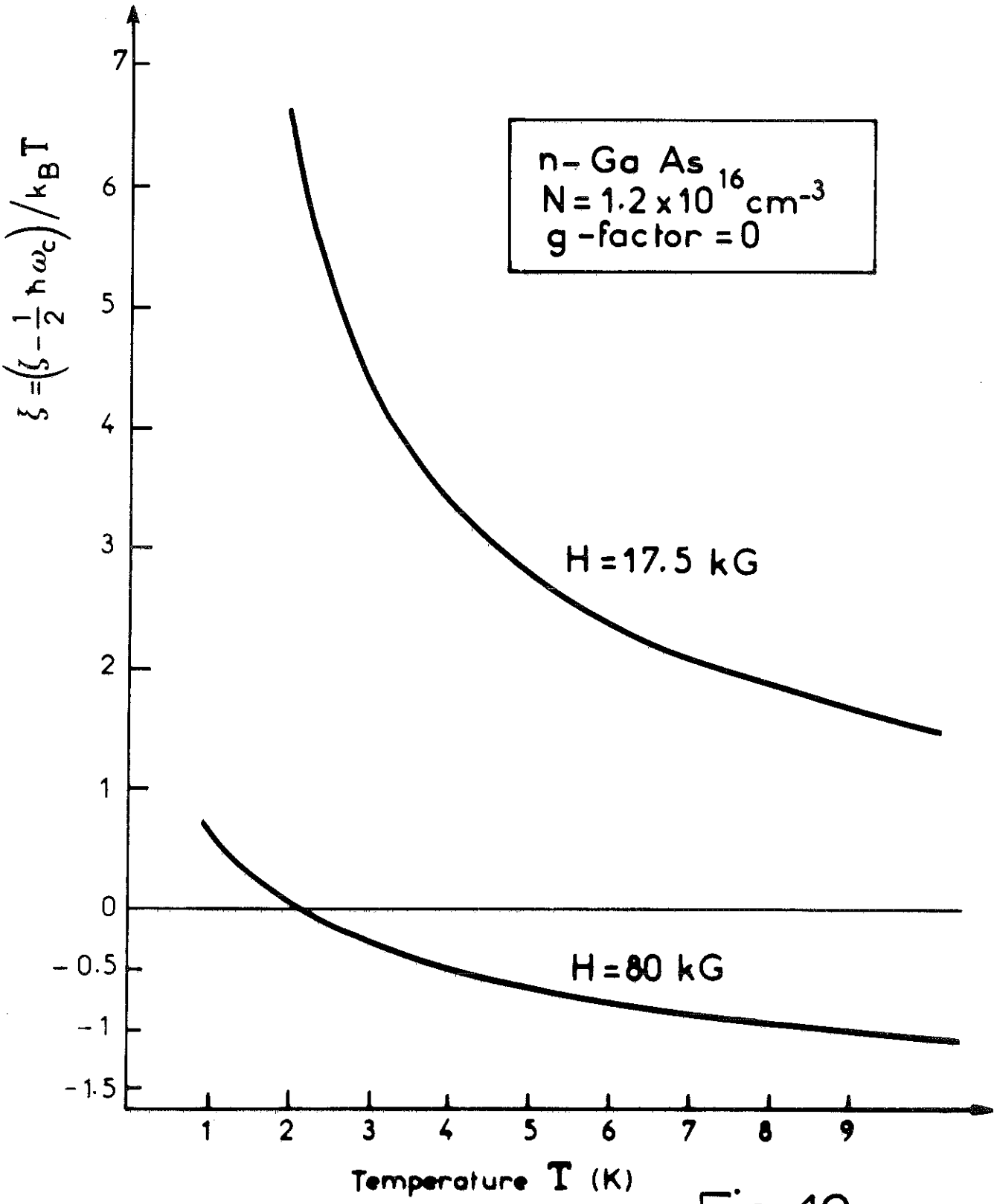
n- Ga As
N = 1.2 x 10^16 cm^-3
g -factor = 0
H = 17.5 kG
H = 80 kG
ζ = (ζ - 1/2 ħω_c) / k_B T
Temperature T (K)
7
6
5
4
3
2
1
0
- 0.5
- 1
- 1.5
1
2
3
4
5
6
7
8
9

Fig. 12

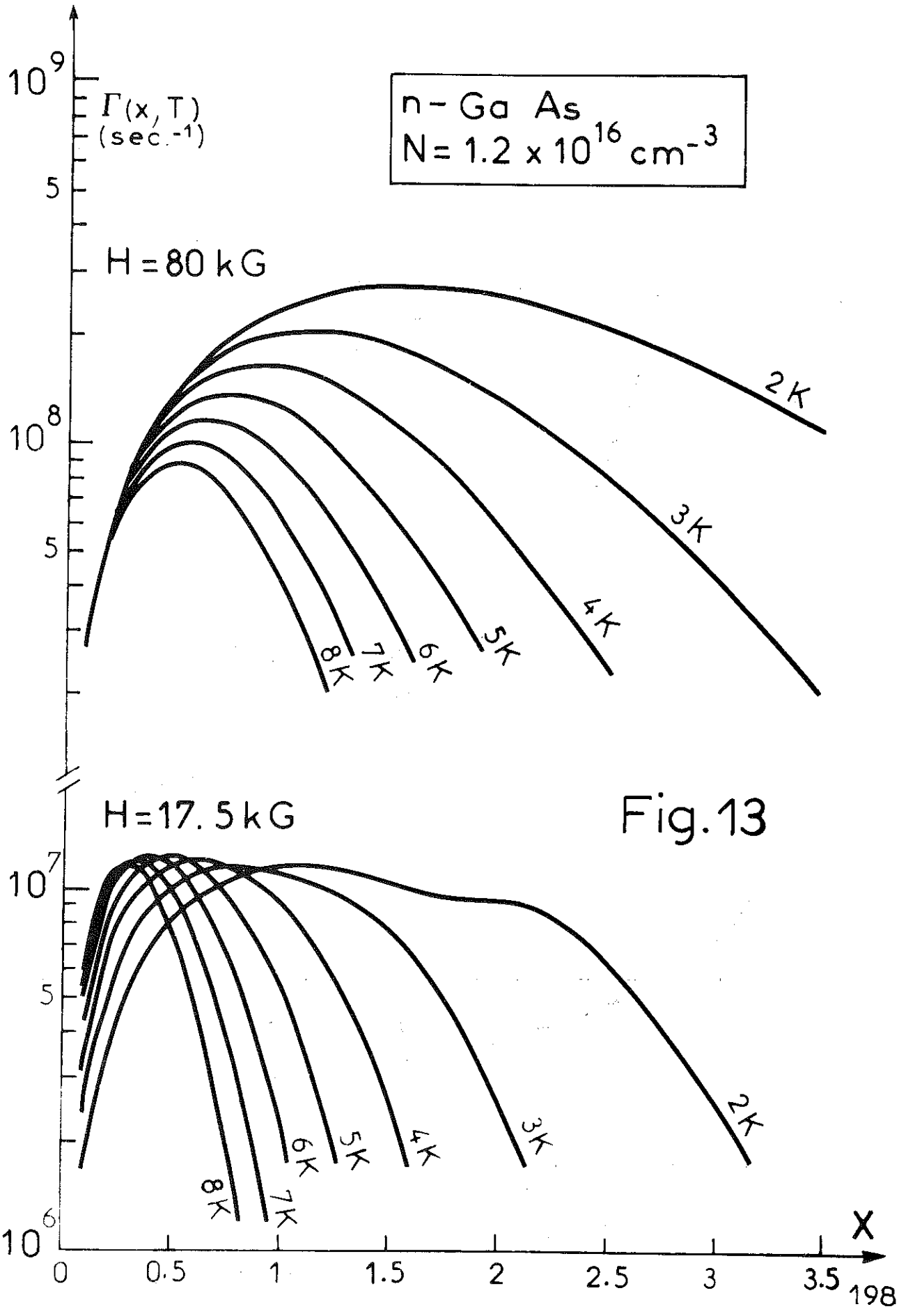
n - Ga As
N = 1.2 x 10^16 cm^-3
Γ(x, T)
(sec.^-1)
H = 80 kG
H = 17.5 kG
2K
3K
4K
5K
6K
7K
8K
10^9
5
10^8
5
10^7
5
10^6
0
0.5
1
1.5
2
2.5
3
3.5
X

Fig.13

ANOMALOUS BEHAVIOR OF THE LOW-TEMPERATURE NERNST-ETTINGSHAUSEN COEFFICIENT OF SEMICONDUCTORS IN STRONG MAGNETIC FIELDS

J.P. Jay-Gerin

(Centre de Recherches sur les Très Basses Températures, C.N.R.S., B.P. 166, Centre de Tri 38042, Grenoble-Cédex, France).

Physics Letters 41A, 7 (28 August 1972).

ABSTRACT

We show that the transition to nondegeneracy induced in a semiconductor at very low temperatures by a sufficiently strong magnetic field should give rise to an anomalous behavior of the Nernst-Ettingshausen coefficient.

It has been shown by Askenazy et al. (1) that a sample of n - type Gallium Arsenide with $N = 3.8 \times 10^{16}$ cm^{-3} electrons at the temperature T = 2 K shows a giant peak in both longitudinal ($\rho_{//}$) and transverse ($\rho_{\perp}$) magnetoresistivity starting at $\approx$ 50 kG, reaching a maximum at $\approx$ 100 kG, and decreasing again to a relatively small and slowly varying value by about 150 kG. This behavior characterizes the transition from degenerate to non-degenerate statistics which takes place when the bottom of the lowest Landau level is driven through the Fermi level.

Recently, the present author (2) has developed a calculation of the thermoelectric power (TEP) of an isotropic semiconductor (GaAs) in the extreme quantum limit when all the carriers are localized in the ground oscillator state with the quantum number n = 0. GaAs was chosen because of its very small spectroscopic g - factor ($g \approx 0.32$), so that Zeeman splitting could be ignored. As a function of magnetic field, the TEP was found to vary monotonically, and no particular effect was expected to occur at the transition to nondegeneracy. Following the lines of this previous work, it is easy to extend the calculation to obtain the Nernst-Ettingshausen (NE) coefficient. The aim of this letter is to show that, unlike the TEP, the NE coefficient should be capable of giving clear evidence of the change in the electron distribution manifested in (1).

Let us consider a semiconductor (GaAs) with a simple parabolic band of effective mass m^*. This adequately describes the situation at sufficiently small carrier concentrations. Let a strong magnetic field $\vec{H} = (0,0,H)$ be along the z axis. We

assume that we are in the extreme quantum limit with all the electrons localized in the lowest Landau level $\underline{n} = 0$, and that $\omega_c\tau >> 1$, where $\omega_c = |e|H/m^*c$ is the cyclotron frequency and τ is the electron relaxation time. We discuss the transport phenomena in the presence of a vanishingly small electric field $\vec{E} = (E,0,0)$ in the direction of the $\underline{x}$ axis, assuming the temperature gradient to be always zero (π-approach method to thermoelectric and thermomagnetic problems (3)). The procedure is to calculate the heat current density $\vec{U}$ due to the presence of $\vec{E}$ under isothermal conditions. The Peltier coefficient π is then given by the equation $\vec{U} = \pi.\vec{J}$, where $\vec{J}$ is the electric current density defined by $\vec{J} = \sigma.\vec{E}$ ($\sigma = \rho^{-1}$). Now, because of the strong electron-phonon interaction, $\vec{U}$ must be considered as a sum of two contributions : $\vec{U}_e$, the usual electronic diffusion part and $\vec{U}_p$, "the phonon-drag" part. As is well known (4), however, $\vec{U}_p$ is greatly predominant over $\vec{U}_e$ at very low temperatures and in high magnetic fields. Accordingly, the thermomagnetic quantities we are concerned with in this letter, namely the TEP and the NE coefficient, can essentially be obtain from $\vec{U}_p$ alone. Consideration of the electronic motion in crossed electric ($\vec{E}$ // Ox) and magnetic ($\vec{H}$ // Oz) fields shows that electrons drift along the $\underline{y}$ direction with the Hall velocity ($-cE/H$). This electron flow drags phonons with itself, and thus induces the Peltier heat $(\vec{U}_p)_y$. Now, using the well-known phenomenological transport equations (5) with the Onsager relations of irreversible thermodynamics and with the above observations, the NE coefficient is written as ($\omega_c\tau >> 1$)

$$A_{NE}(H) \approx \frac{1}{H\,T} \cdot \frac{(U_p)_y}{E}\ \rho_{xx}(H) \qquad (1)$$

with the TEP (2,4)

$$S(H) \approx \frac{1}{T}\ \frac{(U_p)_y}{E}\ \rho_{xy}(H)\ , \qquad (2)$$

where $\rho_{xx}(H)$ and $\rho_{xy}(H)$ are the elements of the magnetoresistivity tensor, given by (6,7)

$$\rho_{xx}(H) = \rho_{\perp} = \frac{\sigma_{xx}}{\sigma_{xx}^2 + \sigma_{xy}^2} \approx \frac{\sigma_{xx}}{\sigma_{xy}^2}\ ,\ |\sigma_{xy}| >> |\sigma_{xx}| \qquad (3)$$

$$\rho_{xy}(H) \approx -\frac{1}{\sigma_{xy}} = -\frac{H}{Nec}\ ,\ \vec{H} = (0,0,H). \qquad (4)$$

Putting Eq.(2) into (1), and using Eqs.(3) and (4), we get

$$A_{NE}(H) \simeq -\frac{Nec}{H^2}\ S(H)\ \rho_{\perp}\ , \qquad (5)$$

where N is the total number of carriers per unit volume, e their charge (e<0 for electrons, e>0 for holes), c is the velocity of light, and $\rho_\perp$ is the transverse magnetoresistivity. Thus, according to Eq. (5), $A_{NE}(H)$ should show an anomalous behavior, similar to that of $\rho_\perp$, as a function of magnetic field at the transition to non-degeneracy when the bottom of the n = 0 Landau level is pushed through the Fermi level.

ACKNOWLEDGMENTS

The author wishes to thank Dr. A. Briggs for a critical reading of the manuscript.

REFERENCES

(1) S. Askenazy, J.P. Ulmet, and J. Léotin/ Solid State Commun., 7, 989 (1969).

(2) J.P. Jay-Gerin/ 13th Intern. Conf. on Low-Temperature Physics (University of Colorado, Boulder, U.S.A., 1972).

(3) C. Herring, T.H. Geballe, and J.E. Kunzler/ Phys. Rev., 111, 36 (1958).

(4) S.M. Puri/ Phys. Rev., 139, A995 (1965).

(5) J.M. Ziman/ "Principles of the Theory of Solids" (Cambridge University Press, Cambridge, 1965), p. 194.

(6) L.M. Roth and P.N. Argyres/ "Semiconductors and Semimetals", vol. 1 (Academic Press, New York and London, 1966), p. 159.

(7) L.E. Gurevich and G.M. Nedlin/ Fiz. Tverd. Tela, 3, 2779 (1961) (English transl.: Sov. Physics-Solid State, 3, 2029 (1962)).

APPENDICE A

CALCUL DE L'ENERGIE LIBRE DE HELMHOLTZ D'UN GAZ D'ELECTRONS "LIBRES" EN REGIME EXTREME QUANTIQUE

Soit un système de N électrons libres se déplaçant sans interactions notables dans une enceinte de volume $\mathcal{V}$ donné (on prendra $\mathcal{V} = 1$) et obéissant à la statistique de Fermi-Dirac. Dans le cadre de l'ensemble canonique généralisé, l'énergie libre de Helmholtz (ou, simplement, énergie libre) d'un tel système est donnée par (voir, par exemple, Peierls 1956, Ziman 1965 et Zeiger et Pratt 1973) :

$$F = N\zeta - k_B T \sum_{\alpha} \mathrm{Log}\left\{1 + e^{-(\varepsilon_\alpha - \zeta)/k_B T}\right\} , \qquad (A\text{-}1)$$

où la sommation porte sur tous les états quantiques à un électron α d'énergie ε_α, ζ est l'énergie de Fermi, T la température et k_B la constante de Boltzmann.

En termes de la densité d'états à un électron, $\mathcal{D}_\sigma(\varepsilon)$, correspondant à la direction de spin σ, on obtient :

$$F = N\zeta - k_B T \sum_{\sigma} \int \mathcal{D}_\sigma(\varepsilon)\, \mathrm{Log}\left\{1 + e^{-(\varepsilon-\zeta)/k_B T}\right\} d\varepsilon . \qquad (A\text{-}2)$$

En intégrant par parties, l'équation (A-2) peut être réécrite sous la forme :

$$F = N\zeta - \sum_{\sigma} \int \mathcal{Z}_\sigma(\varepsilon)\, f(\varepsilon)\, d\varepsilon , \qquad (A\text{-}3)$$

où

$$\mathcal{Z}_\sigma(\varepsilon) = \int_0^{\varepsilon} \mathcal{D}_\sigma(\varepsilon)\, d\varepsilon \qquad (A\text{-}4)$$

et

$$f(\varepsilon) = \frac{1}{e^{(\varepsilon-\zeta)/k_B T} + 1} \qquad (A\text{-}5)$$

est la fonction de distribution de Fermi-Dirac, qui exprime la probabilité d'occupation d'un état d'énergie donnée ε. Comme l'indique clairement l'expression (A-3), le calcul de F se réduit donc essentiellement à la détermination de la fonction $\mathcal{Z}_\sigma(\varepsilon)$. A très basses températures et en présence d'un champ magnétique suffisamment intense, tous les électrons se concentrent sur le niveau de Landau fondamental n = 0 (voir chapitre I). Pour une bande d'énergie parabolique (électrons "libres") de masse effective m^*, on a, en régime extrême quantique,

$$\varepsilon = \frac{1}{2}\hbar\omega_c + \frac{\hbar^2 k_z^2}{2m^*} - \frac{1}{2} g\,\mu_B\,\sigma\,H \qquad \vec{H} = (0,0,H)$$

$$= \frac{1}{2}\hbar\omega_c(1-\gamma\sigma) + \frac{\hbar^2 k_z^2}{2m^*}\,, \qquad \text{(A-6)}$$

où $\omega_c = \frac{|e|\,H}{m^* c}$ est la fréquence cyclotron, g le facteur de Landé des électrons, $\mu_B = \frac{e\hbar}{2m_o c}$ le magnéton de Bohr, $\gamma = g(m^*/2m_o)$, m_o la masse de l'électron libre et $\sigma = \pm 1$.

Les densités d'états des deux spins sont données par (voir chapitre I) :

$$\mathcal{D}_\sigma(\varepsilon) = \frac{1}{(2\pi)^2}\,\frac{1}{2}\hbar\omega_c\,\left(\frac{2m^*}{\hbar^2}\right)^{3/2}\left[\varepsilon - \frac{1}{2}\hbar\omega_c(1-\gamma\sigma)\right]^{-1/2}\,, \qquad \text{(A-7)}$$

de sorte que

$$\mathcal{Z}_\sigma(\varepsilon) = \int_0^\varepsilon \mathcal{D}_\sigma(\varepsilon)\,d\varepsilon$$

$$= \frac{1}{(2\pi)^2}\,\hbar\omega_c\,\left(\frac{2m^*}{\hbar^2}\right)^{3/2}\left[\varepsilon - \frac{1}{2}\hbar\omega_c(1-\gamma\sigma)\right]^{1/2}. \qquad \text{(A-8)}$$

L'expression (A-3), compte-tenu des équations (A-5), (A-6) et (A-8), peut maintenant s'écrire :

$$F(H) = N\zeta - \frac{1}{(2\pi)^2}\,\hbar\omega_c\left(\frac{2m^*}{\hbar^2}\right)^{3/2}(k_B T)^{3/2}\sum_\sigma \int_0^\infty \frac{x^{1/2}\,dx}{e^{(x-\xi_\sigma)}+1}\,, \qquad \text{(A-9)}$$

si on pose :

$$x = \frac{\left[\varepsilon - \frac{1}{2}\hbar\omega_c(1-\gamma\sigma)\right]}{k_B T} \qquad \text{(A-10)}$$

et

$$\xi_\sigma = \frac{\left[\zeta - \frac{1}{2}\hbar\omega_c(1-\gamma\sigma)\right]}{k_B T}\,. \qquad \text{(A-11)}$$

D'après la définition de l'intégrale de Fermi-Dirac d'ordre j (Stoner 1936, Mc Dougall et Stoner 1937 et Blakemore 1962)

$$\mathcal{F}_j(\xi) = \frac{1}{\Gamma(j+1)}\int_0^\infty \frac{x^j\,dx}{e^{(x-\xi)}+1}\,, \qquad \text{(A-12)}$$

où $\Gamma(x)$ symbolise la fonction gamma,
nous avons immédiatement :

$$\int_0^\infty \frac{x^{1/2}\,dx}{e^{(x-\xi_\sigma)}+1} = \Gamma(\tfrac{3}{2})\,\mathcal{F}_{1/2}(\xi_\sigma) = \frac{\sqrt{\pi}}{2}\,\mathcal{F}_{1/2}(\xi_\sigma)\ , \qquad \text{(A-13)}$$

et

$$F(H) = N\zeta - \frac{1}{8\pi^{3/2}}\,\hbar\omega_c\left(\frac{2m^*}{\hbar^2}\right)^{3/2}(k_BT)^{3/2}\,S_+\ , \qquad \text{(A-14)}$$

avec

$$S_+ = \sum_\sigma \mathcal{F}_{1/2}(\xi_\sigma)\,.$$

On peut donner une expression plus compacte de F(H), en explicitant la condition qui permet de définir l'énergie de Fermi ζ, à savoir :

$$N = \sum_\sigma \int \mathcal{D}_\sigma(\varepsilon)\,f(\varepsilon)\,d\varepsilon\ , \qquad \text{(A-15)}$$

soit, compte-tenu des équations (A-5), (A-6), (A-7), (A-10) et (A-11),

$$N = \frac{1}{(2\pi)^2}\,\frac{1}{2}\,\hbar\omega_c\left(\frac{2m^*}{\hbar^2}\right)^{3/2}(k_BT)^{1/2}\sum_\sigma\int_0^\infty \frac{x^{-1/2}\,dx}{e^{(x-\xi_\sigma)}+1}\ . \qquad \text{(A-16)}$$

Comme

$$\int_0^\infty \frac{x^{-1/2}\,dx}{e^{(x-\xi_\sigma)}+1} = \Gamma(\tfrac{1}{2})\,\mathcal{F}_{-1/2}(\xi_\sigma) = \sqrt{\pi}\,\mathcal{F}_{-1/2}(\xi_\sigma)\ , \qquad \text{(A-17)}$$

on obtient :

$$N = \frac{1}{8\pi^{3/2}}\,\hbar\omega_c\left(\frac{2m^*}{\hbar^2}\right)^{3/2}(k_BT)^{1/2}\,S_1\ , \qquad \text{(A-18)}$$

où $S_1 = \sum_\sigma \mathcal{F}_{-1/2}(\xi_\sigma)$. (A-19)

Finalement, en combinant les relations (A-14) et (A-18), on peut réécrire F(H) sous la forme :

$$F(H) = N\left(\zeta - k_BT\,\frac{S_+}{S_1}\right)\ . \qquad \text{(A-20)}$$

APPENDICE B

CHALEUR SPECIFIQUE ET RESISTIVITE DE L'ANTIMONIURE DE GALLIUM DE TYPE p ENTRE 0.3 ET 4 K : UNE ETUDE EXPERIMENTALE

phys. stat. sol. (b) 60, K83 (1973)

Subject classification: 8 and 14.3; 22.2.3

Centre de Recherches sur les Très Basses Températures, C.N.R.S., Grenoble[1])

The Specific Heat and Resistivity of p-Type Gallium Antimonide between 0.3 and 4 K

By

M. SAINT PAUL, J.P. JAY-GERIN, and A. BRIGGS

Recently Cetas et al. (1) have reported specific-heat measurements on gallium antimonide (GaSb) between 1 and 30 K. In order to explain the lowest-temperature data, a term linear in the temperature ($a_1 T$), which was supposed to reflect an electronic contribution to the specific heat, had to be included in the analysis of the results. A calculation using a free-electron model for the conduction carriers present at low temperatures shows that in this specimen a carrier concentration of about 5×10^{17} cm^{-3} at 4 K is required to account for the reported value of a_1. Such a carrier concentration is at least a thousand times greater than that expected for an undoped specimen of GaSb containing $\approx 10^{17}$ cm^{-3} carriers at room temperature.

In an attempt to determine whether the contribution to the specific heat linear in temperature is indeed electronic in origin, we have measured the specific heat of a specimen of GaSb between 0.3 and 4 K, the Hall coefffcient between 4 and 300 K, and the electrical resistivity between 0.3 and 300 K.

The specific heat was measured in a recirculating ^{3}He cryostat by a pulse technique, which has been described in detail elsewhere (2, 3). Temperatures were measured by a germanium thermometer calibrated using a cerium magnesium nitrate magnetic thermometer, which in turn was calibrated between 1 and 4 K against the T_{62} ^{3}He and T_{58} ^{4}He vapour pressure scales. The GaSb single crystal[2]) weighed 10.395 g, and at 300 K was p-type with a carrier concentration of 2×10^{17} cm^{-3}. The measured specific heat is shown in Fig. 1 where C/T is plotted against T^2. The specific heat of GaSb could be fitted, within the accuracy of the experiment, by an

1) B.P. 166, Centre de Tri, 38042 Grenoble-Cedex, France.

2) The GaSb crystal was kindly supplied by Miss A.M. Poujade of the Centre d'Etudes d'Electronique des Solides, Faculté des Sciences, Montpellier, France.

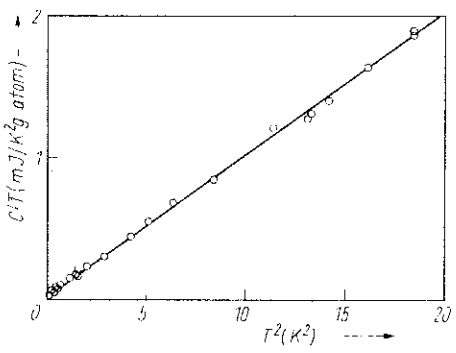

Fig. 1. The measured specific heat C divided by the temperature T as a function of T^2. The straight line has been obtained from the expression $C/T = a_1 + a_3 T^2$, with a_1 and a_3 determined by a least-squares analysis

equation of the form

$$\frac{C}{T} = a_1 + a_3 T^2 = a_1 + \frac{1.94436 \times 10^9}{\Theta_o^3} T^2 (\mu J/K^2 \text{ g-atom}) \quad ,$$

Values of a_1 and Θ_o (Debye temperature at 0 K) were obtained in the usual way by a least-squares fit of a straight line to the experimental data. The values of a_1 and Θ_o so determined were $(3 \pm 2)\mu J/K^2$ g-atom and (267 ± 3)K, respectively.

The electrical resistivity ϱ and the Hall coefficient R_H (= 1/Ne) of a GaSb specimen cut from one end of the specific-heat specimen were measured between 4 and 300 K, using a six-probe technique. The variations with temperature of the carrier concentration N and the resistivity ϱ of the specimen are shown in Fig. 2. The shape of the curves clearly indicates that in the low-temperature region there are two competing conduction processes: ordinary valence band conduction which disappears, and impurity conduction which dominates, as the temperature is reduced. Measurements by Amirkhanov and Amirkanova (4) down to 2 K, and more recently by Matveenko et al. (5) down to 0.1 K, showed no further noticeable change in the temperature dependence of both the electrical resistivity and the Hall coefficient below 4 K. Nevertheless, the resistivity measurements were extended to 0.3 K in order to verify that no anomalous effects occurred in our material. In the temperature range of interest for the specific-heat measurements, the specimen contained a net hole concentration of about 4×10^{15} cm^{-3} (see Fig. 2).

The value of Θ_o agrees well with the value of (270 ± 2)K obtained by (1), but the value we estimate for a_1 is considerably lower. However, in a recent paper (6),

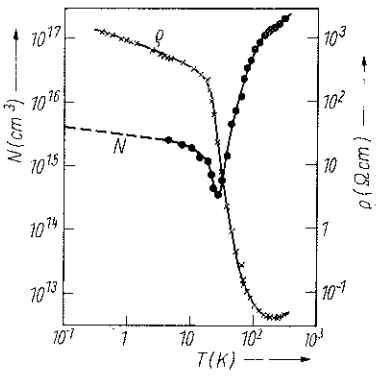

Fig. 2. The carrier concentration N(•) and the electrical resistivity ϱ(×) as a function of temperature T

Holste has carefully reanalyzed the heat-capacity data reported in (1), and published corrected values for the quantities a_1 and Θ_o, which have been calculated using a modified temperature scale for the region 1 to 30 K. The most dramatic effect of the use of this temperature scale was to reduce appreciably the previous value of a_1 (by approximately a factor of 3). The new value of a_1 ($(2.1 \pm 0.8)\mu J/K^2$ g-atom) is in good agreement with the present value which is referred principally to the T_{62} ^{3}He temperature scale. The recalculated value of Θ_o ((268.8 ± 0.5)K), however, is changed little from its previous value.

If only an electronic contribution to the specific heat exists, $a_1 = \gamma$ where γ is the coefficient of the electronic specific heat. The measured value of a_1 has been compared with the value of γ calculated for a degenerate Fermi gas of holes in a parabolic valence band (7), using the following expression:

$$\gamma = a \frac{m^*}{m_o} N^{1/3} \frac{A}{d} , \qquad (2)$$

where $a = (\pi^{2/3} k_B^2 m_o)/(3^{2/3} \hbar^2) = 1.622 \times 10^{-6} \mu J/K^2 cm^2$, k_B is Boltzmann's constant, m_o is the free-electron mass, m^* is the density-of-states effective mass of the carriers, N is the carrier concentration, and A (= 95.47 g) and d (= 5.62 g/cm^3) are the atomic weight and the density of the material, respectively. This assumes that (i) for a pure GaSb crystal the valence band is parabolic and (ii) the addition of impurities to the crystal does not appreciably affect this parabolicity. Furthermore, taking into account the precision of the experiment, and in particular the precision of the determination of the carrier concentration below 4 K, the contributions of the

split-off valence band and of the light-mass valence band have been neglected. It has also been assumed that the carrier concentration does not change significantly below 4 K (4, 5). Then, the value of the coefficient γ calculated, using equation (2), for the heavy-mass valence band with a density-of-states effective mass $m^* = 0.50\ m_o$ (8) is 2.2 $\mu J/K^2$ g-atom, which is in good agreement with the measured value (a_1). Thus, the present measurements indicate that the term linear in T observed in the specific heat of GaSb at low temperatures is electronic in origin.

References

(1) T.C. CETAS, R.C. TILFORD, and C.A. SWENSON, Phys. Rev. 174, 835 (1968).

(2) K.H. GOBRECHT, J.J. VEYSSIE, and L. WEIL, Ann. Acad. Sci. Fennicae 210, 63 (1966).

(3) K.H. GOBRECHT and M. SAINT PAUL, Proc. Third Internat. Cryogenics Conference, Berlin 1970 (p. 235).

(4) KH.I. AMIRKHANOV and D.KH. AMIRKHANOVA, Soviet Phys.-Semiconductors 2, 694 (1968).

(5) A.V. MATVEENKO, S.S. SHALYT, M.L. SHUBNIKOV, and V.S. VEKSHINA, Soviet Phys. - Semiconductors 5, 949 (1971).

(6) J.C. HOLSTE, Phys. Rev. B6, 2495 (1972).

(7) P.H. KEESOM and G.M. SEIDEL, Phys. Rev. 113, 33 (1959).

(8) B. PISTOULET, J.L. ROBERT, and M. MARQUES, phys. stat. sol. 24, 481 (1967).

(Received October 18, 1973)

APPENDICE C

CALCUL DES NIVEAUX D'ENERGIE D'UNE PARTICULE "LIBRE" EN PRESENCE D'UN CHAMP MAGNETIQUE ET D'UN CHAMP ELECTRIQUE CONSTANTS CROISES

L'Hamiltonien d'une particule de masse m^*, de charge e (e<0 ou >0, s'il s'agit d'un électron ou d'un trou), douée de spin $\frac{1}{2}$ et plongée dans un champ magnétique uniforme constant $\vec{H} = (0,0,H)$ et dans un champ électrique uniforme constant $\vec{E} = (E,0,0)$, s'écrit :

$$\mathcal{H}_o = \frac{1}{2m^*} \left(\vec{p} - \frac{e}{c}\vec{A}\right)^2 - e\vec{E}.\vec{r} - \vec{\mu}.\vec{H} , \qquad (C\text{-}1)$$

où $\vec{p} = (p_x, p_y, p_z)$ est l'impulsion de la particule, $\vec{A}$ le potentiel vecteur du champ magnétique au point $\vec{r} = (x,y,z)$ où se trouve la particule ($\vec{H} = \overrightarrow{rot}\ \vec{A}$), $\vec{\mu}$ le moment magnétique propre de la particule et c la vitesse de la lumière.

En général, $\vec{p}$ ne commute pas avec $\vec{A}$, qui est fonction des coordonnées. Cependant, la règle de commutation de l'opérateur d'impulsion et $\vec{A}$, à savoir

$$\vec{p}\,\vec{A} - \vec{A}\,\vec{p} = - i\hbar \operatorname{div} \vec{A} , \qquad (C\text{-}2)$$

nous enseigne que $\vec{p}$ et $\vec{A}$ peuvent avoir simultanément des valeurs déterminées si $\operatorname{div} \vec{A} = 0$. Il est commode ici de choisir le potentiel vecteur du champ uniforme $\vec{H}$ (dirigé parallèlement à l'axe des z) sous la forme

$$A_x = 0, \quad A_y = Hx, \quad A_z = 0 , \qquad (C\text{-}3)$$

qui satisfait automatiquement la condition $\operatorname{div} \vec{A} = 0$ (jauge de Landau).

L'Hamiltonien $\mathcal{H}_o$ devient alors :

$$\mathcal{H}_o = \frac{1}{2m^*}\left[p_x^2 + \left(p_y - \frac{eH}{c}x\right)^2 + p_z^2\right] - eEx - \mu_z H , \qquad (C\text{-}4)$$

où μ_z est la projection du moment magnétique propre de la particule suivant le champ, donnée par

$$\mu_z = \frac{1}{2} g \mu_B H \sigma , \qquad (C\text{-}5)$$

où g est le facteur de Landé, μ_B le magnéton de Bohr et $\sigma = \pm 1$ correspond aux deux valeurs possibles de la projection du spin sur l'axe des z.

Soit $\Psi(x,y,z;\sigma)$ la fonction d'onde de la particule au point $\vec{r}$ avec le spin σ. L'équation de Schrödinger

$$\mathcal{H}_o \, \Psi(x,y,z;\sigma) = E \, \Psi(x,y,z;\sigma)$$

pour les valeurs propres de $\mathcal{H}_o$ s'écrit

$$\frac{1}{2m^*}\left[p_x^2 + \left(p_y - \frac{eH}{c}x\right)^2 + p_z^2\right]\Psi - eEx\Psi - \frac{1}{2}g\mu_B H\sigma\Psi = E\Psi \ . \qquad (C\text{-}6)$$

Puisque μ_z commute avec $\mathcal{H}_o$, et que le coefficient de μ_z dans (C-4) est une constante indépendante des coordonnées, il en résulte que μ_z se conserve et que dans l'équation de Schrödinger (C-6) les variables orbitales et de spin se séparent. $\Psi(x,y,z;\sigma)$ peut donc se mettre sous la forme

$$\Psi(x,y,z;\sigma) = \psi(x,y,z).\chi(\sigma) \ , \qquad (C\text{-}7)$$

produit d'une fonction de coordonnées $\psi(x,y,z)$ par une fonction de spin $\chi(\sigma)$.

On remarque également que $\mathcal{H}_o$ ne contient pas explicitement les coordonnées y et z. Dès lors, les opérateurs p_y et p_z commutent avec $\mathcal{H}_o$, c'est-à-dire que les composantes en y et z de l'impulsion $\vec{p}$ se conservent. Nous pouvons par suite chercher la fonction orbitale $\psi(x,y,z)$ sous la forme :

$$\psi(x,y,z) = C\, e^{\frac{i}{\hbar}(p_y y + p_z z)} \, \textcircled{H}(x) \ , \qquad (C\text{-}8)$$

où C est un facteur normalisant que nous définirons plus bas. En substituant (C-7) et (C-8) dans l'équation (C-6), on obtient l'équation suivante pour la fonction $\textcircled{H}(x)$:

$$\frac{d^2\textcircled{H}(x)}{dx^2} + \frac{2m^*}{\hbar^2}\left[E + \frac{1}{2}g\mu_B H\sigma - \frac{p_z^2}{2m^*} + eEx_o - \frac{1}{2}m^*\left(\frac{cE}{H}\right)^2 - \frac{m^*}{2}\left(\frac{eH}{m^*c}\right)^2 (x - x_o)^2\right]\textcircled{H}(x) = 0 \ , \qquad (C\text{-}9)$$

où l'on a introduit la notation

$$x_o = \frac{c}{eH}\left(p_y + m^*\frac{cE}{H}\right) \ . \qquad (C\text{-}10)$$

Il est facile de voir que l'équation (C-9) coïncide formellement avec l'équation de

Schrödinger pour un oscillateur linéaire oscillant avec la fréquence

$$\omega_c = \frac{|e|H}{m^* c} \qquad \text{(C-11)}$$

autour du point $x = x_o$. Ceci étant, on en déduit aussitôt que la constante

$$E + \frac{1}{2} g\mu_B H\sigma - \frac{p_z^2}{2m^*} + eEx_o - \frac{1}{2} m^* \left(\frac{cE}{H}\right)^2 ,$$

jouant le rôle de l'énergie de l'oscillateur, peut prendre les valeurs $(n + \frac{1}{2}) \hbar\omega_c$, les n étant des entiers ≥ 0. Les niveaux d'énergie de la particule en champs magnétique et électrique uniformes constants croisés sont donc donnés par l'expression :

$$E(n,p_y,p_z,\sigma) = (n+\frac{1}{2}) \hbar\omega_c + \frac{p_z^2}{2m^*} - \frac{1}{2} g\mu_B H\sigma - eEx_o(p_y) + \frac{1}{2} m^* \left(\frac{cE}{H}\right)^2 . \qquad \text{(C-12)}$$

L'énergie représentée par les trois premiers termes dans (C-12), $(n + \frac{1}{2}) \hbar\omega_c + \frac{p_z^2}{2m^*} - \frac{1}{2} g\mu_B H\sigma$, correspond à l'énergie de la particule en l'absence de champ électrique (E = 0) (voir chapitre I). Le terme $-eEx_o(p_y)$ dans (C-12) représente l'énergie potentielle moyenne de la particule dans le champ électrique $\vec{E}$ dirigé le long de l'axe des x. Enfin, le dernier terme dans (C-12), $\frac{1}{2} m^* \left(\frac{cE}{H}\right)^2$, correspond à l'énergie cinétique associée au mouvement de la particule suivant la direction y. En effet, ce terme est relié directement au résultat de la mécanique classique, à savoir qu'une particule en présence de champs magnétique ($\vec{H}$ // Oz) et électrique ($\vec{E}$ // Ox) uniformes constants croisés se déplace, en moyenne, suivant la direction y avec une vitesse d'entraînement égale à la vitesse de Hall ($-\frac{cE}{H}$).

Les fonctions d'onde $\Psi_{n,p_y,p_z}(\vec{r};\sigma)$ correspondantes de $\mathcal{H}_o$ sont égales à :

$$\Psi_{n,p_y,p_z}(\vec{r};\sigma) = \psi_{n,p_y,p_z}(\vec{r}).\chi(\sigma)$$

$$= C\, e^{\frac{i}{\hbar}(p_y y + p_z z)} \, \phi_n\left[x - x_o(p_y)\right].\chi(\sigma) , \qquad \text{(C-13)}$$

où $\phi_n[x - x_o(p_y)]$ est la fonction d'onde normalisée pour un oscillateur harmonique à une dimension de fréquence ω_c dans son n ième état excité et oscillant autour du point $x = x_o(p_y)$, et $\chi(\sigma = \pm 1)$ décrit les deux fonctions de spin correspondant à "spin-up" et "spin-down" le long de la direction z. La constante de normalisation C, qui apparaît dans (C-13), peut être obtenue en écrivant que la particule reste confinée dans une boîte parallélépipédique de volume $\mathcal{V} = L_x L_y L_z$. Par suite, on doit avoir :

$$\int_{\mathcal{V}} \Psi \, \Psi^{*} \, d\vec{r} = 1 \; ,$$

d'où

$$C = \frac{1}{\sqrt{L_y L_z}} \; .$$

BIBLIOGRAPHIE

A.A. ABRIKOSOV : "Introduction to the Theory of Normal Metals" (Edité par H. EHRENREICH, F. SEITZ et D. TURNBULL), Sup. 12, p. 176. Academic Press, New York and London (1972).

Kh. I. AMIRKHANOV, R.I. BASHIROV, and A. Yu. MOLLAEV : Fiz. Tverd. Tela, 13, 849 (1971) [English transl. : Soviet Phys. - Solid State, 13, 701 (1971)].

S. ASKENAZY : "New Developments in Semiconductors" (Edité par P.R. WALLACE, R. HARRIS et M.J. ZUCKERMANN), p. 365. Noordhoff, Netherlands (1973).

S. ASKENAZY, J.P. ULMET, and J. LÉOTIN : Solid State Commun., 7, 989 (1969).

A.C. BEER : "Solid State Physics" (Edité par F. SEITZ et D. TURNBULL), Sup. 4, p. 96. Academic Press, New York and London (1963).

J.S. BLAKEMORE : "Semiconductor Statistics" (Pergamon Press, Oxford, 1962), Appendix B, p. 346.

A.D. BRAILSFORD : Phys. Rev., 149, 456 (1966).

M. CARDONA : J. Phys. Chem. Solids, 24, 1543 (1963).

H.B.G. CASIMIR : Physica, 5, 495 (1938).

T.C. CETAS, C.R. TILFORD, and C.A. SWENSON : Phys. Rev., 174, 835 (1968).

R.B. DINGLE : Proc. R. Soc., A211, 517 (1952).

J. Mc DOUGALL and E.C. STONER : Phil. Trans. Roy. Soc. London, A237, 67 (1938).

L.É. GUREVICH and G.M. NEDLIN : Fiz. Tverd. Tela, 3, 2779 (1961) [English transl. : Soviet Phys. - Solid State, 3, 2029 (1962)].

C. HERRING : Phys. Rev., 96, 1163 (1954).

C. HERRING, T.H. GEBALLE, and J.E. KUNZLER : Phys. Rev., 111, 36 (1958).

C. HERRING, T.H. GEBALLE, and J.E. KUNZLER : Bell System Technical J., 38, 657 (1959).

A.H. KAHN and H.P.R. FREDERIKSE : "Solid State Physics" (Edité par F. SEITZ et D. TURNBULL), vol. 9, p. 257. Academic Press, New York and London (1959).

R. KUBO, S.J. MIYAKE, and N. HASHITSUME : "Quantum Theory of Galvanomagnetic Effect at Extremely Strong Magnetic Fields", in "Solid State Physics" (Edited by F. SEITZ and D. TURNBULL), vol. 17, p. 269. Academic Press, New York and London, 1965.

L.D. LANDAU : Zeitschr. f. Physik, 64, 629 (1930).

L.D. LANDAU and E.M. LIFSHITZ : "The Classical Theory of Fields", p. 62. Pergamon Press, Oxford (1962).

G. LANDWEHR : "The Shubnikov-de Haas Effect and Quantum-Limit Phenomena in Semiconductors" in : "Physics of Solids in Intense Magnetic Fields" (Edited by E.D. HAIDEMENAKIS), p. 415. Plenum Press, New York, 1969.

I.M. LIFSHITZ and A.M. KOSEVICH : Zh. Eksperim. i Teor. Fiz., 29, 730 (1955) [English transl. : Soviet Physics - JETP, 2, 636 (1956)].

D.K.C. MAC DONALD : "Thermoelectricity : an Introduction to the Principles", p. 9, John Wiley & Sons, Inc., New York, London (1962).

Yu. N. OBRAZTSOV : Fiz. Tverd. Tela, 7, 573 (1965) [English transl. : Soviet Phys. - Solid State, 7, 455 (1965)].

R.E. PEIERLS : "Quantum Theory of Solids" (Clarendon Press, Oxford, 1956), p. 75.

S.M. PURI : Phys. Rev., 139, A995 (1965).

L.M. ROTH and P.N. ARGYRES : "Semiconductors and Semimetals" (Edité par R.K. WILLARDSON et A.C. BEER), vol. 1, p. 159. Academic Press, New York and London (1966).

J.C. SLATER : "Insulators, Semiconductors, and Metals" ("Quantum Theory of Molecules and Solids", vol. 3), p. 49. Mc Graw-Hill Book Company, New York (1967).

E.C. STONER : Phil. Mag., 21, 145 (1936).

S.J. WILLIAMSON, S. FONER, and R.A. SMITH : Phys. Rev., 136, A1065 (1964).

J.H. WILSON, W.F. LOVE, and S.C. MILLER : Phys. Rev., 165, 923 (1968).

J.A. WOOLLAM : "Quantum Galvanomagnetic and Thermomagnetic Effects in Graphite to 18 Teslas (180 kG) at Low Temperatures", NASA TN D-7037, 1971.

W. ZAWADZKI : Advanc. Phys., 23, 435 (1974).

H.J. ZEIGER and G.W. PRATT : "Magnetic Interactions in Solids" (Clarendon Press, Oxford, 1973), Appendix 5, p. 573.

J.M. ZIMAN : "Electrons and Phonons" (At the Clarendon Press, Oxford, 1960), p. 396.

J.M. ZIMAN : "Principles of the Theory of Solids" (Cambridge University Press, Cambridge, 1965), p. 274.